TESIS DE LA UNIVERSIDAD DE ZARAGOZA
2025
224

Alejandro Marqués Paola

Implementación de tecnologías de fabricación aditiva en la fabricación sostenible de utillajes y estructuras

Director/es
Elduque Viñuales, Daniel
Javierre Lardiés, Carlos Francisco

ISSN 2254-7606

Prensas de la Universidad
Universidad Zaragoza

Universidad de Zaragoza
Servicio de Publicaciones

ISSN 2254-7606

Universidad Zaragoza
1542

Tesis Doctoral

IMPLEMENTACIÓN DE TECNOLOGÍAS DE FABRICACIÓN ADITIVA EN LA FABRICACIÓN SOSTENIBLE DE UTILLAJES Y ESTRUCTURAS

Autor

Alejandro Marqués Paola

Director/es

Elduque Viñuales, Daniel
Javierre Lardiés, Carlos Francisco

UNIVERSIDAD DE ZARAGOZA
Escuela de Doctorado

2025

Universidad Zaragoza
1542

Tesis Doctoral

Implementación de tecnologías de fabricación aditiva en la fabricación sostenible de utillajes y estructuras

Autor

Alejandro Marqués Paola

Directores:

Dr. Carlos Francisco Javierre Lardiés

Dr. Daniel Elduque Viñuales

Escuela de Ingeniería y Arquitectura

Programa de Doctorado Ingeniería Mecánica

2025

AGRADECIMIENTOS

Al alcanzar la culminación de este camino, no puedo sino recordar y agradecer a todas las personas que, con su apoyo, han sido una parte fundamental de esta tesis.

En primer lugar, quiero expresar mi gratitud a mis jefes, Berta Gonzalvo, Pascual Gracia y José Antonio Dieste, así como a todo el equipo del Centro Tecnológico Aitiip, por proporcionarme los recursos, la orientación y los consejos necesarios para llevar este trabajo a buen término. Gracias por contribuir a mi crecimiento, tanto profesional como personal.

Agradezco también a mis compañeros Alberto Laguía e Iván Monzón, por acogerme desde el primer día como uno más, por su apoyo constante, por todo lo que me han enseñado y por inspirarme a ser el ingeniero que soy hoy. Mi objetivo siempre ha sido, y seguirá siendo, aspirar a alcanzar vuestra excelencia profesional. No puedo dejar de mencionar a Julio Vidal, quien, junto a Alberto e Iván, ha sido una parte indispensable de este ciclo tan importante de mi vida.

A mis directores de tesis, Carlos Javierre y Daniel Elduque, les agradezco profundamente su incansable dedicación, su disponibilidad infinita, su apoyo constante y su guía a lo largo de todo este trayecto.

A mis amigos, que siempre han sido un apoyo y un escape. Porque siempre han estado, y son una parte esencial de mi vida.

A mi familia, mi más sincero agradecimiento. A mis padres, Manuel Marqués y Fuen Paola, por haberme apoyado en todo momento y haberme formado como la persona que soy hoy.

A mis tíos y abuelos, por educarme como a un hijo y por enseñarme que lo más importante siempre es ser una buena persona. Y, especialmente, a mi abuelo Manuel, al que no puedo dejar de echar de menos en los momentos significativos de mi vida.

A mi hermana Ruth, por ser tan diferente y a la vez tan igual en tantas cosas, y enfocar la vida siempre de la manera más imprevisible e inspiradora.

Finalmente, a Teresa, gracias por ser tanto la calma y cordura cuando lo necesito, como una fuente constante de originalidad y diversión. Todo es mejor a tu lado. Te quiero.

TESIS POR COMPENDIO DE PUBLICACIONES

La presente tesis doctoral titulada: Implementación de tecnologías de fabricación aditiva en la fabricación sostenible de utillajes y estructuras, es un compendio de trabajos previamente publicados por el doctorando en medios científicos relevantes en el ámbito de conocimiento.

ARTÍCULO 1:

Marqués, A.; Dieste, J.A.; Monzón, I.; Laguía, A.; Javierre, C.; Elduque, D. Analysis of Energy and Material Consumption for the Manufacturing of an Aeronautical Tooling: An Experimental Comparison between Pure Machining and Big Area Additive Manufacturing. *Materials* 2024, *17*, 3066, doi:10.3390/ma17133066.

Impact Factor: 3.1; Q1 (JCR 2023)

ARTÍCULO 2:

Marqués, A.; Dieste, J.A.; Monzón, I.; Laguía, A.; Gracia, P.; Javierre, C.; Clavería, I.; Elduque, D. Improvements in Injection Moulds Cooling and Manufacturing Efficiency Achieved by Wire Arc Additive Manufacturing Using Conformal Cooling Concept. Polymers (Basel) 2024, 16, doi:10.3390/polym16213057.

Impact Factor: 4.7; Q1 (JCR 2023)

ARTÍCULO 3:

Arrè, L.; Laghi, V.; Marqués, A.; Palermo, M. Tubular Sandwich Cross-Sections Fabricated with Wire Arc Additive Manufacturing for Jumbo Structural Members. *Structures* 2024, *67*, doi:10.1016/j.istruc.2024.106689.

Impact Factor: 3.9; Q1 (JCR 2023)

ARTÍCULO 4:

A. Marqués, J. Dieste, I. Monzón, C. Javierre and D. Elduque, rCF LM PAEK press-moulding process optimization through the introduction of a WAAM mould core, Materiales Compuestos (2024). Vol. 08 - COMUNICACIONES MATCOMP21 (2022) Y MATCOMP23 (2023), (Núm. 6 - Fabricación y Aplicaciones Industriales), 35 URL https://www.scipedia.com/public/Marques*_et_al_2024a

Proceeding con revisión académica por pares

RESUMEN

La fabricación aditiva, conocida popularmente como impresión 3D, ha transformado los procesos de producción al permitir la creación de objetos capa por capa a partir de modelos digitales, siendo su principal uso inicial el "prototipado rápido". Sin embargo, su integración completa en entornos industriales con altos requerimientos mecánicos aún enfrenta desafíos significativos.

En este contexto, el doctorando ha desarrollado una estrategia integral para la implementación de tecnologías de fabricación aditiva de grandes dimensiones, enfocándose específicamente en la tecnología metálica WAAM (*Wire Arc Additive Manufacturing*) dentro de entornos industriales exigentes.

En primera instancia, se abordó la sostenibilidad del proceso mediante la fabricación y análisis de dos utillajes de conformado simétricos: uno producido con tecnología aditiva y otro mediante métodos convencionales. Este estudio incluyó la evaluación comparativa de consumos eléctricos y de material en ambos casos, destacando las ventajas ambientales del utillaje fabricado mediante WAAM, con reducciones significativas en el material consumido, el material descartado y el consumo energético. Asimismo, se realizó un análisis metrológico detallado del utillaje WAAM para identificar optimizaciones de diseño que incrementaran aún más la sostenibilidad del proceso.

Adicionalmente, se analizó el proceso de diseño y fabricación de un utillaje de inyección optimizado, aprovechando las capacidades que ofrecen los procesos de fabricación aditiva, como la creación de canales de refrigeración internos complejos, inviables mediante técnicas convencionales, contribuyendo a la mejorar en su rendimiento.

Este análisis se complementó con la evaluación de un caso práctico, utilizando un utillaje fabricado aditivamente en un proceso industrial real. Estos estudios permitieron verificar la idoneidad de la tecnología WAAM para la producción de componentes industriales de gran tamaño.

Finalmente, se examinó la aplicación de la tecnología WAAM en la fabricación de productos finales con altos requerimientos mecánicos, enfocándose en el sector de la construcción. Para ello, se diseñaron y fabricaron diversas estructuras tipo columna con configuraciones "sándwich" auto-reforzadas, optimizadas para aprovechar las capacidades del proceso WAAM y alcanzar altas propiedades mecánicas.

En conclusión, este trabajo demuestra el potencial de la tecnología WAAM para integrarse plenamente en entornos industriales, destacando beneficios notables en términos de diseño, sostenibilidad y eficiencia en comparación con los métodos tradicionales. Además, se resalta su capacidad para reducir significativamente el consumo de material y energía, consolidándose como una alternativa prometedora para la producción en sectores con exigencias técnicas elevadas.

ABSTRACT

Additive manufacturing, popularly known as 3D printing, has transformed manufacturing processes by enabling the creation of 3D objects layer by layer from digital models, with its main initial use being “rapid prototyping”. However, its full integration in industrial environments with high mechanical requirements still faces significant challenges.

In this context, the PhD student has developed a comprehensive strategy for the implementation of large-scale additive manufacturing technologies, focusing specifically on WAAM (Wire Arc Additive Manufacturing) technology within demanding industrial environments.

In the first instance, the sustainability of the process was addressed through the fabrication and analysis of two symmetrical forming tools: one produced using additive technology and the other using conventional methods. This study included the comparative evaluation of electrical and material consumption in both cases, highlighting the environmental advantages of the tooling produced by WAAM technology, with significant reductions in consumed material, discarded material and energy consumption. A detailed metrological analysis of the WAAM tooling was also performed to identify design optimizations that would further increase the sustainability of the process.

Additionally, the design and manufacturing process of an optimized injection tooling was analyzed, taking advantage of the capabilities offered by additive manufacturing processes, such as the creation of complex internal cooling channels, unfeasible by conventional techniques, contributing to the improvement of its performance.

This analysis was complemented with the evaluation of a case study, utilizing an additively manufactured tooling in a real industrial process. These studies verified the suitability of WAAM technology for the production of large industrial components.

Finally, the WAAM technology application in the manufacturing of final products with high mechanical requirements was examined, focusing on the construction sector. For this purpose, several column-type structures named Tubular Sandwich Sections (TSS), were designed and fabricated, optimized to take advantage of the capabilities of the WAAM process and to achieve high mechanical properties.

In conclusion, this research demonstrates the potential of WAAM technology to be fully integrated into industrial environments, highlighting remarkable benefits in terms of design, sustainability and efficiency compared to traditional methods. In addition, its ability to significantly reduce material and energy consumption is highlighted, consolidating it as a promising alternative for production in sectors with high technical requirements.

ÍNDICE

LISTA DE ACRÓNIMOS

ABS (Acrylonitrile Butadiene Styrene): *Acrilonitrilo Butadieno Estireno, un termoplástico común en impresión 3D.*

ALM (Additive Layer Manufacturing): *Fabricación aditiva por capas.*

ASTM (American Society for Testing and Materials): *Organización de estándares internacionales*

BAAM (Big Area Additive Manufacturing): *Fabricación Aditiva de Gran Escala, una técnica de impresión 3D industrial.*

BJT (Binder Jetting Technology): *Tecnología de Inyección de Unión, un método de fabricación aditiva basado en aglutinantes.*

BTF (Buy To Fly): *Ratio que compara el peso del material comprado con el peso del material mecanizado.*

CAD (Computer-Aided Design): *Diseño Asistido por Computadora, creación de modelos digitales.*

CAM (Computer-Aided Manufacturing): *Manufactura Asistida por Computadora, software para control de máquinas.*

CC (Conformal Cooling): *Estrategia de diseño de sistemas de refrigeración*

CMT (Cold Metal Transfer): *Soldadura por Transferencia de Material Frío, técnica de soldadura.*

CNC (Computer Numerical Control): *Control Numérico Computarizado, control de máquinas herramienta.*

DED (Directed Energy Deposition): *Deposición Directa de Energía, técnica de fabricación aditiva.*

DMLS (Direct Metal Laser Sintering): *Sinterizado Directo de Metal por Láser, una técnica de fabricación aditiva.*

EBM (Electron Beam Melting): *Fusión por Haz de Electrón, una técnica de fabricación aditiva.*

FDM (Fused Deposition Modeling*): Modelado por Deposición Fundida, técnica de impresión 3D.*

FFF (Fused Filament Fabrication): *Fabricación por Filamento Fundido, método común de impresión 3D.*

GMAW (Gas Metal Arc Welding): *Soldadura de Arco con Gas Metálico, método de soldadura.*

HAM (Hybrid Additive Manufacturing): *Manufactura Híbrida Aditiva, combinación de métodos tradicionales y aditivos.*

HF (Hot Forming): *Conformado en caliente.*

ISO (Internacional Organization for Standardization): *Organización Internacional de Normalización o Estandarización*

LCA (Life Cycle Assessment): Metodología que evalúa los impactos ambientales asociados a todas las etapas del ciclo de vida de un producto

LCC (*Life Cycle Costing*): Enfoque económico que analiza los costos totales de un producto o proceso a lo largo de su ciclo de vida

LMD (Laser Metal Deposition): *Deposición de Metal por Láser, una técnica de fabricación aditiva.*

LPBF (Laser Powder Bed Fusion): *Técnica de fabricación aditiva. Utiliza una fuente láser de alta potencia para fundir polvo capa a capa para fabricar componentes metálicos.*

MAG (Metal Active Gas Welding): *Soldadura de Gas Activo Metálico, técnica de soldadura*

MAM (Metal Additive Manufacturing): *Manufactura Aditiva de Metales, proceso de impresión 3D metálica.*

MEX (Material Extrusion): *Extrusión de Material, tecnología de fabricación aditiva.*

MIG (Metal Inert Gas Welding): *Soldadura de Gas Inerte Metálico, técnica de soldadura.*

MJF (MultiJet Fusion): *Fusión MultiJet, método de impresión 3D.*

PBF (Powder Bed Fusion): *Fusión de Lecho de Polvo, una técnica de impresión 3D.*

PU A (Polyurethane Component A): *Poliuretano Componente A, reactivo en la producción de plásticos.*

PU B (Polyurethane Component B): *Poliuretano Componente B, reactivo en la producción de plásticos.*

RTM (Resin Transfer Moulding): *Moldes de transferencia de resina para el sector aeronáutico.*

SHL (Sequential Head Laser Strategy): *Estrategia de Cabezal de Láser Secuencial, en fabricación aditiva.*

SLA (Stereolithography): *Estereolitografía, un método de impresión 3D.*

SLM (Selective Laser Melting): *Fusión Selectiva por Láser, una técnica de fabricación aditiva.*

SLS (Selective Laser Sintering): *Sinterizado Selectivo por Láser, una técnica de fabricación aditiva.*

UNE (Asociación Española de Normalización): *Organismo de Normalización en España, designado por el Ministerio de Economía, Industria y Competitividad ante la Comisión Europea*

VPP (Vat Photopolymerization): *Fotopolimerización por Volumen, tecnología de impresión 3D.*

WAAM (Wire Arc Additive Manufacturing): *Fabricación Aditiva por Arco y Alambre, método industrial.*

Capítulo 1

Introducción y objetivos

En este capítulo se describe el punto de partida del doctorando en el desarrollo de su tesis. Describiendo sus motivaciones y objetivos para el desarrollo de una tesis doctoral centrada en el ámbito de la fabricación aditiva metálica de grandes componentes y la sostenibilidad. Con el propósito de que los resultados del presente desarrollo e investigación contribuyan a generar avances significativos en el ámbito de la fabricación aditiva, se busca fomentar su integración tanto en la industria como en la sociedad, promoviendo así un progreso alineado con los principios de sostenibilidad.

Contexto

La fabricación aditiva (AM), también conocida como impresión 3D, es una técnica avanzada utilizada para la fabricación de geometrías y estructuras complejas mediante la acumulación de material en forma de capas superpuestas, utilizando datos de modelos 3D. Esta tecnología ha supuesto una transformación en el campo de las técnicas de producción. Su facilidad de uso, compactibilidad y rapidez han acercado la fabricación a nivel de usuario, creando una comunidad dedicada a la impresión 3D, con millones de usuarios a nivel global. A nivel industrial, la tecnología aditiva ha revolucionado el concepto de prototipado rápido, cambiando la forma de enfocar la fase de diseño industrial. Además, permite implementar pequeños cambios o rediseños de manera rápida en diseños industriales ya cerrados, con objetivo de optimizarlos.

Dentro del ámbito de las tecnologías de fabricación aditiva, es importante distinguir entre los distintos procesos de fabricación existentes. Estos procesos atienden a las definiciones especificadas por la norma ISO/ASTM 52900:2022 [1]:

- BJT - Inyección de Aglutinantes (*Binder Jetting*): Consiste en depositar un adhesivo líquido de forma selectiva para unir partículas de material en polvo, como plástico, metal o cerámicas. Las piezas obtenidas requieren sinterización posterior para alcanzar las propiedades mecánicas finales.
- DED - Deposición por Energía Dirigida (*Directed Energy Deposition*): Utiliza una fuente de energía térmica focalizada (como un láser o haz de electrones) para fusionar material mientras se deposita. Los materiales empleados suelen ser polvo o hilo metálico, permitiendo aplicaciones de reparación y fabricación directa.
- MEX - Extrusión de Material (*Material Extrusion*): Este proceso dispensa material a través de una boquilla u orificio, creando piezas capa por capa. Trabaja con filamentos termoplásticos, granza, líquidos o pastas, y es ampliamente usado en aplicaciones domésticas e industriales.
- MJT - Inyección de Material (*Material Jetting*): Mediante la deposición selectiva de gotas de material líquido, como polímeros fotopolimerizables o ceras, permite crear piezas con alta resolución y acabado superficial.
- PBF - Fusión en Lecho de Polvo (*Powder Bed Fusion*): Utiliza energía térmica, como láseres, para fusionar selectivamente regiones de un lecho de polvo micronizado (metales, plásticos o cerámicas), logrando piezas de gran precisión.
- SHL - Laminado de Hojas (*Sheet Lamination*): Une láminas de material, como metales, plásticos o papel, para formar objetos tridimensionales. Es ideal para prototipos y aplicaciones de menor exigencia mecánica.
- VPP - Fotopolimerización (*Vat Photopolymerization*): Trabaja con resinas líquidas fotopolimerizables, curadas mediante exposición a luz. Ofrece alta precisión en piezas, siendo limitada a aplicaciones con resinas específicas.

La gran cantidad de materiales disponibles para los procesos de fabricación aditiva ejerce un rol esencial en su pronta adopción dentro del mercado, tanto industrial como a nivel usuario. Estos materiales presentan variaciones en su forma y características, dependiendo de su utilización en las tecnologías previamente enumeradas. No obstante, pueden agruparse en tres categorías principales: termoplásticos (principalmente poliamidas), metálicos y cerámicos. Esta clasificación facilita la selección de materiales específicos, según los requerimientos de acabados estéticos, propiedades mecánicas de alto rendimiento, resistencia a temperatura, entre otros. En el campo de la fabricación aditiva, el Centro Tecnológico Aitiip, ubicado en Zaragoza, ha demostrado ser una institución puntera a nivel internacional. Su amplia experiencia se refleja en la participación en numerosos proyectos internacionales, abarcando tanto la innovación en procesos aditivos avanzados como el desarrollo de nuevos materiales específicamente diseñados para este tipo de fabricación.

Prueba de ello es el proyecto KRAKEN, desarrollado en el marco del Programa de Investigación e Innovación Horizonte 2020 de la Unión Europea bajo el acuerdo de

subvención nº 723.759 [2]. Este proyecto, iniciado en 2016, se erigió como el sistema de fabricación aditiva más grande del mundo. Su revolucionario sistema se basó en el montaje de un cabezal de impresión aditiva en un sistema robótico, anclado a un puente grúa, logrando dimensiones de fabricación de hasta 20 x 6 metros y una altura máxima de 3 metros, como se muestra en la Ilustración 1. En este sistema de fabricación aditiva, basado en la tecnología extrusión de material, se incorporó la fabricación aditiva metálica WAAM y la extrusión de resina de poliuretano bicomponente. De esta manera, el mismo sistema de impresión aunó dos materiales distintos, materiales metálicos y termoplástico. Además, el sistema KRAKEN estaba provisto con un cabezal de fresado, por lo que unificaba ambos sistemas de fabricación, aditiva y sustractiva, siendo capaz de combinarlos en un sistema denominado *HAM (Hybrid Additive Manufacturing).*

Ilustración 1 Sistema robotizado de fabricación híbrida KRAKEN. Fotografía tomada en las instalaciones de la Fundación Aitiip.

La presente tesis se enmarca en el desarrollo del sistema de fabricación aditiva KRAKEN y en los proyectos derivados de esta línea de investigación. Estos avances han permitido explorar y aprovechar las capacidades de la fabricación aditiva, destacando su potencial para producir componentes de gran tamaño y alta complejidad, ampliando así las posibilidades en aplicaciones industriales.

Justificación de la importancia del estudio

Las tecnologías de fabricación aditiva han revolucionado las técnicas de producción gracias a su facilidad de uso, rapidez y versatilidad. Sin embargo, estos procesos aditivos tienen desventajas remarcables, que lastran su completa implementación en diversos sectores de la industria.

Los procesos de fabricación aditiva, al ser significativamente más recientes que los métodos de fabricación convencionales, presentan un menor grado de implementación industrial y desarrollo en términos de automatización. Además, el conocimiento técnico necesario para dominar estas tecnologías es menos extendido, lo que demanda una mayor especialización y la incorporación de programas de formación específicos para su adecuada aplicación.

Esta falta de implementación industrial se ve reflejada a su vez en la en la falta de conceptualización de las capacidades de diseño para fabricación aditiva. Esta tecnología permite la fabricación de diseños complejos, inalcanzables para métodos de fabricación convencionales, pero a su vez, tiene sus propias restricciones de diseño, de manera que es necesario que se optimicen al máximo sus posibilidades de fabricación y las propiedades mecánicas finales de la pieza fabricada.

En referencia a los objetos fabricados por fabricación aditiva, las propiedades mecánicas requeridas por los diversos sectores industriales limitan el uso de materiales termoplásticos para aplicaciones con requerimientos medio-altos. Además, los procesos de extrusión de material (MEX) cuyo material de aporte es termoplástico muestran unas propiedades mecánicas anisótropas, altamente dependientes de la dirección de impresión. De esta manera, los materiales metálicos se erigen como los más adecuados para procesos industriales. Estos procesos aditivos metálicos son más complejos que los requeridos para el uso de termoplásticos, y por ello se encuentran menos desarrollados e implementados actualmente, en especial los basados en la tecnología de extrusión de filamento.

Por otro lado, el tiempo de fabricación representa una de las principales limitaciones en los procesos de fabricación aditiva. Si bien la posibilidad de almacenar fácilmente el material facilita tiempos de producción rápidos para piezas pequeñas y específicas, el tiempo de fabricación incrementa de manera significativa para componentes de mayor tamaño. Asimismo, en la producción de grandes lotes de piezas, los métodos de fabricación tradicionales están ampliamente optimizados, permitiendo reducir considerablemente el tiempo total de producción. Por el contrario, en los procesos aditivos, el tiempo de fabricación tiende a incrementarse de forma lineal con el número de piezas, lo que limita su competitividad frente a métodos convencionales en este ámbito.

Además, una de las limitaciones clave en la implementación de la fabricación aditiva radica en la precisión de las piezas producidas. En los sistemas aditivos, tanto metálicos como no metálicos, se observa que un aumento en la tasa de deposición afecta negativamente la precisión final, ya que la calidad superficial de las capas queda condicionada por el tamaño de los cordones depositados. Por este motivo, para alcanzar las tolerancias dimensionales requeridas en las piezas finales, suele ser necesario recurrir a procesos de fabricación sustractiva como etapa complementaria.

Por otro lado, las restricciones de tamaño impresión de los equipos de fabricación aditiva comerciales limitan de sobremanera las piezas finales a obtener. En el caso de las tecnologías basadas en fusión de lecho de polvo (BJT, DED, MJT, PBF y VPP), los tamaños comerciales máximos de áreas de impresión alcanzar áreas de 1000x1000x1000 mm. Este hecho se debe a la necesidad de un sistema cerrado de aportación de polvo de material, y en algunos casos de la necesidad de crear una atmósfera adecuada al proceso. Estas restricciones, sumadas a la lentitud del proceso, restringen su uso industrial.

Las tecnologías de extrusión de material, gracias a su mayor tasa de aporte, y a su independencia de un área acotada de impresión, abren la puerta a la fabricación de grandes estructuras y utillajes. Las amplias posibilidades que abre este desarrollo en el campo de la fabricación industrial han sido la principal motivación para la realización de esta tesis.

Las limitaciones de los procesos de fabricación aditiva en su adopción industrial pueden sintetizarse en los siguientes aspectos:

- Competencia con tecnologías tradicionales: Las tecnologías aditivas enfrentan desafíos frente a métodos de fabricación convencionales ya consolidados y optimizados en la industria.
- Limitaciones de diseño: Es necesaria una revisión de los conceptos básicos de diseño de pieza y una adaptación a las posibilidades de la tecnología.
- Propiedades mecánicas: Dependiendo del proceso aditivo y el material seleccionado, las piezas fabricadas pueden presentar propiedades mecánicas reducidas, o anisotropías, lo que limita su rendimiento en ciertos entornos.
- Tiempo de fabricación: Los procesos aditivos requieren de un tiempo de fabricación aumentado en comparación con las tecnologías tradicionales, especialmente en la producción de piezas grandes o en lotes a gran escala.
- Precisión dimensional: La calidad y tolerancia dimensional de las piezas aditivas es inferior en comparación con métodos tradicionales, lo que a menudo requiere procesos secundarios de mecanizado.
- Restricciones de tamaño: La capacidad de fabricar componentes de gran escala es limitada, restringiendo la aplicación de estas tecnologías a piezas pequeñas o medianas.

Este conjunto de desafíos subraya la necesidad de avances tecnológicos y optimizaciones en los procesos de fabricación aditiva para su implementación más amplia en la industria.

En el estudio realizado dentro del marco de la tesis doctoral, se plantean estrategias de fabricación aditiva metálica, basadas en la tecnología de extrusión de material, para la fabricación de componentes estructurales y utillajes metálicos. Se abordará tanto desde un punto de vista de diseño, planteando la optimización de los productos fabricados respecto a su alternativa fabricada por métodos de fabricación tradicionales, como desde una perspectiva de sostenibilidad, estudiando los consumos eléctricos y de material del proceso. De esta manera se valorarán las posibilidades de implementación de esta tecnología en la industria para la fabricación de productos intermedios y finales.

La combinación de los estudios presentados pretende demostrar las virtudes del proceso de fabricación aditiva metálica, específicamente la tecnología WAAM, para la producción de utillajes y estructuras. Este análisis abarca tanto las mejoras técnicas obtenidas, como los beneficios asociados en términos de sostenibilidad.

La relevancia de este estudio no solo radica en la validación de la idoneidad de la tecnología WAAM como una solución industrial eficiente, sino también en establecer pautas claras de diseño y fabricación que optimicen su desempeño frente a los métodos convencionales. Estas directrices tienen como objetivo facilitar su integración en entornos industriales, mejorando su competitividad y promoviendo un uso más amplio y eficiente de esta tecnología en sectores con altos requerimientos mecánicos y/o de proceso.

Objetivos, alcance y metodología

A partir de las limitaciones identificadas durante la revisión técnica de las tecnologías de fabricación aditiva para componentes de gran tamaño, se han definido los objetivos de la investigación, diferenciándolos en objetivos generales y específicos. Asimismo, se ha delimitado el alcance del trabajo y detallado la metodología aplicada a lo largo del desarrollo de la tesis.

Objetivo principal

El objetivo de esta investigación es evidenciar que los procesos de fabricación aditiva, en particular la fabricación aditiva metálica, representan una mejora significativa frente a los métodos de fabricación convencionales. Esta mejora se evalúa tanto desde la perspectiva de la optimización del proceso, como desde el enfoque de la sostenibilidad, poniendo el foco en la producción de componentes de gran tamaño, tanto intermedios como finales.

En el contexto de esta investigación, la hipótesis planteada se evaluará a través de la fabricación y el análisis de componentes industriales de gran tamaño destinados a sectores como la construcción, la industria aeronáutica y la automoción. Este enfoque pone de manifiesto la versatilidad de esta tecnología, y su potencial para marcar una diferencia significativa en una amplia variedad de aplicaciones industriales.

Objetivos específicos

Con el propósito de fomentar la integración de las tecnologías de fabricación aditiva metálica, en la industria para la producción de componentes intermedios y finales, trascendiendo su aplicación exclusiva al ámbito del prototipado rápido, se han establecido los siguientes objetivos específicos:

1. Diseño y fabricación de utillaje de gran tamaño para implementación industrial en procesos de moldeo. Diseño y fabricación paralela de un molde simétrico mediante técnicas convencionales de fabricación.
    a. Validación del desempeño de los utillajes desarrollados mediante la implementación del proceso industrial, orientado a la producción de piezas finales.

   b. Estudio y comparación de los consumos eléctricos y de material en utillajes realizados mediante proceso de fabricación aditiva y proceso de fabricación convencional, analizando posibles optimizaciones en la fabricación aditiva del utillaje.
2. Diseño y fabricación un molde de gran tamaño refrigerado mediante canales internos optimizados siguiendo el principio de *Conformal Cooling* (CC).
   a. Simulación del ciclo de enfriamiento del molde y análisis de rendimiento comparado con el de un molde teórico equivalente, diseñado con canales internos idóneos para su fabricación mediante métodos convencionales.
   b. Fabricación de dicho molde mediante tecnología aditiva y análisis de consumo de material. Este consumo es comparado con el material requerido para la fabricación del molde teórico equivalente.
3. Diseño y fabricación de secciones tubulares en estructura sándwich optimizadas para su fabricación mediante tecnología aditiva.
   a. Simulación del comportamiento de las secciones tubulares optimizadas contra soluciones estructurales implementadas en la actualidad.

Esquema de toma de decisiones

Para estructurar y justificar las decisiones tomadas a lo largo de la tesis, se ha desarrollado el diagrama que se presenta en la Ilustración 2. Este diagrama detalla las tecnologías, materiales y procesos considerados en el marco de la investigación. La elección de cada tecnología está orientada al desarrollo de soluciones específicas para la fabricación de grandes componentes, evaluando distintos enfoques y perspectivas clave para asegurar su viabilidad industrial. La premisa inicial desde la que se parte es el conocimiento de los procesos de fabricación aditiva, sus posibilidades y restricciones. Por ello, se asimilarán los conocimientos necesarios en cuanto a posibilidades de diseño y restricciones por parte del doctorando.

El objetivo final, por tanto, será la demostración de la viabilidad de la implementación de los procesos aditivos en un entorno industrial solventando las problemáticas subrayadas en el apartado anterior.

En relación con los materiales empleados, se plantearán los materiales más utilizados en la fabricación aditiva, como anteriormente se ha mencionado. Estos son los materiales termoplásticos, los cerámicos y los metálicos. Para, los materiales de aporte cerámicos y termoplásticos, debido a sus propiedades mecánicas limitadas, no satisfacen completamente los requerimientos de ambientes industriales exigentes. No obstante, los materiales termoplásticos son los más utilizados en la industria de fabricación aditiva, siendo sus procesos de fabricación los más perfeccionados y optimizados. En el caso de los materiales metálicos, mecánicamente se postulan como los más adecuados. Sin embargo, los procesos de fabricación aditiva metálica se encuentran menos maduros que sus homólogos para material termoplástico.

Respecto a los tiempos de fabricación requeridos, estos son dependientes de la tecnología de fabricación empleada. Las tecnologías de gran aporte de material, como en el caso de la tecnología MEX, alcanzan un menor tiempo de fabricación, en detrimento de la calidad superficial y precisión de la pieza final. Por lado, las tecnologías aditivas basadas en lecho de polvo, como la PBF, cuentan con una gran precisión y una excelente calidad, pero en detrimento de sus tiempos de fabricación, que son sustancialmente mayores. Estos tiempos de fabricación son inversamente proporcionales al aporte de material, al que se hace referencia en el esquema de toma de decisiones.

En lo que respecta a los procesos, el tamaño máximo de las piezas fabricables representa una limitación crítica. La adopción industrial completa de la fabricación aditiva dependerá de la capacidad de estas tecnologías para adaptarse a la producción de componentes de gran tamaño. En el esquema de toma de decisiones se han incluido las soluciones comerciales de mayor tamaño en la actualidad.

Finalmente, las tecnologías específicas de fabricación de cada que cumplimentan las anteriores características explicadas se muestran en el último eslabón del esquema. Cabe mencionar que tecnologías aditivas como el *binder jetting* se repiten para varios materiales, sin embargo, sus dimensiones máximas de proceso variarán dependiendo del material de impresión en el que la impresora 3D se capaz de trabajar.

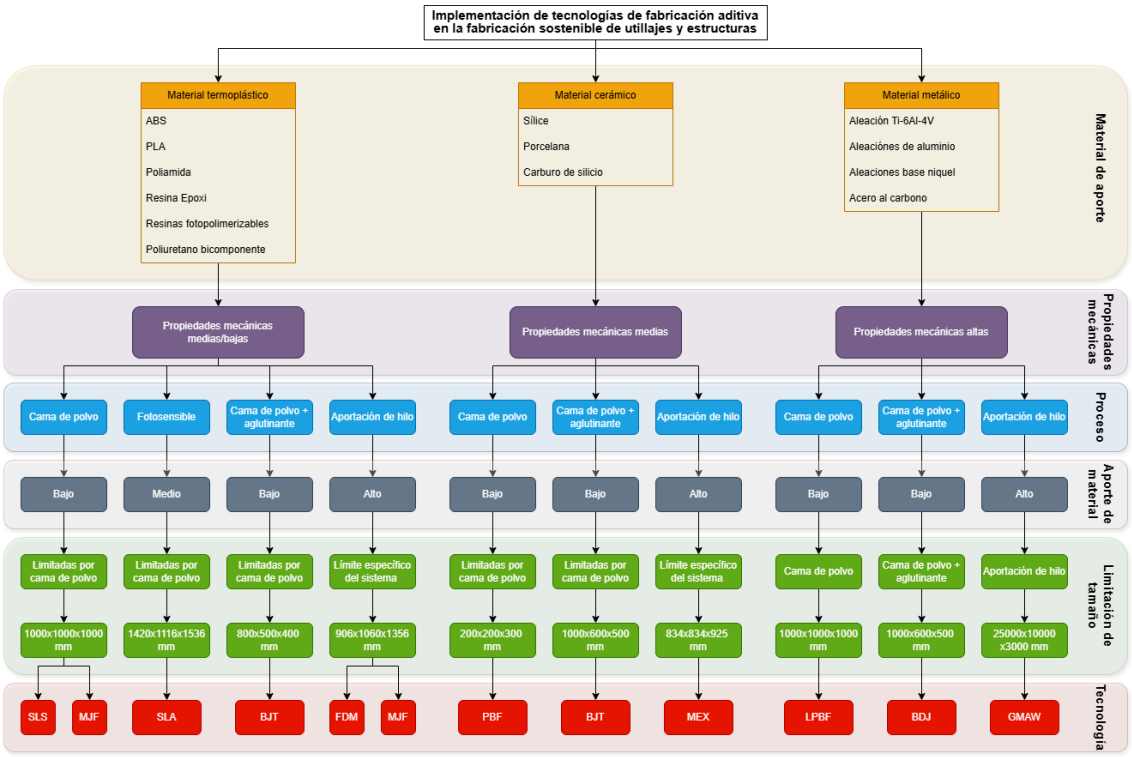

Ilustración 2 Esquema de toma de decisiones

Alcance

La realización de esta tesis sigue un hilo conductor basado en la integración total de la tecnología aditiva en la industria. En este contexto, el doctorando diseñará una estrategia integral que abarca todas las etapas necesarias para la implementación de la tecnología de fabricación aditiva de grandes dimensiones. El esquema de toma de decisiones desarrollado permite visualizar el camino hacia la integración industrial de la tecnología aditiva. Los requerimientos mecánicos altos derivados del ecosistema industrial y la casi inexistente limitación de tamaño de fabricación de piezas, hacen que el estudio se enfoque hacia la tecnología aditiva metálica basada en el proceso GMAW. Específicamente, la tecnología WAAM, basada en dicho proceso, se erige como la principal solución al problema planteado. Este enfoque se estructurará en torno a la producción de cuatro artículos científicos, los cuales describirán de manera exhaustiva el ciclo completo del proceso de fabricación aditiva.

Desde la conceptualización y diseño inicial de las piezas y estructuras industriales hasta la optimización de sus características, la fabricación efectiva de los prototipos, el análisis detallado de los parámetros y resultados del proceso, y, finalmente, la validación del desempeño de las piezas fabricadas bajo condiciones industriales reales, cada etapa será abordada con el objetivo de demostrar la viabilidad y eficiencia de esta tecnología en aplicaciones industriales complejas.

Se han identificado dos sectores estratégicos para evaluar y validar la tecnología de fabricación aditiva WAAM de grandes dimensiones: la industria del moldeo y la industria de la construcción. En el primer caso, se pretende analizar la viabilidad de integrar esta tecnología en la fabricación de utillajes intermedios, aprovechando sus ventajas en términos de personalización y optimización de diseño. Por otro lado, en el ámbito de la construcción, se plantea su aplicación directa en la fabricación de elementos finales, explorando su potencial para satisfacer las demandas estructurales específicas y contribuir a la innovación en este sector.

El alcance de esta investigación, por tanto, busca tener un impacto significativo en el panorama industrial actual, presentando la integración de la fabricación aditiva como una realidad. Por ello, este estudio, se enfoca en la fabricación aditiva WAAM, demostrando sus importantes ventajas desde la perspectiva del diseño de elementos complejos, la optimización de procesos y la sostenibilidad.

Metodología

Con el propósito de justificar la integración industrial de la tecnología aditiva WAAM, se desarrollará un estudio integral que abarque desde las etapas iniciales de diseño aditivo, remarcando sus capacidades y limitaciones, hasta la validación final de piezas en entornos industriales reales. Este enfoque, estructurado en una progresión metodológica, permitirá una evaluación completa del proceso. La metodología seguida se detalla a continuación:

1. **Búsqueda bibliográfica**: Se realizará un análisis exhaustivo para definir el estado del arte de las tecnologías aditivas, con énfasis en la tecnología WAAM. Este análisis incluirá no solo referencias relacionadas con esta tecnología, sino también un estudio de las industrias objetivo de su integración, con la finalidad de identificar oportunidades y desafíos.
2. **Diseño y optimización**: Se desarrollarán diseños adaptados a los requerimientos específicos del proceso WAAM, optimizando las estructuras y piezas finales para aprovechar las capacidades de la tecnología, como la fabricación de geometrías complejas y estructuras reforzadas.
3. **Análisis de estructuras/piezas a fabricar**: Las piezas diseñadas serán evaluadas en términos de rendimiento estructural y eficiencia del proceso. Este análisis se realizará frente a piezas análogas industriales teóricas o reales, permitiendo verificar que las optimizaciones implementadas contribuyen a una mejora en el desempeño del proceso y de las piezas fabricadas.
4. **Fabricación WAAM**: Las piezas serán fabricadas mediante el proceso WAAM, registrando datos críticos como consumo energético y material. Esta etapa tendrá como objetivo identificar áreas clave para optimizar la sostenibilidad del proceso en comparación con métodos convencionales.
5. **Análisis de datos y comparación**: Los datos obtenidos del proceso WAAM serán comparados con los de piezas equivalentes, ya sea reales o teóricas, fabricadas mediante tecnologías tradicionales. Este análisis tiene como objetivo validar las ventajas del proceso WAAM, con énfasis en su eficiencia, sostenibilidad y capacidad de ahorro de recursos.
6. **Testeo en condiciones reales**: Las piezas fabricadas mediante WAAM se someterán a pruebas en entornos industriales reales permitiendo la validación de utillajes de moldeo optimizados y verificando su desempeño satisfactorio en aplicaciones prácticas. Además, se realizarán pruebas preliminares en la industria de la construcción, validando estructuras tubulares auto-reforzadas diseñadas para entornos de alta exigencia mecánica.

A través de esta metodología, se pretende verificar el potencial del proceso WAAM como una solución industrial viable, capaz de producir componentes metálicos grandes y funcionales con elevados estándares de rendimiento, al tiempo que se optimizan los recursos empleados en su fabricación.

Esquema y desarrollo del documento

La estructura de esta tesis ha seguido el modelo de compendio de artículos, todos ellos basados en un hilo conductor común. Estos estudios, publicados en forma de cuatro artículos independientes, forman el hilo conductor de la tesis, cuya premisa es la implementación de tecnologías de fabricación aditiva en la fabricación sostenible de utillajes

y estructuras. La organización de dichos artículos publicados se muestra de manera esquemática en la Ilustración 3.

En cuanto al documento en sí, su estructura se aborda de la siguiente manera:

En primer lugar, la tesis introduce el contexto y la justificación del estudio, considerando las premisas, el alcance y los objetivos planteados. Posteriormente, se incluye un estado del arte que analiza en detalle la evolución de la tecnología aditiva, desde sus inicios hasta su aplicación en el ámbito industrial, con un enfoque específico en la fabricación aditiva metálica, eje central de este trabajo, y su relación con los objetivos propuestos.

El desarrollo técnico se estructura a través de los artículos publicados, siguiendo el hilo conductor definido en la sección Alcance. La sección de resultados presenta los logros alcanzados durante la investigación, junto con una discusión sobre su impacto. Además de los artículos, se detalla la contribución de las investigaciones en la publicación de patentes y en el desarrollo de proyectos europeos de investigación.

Las conclusiones sintetizan el trabajo realizado, destacando los resultados obtenidos y cerrando el hilo conductor planteado. También se incluyen las contribuciones originales al estado de la técnica y se proponen líneas de investigación futura para continuar mejorando los procesos estudiados.

Finalmente, el documento incorpora una sección de bibliografía que recopila todas las fuentes consultadas, así como listas de figuras, gráficos, tablas y acrónimos con su respectiva ubicación en el texto. En los anexos se encuentran los artículos y las patentes publicadas durante el desarrollo de la tesis.

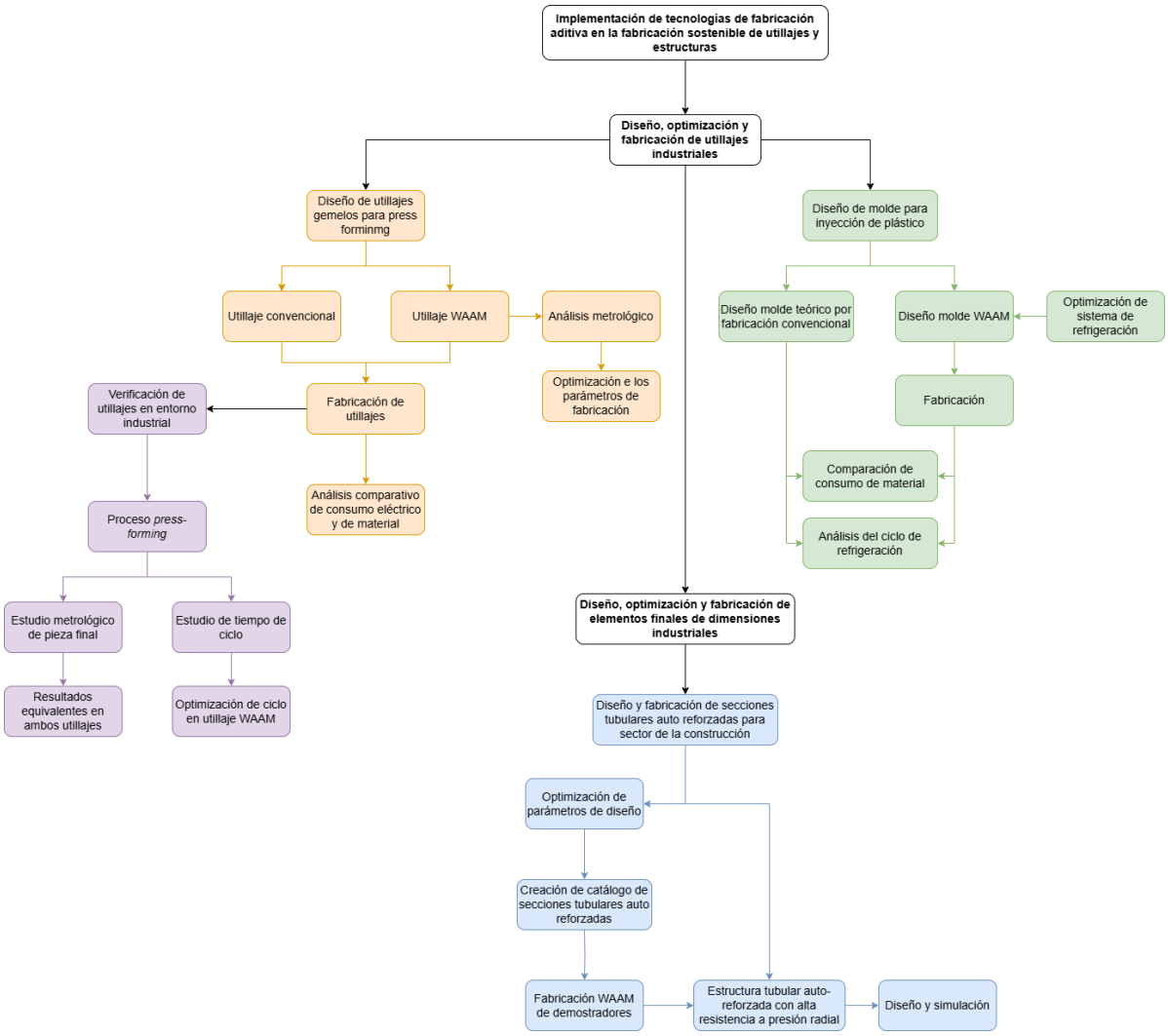

Ilustración 3 Diagrama de trabajos realizados

Capítulo 2

Estado del arte

Este capítulo aborda la evolución de la tecnología de fabricación aditiva, desde sus inicios hasta su consolidación no solo en la industria, sino también en la sociedad, donde ha ganado gran aceptación y ha fomentado la formación de una comunidad activa. Como introducción al ámbito de la fabricación aditiva, se analizan las principales diferencias con respecto a los métodos de fabricación convencional, destacando los casos en los que la impresión 3D puede complementar o incluso reemplazar estas tecnologías, además de señalar sus limitaciones inherentes.

Tras definir el concepto de fabricación aditiva, se exploran las principales tecnologías actuales, detallando sus características, limitaciones y aplicaciones específicas diferenciándolas en tecnologías de fabricación de lecho de polvo y tecnologías de fabricación por extrusión de material. Una vez establecida esta base, el enfoque se centra en el proceso de fabricación por extrusión de material, específicamente en el proceso WAAM, resaltando su potencial como alternativa eficiente y sostenible frente a los métodos de fabricación tradicionales. Se abordan los materiales más comunes empleados en esta tecnología, con especial atención al acero al carbono, que constituye el eje central del estudio, tal y como se ha explicado en la introducción, relacionándolo con sus aplicaciones industriales.

Además, se discuten las especificaciones de diseño asociadas al proceso WAAM, incluyendo sus limitaciones técnicas y requisitos específicos, así como las posibilidades de optimización geométrica que no son factibles con métodos de fabricación convencional. El capítulo también subraya la relevancia de la sostenibilidad en el proceso, centrándose en el análisis del consumo eléctrico y de material, y destacando las oportunidades industriales futuras que esta tecnología ofrece.

Como conclusión, se examina la integración de la tecnología WAAM en diversos sectores industriales, proponiendo escenarios en los que puede complementar o reemplazar las

tecnologías de fabricación tradicionales, consolidando su papel como una solución viable y sostenible para los desafíos actuales de diseño y producción.

Origen de la fabricación aditiva

La fabricación aditiva (AM), también conocida como impresión 3D, es una técnica avanzada utilizada para la fabricación de geometrías y estructuras complejas mediante la acumulación de material en forma de capas superpuestas, utilizando datos de modelos 3D [3,4]. En base a esta tecnología, gracias a su capacidad de producir piezas directamente a partir de un archivo CAD (*Computer-Aided Design*), eliminando la dependencia de los requerimientos tradicionales de fabricación, como el desarrollo de un plan de procesamiento, el acopio de materiales o el empleo de máquinas-herramienta específicas, ha sentado las bases de lo que hoy se conoce como prototipado rápido [5]. El impacto de esta tecnología en gran variedad de industrias, sumada a sus ventajas previamente remarcadas, han conferido a la fabricación aditiva el título de la "tercera revolución industrial" [6].

El origen de la fabricación aditiva se remonta a la década de los 80. El Dr. Kodama, en el Instituto Municipal de Investigación Industrial de Nagoya [7], propone en 1981 la primera aproximación a esta tecnología mediante la utilización de protopolímero, el cual se endurecía con la aplicación de luz ultravioleta. Esta idea sentó las bases para desarrollos futuros en el campo de la fabricación aditiva, destacando la invención de la primera tecnología de estereolitografía (*Stereolithography* - SLA), creada por Chuck Hull en 1986 [8], y la fabricación con filamento fundido (*Fused Filament Fabrication* - FFF), desarrollada por Scott y Lisa Crump en 1989 [9]. Estas innovaciones representan los precursores de los dos principales grupos de tecnologías en fabricación aditiva.

En la actualidad, los procesos de fabricación aditiva han sido integrados tanto en el ámbito industrial como en aplicaciones dirigidas a usuarios no especializados. Este hecho se debe en gran medida a la popularización de los dispositivos de impresión 3D, distribuidos mundialmente por una gran cantidad de compañías, siendo el usuario no especializado su principal target. Estas impresoras comerciales están basadas en su mayoría en tecnologías de filamento fluido de material polimérico, al ser fáciles de ensamblar, reparar y modificar, y al ser este proceso el más sencillo a nivel de producción. Gracias a su gran popularidad, se ha creado una importante comunidad de usuarios, que comparten ficheros CAD, soluciones de fabricación, datos de procesabilidad de materiales, etc. Esta circunstancia alimenta la rama más industrial de la fabricación aditiva [10,11], proveyendo a esta de retroalimentación constante de sus consumidores a nivel usuario. Como resultado, la fabricación aditiva ha impulsado un notable crecimiento en la industria, consolidándose progresivamente en los procesos industriales. Su proyección futura es ampliamente favorable, evidenciando un potencial significativo para su expansión y evolución [12].

La incorporación de la fabricación aditiva en el ámbito industrial ha conducido a la publicación en España de la Norma UNE-EN ISO/ASTM 52910:2020: Fabricación aditiva. Diseño. Requisitos, directrices y recomendaciones (ISO/ASTM 52910:2018) [13]. Esta normativa proporciona directrices aplicables al diseño de productos, dispositivos, sistemas, componentes o piezas fabricados mediante cualquier tecnología de fabricación aditiva, facilitando la identificación de consideraciones de diseño y la maximización de las capacidades inherentes a estos procesos. La elaboración de esta norma ha surgido de la adaptación al catálogo nacional de los grupos ISO/TC 261 *Additive Manufacturing* [14] y *ASTM F42 Additive Manufacturing Technologies*.

Diferencias entre fabricación aditiva y fabricación convencional

Como se ha mencionado, la fabricación aditiva tiene ventajas importantes respecto a la fabricación convencional en situaciones específicas. Estas diferencias fundamentales residen en su enfoque específico, su metodología y su aplicación, resumidas en los siguientes seis puntos:

1. Principio de fabricación. La fabricación convencional se puede considerar un proceso sustractivo, en el que un bloque de materia prima de tamaño mayor al de la pieza final es procesado mediante la extracción de material, mediante procesos como el fresado, corte o taladrado, hasta la obtención de la pieza objetivo. Por el contrario, en los procesos de fabricación aditiva, el proceso se basa en el aporte de material, creando la pieza final correspondiente al modelo CAD mediante la adición de capas.
2. Flexibilidad de diseño. Los métodos de fabricación convencional cuentan con las limitaciones intrínsecas de las máquinas-herramientas y equipos utilizados. Debido a ello, los diseños a fabricar deben ser adaptados a dichas restricciones, limitando la complejidad de las piezas a fabricar. Sin embargo, los procesos de fabricación aditiva se independizan de estas restricciones de fabricación, permitiendo la fabricación de estructuras complejas e intrincadas, inalcanzables por métodos de fabricación convencionales [15], como serían las estructuras internas. Esto no implica que los procesos de fabricación aditiva carezcan de limitaciones inherentes en cuanto al diseño para su fabricación, aspecto que será analizado en detalle en secciones posteriores. No obstante, estos procesos ofrecen una capacidad significativamente superior para la creación de geometrías complejas en comparación con los métodos de fabricación convencional. Cabe resaltar en este apartado las limitaciones dimensionales de los procesos aditivos, siendo dependientes de la tecnología y material utilizados, que restringen el tamaño máximo de las piezas a fabricar [16].
3. Costes de producción. Los costes de producción de un producto realizado mediante métodos de fabricación convencionales son proporcionales a la

complejidad de la pieza. Sin embargo, las producciones en masa reducen los costes de la producción de cada elemento individual, al amortizar las herramientas y los procesos de mecanizado. Por esto, la fabricación convencional es adecuada para grandes lotes de piezas. En el caso de la fabricación aditiva, el coste de fabricación es independiente de la complejidad de la geometría final, siendo este directamente proporcional al volumen final de la pieza. Por ello, la fabricación aditiva es adecuada para series cortas o prototipos.

4. Materiales. Los procesos de fabricación convencional cuentan con una extensa trayectoria de aplicación industrial, lo que ha propiciado el desarrollo de soluciones avanzadas de máquina-herramienta, adaptadas al procesamiento de una amplia variedad de materiales. En contraste, la fabricación aditiva, al ser una tecnología relativamente reciente, presenta una limitación en la variedad de materiales disponibles para su procesamiento. Los materiales más comúnmente empleados son los termoplásticos [17,18], aunque también se han desarrollado aplicaciones utilizando materiales cerámicos [19] y metálicos [20].
5. Tiempo de fabricación. Al igual que se ha mencionado para los costes de producción, los tiempos necesarios para fabricar productos realizados mediante métodos de fabricación convencionales son proporcionales a la complejidad del diseño de éstos. Sin embargo, este tiempo de producción elevado se rentabiliza en la fabricación de grandes series. Por el contrario, los procesos aditivos eliminan pasos de la producción, como el cambio de herramientas, sin embargo, el proceso de fabricación se mantiene constante independientemente de las piezas a producir, siendo mejorado en la fabricación de grandes series de productos por los métodos de fabricación convencionales.
6. Sostenibilidad. Los procesos de fabricación convencionales parten de una materia prima, de la cual comúnmente extraen material hasta formar el elemento final. Como resultado, estos procesos generan una cantidad significativa de desechos, cuyo volumen depende directamente de la discrepancia entre el tamaño de la materia prima adquirida y la geometría final del componente a fabricar. En contraposición, los procesos de fabricación aditiva permiten la obtención directa de piezas finales, requiriendo, en función del tipo de tecnología empleada, un mínimo o incluso ningún proceso de acabado posterior. Esto se traduce en una optimización significativa del material empleado durante la fabricación [21]. Esta optimización en el uso de material se plasma también en el consumo eléctrico del proceso [22], como será desarrollado más adelante.

En resumen, mientras la fabricación convencional sigue siendo la opción preferida para la producción en masa de piezas estándar, la fabricación aditiva sobresale en la personalización, la producción de prototipos y la fabricación de geometrías complejas, con una mayor eficiencia en el uso de recursos.

Tecnologías de fabricación aditiva

En referencia a las tecnologías de fabricación aditiva existentes, su diferenciación se puede realizar en base a diferentes criterios. En el capítulo Introducción y objetivos se han presentado los diferentes procesos de fabricación aditiva atendiendo a su especificación ISO/AST. En este apartado, dicha diferenciación se realizará en función a su tecnología de deposición y consolidación del material, característica que se relaciona directamente con las capacidades dimensionales del proceso. Por ello, diferenciaremos 2 grandes grupos de tecnologías: tecnologías de lecho de polvo y tecnologías de extrusión de material.

Tecnologías de lecho de polvo

En las tecnologías de fabricación aditiva por lecho de polvo, el material inicial se presenta en forma de polvo, que se extiende en capas uniformes sobre una superficie. Cada capa se consolida selectivamente mediante una fuente de energía, como un láser o un haz de electrones, que sinteriza o funde el material según el diseño [23]. De esta manera, se consolida una capa de material, que es cubierta por una nueva capa de polvo, consolidándose de nuevo, y repitiendo este proceso capa a capa hasta completar la geometría. Entre las tecnologías más relevantes dentro de este grupo se encuentran: la sinterización selectiva por láser (*Selective Laser Sintering* - SLS) [24], que utiliza un láser para sinterización de polvo termoplástico; la fusión selectiva por láser (*Selective Laser Melting* - SLM) [25], también basada en la consolidación selectiva mediante láser, pero específicamente orientada al procesamiento de materiales metálicos; y la fusión por haz de electrones (*Electron Beam Melting* - EBM) [26], que emplea un haz de electrones para fusionar y consolidar las capas de material metálico. Un esquema del concepto de fabricación aditiva mediante tecnología de lecho de polvo, específicamente SLM, se muestra en la Ilustración 4. Como se puede apreciar, esta tecnología posee la capacidad de procesar una amplia diversidad de materiales, destacando especialmente la fabricación aditiva metálica (*Metallic Additive Manufacturing*, MAM).

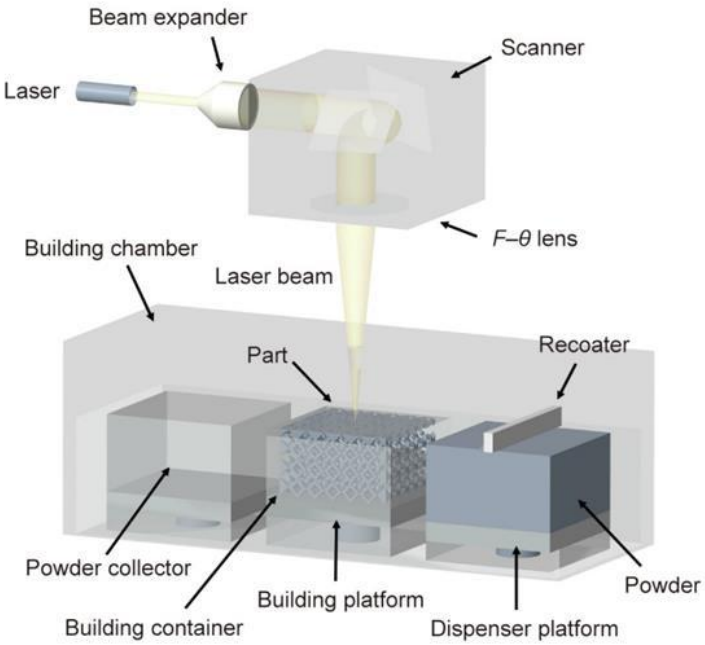

Ilustración 4 Definición esquemática del proceso SLM [27]

Este grupo de tecnologías de lecho en polvo destaca por su capacidad de fabricación de piezas de alta complejidad geométrica, alta calidad superficial y propiedades mecánicas avanzadas [28,29]. Cabe destacar la calidad de detalle alcanzada por esta tecnología, permitiendo minimizar o incluso eliminar por completo los procesos de acabado posteriores. Una de las cualidades más valoradas de esta tecnología es la isotropía de sus propiedades mecánicas, atribuida a las particularidades inherentes a su proceso de consolidación.

Como contrapunto, se debe mencionar el prolongado tiempo de proceso requerido por estos procesos, y su consumo eléctrico elevado en comparación con las tecnologías de extrusión de material [30]. Un aspecto aún más relevante de estas tecnologías es la limitación en el tamaño de las piezas que pueden fabricarse, determinada por las dimensiones de la cama de polvo y los sistemas diseñados para el depósito y distribución de polvo en la cama de fabricación. Las tecnologías basadas en lecho de polvo requieren una estructura cerrada y hermética para evitar la contaminación por impurezas externas, lo que restringe adicionalmente las dimensiones de fabricación. Como resultado, estas tecnologías de fabricación aditiva de lecho de polvo se encuentran principalmente limitadas a la producción de piezas de tamaño pequeño.

Tecnologías de extrusión de material

Esta tecnología se basa en la extrusión continua de material, generalmente en forma de filamento. El material se deposita capa a capa, siguiendo el diseño del modelo CAD. La consolidación del material depositado ocurre debido al enfriamiento de éste en la mayoría de los casos, como en los procesos de filamento fundido (*Fused Filamente Fabricatión* – FFF) [31] o los procesos de deposición fundida (*Fused Deposition Modeling*

- FDM) [32]. Un esquema del concepto de fabricación aditiva mediante extrusión de material, específicamente FDM, se muestra en la Ilustración 5. Por norma general, las tecnologías aditivas basadas en extrusión de material son procesos endotérmicos, los cuales requieren de una fuente de calor externa para realizar el proceso de extrusión. No obstante, en procesos como la extrusión de poliuretano bicomponente [33], se pueden observar reacciones exotérmicas que ocurren durante la mezcla y posterior extrusión de ambos elementos (*PU A + PU B*).

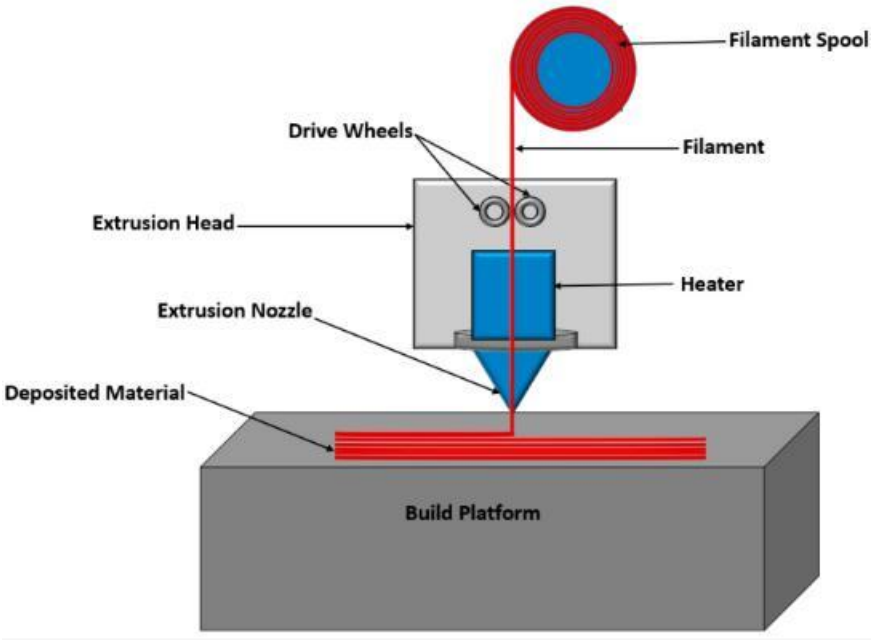

Ilustración 5 Esquema simplificado de un proceso de fabricación aditivo FDM [34]

Esta tecnología se caracteriza por su simplicidad operativa, bajo costo y amplia accesibilidad. Por ello, se ha convertido en la opción preferida para prototipado rápido y para aplicaciones funcionales con geometrías menos complejas [35]. Además, es la tecnología más utilizada fuera del ámbito industrial. Sin embargo, cuenta con problemáticas tales como la baja calidad superficial, la necesidad de material de soporte para diseños específicos, y la posible anisotropía en las propiedades mecánicas de las piezas impresas. Ésta es dependiente del material y del proceso específico de impresión, siendo más notable en las tecnologías FFF con aporte de material termoplástico [36,37], y prácticamente inexistente en tecnologías con aporte de material metálico.

Otra de las características destacables de las tecnologías de extrusión de material, es su área de trabajo. Al ser el sistema de extrusión no dependiente de las restricciones geométricas del lecho de polvo, el área de impresión alcanzable por esta tecnología no tiene limitaciones geométricas más que las del propio diseño de los ejes del dispositivo de impresión. Por ello, esta tecnología es la más indicada para la impresión de diseños de gran tamaño, concepto denominado *Big Area Additive Manufacturing* (BAAM) [38].

En relación con los materiales empleados en esta tecnología aditiva, se encuentra una amplia variedad. Los materiales termoplásticos destacan como los más utilizados, especialmente en forma de filamento para procesos de FFF, debido a su diversidad en colores, acabados y propiedades, así como a su extensa disponibilidad en el mercado. No obstante, tal como se ha señalado previamente, el desarrollo y la aplicación de materiales cerámicos y metálicos, en el ámbito de la fabricación aditiva por extrusión de material, han alcanzado un nivel de avance considerable en la actualidad.

Tecnología WAAM

En este estudio, se hará hincapié en las tecnologías de fabricación aditiva metálica (MAM), específicamente en la tecnología de fabricación *Wire Arc Additive Manufacturing* (WAAM) [39–41]. En esta tecnología de fabricación aditiva metálica, basada en la Soldadura por Arco Metálico con Gas (*Gas Metal Arc Welding - GMAW*) [42] el calor del arco generado entre el electrodo consumible y la pieza se utiliza para fundir las superficies del metal base y la punta del electrodo. El metal fundido del electrodo se transfiere a la pieza a través del arco, depositándose sobre la capa anteriormente aportada y ya solidificada [43]. La antorcha de soldadura proporciona una atmósfera protegida con gas de soldadura, la entrada del hilo y la corriente de soldadura. Esta antorcha se incorpora en un sistema de movimiento, que puede ser un sistema de 3 ejes o un robot colaborativo más complejo. El proceso descrito de la fabricación WAAM se encuentra representado en la Ilustración 6. Este sistema es independiente de una cama de polvo o atmósfera hermética, ya que la atmósfera de soldadura necesaria es generada directamente por la propia tobera en la zona de soldadura. Por ello, no presenta limitaciones dimensionales de construcción, salvo aquellas impuestas por la estructura de soporte del cabezal de soldadura.

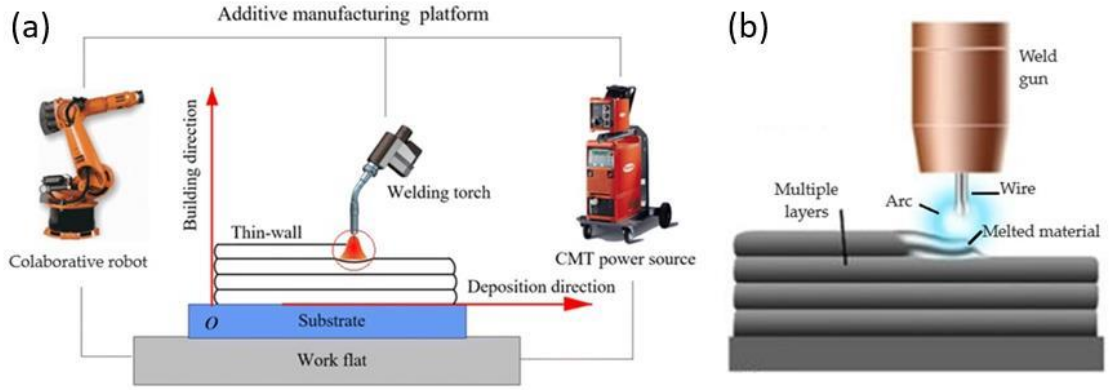

Ilustración 6 Sistema de fabricación aditiva WAAM (a) y detalle del cabezal de soldadura (b)

Es importante destacar que este proceso de fabricación aditiva se fundamenta en la superposición sucesiva de capas, ya que se encuentra basado en tecnologías aditivas de extrusión de material. Debido a esta característica, las superficies laterales de estas construcciones presentan una geometría similar a la que se muestra en la Ilustración 7. Por este motivo, el proceso WAAM se considera una tecnología *Near to Net Shape*, lo

que significa su producto impreso es muy similar a su forma final. Esto significa que, una vez finalizado el proceso, el resultado obtenido requiere de un proceso de acabado por CNC. La superficie lateral irregular es el resultado de un compromiso alcanzado mediante la optimización de los parámetros de la temperatura de soldadura (dependiente de la corriente eléctrica), y de la velocidad de impresión [44]. Estos parámetros afectan a la altura del cordón de soldadura y a su anchura, que son inversamente proporcionales. Los parámetros de construcción de WAAM establecidos afectan a la calidad de la superficie final [45–47]; sin embargo, el estudio de Lopes et al. [48] muestra que el comportamiento mecánico de los componentes fabricados no está influenciado por el proceso de fresado posterior.

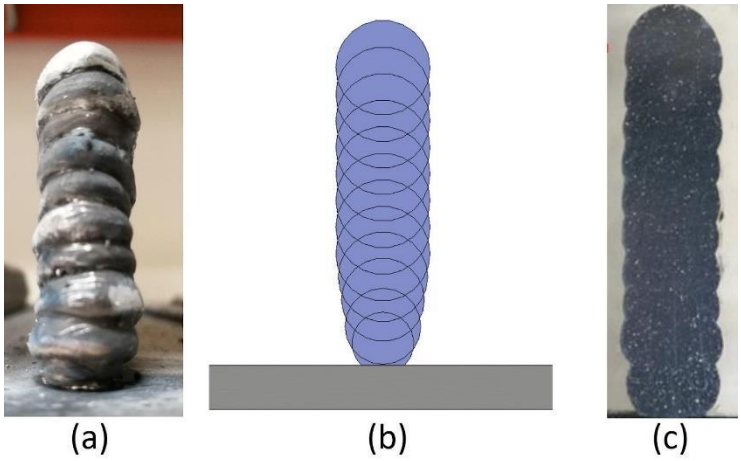

Ilustración 7 Estructura solapada del cordón de soldadura en el proceso WAAM. (a) Fotografía de la estructura. (b) Representación geométrica de la distribución de los cordones de soldadura. (c) Fotografía de una sección transversal de la estructura.

Cabe resaltar los parámetros más relevantes del proceso WAAM, los cuales afectan a la pieza final impresa. Principalmente su efecto se hace patente en la anchura y altura del cordón de soldadura extruido, así como en la calidad de éste:

- Velocidad de impresión. Velocidad a la que la antorcha de soldadura se mueve durante el proceso WAAM.
- Aporte de hilo: Volumen de material de aporte por segundo suministrado.
- Altura de capa: Distancia entre capas, definida en el eje vertical.
- Ángulo del electrodo: Inclinación del sistema de soldadura WAAM respecto a la horizontal de la capa previamente extruida o base.
- Voltaje eléctrico. Este parámetro determina la longitud del arco en soldadura, que es la distancia entre el baño de soldadura fundido, y el alambre de metal de aportación en el punto de fusión dentro del arco.
- Intensidad. Esta variable de la corriente de soldadura afecta a la cantidad de material depositado durante el proceso WAAM.
- Caudal de gas de soldadura. Un caudal inadecuado puede provocar problemas de oxidación, porosidad o crecimiento inadecuado de la pieza.

- *Stick-out*. Término que hace referencia a la distancia desde la tobera hasta la construcción WAAM. Un *stick-out* demasiado grande puede resultar en fallo del arco de soldadura, mientras que, si se trata de un valor demasiado pequeño, significa que la tobera está demasiado cerca de la construcción, pudiendo llevar a colisiones o incluso a la soldadura de la tobera.
- Temperatura. Un exceso de temperatura puede causar un flujo excesivo del material depositado, aumentando la anchura del cordón y reduciendo su altura. Esto afecta negativamente al crecimiento y precisión de la pieza. Por ello, es esencial evitar acumulaciones de calor mediante una planificación adecuada del ruteo, asegurando una distribución térmica uniforme durante el proceso.

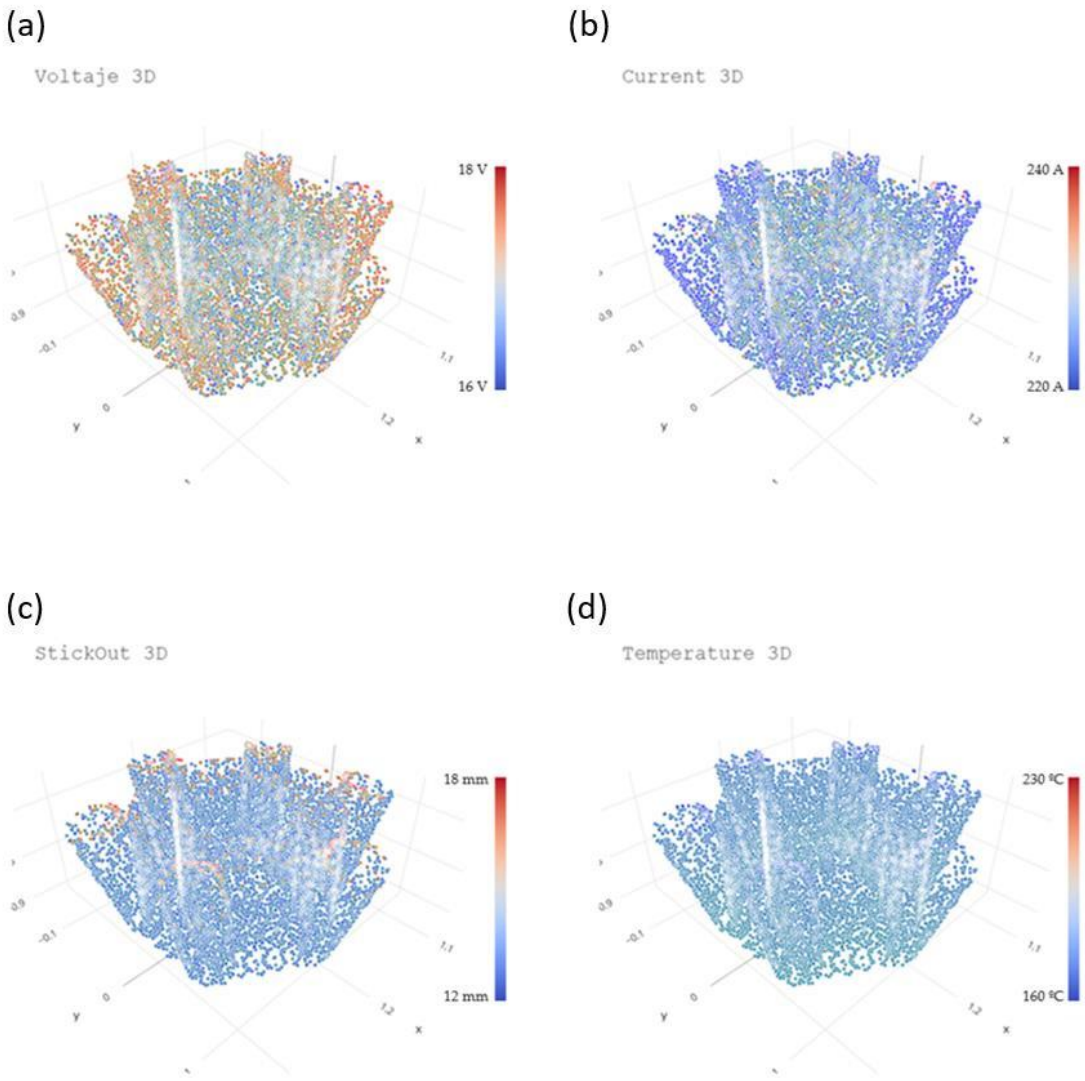

Ilustración 8 Parámetros de proceso WAAM recogidos durante la fabricación de una estructura compleja: (a) voltaje, (b) Intensidad, (c) Stick-out y (d) Temperatura.

Para grandes construcciones, es deseable un cordón de soldadura estrecho, que permita un crecimiento rápido de la pieza en altura, pese a que reduzca la penetración de la

soldadura en la capa inferior [49].Estos parámetros de fabricación afectan a las propiedades finales del material, quedará definida por los requerimientos finales de la construcción[50–54].

En este repaso de los parámetros más relevantes para el proceso de soldadura se han obviado elementos tan importantes como el material de aporte y el gas de soldadura utilizado, ya que serán descritos con mayor detalle en el apartado siguiente.

El análisis del proceso de fabricación aditiva WAAM y su parametrización se fundamenta en los desarrollos realizados por Iván et al. [55] en su tesis doctoral, la cual establece los principios básicos para procesos WAAM de grandes dimensiones. Estos avances constituyen la base del estudio actual y también inspiran la investigación en curso de Alberto Laguía, enfocada en la parametrización detallada del proceso WAAM. Este trabajo aprovecha los hallazgos de ambas tesis como puntos de partida esenciales para su desarrollo, integrando sus contribuciones para avanzar en la implementación industrial de esta tecnología.

Materiales

El proceso WAAM es realizable con una amplia variedad de materiales metálicos, sin embargo, los parámetros de fabricación son dependientes del material utilizado. Esto puede atribuirse a los cambios introducidos en la fuente de calor, la alimentación del filamento, el laminado, las condiciones de procesamiento y las técnicas de calentamiento para mejorar y optimizar el proceso de fabricación [56]. Los materiales de aporte de mayor relevancia en aplicaciones industriales son los siguientes:

- Aleación Ti-6Al-4V. Ampliamente utilizada en la industria aeroespacial, a lo largo de los años se ha trabajado más en la mejora del rendimiento de la aleación [57]. Además, la aleación de titanio se utiliza para muchas aplicaciones ligeras, ya que se caracteriza por su sobresaliente resistencia mecánica. Sin embargo, este material es relativamente más caro, por lo que las tecnologías de fabricación que optimizan su consumo de material, como en el caso del WAAM, adquieren una especial importancia[58]. Sin embargo, proceso WAAM en esta aleación puede generar tendencias anisotrópicas en las propiedades mecánicas de la pieza fabricada, como en el caso de la resistencia a tracción [59].
- Aleaciones de aluminio. Las más importantes áreas de aplicación de las aleaciones de aluminio producidas mediante tecnología WAAM incluyen los sectores aeroespacial, automovilístico, naval y energético, en los que las estructuras ligeras, la resistencia a la corrosión y la alta resistencia son fundamentales. En este material, el aporte térmico del proceso influye significativamente en la microestructura y las propiedades mecánicas de los componentes, provocando defectos como tensiones residuales, distorsión, porosidad y grietas [60]. La Ilustración 9

muestra un ejemplo de construcción de torre de aluminio SuperGlaze 5356, definido según EN ISO 18273 como S Al 5356 (AlMg5Cr(A)) [61].

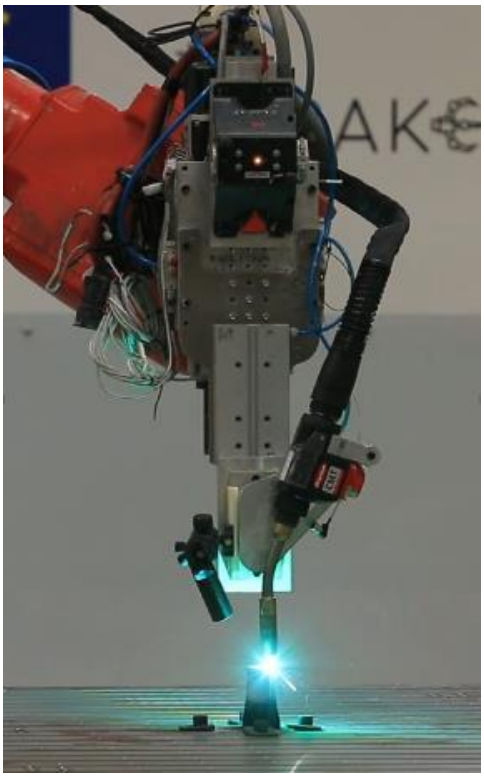

Ilustración 9 Fabricación de torre de aluminio mediante proceso WAAM operado por robot colaborativo. Fotografía tomada en las instalaciones de la Fundación Aitiip.

- Las superaleaciones base níquel (Ni). Las aleaciones a base de níquel tienen una buena resistencia a la corrosión y presentan unas excelentes propiedades mecánicas [62]. Estas propiedades se mantienen incluso a temperaturas elevadas, lo que da lugar a una amplia gama de aplicaciones industriales. Respecto a su utilización como material de aporte en la tecnología WAAM, los resultados obtenidos muestran una gran dependencia de la selección de las técnicas WAAM y los parámetros de entrada. Estos efectos se hacen visibles en la microestructura resultante, y la aparición de defectos que pueden influir en las propiedades mecánicas finales. Las superaleaciones utilizadas en el proceso WAAM basadas en Ni muestran una microestructura y unas propiedades mecánicas no homogéneas desde las capas inferiores a las superiores [63].
- Acero al carbono. Las aleaciones de acero al carbono figuran entre los materiales más ampliamente empleados en el ámbito industrial[64]. Su aplicación mediante la tecnología WAAM ha sido validada en sectores de gran relevancia, como la industria militar [65], construcción [66–68], ferroviaria [69] y nuclear [70], destacando por su versatilidad y propiedades mecánicas superiores en entornos exigentes. Estas propiedades pueden atribuirse a su comportamiento mecánico isotrópico, validado por los ensayos realizados por Laghi et al. [71] y respaldado

por análisis microestructurales que evidencian una microestructura notablemente homogénea en las construcciones fabricadas mediante tecnología WAAM. Un ejemplo de cordón de soldadura fabricado en acero al carbono se detalla en la Ilustración 10.

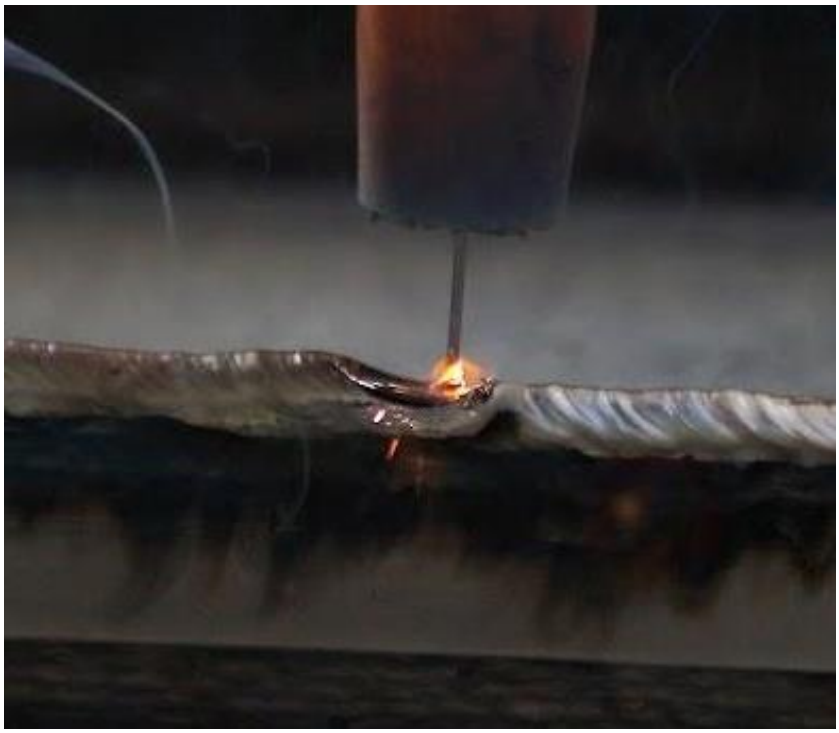

Ilustración 10 Detalle de fabricación de estructura utilizando acero al carbono como material de aporte

Además del material de aporte, cabe resaltar la importancia del gas de soldadura utilizado durante el proceso. La función de este gas es creación de una atmósfera idónea para el proceso de soldadura, desplazando el oxígeno y otros gases atmosféricos, aumentando la ionización del arco eléctrico, y por lo tanto la energía térmica transferida, lo que resulta en una mayor penetración del metal base y un arco más estable. Este desplazamiento de gas atmosférico en la zona de soldadura previene además la oxidación durante el proceso. Las especificaciones del proceso de soldadura utilizado en la tecnología WAAM (MIG o MAG comúnmente) definen la utilización de un gas inerte o activo. El caudal de éste requiere un importante proceso de optimización. Un caudal insuficiente no será capaz de desplazar el volumen de aire atmosférico, siendo incapaz de crear la atmosfera idónea para la soldadura. Sin embargo, un caudal demasiado elevado puede crear un enfriamiento indeseado de la zona de deposición debido a la convección forzada [72,73].

Esta tesis doctoral se centra en la tecnología WAAM utilizando acero al carbono como material de aporte, debido a su alta versatilidad y amplia utilización en el ámbito industrial. Este material destaca no solo por su gran disponibilidad y facilidad de adquisición, sino también por su aplicabilidad en una amplia variedad de sectores, tanto en componentes intermedios, como utillajes y moldes, como en productos finales, tales como

estructuras constructivas. Su disponibilidad, combinada con excelentes propiedades mecánicas, lo posiciona como una opción idónea para la fabricación de grandes componentes, manteniendo una relación coste-propiedades mecánicas altamente competitiva. Estas características, junto con su potencial de integración en la industria, lo convierten en un candidato ideal para el desarrollo de esta tesis, enfocada en la implementación sostenible de la tecnología aditiva WAAM aplicada a la fabricación de utillajes y estructuras.

Diseño

Los procesos de fabricación aditiva permiten la producción de estructuras complejas imposibles de fabricar por métodos de fabricación convencionales. La introducción de estas tecnologías aditivas metálicas en los sectores industriales requiere la reevaluación de los conceptos de diseño utilizados hasta el momento. Estas nociones están adaptadas, y por tanto restringidas, a los métodos de producción convencionales, y deben adecuarse a las nuevas posibilidades de la tecnología aditiva, y a su vez tomar en consideración sus restricciones.

La tecnología de fabricación WAAM es un proceso es relativamente joven y, por lo tanto, no está desarrollado al mismo nivel que los sistemas de fabricación convencionales. Un punto delicado a tener en cuenta es la limitada calidad de las superficies impresas, lo que hace indispensable un postprocesado de las superficies con requisitos de acabado de precisión [74]. La consecuencia de estas circunstancias es la necesidad de diseñar un CAD (diseño asistido por ordenador) específico para fabricación aditiva debido a la necesidad de eliminar material para conseguir una pieza final de alta calidad. Un ejemplo de fabricación WAAM donde se visualiza el resultado del proceso de mecanizado posterior es la Ilustración 11. Este CAD específico se denomina CAD adaptado al proceso WAAM. En este CAD se debe tener un sobre-espesor de diseño en la superficie exterior, que luego se mecanizará. El criterio de sobre-espesor requerido para cumplir con las especificaciones de acabado varía en función del autor, el proceso de soldadura WAAM empleado y el material utilizado. No obstante, una cifra de referencia ampliamente aceptada es un excedente de 10 mm [75–77]. Este sobre-espesor también sirve como elemento de seguridad en caso de fallo del proceso de impresión.

Ilustración 11 Construcción WAAM tras primera etapa de postprocesado

Cabe resaltar que el proceso WAAM requiere de una base metálica sobre la que poder depositar las primeras rutas de soldadura aditiva. Por ello, se debe tener en cuenta si esta base metálica forma parte de la pieza final, y, en el caso de no ser así, se deberán considerar en la etapa de diseño varias capas de sacrificio, que ayudarán a la eliminación de esta base mediante su corte. Las características mencionadas en este párrafo se muestran en la Ilustración 12.

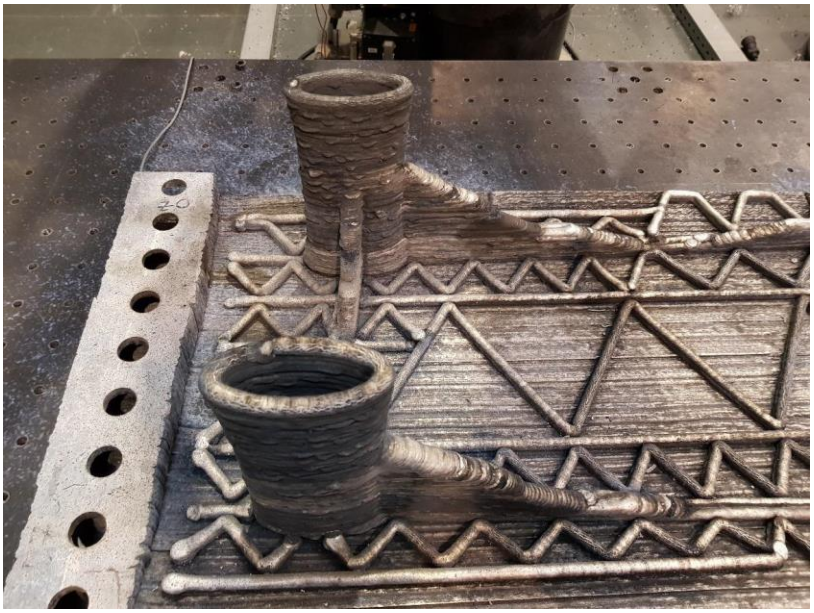

Ilustración 12 Proceso aditivo WAAM aplicado sobre base metálica

Otra circunstancia que debe tenerse en cuenta durante la fase de diseño es la temperatura de proceso del sistema WAAM. Durante este proceso aditivo, el material alcanza temperaturas de hasta 450°C, dilatando la geometría. Para compensar esta dilatación, la pieza se diseña teniendo en cuenta esta contracción, de forma que el utillaje en frío cumpla con la geometría objetivo. Este aumento de la temperatura puede resultar problemático, ya que su acumulación a lo largo del proceso crea zonas puntuales donde los cordones de soldadura no alcanzan la altura adecuada, debido a que requieren un mayor tiempo de solidificación [78]. Esos puntos calientes deben ser evitados durante el ruteo del proceso aditivo, implementando rutas de impresión que eviten concentraciones de puntos en zonas concretas.

A diferencia de otras tecnologías de AM, el proceso WAAM se realiza sin ninguna estructura de soporte adicional. En consecuencia, las construcciones sin soporte realizadas mediante este método de impresión pueden sufrir errores de precisión o incluso desprendimiento de material en zonas donde los ángulos de los voladizos son demasiado elevados [79–81]. En este sentido, los estudios realizados por Liu et al. [82] demostraron que las paredes delgadas de construcción con una inclinación teórica de 25º presentaban un error de hasta el 6%. Esta característica se muestra en la Ilustración 13. Como en el caso del sobre-espesor de diseño, el CAD adaptado al proceso WAAM debe tener en cuenta estas características. Esta restricción también aplica a ciertas características constructivas, como roscas o pequeños agujeros que deben ser fabricados en la segunda etapa de postprocesado, como se esquematiza en la Ilustración 13.

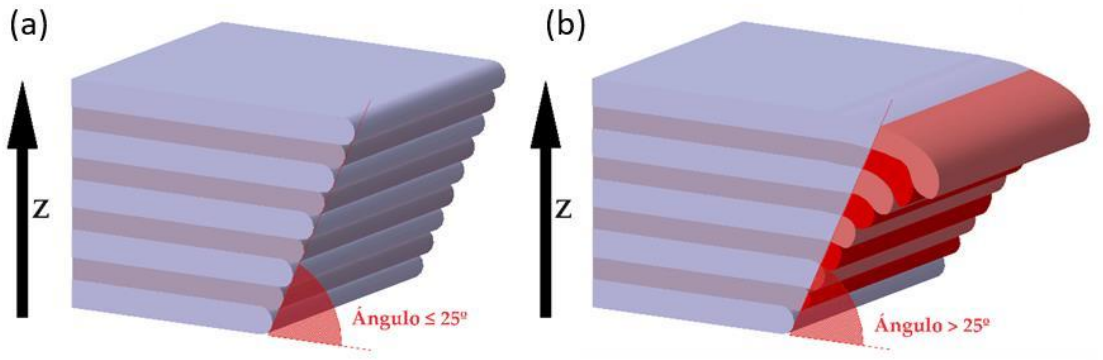

Ilustración 13 Esquema de diseño WAAM. Definición de diseño con restricción de ángulo de voladizo. (a) Construcción correcta (ángulo de voladizo ≤ 25º). (b) Construcción incorrecta, con desplome (en rojo) (ángulo de voladizo > 25º)

Teniendo en cuenta las limitaciones de diseño presentadas para la fabricación de aberturas o vanos en la dirección Z de la estructura, estos conceptos deben adaptarse al proceso de fabricación. La tecnología de fabricación WAAM es capaz de la fabricación de estos diseños con vaciados en la estructura, sin embargo, el diseño de éstos debe realizarse con un cierre progresivo, respetando el ángulo de desplome máximo. Esta estructura con formato de gota de agua, como se muestra en la Ilustración 14, podrá utilizarse para la fabricación de complejos vaciados internos, que podrían tener como objetivo la reducción del peso de la pieza final.

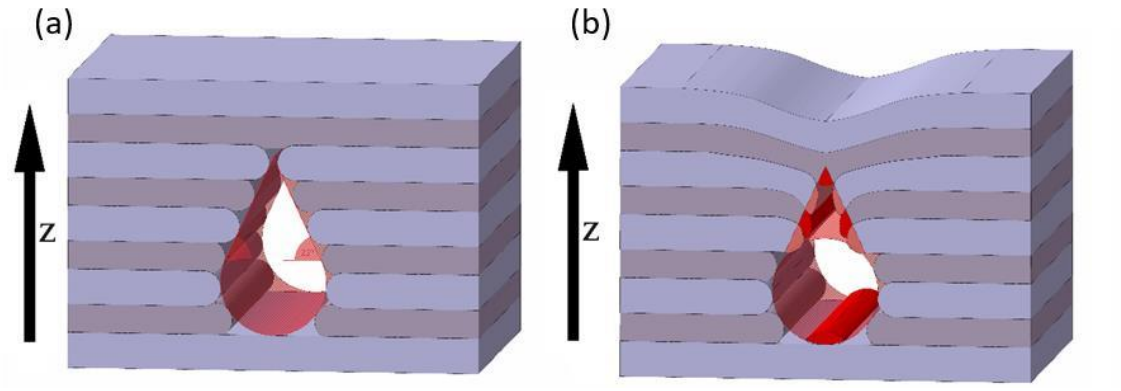

Ilustración 14 Esquema de diseño WAAM. Concepto de diseño de aberturas. (a) Construcción WAAM adaptada (ángulo de voladizo ≤ 25º, estructura de gota de agua). (b) Construcción incorrecta, sin diseño interno adaptado (desplome en rojo)

Respecto a la reducción de material en diseños concretos, la flexibilidad de diseño del proceso WAAM permite concebir diseños donde se optimiza al máximo la cantidad de material utilizado. Por ello, se pueden crear modelar elementos con características específicas que maximizan la eficiencia del material empleado, que serían inviables de mecanizar mediante métodos de fabricación convencionales debido a que el costo asociado a la ejecución de los vaciados propuestos resultaría desproporcionado en relación con los beneficios obtenidos.

Otro caso concreto que optimiza las capacidades de la fabricación WAAM es la fabricación de canales internos. Estos canales pueden utilizarse como sistemas de calentamiento y/o refrigeración, y se utilizan en moldes para procesos como la inyección de plástico o el *hot-forming*. El diseño de los canales térmicos del utillaje WAAM puede optimizarse para adecuarse a la geometría de la pieza, optimizando la transferencia de temperatura. Este concepto de diseño se denomina *Conformal Cooling* (CC) [83–86], y permite reducir tiempos de ciclo en el proceso industrial subsecuente [87], además de optimizar la distribución de calor a lo largo de la pieza. La distribución de la temperatura en el molde y su velocidad de enfriamiento son fundamentales para la calidad de la pieza inyectada. Un enfriamiento insuficiente o no uniforme puede afectar a la geometría de la pieza, encogiéndola o deformándola en el caso de los procesos de inyección [88,89]. En estos procesos, además, una distribución no uniforme de la temperatura también puede causar efectos indeseables en la pieza, que pueden observarse en su acabado superficial (como zonas de acabado superficial pobre o la aparición de zonas brillantes) [90].

Sostenibilidad

Como se ha mencionado anteriormente, los procesos de fabricación aditiva destacan por su elevada capacidad para maximizar la eficiencia en el uso de material necesario en la producción de una pieza final. Además, al emplear únicamente la cantidad mínima de material necesaria, se logra reducir significativamente el consumo energético asociado al proceso de fabricación. En consecuencia, el proceso de fabricación aditiva WAAM se

posiciona como una alternativa prometedora para lograr una disminución tanto en el consumo energético como en el uso de material, en comparación con los productos fabricados mediante métodos convencionales.

Consumo de material

La reducción de consumo de material se debe tanto a los requerimientos específicos de fabricación como a las posibilidades de diseño desarrolladas en el apartado Diseño. Su principal bondad es la fabricación de estructuras *Near to Net Shape*, en la que la pieza resultado dista poco de la pieza final, que alcanzará tras la segunda fase de postprocesado requerida en las superficies con requerimientos de acabado. Esta característica, sumada a la posibilidad de creación de estructuras complejas, con vaciados de material no realizables mediante métodos de fabricación convencionales, permite reducir el material utilizado al mínimo [91,92]. Por ello, una vez optimizado al máximo el diseño de la pieza, el parámetro más influyente en el consumo de material del proceso WAAM es el sobre-espesor de impresión.

Como se ha mencionado, el sobre-espesor es un parámetro de seguridad que genera un grosor de pared extra, que será eliminado posteriormente. Este criterio genera suficiente material para garantizar su eliminación en la segunda fase de mecanizado, permitiendo conseguir superficies que alcancen los requerimientos de acabado necesarios. Además, elimina errores de falta de material producibles debido a la naturaleza del proceso, como falta de material en interfases de cordones o sobre-calentamiento.

En la tecnología WAAM, la optimización del sobre-espesor de diseño se posiciona como uno de los objetivos prioritarios para investigaciones futuras. Su reducción podría traducir en una disminución significativa del consumo de material y una disminución significativa del consumo energético durante la impresión y el mecanizado necesario para eliminar dicho excedente

Consumo eléctrico

El caso específico del consumo eléctrico mantiene similitudes con lo expuesto en cuanto a consumo de material. El parámetro de sobre-espesor puede suponer una diferencia en el consumo final de fabricación, al conllevar inevitablemente un aumento del tiempo de proceso de impresión. Sin embargo, su valor es despreciable respecto al consumo global de un proceso WAAM de grandes dimensiones.

El consumo eléctrico total de un proceso WAAM por tanto es, al igual que en el caso del consumo de material, dependiente de la geometría impresa y del equipo de utilizado. El sistema WAAM requiere de un equipo de soldadura y un sistema motriz para este, que puede ser desde un sistema simple de 3 ejes hasta robots colaborativos de 6 ejes. Por ello, la asunción de un valor de consumo eléctrico del proceso no puede ser universalizada.

Según la bibliografía consultada [93,94], el proceso de desbaste presenta un mayor consumo energético debido a la considerable cantidad de material eliminado y a las elevadas fuerzas de corte que este requiere. En contraste, el proceso de acabado implica un consumo energético significativamente inferior, ya que se centra en la eliminación mínima de material necesaria para alcanzar la precisión dimensional y la calidad superficial deseadas.

Un análisis detallado del consumo energético en el fresado [95] revela que los parámetros de corte, como la velocidad de avance y la profundidad de corte, influyen directamente en la energía utilizada. Durante el desbaste, el objetivo es maximizar la productividad, lo que resulta en un mayor consumo eléctrico. Por otro lado, el acabado se enfoca en la precisión, reduciendo la demanda energética al minimizar las fuerzas de corte y la vibración de la herramienta.

Debido a la cualidad de la fabricación aditiva WAAM de fabricar piezas bajo el concepto *Near to Net Shape*, los resultados impresos no requieren de procesos de desbaste. Al necesitar solo de procesos de acabado, el consumo eléctrico total se reduce al proceso de acabado, menos exigente en cuanto a consumo eléctrico. Además, únicamente las áreas que exigen un acabado específico deben ser sometidas a postprocesado, lo que permite disminuir la extensión total de las superficies a mecanizar o, en ciertos casos, prescindir completamente del mecanizado, eliminando así este consumo energético del balance total del proceso. Por consiguiente, es posible concluir que los componentes producidos mediante el proceso WAAM tienen el potencial de disminuir el consumo energético en comparación con los métodos de fabricación convencionales.

Por ello, la tecnología aditiva WAAM se posiciona como una realidad sostenible en la fabricación de grandes estructuras metálicas [96,97], siendo sus principales fortalezas la disminución de material consumido durante la fabricación, el ahorro energético asociado a la eliminación del proceso de fresado desbaste durante su fase de mecanizado y la significativa reducción de residuos generados como resultado de estas dos condiciones.

Aplicaciones

Las aplicaciones del proceso de fabricación aditiva WAAM han sido mencionadas de manera tangencial a lo largo del Estado del Arte. Es importante destacar que, aunque esta tecnología es adaptable a diseños de cualquier tamaño alcanzable por el sistema de movimiento en el cual se instale y nivel de complejidad, su mayor potencial se encuentra en la fabricación de piezas o estructuras metálicas de grandes dimensiones con geometrías complejas.

En este contexto, el proceso WAAM alcanza su máxima eficacia al permitir la producción de estructuras que no pueden ser obtenidas mediante métodos convencionales de fabricación. Ejemplos de estos conceptos incluyen vaciados internos, diseños autoreforzados y sistemas de conductos para refrigeración. La capacidad de generar piezas

cercanas a la forma final (*Near to Net Shape*) no solo posibilita una significativa reducción del peso en los productos finales, sino que, desde una perspectiva de sostenibilidad, optimiza el consumo de material y minimiza las áreas requeridas para el mecanizado en procesos de postprocesado. Esto se traduce en una notable disminución tanto del consumo de material como del gasto energético asociado.

Entre los sectores industriales que más se benefician de las ventajas de este proceso destacan la industria dedicada a la fabricación de moldes y la industria de la construcción, donde estas capacidades pueden ser aprovechadas de manera óptima.

Industria de la fabricación de moldes

La industria de fabricación de moldes puede clasificarse según los procesos específicos para los cuales están diseñados los moldes. Sin embargo, de manera general, estos requieren propiedades mecánicas excepcionalmente altas debido a las exigencias de los procesos industriales a los que están destinados. Además, al tratarse comúnmente de aplicaciones orientadas a la producción de grandes lotes, los moldes deben soportar ciclos de fabricación extremadamente cortos. En este contexto, las aplicaciones de la tecnología WAAM destacan como particularmente adecuadas.

En primer lugar, la capacidad de WAAM para fabricar diseños complejos permite optimizar el peso de los moldes sin comprometer sus propiedades mecánicas. Esta optimización generalmente se traduce en una reducción significativa del peso del molde, lo que disminuye su inercia térmica [98] y, a su vez, permite acortar los tiempos de ciclo [99,100].

Además, la capacidad del proceso WAAM para incorporar conductos internos personalizados, adaptados a la geometría de la pieza final, ha sido discutida previamente en el apartado de diseño. Este enfoque, conocido como *Conformal Cooling*, facilita la reducción de los ciclos térmicos y permite una distribución precisa y uniforme de la temperatura a lo largo de la estructura del molde [101,102]. Como resultado, se logra una homogeneización de la temperatura durante el proceso, reduciendo el riesgo de deformaciones en las piezas fabricadas. Este concepto de diseño ha sido testeado hasta la fecha en utillajes de pequeño tamaño (100x100x100 mm), con resultados prometedores [103], y su escalado presenta un desafío por las limitaciones de las soluciones de fabricación aditiva actuales.

Estas características hacen que la tecnología de fabricación aditiva WAAM sea especialmente adecuada para su aplicación en la industria de fabricación de moldes. No obstante, es necesario realizar investigaciones más exhaustivas para validar el rendimiento de los moldes tras múltiples ciclos de fabricación, especialmente en procesos con altos requerimientos mecánicos, como los asociados a la inyección de plásticos. Además, la principal limitación encontrada para la implementación de tecnologías aditivas en la industria es la restricción dimensional encontrada en los sistemas actuales. El proceso WAAM, al ser un proceso cuyas restricciones dimensionales son dependientes del sistema de movimiento planteado, puede suplir esta problemática.

Industria de la construcción

Los avances en programas informáticos de diseño asistido por ordenador (CAD), modelado tridimensional y métodos de fabricación digital han abierto posibilidades para explorar formas estructurales complejas e innovadoras, como diseños de forma libre, cáscaras, o estructuras reticulares [104,105]. El uso de estas herramientas de software ha permitido a los diseñadores emplear métodos computacionales en la exploración de nuevas soluciones estructurales [106]. Sin embargo, los métodos de fabricación convencionales no siempre son capaces de realizar de manera óptima los diseños conceptualizados, por lo que la fabricación aditiva se erige como una solución. Específicamente, la tecnología WAAM muestra un alto potencial para aplicaciones de ingeniería estructural. Esta tecnología ofrece la libertad de diseño y la capacidad de reforzar componentes requerida para la implementación de estas soluciones. El ejemplo más reconocible de la utilización de la tecnología WAAM en construcción es la construcción del puente de MX3D en Ámsterdam [107].

Como en el caso de la fabricación de moldes, la principal barrera para la completa adopción de los procesos de fabricación aditiva convencionales en la industria radica en la limitación del tamaño de las piezas que pueden producirse. En este contexto, la tecnología WAAM se perfila como una solución viable, ya que permite la fabricación de componentes de acero, ampliamente empleado en el sector de la construcción, sin restricciones de dimensiones y con propiedades mecánicas satisfactorias. Asimismo, como se ha descrito previamente, este proceso es apto para la creación de estructuras complejas, diseñadas mediante herramientas avanzadas de software.

Capítulo 3

Resultados y trabajos realizados

Este capítulo se organiza en dos secciones principales. La primera aborda los nexos de unión y las interrelaciones entre las distintas investigaciones realizadas, con el objetivo común de trazar y demostrar el potencial de la integración de la tecnología WAAM en un entorno industrial para la fabricación de estructuras intermedias y finales. Se hace especial énfasis en las ventajas que esta tecnología ofrece en términos de eficiencia del proceso y sostenibilidad, vinculando así el propósito de cada trabajo con el marco global de la investigación.

La segunda sección presenta cada uno de estos trabajos de manera individual. La organización de los artículos no seguirá un esquema estrictamente lineal en el tiempo, dado que, en algunos casos, la fecha de publicación no coincide con el orden cronológico del desarrollo de la investigación. Además, se incluye un breve resumen en castellano de cada trabajo, destacando las ideas principales y los resultados más relevantes obtenidos en cada caso.

Finalmente, el capítulo recopila algunos de los proyectos y actividades en los que el doctorando ha participado durante este periodo, remarcando el carácter industrial en el que se ha enmarcado esta investigación. Estas experiencias han sido fundamentales para el desarrollo de las investigaciones incluidas en la tesis, así como de otras iniciativas en un entorno multidisciplinar e internacional. Este apartado resalta el carácter colaborativo de los estudios realizados y refleja el conocimiento integral del doctorando sobre los aspectos clave de una investigación: desde la conceptualización de la idea hasta la obtención de conclusiones, pasando por su ejecución y la difusión de los resultados obtenidos.

Justificación de la unidad temática & Presentación de los trabajos

Desarrollo del esquema de toma de decisiones

Siguiendo el esquema de toma de decisiones presentado en la introducción, se realizó una investigación inicial para identificar la tecnología aditiva más adecuada para alcanzar el objetivo planteado: implementar industrialmente un proceso de fabricación aditiva de gran escala. Por ello, se partió de la Ilustración 2 para la selección de la tecnología aditiva sobre la que se realizó el estudio.

El enfoque inicial del análisis se centró en tres grandes grupos de materiales de aporte: termoplásticos, metálicos y cerámicos. Los materiales termoplásticos fueron descartados debido a sus propiedades mecánicas medias/bajas, insuficientes para cumplir los altos requerimientos mecánicos de industrias como la construcción o la industria del moldeo. En contraste, los materiales metálicos y cerámicos presentan propiedades mecánicas medias y altas, aunque los cerámicos enfrentan limitaciones como su alta fragilidad, una característica que, dependiendo la aplicación específica, podría considerarse asumible.

La elección del proceso aditivo está directamente relacionada con el material de aporte. Tanto para materiales cerámicos como metálicos, las principales tecnologías disponibles son la fabricación aditiva por cama de polvo, la fabricación aditiva por cama de polvo con aglutinante y la aportación de hilo.

Las tecnologías basadas en cama de polvo (incluyendo las basadas en cama de polvo más aglutinante), aunque ofrecen importantes ventajas en diseño y sostenibilidad, presentan una baja velocidad de fabricación, debido a su limitada capacidad de aporte de material por capa. Esto las hace no competitivas para aplicaciones industriales que requieren tiempos de producción reducidos. Por esta razón, se descartaron como opción viable.

En contraste, las tecnologías de aportación de hilo destacan por su alta tasa de aporte de material, lo que permite fabricar estructuras de gran tamaño en tiempos más reducidos. Si bien estas tecnologías pueden producir superficies finales de menor calidad, este aspecto no es determinante, dado que todos los procesos aditivos analizados requieren una etapa posterior de mecanizado para alcanzar los estándares de acabado superficial requeridos.

Finalmente, se evaluó la capacidad para fabricar piezas de gran tamaño, un requerimiento esencial para aplicaciones industriales. En este aspecto, la tecnología GMAW metálica de aporte de hilo sobresalió frente a su contraparte cerámica, al estar basada en un proceso industrialmente maduro, como la soldadura. Debido a ello, ofrece mayores posibilidades dimensionales en comparación con las impresoras 3D cerámicas de mayor tamaño disponibles en el mercado.

Considerando las especificaciones iniciales, como propiedades mecánicas elevadas, alta capacidad de aporte de material y la posibilidad de fabricar piezas de gran escala, se

seleccionó la tecnología aditiva GMAW para este estudio, específicamente en su variante WAAM, derivada de GMAW. Esta elección cumple con los requisitos de integración industrial y asegura la viabilidad del proceso para los objetivos establecidos en la tesis. El desarrollo de esta toma de decisiones ha sido plasmado en la Ilustración 15.

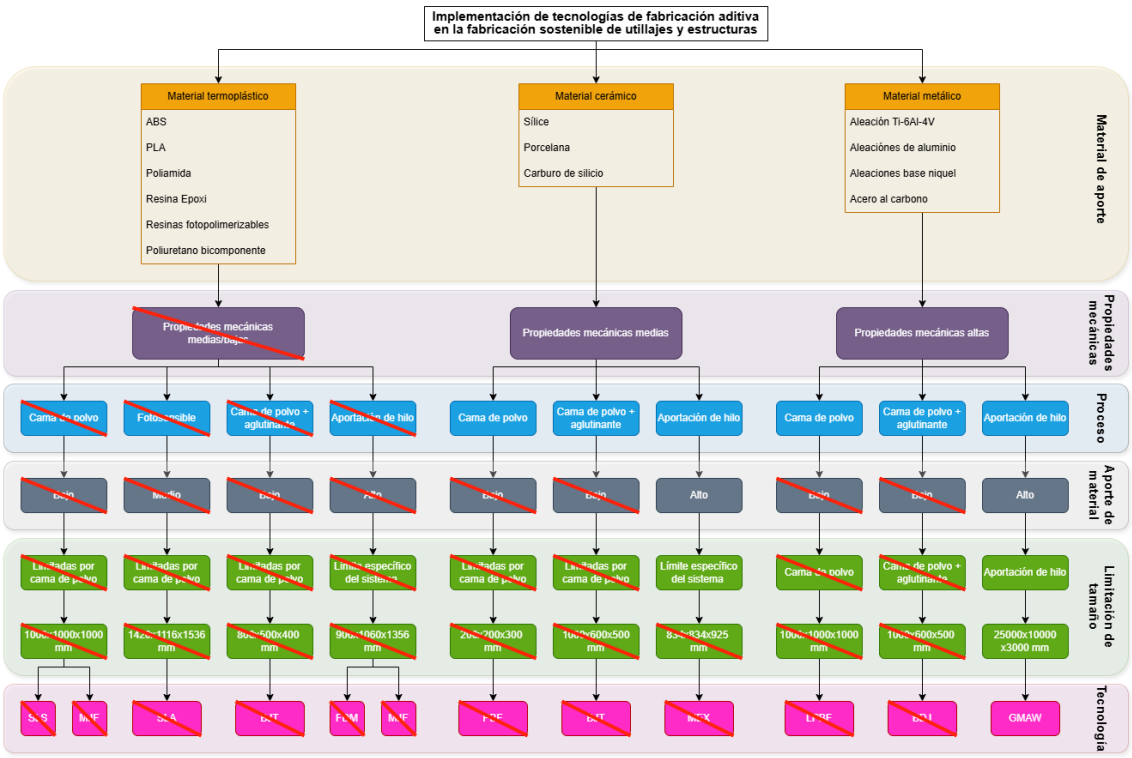

Ilustración 15 Esquema de toma de decisiones final

Hilo conductor de la investigación

La investigación consolidada en el marco de esta tesis doctoral ha tenido como propósito validar la viabilidad de la tecnología aditiva WAAM para la fabricación de piezas intermedias y finales de gran tamaño, promoviendo su integración en el entorno industrial como una solución sostenible frente a desafíos de diseño complejos. Como se ha detallado previamente, la tecnología WAAM ofrece una amplia gama de materiales de aporte; en este estudio, se ha elegido el acero al carbono debido a sus destacadas propiedades mecánicas y su extendida aplicación en la industria.

En este marco, el doctorando ha diseñado una estrategia que cubre todas las fases esenciales del proceso, desde la conceptualización hasta la validación final, plasmada en el desarrollo de cuatro artículos científicos que detallan exhaustivamente el ciclo completo de esta tecnología.

Como punto de partida de la fabricación de piezas y estructuras industriales, se realizó la fabricación de un molde de *press-forming* mediante proceso aditivo WAAM, a la vez que un molde simétrico realizado por técnicas de fabricación convencionales. En este

primer paso del estudio se evaluó la posibilidad de la fabricación aditiva WAAM en elementos de grandes dimensiones, al tratarse de un molde metálico de dimensiones 500x450x150 mm aproximadamente. El molde WAAM fabricado fue diseñado y optimizado para adecuarse al proceso de fabricación aditiva.

El éxito en la fabricación del utillaje WAAM sentó las bases de los procesos de fabricación posteriores. Durante el proceso de fabricación, los datos recopilados evidenciaron una notable reducción tanto en el consumo eléctrico como en el uso de material en el proceso WAAM en comparación con los métodos de fabricación convencionales. Adicionalmente, un análisis metrológico realizado sobre la pieza WAAM antes de su mecanizado permitió identificar oportunidades para optimizar aún más el proceso. Estas optimizaciones lograron disminuir adicionalmente el consumo de recursos, consolidando así la sostenibilidad del proceso demostrada en este primer caso de estudio.

Para la completa validación del proceso WAAM en la fabricación de piezas industriales, se testeó el utillaje fabricado junto con su análogo realizado por procesos convencionales para el proceso *press-forming*. Los resultados obtenidos demostraron un desempeño satisfactorio, confirmando la viabilidad de implementar el proceso WAAM en aplicaciones industriales.

Partiendo de la verificación del proceso WAAM alcanzada, y con el objetivo de aprovechar las capacidades de diseño de elementos complejos, se propuso la fabricación de un nuevo molde de grandes dimensiones. En este caso, se trató de un molde de inyección, con el objetivo de verificar el proceso de fabricación WAAM en una diversidad de procesos industriales.

Este molde fue fabricado según el concepto de *Conformal Cooling*, definido anteriormente, de manera que se optimiza teóricamente el ciclo de refrigeración de dicho molde. El diseño complejo WAAM fue analizado contra con un molde análogo teórico, diseñado para su fabricación por métodos de fabricación convencionales. Los resultados mostraron una reducción del tiempo de ciclo y una mayor homogeneidad de extracción de calor para el molde WAAM. La fabricación satisfactoria de este molde fue monitorizada, permitiendo el análisis del consumo de material, utilizado para el estudio de la sostenibilidad del proceso.

Tras la demostración de la capacidad de fabricación de utillajes complejos para diferentes procesos de moldeo, se enfocó el estudio en la fabricación de elementos finales. Por ello, se decidió optar por la industria de la construcción para cerrar el ciclo de estudios de la implementación del proceso WAAM.

Para la demostración de la implementación de la tecnología WAAM en esta industria, se adoptó un enfoque alternativo. En este caso, se diseñaron estructuras tipo columna con configuraciones auto-reforzadas de diseño tipo “sándwich”, aprovechando las capacidades del proceso WAAM para desarrollar un catálogo de estructuras adaptadas a los

parámetros de diseño requeridos. Estos parámetros, optimizados mediante simulaciones computacionales para satisfacer exigencias estructurales específicas, son el diámetro exterior (D_{ext}), el diámetro interior (D_{int}), el número de refuerzos (N_w) y el espesor de pared (t).

Esta optimización permitió obtener secciones transversales compactas, ideales cuando se prioriza una alta ductilidad frente a fuerzas axiales y momentos de flexión, incluso si ello implica sacrificar cierta eficiencia en el uso del material. Por otro lado, se identificaron secciones transversales esbeltas como opciones más adecuadas para estructuras que buscan maximizar la eficiencia en el uso de recursos. Estas variaciones pueden apreciarse en la Ilustración 16. La viabilidad de este enfoque fue validada mediante la fabricación de demostradores representativos del catálogo propuesto.

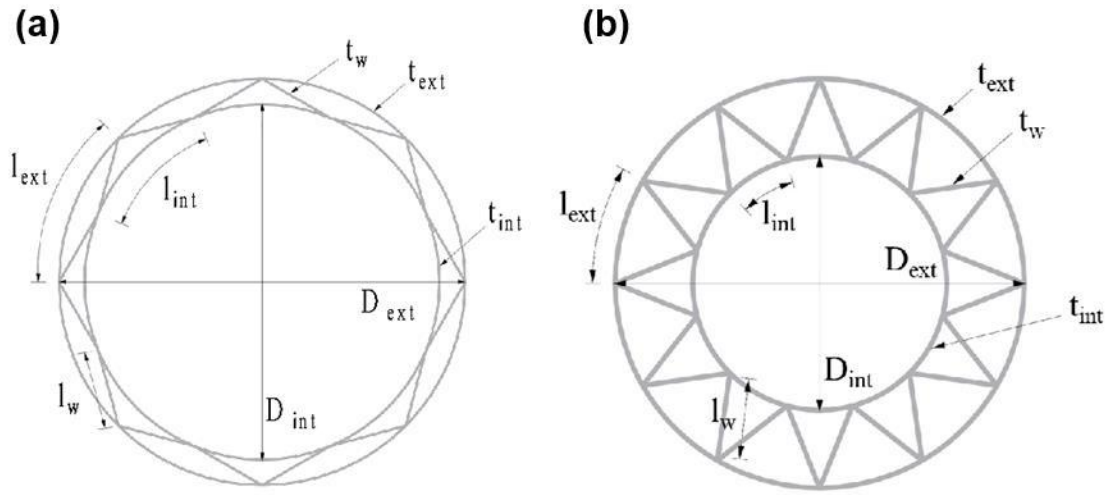

Ilustración 16 Estructuras tubulares auto-reforzadas esbelta (a) y compacta (b)

Por último, en base a los desarrollos realizados en la fabricación de estructuras auto-reforzadas, un demostrador final estructural para aplicaciones marítimas de elevadas presiones radiales fue analizado. Este diseño mostró un desempeño significativamente superior a las estructuras comerciales actuales, consolidando el potencial de la tecnología WAAM en aplicaciones estructurales avanzadas.

Artículos publicados para el compendio

Artículo 1

Analysis of Energy and Material Consumption for the Manufacturing of an Aeronautical Tooling: An Experimental Comparison between Pure Machining and Big Area Additive Manufacturing

Alejandro Marqués, Jose Antonio Dieste, Iván Monzón, Alberto Laguía, Carlos Javierre y Daniel Elduque. (2024).

Materials, 17, 3066

DOI: 10.3390/ma17133066

Impact Factor: 3.100 (JCR 2023); Q1 Materials science and engineering.

Este artículo aborda la fabricación de dos utillajes gemelos de gran tamaño destinados al proceso de press-forming. Uno de ellos fue producido mediante métodos convencionales de fabricación, mientras que el otro fue desarrollado utilizando tecnología aditiva WAAM. En ambos casos, el diseño de los utillajes fue adaptado a las particularidades de la tecnología empleada, y se llevó a cabo un monitoreo exhaustivo durante el proceso de fabricación.

En primer lugar, se realizó un análisis comparativo de los diseños, destacando las especificaciones técnicas asociadas a cada método. Este análisis enfatizó la reducción de peso lograda en el utillaje fabricado mediante tecnología WAAM, así como la inclusión de canales térmicos adaptativos, posible gracias a la capacidad de esta tecnología para fabricar diseños complejos.

A continuación, se evaluaron los consumos de material y energía eléctrica involucrados en la fabricación de ambos utillajes. En el caso de WAAM, se demostró su capacidad para producir piezas Near Net Shape, lo que resultó en una reducción significativa del consumo de material en comparación con los métodos tradicionales. Respecto al consumo eléctrico, el análisis consideró no solo la fase de fabricación aditiva, sino también el posterior mecanizado CNC necesario para el acabado. Los resultados indicaron un ahorro energético significativo en el proceso aditivo frente al convencional. Los resultados obtenidos evidenciaron una mejora significativa en la sostenibilidad del utillaje fabricado mediante tecnología WAAM en comparación con el método tradicional.

Finalmente, se realizó un análisis detallado de los parámetros de diseño y fabricación del utillaje WAAM. A través de un estudio metrológico, se evaluó la correlación entre el modelo CAD adaptado al proceso WAAM, que incorpora un sobre-espesor de diseño, y la pieza impresa final. Este análisis permitió explorar la posibilidad de reducir el sobre-espesor de diseño, determinar su valor mínimo y cuantificar el ahorro de material que esta optimización representaría.

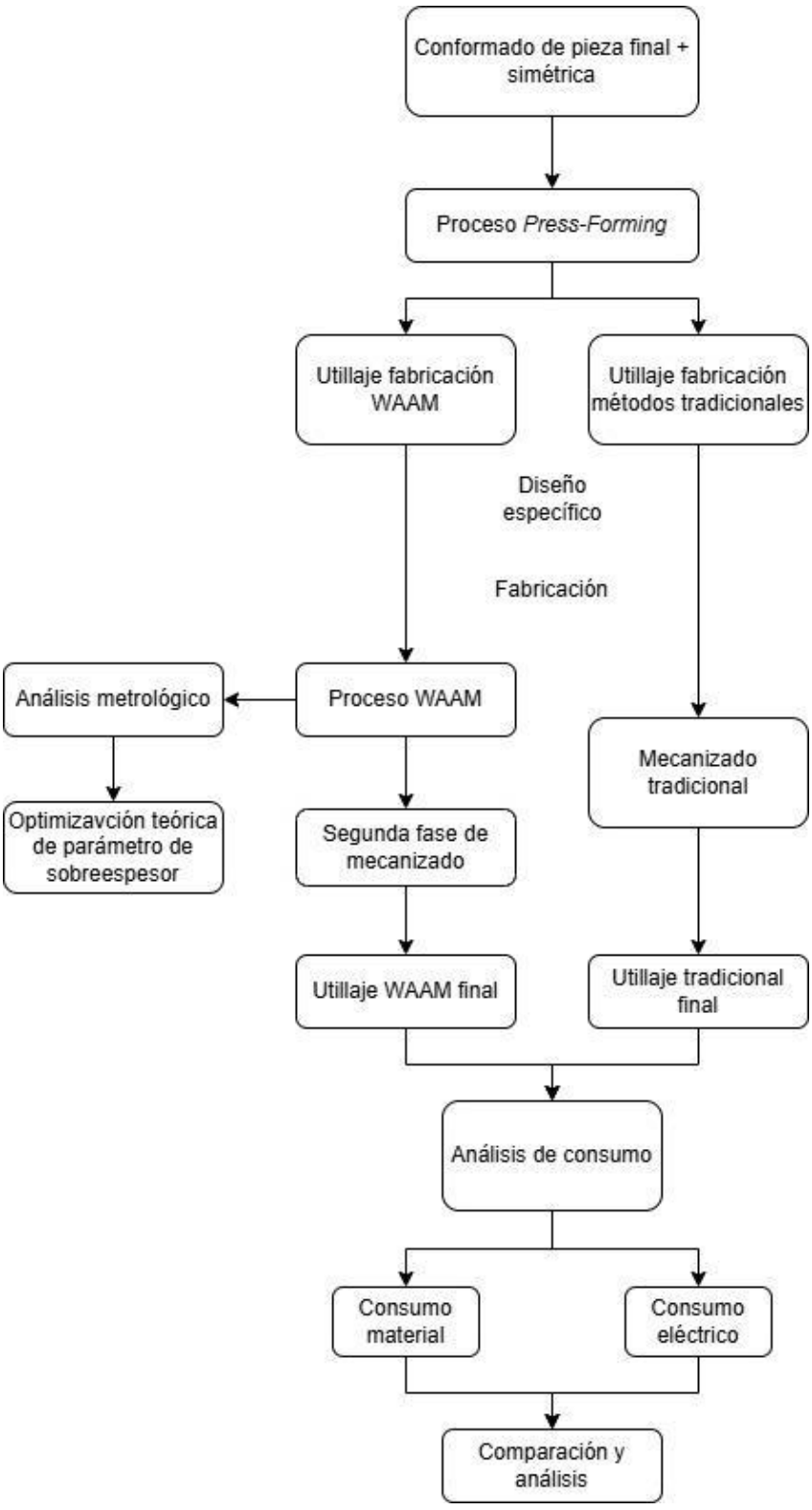

Ilustración 17 Esquema de los trabajos realizados en el artículo 1 para el análisis y optimización d la fabricación aditiva WAAM en utillaje de grandes dimensiones

materials

MDPI

Article

Analysis of Energy and Material Consumption for the Manufacturing of an Aeronautical Tooling: An Experimental Comparison between Pure Machining and Big Area Additive Manufacturing

Alejandro Marqués [1,*], Jose Antonio Dieste [1], Iván Monzón [1], Alberto Laguía [1], Carlos Javierre [2] and Daniel Elduque [2]

[1] R&D Department, Fundación Aitiip, Polígono Industrial Empresarium, C/Romero, No. 12, 50720 Zaragoza, Spain; joseantonio.dieste@aitiip.com (J.A.D.); ivan.monzon@aitiip.com (I.M.); alberto.laguia@aitiip.com (A.L.)
[2] Department of Mechanical Engineering, University of Zaragoza, C/María de Luna, 50720 Zaragoza, Spain; carlos.javierre@unizar.es (C.J.); delduque@unizar.es (D.E.)
* Correspondence: alejandro.marques@aitiip.com

Abstract: Additive manufacturing (AM) has been fully incorporated into both the academic and the industrial world. This technology has been shown to lower costs and environmental impacts. Moreover, AM-based technologies, such as wire arc additive manufacturing (WAAM), have been proven suitable for the manufacturing of large products with significant mechanical requirements. This study examines the manufacture of two aeronautical toolings: first, using conventional techniques, and second, using a big area additive manufacturing (BAAM) process, specifically WAAM technology, followed by second-stage hybrid machining. Both toolings can be considered interchangeable in terms of design and performance. Energy and material consumption were analysed and compared throughout both tooling procedures. The results show the important optimisation of both procedures in manufacturing WAAM tooling, encompassing the additive process and second-stage hybrid machining. Nevertheless, the time required for WAAM tooling manufacturing increased significantly compared to conventional manufacturing tooling. Moreover, based on metrology data from the AM process, a theoretical study was conducted to assess different design optimisations for WAAM tooling manufacturing and determine their influence on material and energy consumption. These theoretical results improve those already obtained regarding energy and raw material savings.

Keywords: additive manufacturing; big area additive manufacturing; energy consumption; material consumption; wire arc additive manufacturing; aeronautical tooling

Citation: Marqués, A.; Dieste, J.A.; Monzón, I.; Laguía, A.; Javierre, C.; Elduque, D. Analysis of Energy and Material Consumption for the Manufacturing of an Aeronautical Tooling: An Experimental Comparison between Pure Machining and Big Area Additive Manufacturing. *Materials* **2024**, *17*, 3066. https://doi.org/10.3390/ma17133066

Academic Editor: Guozheng Quan

Received: 14 May 2024
Revised: 4 June 2024
Accepted: 9 June 2024
Published: 21 June 2024

1. Introduction

Due to the material and energy crisis [1,2] and following the environmental awareness trend of the last few years [3–7], additive manufacturing (AM) has been gaining relevance in the industrial environment. In this vein, the *Annual Additive Manufacturing Trend Report* produced by HUBS, which looks at the international trends and uses for AM based on responses from 1504 engineering businesses, shows a significant increase in the use of AM technologies in the past year. It also highlights the increased media exposure of these technologies since the COVID-19 pandemic, as the ability to create PPE (Personal Protective Equipment) rapidly made the technology very popular [8]. Moreover, this technology has already proven its ability to be fully implemented in the industry [9–11], being used to manufacture functional metallic parts and entering an increasing number of industrial fields, such as nuclear [12,13], construction [14,15], railway [16], and military applications [17]. Its capacity to create complex geometries and maintain good mechanical properties [18–21] while potentially saving materials and energy compared to conventional manufacturing

strategies [22–24] has made it a widely researched technology. In engineering, we highlight the procedure known as BAAM (big area additive manufacturing), which is nothing more than a dimensional specification of the AM process. The term BAAM encompasses additive manufacturing machines capable of working in larger dimensions than those limited by standard 3D printers, being able to reach printed volumes of several cubic metres [25–29].

As reflected in the previous paragraph, AM is a widely used manufacturing process in many industries and, in addition to the characteristics mentioned above, another of its benefits is the ability to work with various types of materials. The different printing processes encompassed by AM allow for the use of not only metallic materials [30–32] but also more complex materials, such as composites [33–36], recycled materials [37,38], and biological materials [39,40]. This article focuses on metal additive manufacturing (MAM) since its ultimate goal, as explained later, is manufacturing a functional core mould.

In order to introduce metallic additive manufacturing (MAM) technologies, two groups stand out from the rest, depending on their feeding material: powder-feed technologies and wire-feed technologies. Within these groups, the most representative AM technologies are Laser Metal Deposition (LMD) and Powder Bed Fusion (PBF) when referring to powder-feed technologies, and wire arc additive manufacturing (WAAM) when referring to wire-feed technologies.

According to ISO/ASTM 52,900:2021 [41], Powder Bed Fusion is a standard process, in which thermal energy selectively fuses regions of a powder bed [42]. This AM technology creates extremely complex geometries with a high surface finish and small details. Its main limitation is the reduced size of its printed area, limited by the printer size (400 × 400 mm in general). On the other hand, WAAM is a fusion manufacturing process, in which the heat energy of an electric arc is employed for melting the electrodes and depositing material layers for wall formation or for the simultaneous cladding of two materials to form a composite structure [43,44]. This technology creates large final geometries with low surface finish quality, demanding hybrid machining on surfaces with high geometrical demands [45]. Moreover, it is a constantly evolving technology, whose future applications in the field of metal part repair are being extensively researched [46].

Several studies have developed modelling methods comparing manufacturing processes with pure machining, studying the optimal strategy for specific part manufacturing. Several authors [47–49] introduced a decision-making model to calculate the suitability of choosing a PBF procedure versus a pure machining one. The study conducted by Campatelli et al. [50] specifically compares the WAAM-subtractive process (WAAM manufacturing with a manufactured finishing process) with a pure subtractive manufacturing process for the same final geometry, a blade designed according to the NACA 9403 standard [51], with a 100 mm chordal length and made of EN S235JR structural steel.

In this case, the WAAM method is Gas Metal Arc Welding (GMAW)-based additive manufacturing [52]. In the GMAW procedures, the heat of the arc generated between the consumable electrode and the workpiece is used to melt the surfaces of the base metal and the tip of the electrode. The molten metal from the electrode is transferred to the workpiece through the arc, where the substrate is deposited. The welding torch provides the weld with an inert-gas-protected atmosphere, wire input, and welding current [53]. This technology's main advantages are a higher deposition rate, lower equipment cost, and fewer residue issues. However, a primary concern in this technique is the deterioration of the surface quality on the side face of the fabricated parts, making it necessary to post-process surfaces that require precision finishing [54–56].

Three criteria were applied to select the most suitable MAM technology for study: the accomplishment of BAAM conditions, energy consumption, and material consumption. As mentioned before, Powder Bed Fusion technology is constrained by its printing area, limiting the possibilities of this technology. Furthermore, its low feeding rate makes this technology the least optimal to achieve BAAM constructions [57]. Within the second selected criteria, energy consumption was considered regardless of its final geometry complexity [58]. Several studies conclude that Powder Bed Fusion technologies require

an energy demand higher than one order of magnitude to accomplish the same printed geometry as WAAM technology [59].

The WAAM manufacturing process is based on the superposition of layers. Due to this feature, the lateral surfaces of these constructions show a geometry similar to the one displayed in Figure 1. For this reason, the WAAM process is considered a Near to Net Shape technology. Once the process has ended, the result obtained is not the final part but a rough previous workpiece that an NC machine should finish. Settled WAAM building parameters affect the final surface quality [60–62]; nevertheless, the study by Lopes et al. [63] shows that the mechanical behaviour of the as-built components does not significantly influence the milling process.

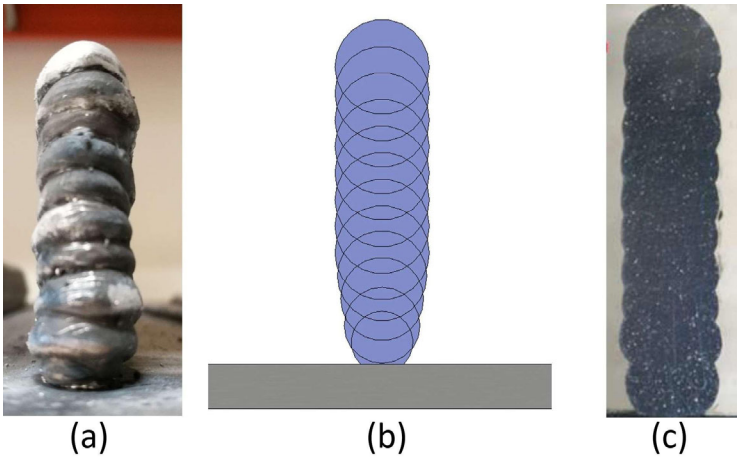

Figure 1. Overlapping weld bead structure in the WAAM process. (**a**) A photograph of the structure. (**b**) A geometric representation of the distribution of weld seams. (**c**) A photograph of a cross-section of the structure.

This uneven lateral surface results from a compromise reached by optimising the parameters of the welding temperature (dependent on electrical current) and printing speed [64]. These parameters affect the height of the weld bead and its width, which are inversely proportional.

For large constructions, a narrow weld bead is desirable, allowing high bead growth, even though it reduces the weld penetration into the bottom layer and creates the aforementioned rounded ball-shaped bead [65]. Moreover, these parameters affect the material's final properties, so their range of modification is modified based on the experience accumulated with this technology and the existing literature [66–70].

This study aims to compare a pure subtractive manufacturing process versus a whole BAAM process in the manufacturing of aeronautical tooling, focusing on energy and material consumption. For this purpose, two twin toolings were constructed, one manufactured by pure machining and the other one manufactured by a combination of WAAM technology and a second-stage machining process. Throughout both processes, energetic inputs have been controlled, both in the AM process and pure milling, as well as the total material consumed. Additionally, in this study, different WAAM design strategies have been subjected to a sensitivity analysis, comparing the different theoretical outputs obtained with those used on the real printed WAAM tooling.

2. Materials and Methods

As introduced, this article compares the energetic and material outputs obtained from two similar toolings produced from two different manufacturing methods. One was produced by conventional manufacturing methods, i.e., starting from a block of raw material and carrying out milling processes on a numerical control (NC) machine until the final geometry was obtained. On the other hand, the second tooling was produced

from scratch by an AM method, and subsequently underwent a series of milling processes in an NC machine until reaching the desired final geometry. Due to the data provided by researchers in the previous paragraphs, the WAAM process was chosen as the most optimal AM process for the selected application. Owing to the size of the final tooling (500 × 450 × 150 mm approximately), the additive manufacturing procedure is considered a BAAM process.

As mentioned in the previous section, the additive manufacturing process characteristics condition both the part's design process procedures and its subsequent construction. One of the most notable restrictions is the mentioned rounded ball-shaped bead. Its irregular geometry, which extends in all areas perpendicular to the printing direction, forces a specific printing Computer-Aided Design (CAD) architecture for the AM parts, in which an over-thickness is implemented on the outer surfaces. This specific CAD has been named the WAAM-process-adapted CAD. Moreover, to avoid problems related to small failures in the printing procedure [71–73], such as a lack of material or occasional welding errors, every surface was designed with this over-thickness during the WAAM-process-adapted CAD. This over-thickness was initially set at 10 mm. To achieve this theoretical 10 mm over-thickness, previous printing tests in the same environment were reviewed. All parameters, such as the printing strategy, weld control software, and printing materials (filler material and inert gas), were previously tested, although always on smaller constructions. These tests concluded that a safety over-thickness of 5 mm was sufficient to ensure the construction of the original geometry in small parts. However, as this construction was much larger than those carried out for the tests, and considering the investment in time and material, it was decided to increase the theoretical over-thickness. This way, the chances of a specific welding error resulting in an area lacking material were reduced, although this meant an increase in the material consumed and the printing time.

In contrast with other AM technologies, the WAAM process is performed without any extra supporting structure. Consequently, support-free constructions performed by this printing method may suffer from errors of precision or even material detachment in areas where the cantilever angles are too high [74,75]. Liu et al. [76] showed that thin walls of construction with a theoretical 25° inclination showed an error of up to 6%. As in the case of the design over-thickness, the WAAM-process-adapted CAD was designed conservatively considering, in addition to the abovementioned article, the experience gained from previous tests. Therefore, the maximum design cantilever angle was set at 20°.

Focusing on the tools to be studied, the first tooling was manufactured in a common NC machine with a pure machining method. To clearly differentiate the machining procedures applied to each tooling, this traditional machining method was named pure machining. At the same time, the twin tooling mentioned above was an AM technology-made tooling, finished by a second-stage hybrid-machining process, referred to as hybrid mechanisation in this article. The main differences in both toolings were the design specifications, in order for them to work with the respective procedure restrictions but be exchangeable during the final complete aeronautical tooling.

Referring to machining procedures, both pure and second-stage WAAM technology hybrid-machining processes were performed using a 5-Axis NC machine. The machining process executed was a milling process, and the chosen machining centre was a CME FCM 400 (Figure 2). The energetic input information for this procedure was characterised according to the measured inputs obtained in real-time.

The NC machine electric consumption, throughout both toolings' machining processes, was recorded by a Circutor C-80 system analyser [77], which displays and stores power consumption data. It should be noted that this study included a gate-to-gate analysis regarding the additive and subtractive manufacturing processes. Therefore, the energy needed to manufacture the raw block, welding wire, and shielding gas was not considered.

Figure 2. The 5-Axis NC machine, CME FCM 400. Photograph taken at the facilities of Fundación Aitiip.

On the other hand, regarding the WAAM tooling, an AM system designed to fabricate large parts was used. This system was developed in the KRAKEN project within the framework of the European Union's Horizon 2020 Research and Innovation Program under grant agreement No. 723,759 [78]. The Kraken system is based on a robotic arm (COMAU NJ130) [79] mounted on a gantry crane. This distribution removes the dimensional restrictions on the gantry crane structure, so the working space is not limited by the machine itself but to the assembly space available within the gantry crane structure. Figure 3 displays an overview of the Kraken system. The mentioned robotic arm counts on interchangeable heads and can perform milling, polymer resin extrusion, and additive manufacturing processes based on WAAM technology. The combination of crane mobility with the WAAM process head enables the manufacturing of BAAM parts.

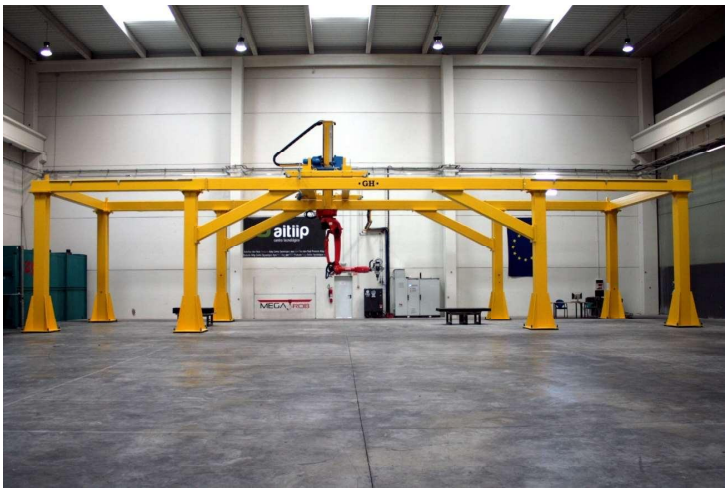

Figure 3. KRAKEN—Hybrid manufacturing robotic system. Photograph taken at the facilities of Fundación Aitiip.

Regarding software, robot movements are programmed directly from CAM software (HyperMILL CAD/CAM 2023) [80] to automatically guide the robot's path. The movements obtained are post-processed for ISO G-Code language. The file obtained is simulated in an Off-line Programming Software (Ultimaker Cura 2023) [81] to avoid collisions and singularities and ensure that all the movements are within the reach scope of the robot. The power source platform utilised in this procedure was a Fronius TPS 400i [82].

The robotic arm position was recorded in real-time. At the same time, the construction height was measured by a laser distance sensor (Keyence CMOS Multi-Function Analogue Laser Sensor) [83] installed in the welding torch, and the temperature was controlled by

a temperature sensor (OPTRIS—3MH CF) [84]. These height and temperature sensors created two independent security loops:

1. A distance control system at the WAAM torch was programmed to control the 'layers' height. This system measures the distance between the torch and the last welded layer, comparing that input data with the theoretical distance of the printing simulation. If the measured data are within a predetermined scale, the procedure continues. Otherwise, the program skips a printing layer if the distance measured is smaller than the theoretical distance or repeats it if it is higher.
2. The temperature sensor creates a second security loop, in which the last printing layer temperature is measured. This sensor is installed in the welding head, 25 mm behind the welding torch, measuring the temperature of the weld bead immediately after its deposition. High layer temperatures lead to geometrical inconsistencies in the geometry, and if too low, lead to interlayer-adhesion problems. This second low-temperature issue is less common and problematic. Thus, a minimum time between layers was used to ensure a layer temperature lower than 250 °C, even if geometrical singularities distort the temperature signal.

Data collection for the WAAM process was carried out based on the main welding equipment (Fronius TPS 400i), which measures the material supplied, whose parameter is defined as the WFR (Wire Feed Rate), electric current, and the voltage of the system, transferring them to a database via a Profibus communication.

Finally, based on the results obtained for the already-printed WAAM tooling, a sensitivity analysis was performed to test the over-thickness parameter selected. An assimilation with different design over-thicknesses for WAAM-process-adapted CAD was performed. These theoretical toolings were correlated with the real toolings, employing their designed volume parameters. By performing this assimilation, outputs comparable to the final test results were obtained theoretically.

The final aim of these theoretical models is to calculate the minimum over-thickness parameter designed for the WAAM-process-adapted CAD to minimise both material and energy consumption. This parameter should also achieve geometrical restrictions and not compromise the correct functioning of the tooling during the process.

2.1. Case Study

Both pure machining and the WAAM tooling are part of the INNOTOOL project [85] in the Clean Sky 2 program within the Horizon 2020 framework, whose objective is the development of a thermoplastic press-forming tool for an advanced rear-end closing frame prototype and tooling 4.0 for the assembly and transportation of the advanced rear-end prototype. This rear-end prototype consisted of two symmetrical thermoplastic parts, each created using a symmetric mould, whose core part was created following the two stated manufacturing procedures. These similar toolings (Figure 4) could be assimilated as equal, allowing for a direct comparison between their energy and material consumption inputs. Both toolings achieve final dimensions of 500 × 450 × 150 mm.

The final products obtained by the two twin toolings were two high-load composite frames, which were integrated into an aircraft rear-end fuselage demonstrator. Composite materials respond to the current trend of reducing metallic materials in the transport industry [86,87]. This rear-end demonstrator was built up for validation purposes regarding safety certification and to structure the systems' integration concepts up to full scale.

The process performed using these toolings was a press-forming procedure, in which a thermoplastic sheet is heated to a high temperature and fed into the tooling (core and cavity) and where, through a high-speed procedure, high pressure and high temperature are applied to produce a final part. This high temperature in the tooling is achieved by internal channels, through which high-temperature oil circulates. To achieve uniformity in the heating of the mould, the design attempts to adapt the oil channels to the geometry of the final part in the most appropriate way [88,89]. Also, a minimum weight is sought in the tooling so that its thermal inertia decreases, and, therefore, its cycle times. The tooling

design was adapted to each manufacturing process, as described below. Also, at this point, both processes are described.

Figure 4. Final tooling comparison between (**a**) WAAM tooling and (**b**) pure machining tooling.

2.1.1. Tooling Differences

The design differences between AM and pure machining toolings are highlighted in this section. Each process has its own singularities and restrictions that apply to each CAD design. Figure 5 displays the WAAM tooling's final design and pure machining tooling's final design. In both of them, their inner channels are highlighted. This figure also displays the hole plugs in the mould area of pure machining tooling. These differences are outlined and justified below.

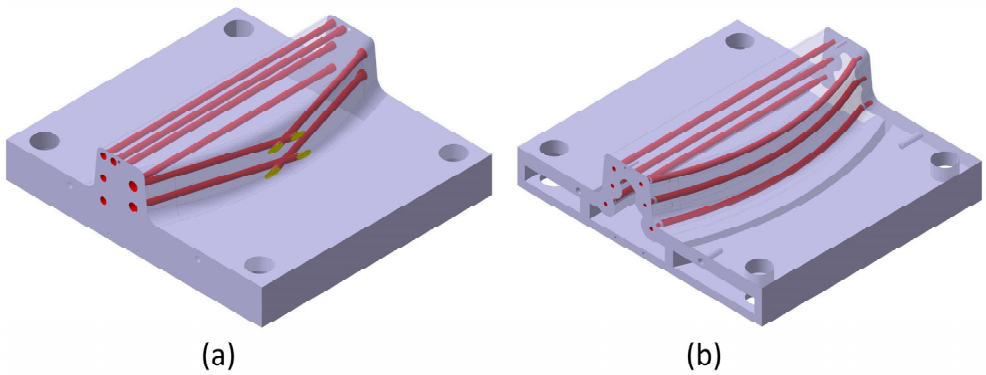

Figure 5. CAD design of both tooling, with internal channels highlighted in red (**a**) Pure machining tooling CAD design and (**b**) WAAM tooling CAD design.

Pure machining tooling:

1. Only a final design CAD is needed.
2. The internal channels can only be designed straight due to machining limitations. For this reason, they cannot be adapted to the final shape of the tooling. These drills are designed straight through the tooling and drilled in a step before finishing.
3. In an extra process, these drills are subsequently plugged (manually) and re-machined, as shown in Figure 5.
4. All construction singularities (threaded holes, reference holes, and holes for guideways) are performed during the same procedure.
5. Due to machining area limitations, the inner tooling part is not emptied, as in WAAM tooling.

WAAM Tooling:

1. Any construction singularity, such as screw drills located on surfaces perpendicular to the growth direction, is eliminated during the WAAM design and machined in the posterior hybrid-machining process.

2. The main tooling is constructed over a metallic plate larger than the tooling used as a printing base. When the WAAM process starts, extra layers are constructed over the plate and eliminated in the hybrid machining procedure, as shown in Figure 6.
3. This figure also displays the printing direction, which is perpendicular to the theoretical base of the mould. This arrangement allows us to cast the inside of the part.
4. As highlighted in Figure 5, the final tooling has internal heating channels. These channels follow the curved surface of the final thermoplastic part, homogenising the temperature distribution in the mould and increasing its heating rate.
5. The design respects the restriction of a growth angle smaller than 20° relative to its horizontal plane.
6. The printing process allows the tooling inner part to be designed as empty (design supported by FEM analysis).

Figure 6. WAAM tooling printing over a metallic plate.

2.1.2. Pure Machining Tooling

The pure machining process covers all roughing, drilling, and finishing processes from a raw steel block of nominal dimensions plus 5 millimetres of growth. These shape specifications cause the initial block size to be 510 × 460 × 158 mm. First, the bores used for positioning the part in the machine were drilled. Then, the drill holes for the thermal channels were produced. After that, a rough procedure eliminated any existing extra material. Then, drilling operations were conducted, and the finishing process was used to reach dimensional tolerances where needed.

As mentioned, the inner heating channels need to be manufactured in three stages:

1. First, a drilling process was carried out before the roughing process, creating through-holes that pass through the workpiece.
2. Then, rough milling of the area was carried out, approximating its geometry to the final geometry.
3. Afterwards, a re-tapping procedure was conducted to blind these through holes, creating the internal heating circuit.

Finally, leftover material from the plugs used in the channels was removed in the subsequent pre-finishing and finishing procedures. The following diagram (Figure 7) shows an overview of the machining processes carried out on the NC machine.

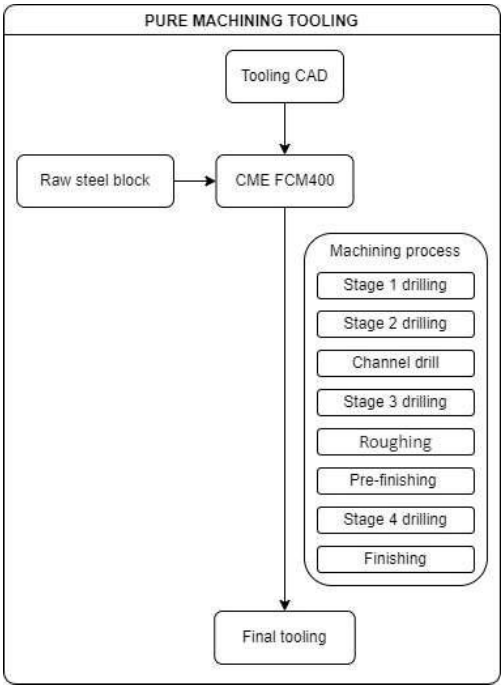

Figure 7. Pure machining tooling manufacturing diagram.

2.1.3. WAAM Tooling

First, the input material for the AM process must be selected. For this BAAM process, the chosen wire material was G42 4 M21 3Si1 (ISO specification). This carbon steel electrode offers excellent weldability, with many deoxidising elements for welding in which strict cleaning practices cannot be followed.

The printing strategy carried out for the WAAM process was the following:

1. Over the aforementioned metallic plate, five extra layers of the inferior final figure were printed. This strategy assures the orthogonality of the final construction and creates an extra height that ensures the ease of plate removal.
2. Based on the Figure 8 cutting, the WAAM strategy was the following for each layer:
    a. First, the contour of the tooling was printed.
    b. In the second stage, the contour of the inner channels was printed.
    c. Subsequently, the inner part was fulfilled following Figure 8's pattern, ending the layer.
    d. The next layer started on a randomly selected point of the contour, avoiding, in this way, heat concentrations in specific areas.
3. The WAAM process input data are provided in Table 1.
4. The WFR is variable and adaptable to the geometry, printing route, and weld specifications. Its main value is also shown in Table 1.

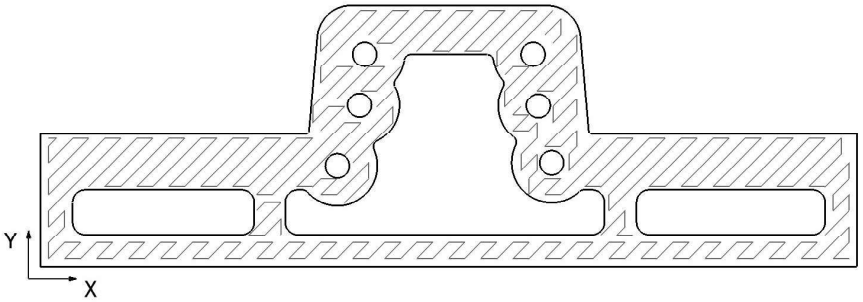

Figure 8. WAAM process printing route details. The lines shown represent the route followed by the WAAM system to build each layer, with the darker lines indicating the contours of the workpiece.

Table 1. WAAM process parameters.

Process Parameters for WAAM Deposition		
Process parameters	Details	Value
Speed	Welding speed	0.02 m/s
	Wire feed rate	8.64 ± 0.81 m/min
	Deposition rate	0.077 kg/min
Distance and angle	Layer height	1.2 mm
	Electrode to layer angle	90°
Shield gas	Shield gas type	ISO 14175-M20-ArC-8 [90] (CO_2 8% Ar 92%)
	Shield gas flow rate	15 L/min

Once the AM process ends, WAAM tooling hybrid machining starts with a cutting procedure to separate the printing base plate from the final tooling. After that, the roughing process only mills the areas that are to be subsequently subjected to drilling or finishing processes and the areas that require the removal of extra material printed in the WAAM process due to mechanical or procedure specifications.

The internal channels of the WAAM tooling were designed based on the experience gained from previous constructions using the WAAM method, as well as from previous tests. Their design and manufacture are considered successful after testing the internal channel system with thermal oil.

The following diagram (Figure 9) summarises the tooling manufacturing, including an enumeration of the different machining processes carried out on the NC machine.

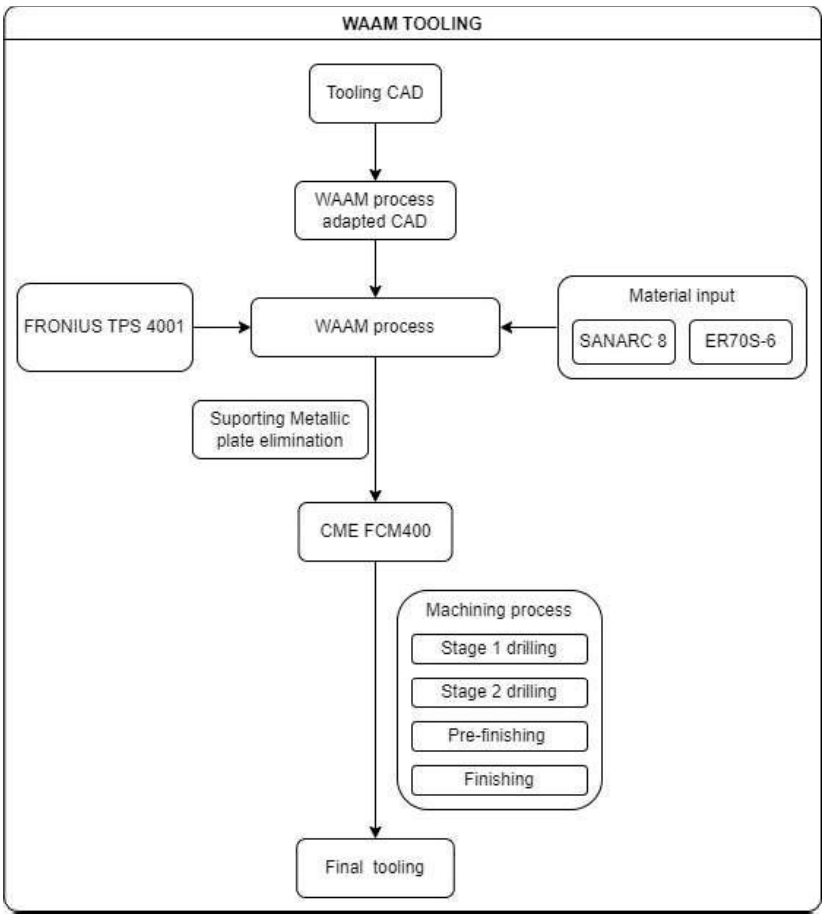

Figure 9. WAAM tooling manufacturing diagram.

3. Results

3.1. Pure Machining Tooling

3.1.1. Energy Consumption

Energetic input information for this procedure was characterised by the measured inputs obtained in real-time. In the case of pure machining tooling, the whole process was performed by the CME FCM400 and lasted 9.69 h. This procedure includes the drilling and rough milling channels and a pre-finishing and finishing step. The manual channel plugging step time was not included. The total amount of electric energy consumed across the process was 696.228 kWh.

3.1.2. Material Consumption

For the pure machining tooling, as aforementioned in the Milling Process section, the original raw material was a 510 × 460 × 158 mm raw steel block (Figure 10), whose density was 7860 kg/m^3. Two stages in Table 2 related to tooling weight are differentiated:

1. The material consumed weight.
2. The final tooling weight.

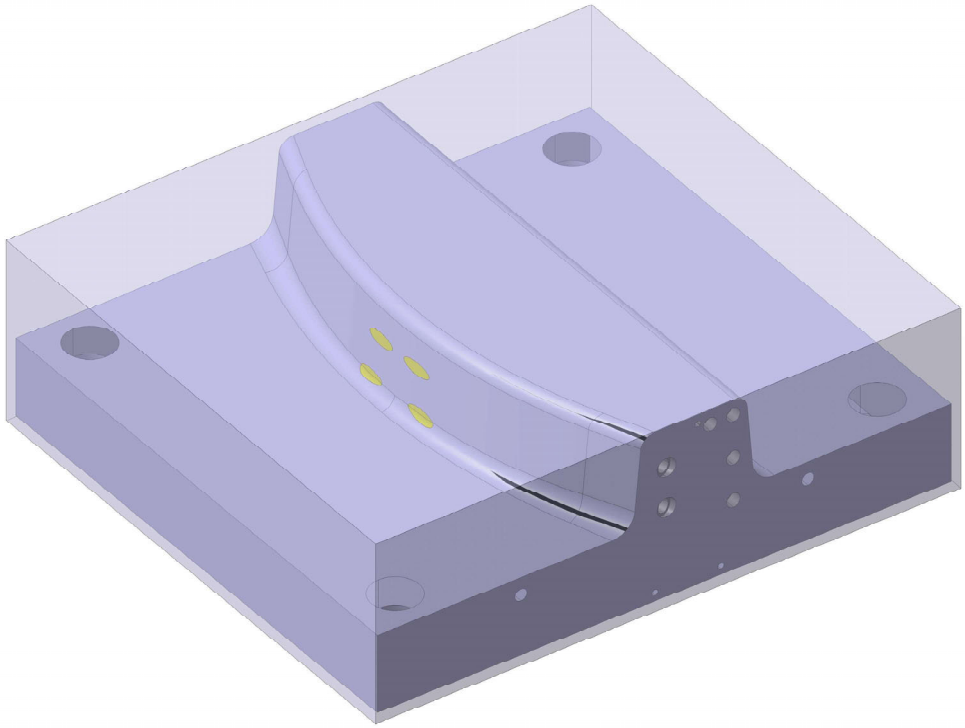

Figure 10. Raw material vs. final tooling in pure machining tooling.

Table 2. Pure machining tooling material consumption.

Pure Machining Tooling	
Material consumed weight	291.345 kg
Final tooling weight	152.747 kg
Material discarded	47.57%

These states refer to the amount of raw material consumed in the process (raw steel block in this case) and, secondly, the mass of material held in the final tooling. From these two states, it is possible to find the percentage of the material used concerning the material expended and, therefore, the amount of material discarded in each procedure.

3.2. WAAM Tooling

3.2.1. Energy Consumption

The technology required to perform the WAAM process, based on Kraken products, requires specific equipment to allow the welding system to work. All the elements around the AM system are already summarised in Table 1. Regarding support systems around the weld, all the energetic inputs are reviewed in Table 3. Under the concept of 'General', all installed sensors and control software are summarised. It must be mentioned that the Kraken MAM system only actuates the gantry crane system when the construction size exceeds the operating range of the robotic arm. In this case, the final construction dimensions are achievable by the robotic arm, so gantry crane fuel inputs are considered negligible. These consumptions were previously characterised during actual WAAM operations before the study.

Table 3. KRAKEN system power consumption.

Energy Inputs	Average Power Consumption
Gantry crane	1.890 kWh
Robotic arm	0.440 kWh
General	2.15 kWh

The global WAAM printing process lasted 37.48 h in terms of the pure printing time. Throughout that time, the printing software recorded the position, wire feed rate, electric current, arc voltage, and layer height data. It must also be specified that, during additive manufacturing, no extra stop was required for cooling the workpiece. This stabilisation stop is common in WAAM systems. However, due to the large size of the part, the printing time itself was long enough to stabilise the part temperature.

It should be highlighted that the recorded data were post-processed, eliminating welding stops. This decision allows us to focus on the power consumption data obtained during the AM process, facilitating its later treatment. However, these times added to the welding were recorded and used for the final calculation of the power consumption and process times. The downtime measured during the process amounted to 4.58 h. These stoppages were due to the following causes:

1. The programming robot travelling between welding cordons.
2. The programming robot travelling between layers.
3. Not programming stops due to welding material replacement (wire or gas).

This article focuses on electric consumption, dependent on the electric current (Figures A1 and A2) and arc voltage (Figures A3 and A4). Both inputs follow a normal distribution; consequently, Figures A5 and A6 also comply with this distribution. The large number of atypical values recorded in graphical areas between 0 and the lower statistical variance value should be mentioned. These atypical values could result from the WAAM process stability across the weld, which could be affected by different external inputs. These inputs, in general terms, result from robotic arm positioning errors or process singularities, such as specific areas with a large grouping of printing points, layer changes, or alternation between welding seams.

The total amount of electrical energy consumed by the system, combining the consumption of the WAAM process itself, the consumption of the robotic arm, and the control software, is shown in Table 4.

Table 4. WAAM process deposition power.

WAAM Process Deposition Power	
Current	226.26 ± 21.66 A
Arc voltage	17.39 ± 0.97 V
Electric power	3945.00 ± 377.36 W

Once the AM process ends, the same NC machine is used to manufacture the pure machining tooling; therefore, the machining system inputs are the same as those presented in Table 5. The machining process energy consumption (311.365 kWh) overcomes the WAAM process (245.259 kWh). However, the sum of the two (568.515 kWh) is still less than the single tooling machining process of pure machining tooling (696.228 kWh). Under the concept of WAAM process energy consumption, we include both the pure consumption of the AM process (245.259 kWh) and the consumption of the system during secondary operations (11.891 kWh).

Table 5. Total electric energy consumption during WAAM tooling.

	Machining Process (kWh)	WAAM Process (kWh)	TOTAL (kWh)
WAAM Tooling	311.365	257.150	568.515

Referred to as WAAM tooling, the primary printing procedure eliminates the channel drilling and roughing processes (the most time-consuming) and keeps only the pre-finishing and finishing processes. Thanks to this step reduction, the machining time falls to 3.66 h.

3.2.2. Material Consumption

Regarding material consumption, specific considerations mentioned in Section 2.1.3 were considered. Figure 11 shows the WAAM tooling CAD design versus WAAM-process-adapted CAD. The recorded data of WFR determined the WAAM process material consumption. The statistical analysis of the data collected from the WFR is presented in Figures A7 and A8, which follow a normal distribution. The total wire expenditure weight is shown in Table 6.

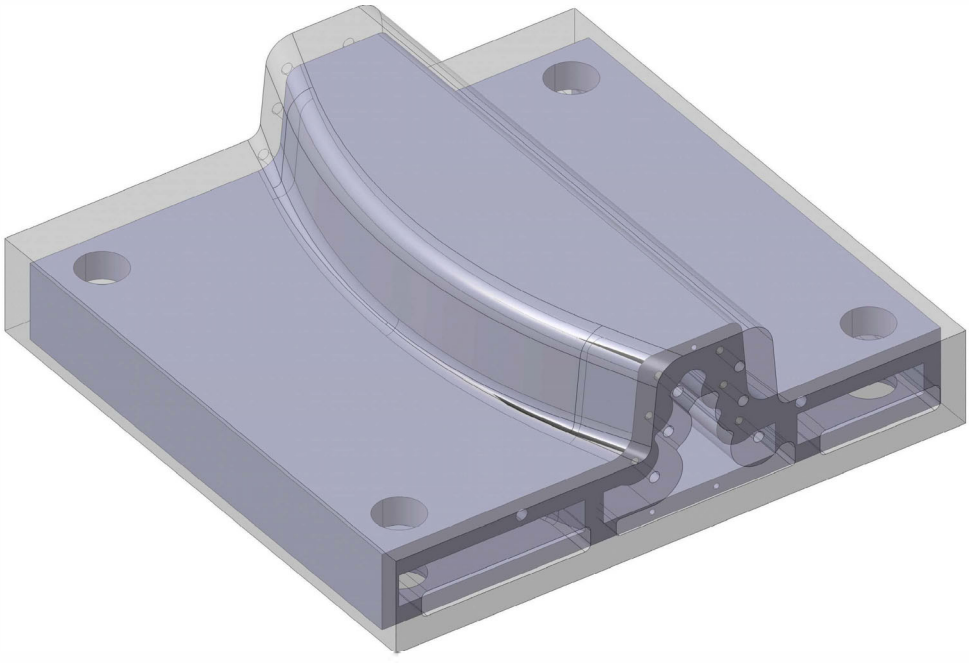

Figure 11. Raw material vs. final tooling in WAAM tooling.

Table 6. WAAM tooling material consumption.

WAAM Process Deposition Power	
Material consumed weight	173.091 kg
Final tooling weight	90.960 kg
Material discarded	47.45%

The final results of material consumption and material discarded for WAAM tooling are shown in Table 6.

3.3. Sensitivity Analysis of the WAAM Over-Thickness

Once the data obtained from the WAAM tooling are processed, the question arises as to whether the additive manufacturing process could be optimised in such a way that it would be even more favourable in terms of electricity and material consumption. As previously mentioned, over-thickness is a safety measure considered in the design phase of the parts manufactured using WAAM technology, whereby a part thickness more significant than the final thickness is designed to minimise the effect of defects in the welding procedure. This over-thickness is machined later in the precision-finishing phase in the necessary areas. Based on this premise, several over-thicknesses were tested theoretically for the WAAM-process-adapted CAD on which the tooling AM process is based. It should be mentioned that the 10 mm over-thickness given to the original CAD responds to conservative criteria, seeking to minimise the possibility of errors and not the optimisation of the procedure.

To carry out this study, the WAAM-process-adapted CAD was modified, increasing the over-thicknesses to a final 20 mm and reducing it to 1.5 mm. Considering that the WAAM-process-adapted CAD cannot have an over-thickness of 0 mm, as the very concept of over-printing layers in the WAAM process would make it impossible not to incur areas of material shortage, a minimum over-thickness of 1.5 mm was used to optimise the print as much as possible while trying to avoid such areas of material shortage. On the other hand, logic dictates that any design thickness greater than the original 10 mm would increase both material consumption and energy costs. However, higher values of over-thickness will be tested to examine the implications of consumption. For these over-thicknesses of more than 10 mm, the advantages derived from the AM process were reduced or even disappeared. The WAAM-process-adapted CAD derived from high over-thicknesses makes it impossible to perform the internal emptying of the part. Consequently, the tooling cannot be made lighter than the pure machining tooling. However, values of less than 10 mm significantly reduced material consumption.

3.3.1. Theoretical Energy Input

The theoretical results obtained from the performed toolings are shown in Figure 12. This graph shows the energy expenditure for the additive manufacturing procedure and the subsequent second-stage hybrid-machining process.

The WAAM tooling is not machined in its casting areas in any case, and the function of these zones is only weight reduction; therefore, they do not require any machining process. These areas only represent the additive manufacturing phase, and only the functional part of the tooling shall be machined.

It is also worth noting that when the machining thickness exceeds 10 mm, an extra machining process, rough milling, should be added to the ones already applied to the WAAM tooling. Nevertheless, rough milling is much less energy-consuming than the later finishing operations, so its relevance to the total energy consumption is minor.

The calculated energy inputs show a higher relevance of the over-thickness parameter in the WAAM printing process than in the subsequent machining. In the case of the most negligible printing thickness, 1.5 mm, energy savings of 44.53% are achieved in the WAAM process and 24.81% in the subsequent machining, with a total theoretical energy saving of 33.73% for the original WAAM tooling manufactured. On the other hand, for the most unfavourable case of over-thickness, 20 mm, the terms of energy consumption soar. The power consumption of WAAM printing increases by 276.09%, and that of the subsequent machining increases by 201.69%, compared to the original 10 mm WAAM-process-adapted CAD. Consequently, the total electric consumption increases by 235.34%. As mentioned above, the most electrically demanding machining procedures are the finishing processes, which are the same for all toolings 10 mm thick or more. From this thickness, a rough milling process was carried out until this thickness was reached, making this procedure

much less electrically demanding. For this reason, the machining energy consumption does not increase linearly with the WAAM print consumption from 10 mm over-thickness.

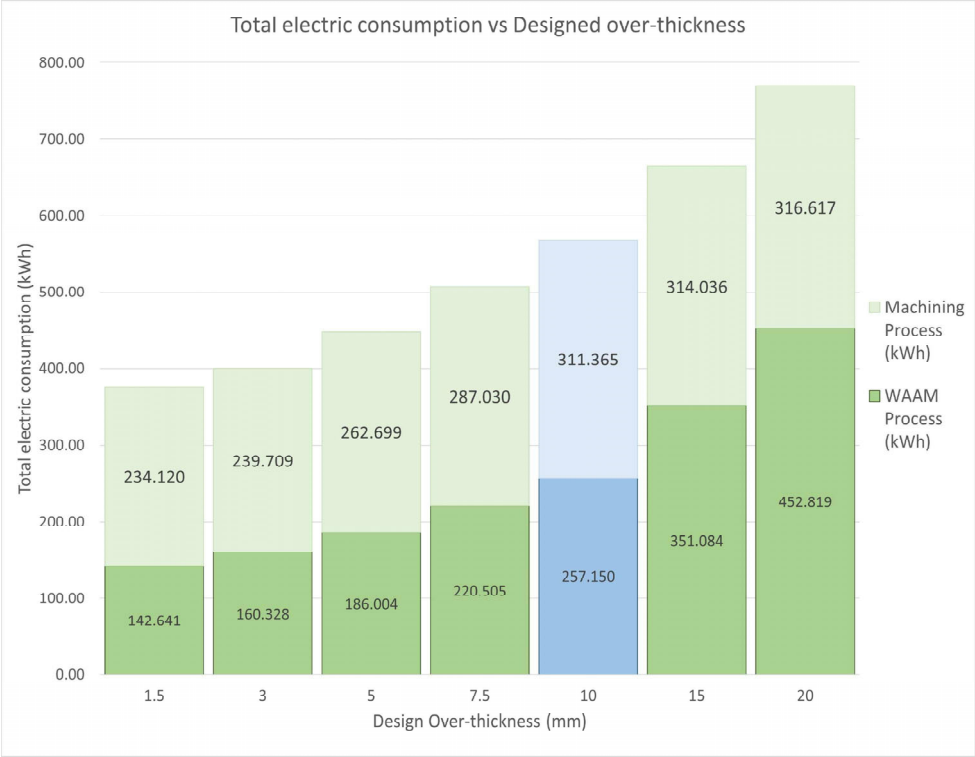

Figure 12. Theoretical over-thickness energy inputs. Green columns display theoretical results meanwhile blue column shows the actual data obtained.

3.3.2. Theoretical Energy Input

As in the previous section, the theoretical result of material consumption during AM operations, based on the WAAM tooling results, is shown in Figure 13.

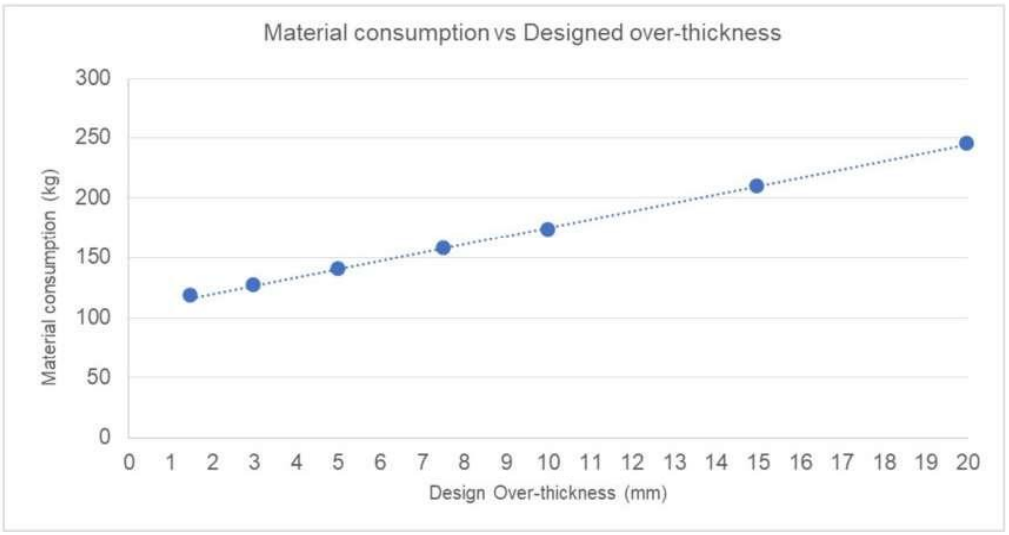

Figure 13. Material consumption vs. design over-thickness. The graph shows the linear growth of the amount of material consumed during the WAAM process (kg) with reference to the over-thickness considered in WAAM-process-adapted CAD.

The minimum 1.5 mm over-thickness of the WAAM-process-adapted CAD over-thickness displays a theoretical reduction of 32.01% of the raw material consumption compared to the 10 mm thick construction. This results in a better use of material, reducing the percentage of theoretically discarded material to 22.70% of the final tooling.

On the other hand, for over-thicknesses greater than 10 mm, the increase in material theoretically consumed scales up to 241.90% in the worst case (20 mm over-thickness). Consequently, the discarded material increases, although in several areas, this material is not removed in the second-stage hybrid machining, increasing the final weight of the tooling. This would be the case of the aforementioned inner voids, which, due to this over-thickness, would practically disappear and later challenge the machine.

Finally, the last parameter to be commented on is the process time. Figure 14 displays the total consumed time with the accumulation of the WAAM process time plus the hybrid machining time. As observed, the AM process time covers most of the entire process time. decreasing by 32.01% for the most favourable case compared to a manufactured tooling over-thickness of 10 mm. For the hybrid machining process times, as mentioned above, by increasing the over-thickness to more than 10 mm, a rough milling procedure was added to the operations to be carried out. This procedure is faster than the finishing milling processes, so the increase in time was less significant.

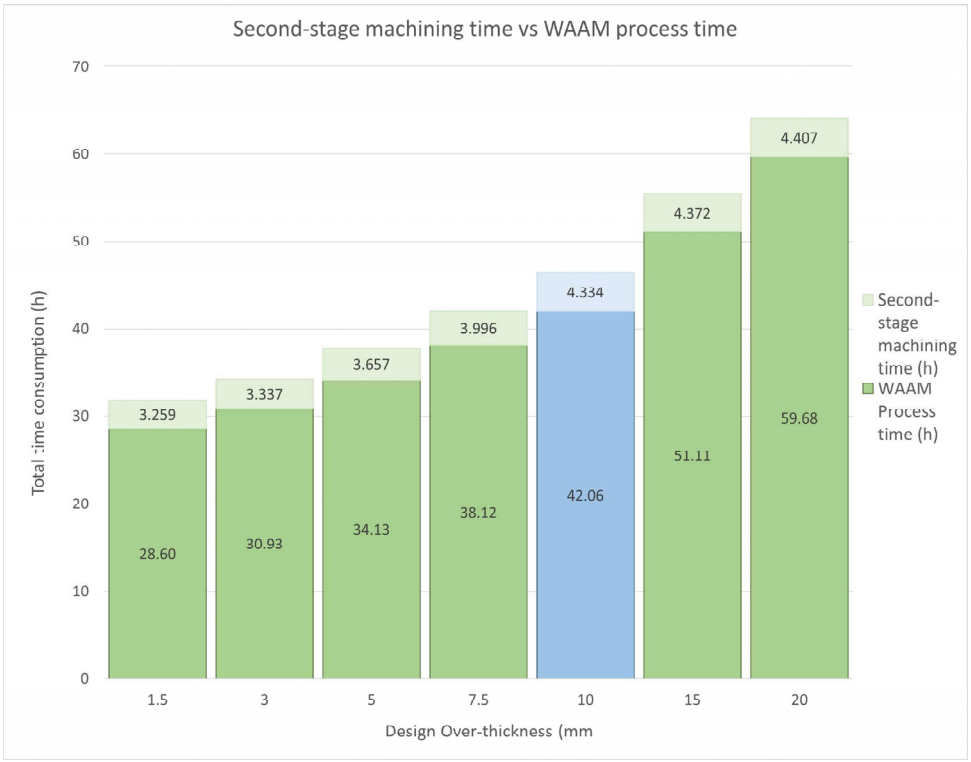

Figure 14. Hybrid machining time vs. WAAM process time. Green columns display theoretical results meanwhile blue column shows the actual data obtained.

As shown in Figure 14, the most favourable total process time with a 1.5 mm over-thickness is 31.855 h, and the most unfavourable time at a 20 mm over-thickness is 64.092 h. Even in the most favourable scenario, the WAAM tooling manufacturing process continues to be three times slower than pure machining manufacturing.

3.3.3. WAAM Tooling Metrology

After the AM operation, a metrology studio was performed against the WAAM tooling. Using a T-SCAN type measurement scanner [83], a 3D point cloud was obtained. This point

cloud was compared with the WAAM-process-adapted CAD through a best-fit procedure, and the metrology studio was performed against the WAAM-process-adapted CAD.

The results clearly show differentiated zones in which over-thickness layers are interspersed with large areas of below-grade thicknesses (Figure 15). This zone differentiation clearly shows the construction boundary layer between the sections, with excess material compared to the theoretical value and those with a lack of material. This effect is caused by the thermal expansion of the material during the additive process. As explained previously, the WAAM process deposits material at high temperatures and is thus in a state of thermal expansion. This characteristic is considered in the design process. As a result, the final part shrinks slightly when the process is finished and cools down. If the entire part is printed continuously, the thermal shrinkage affects the entire workpiece. However, if a prolonged stop is made throughout the build process, the workpiece shrinks and shifts its geometry slightly away from the printing route. Therefore, when the printing process is resumed at the same point, the printed layer is displaced in the direction of shrinkage, causing the next layer not to be deposited fully aligned with the previous one. Accordingly, this new weld bead will not be deposited in its ideal position concerning the previous layer but deposited off-centre, creating an overhang and, therefore, increasing in width and decreasing in height.

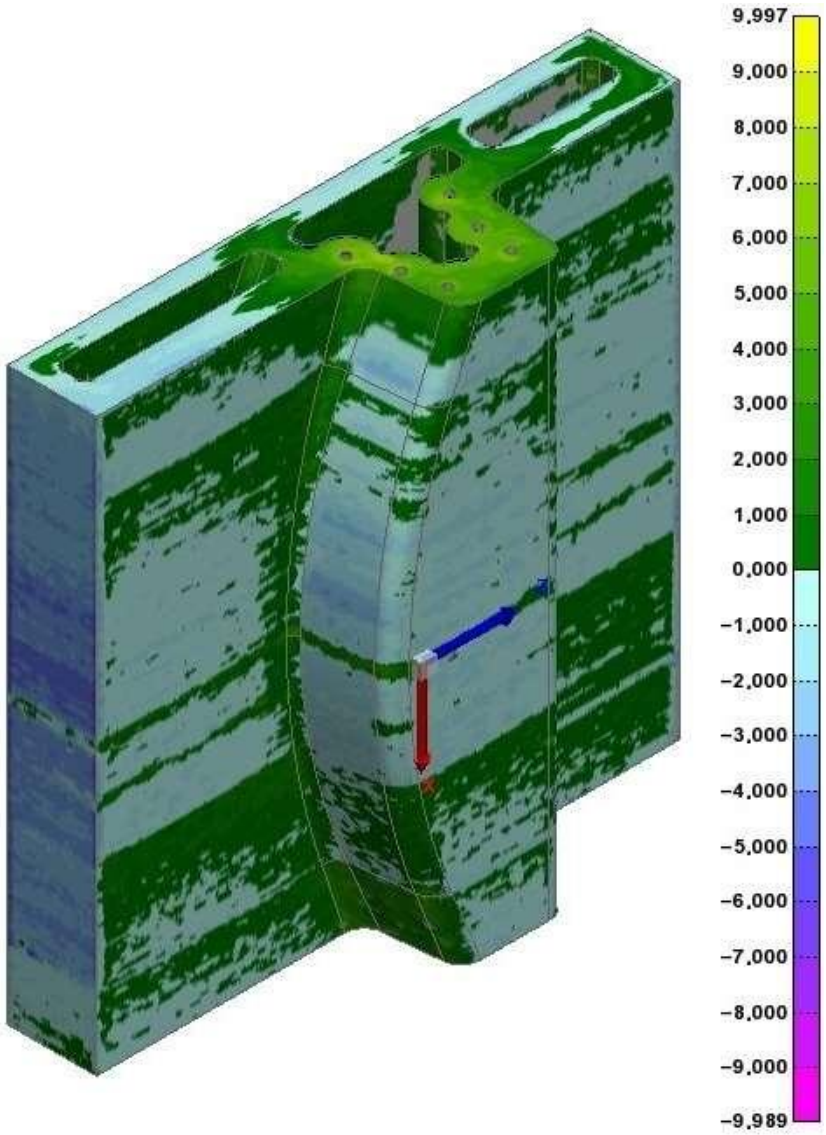

Figure 15. WAAM tooling metrology studio. Data are shown in mm.

For this reason, the areas in which construction stops tend to be out of level, having excessive thicknesses. This feature is not critical for tool printing and subsequent second-stage hybrid machining, as these wider layers will be machined afterwards in any case. This anomaly is clearly visible in the image, with weld beads deposited after a process stop.

One important point to highlight is that the extra deposited material is not problematic for ensuring the quality of the final product, and areas with excess material are mechanised in subsequent procedures. However, under-material areas can be problematic if the under-material exceeds the over-thickness designed in the WAAM-process-adapted CAD, as it makes it impossible for the final part to reach the dimensions after the second-stage hybrid-machining process.

During the metrology process, several studios were made of the section of the punch area of the mould, as this was the most compromised tooling area. Of the multiple measurements performed, the most unfavourable one was taken, as shown in Figure 16. In this image, the mentioned thermal dilatation process could be appreciated.

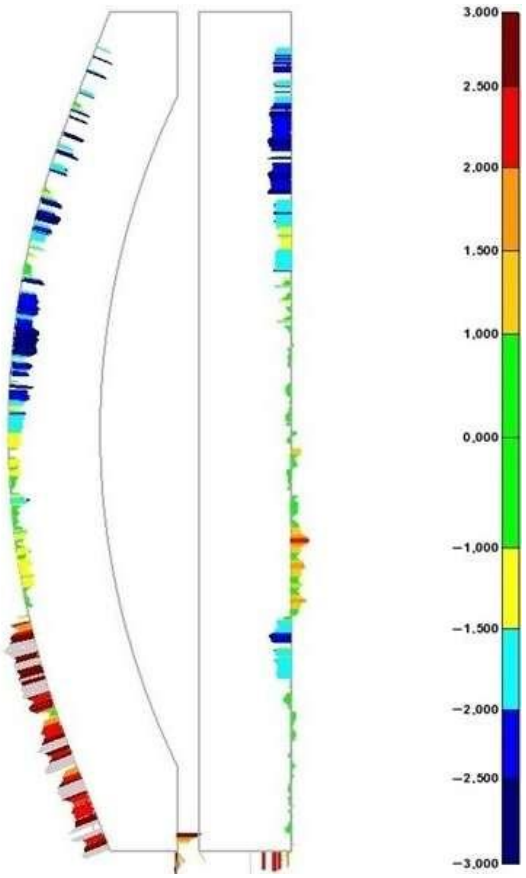

Figure 16. WAAM tooling metrology studio—punch section. Data are shown in mm.

The data obtained from the metrology studio show a −3 mm maximum negative AM deviation concerning the WAAM-process-adapted CAD in the areas where the lack of material is more accentuated. These data suggest that a minimum 3 mm over-thickness should be applied to the WAAM-process-adapted CAD in order to obtain the first AM product available to achieve the final tooling geometrical specifications. This fact discards the calculated theoretical over-thickness of 1.5 mm but makes the next estimated value of 3 mm feasible. The values of the positive deviations overcome the 3 mm in the tested area, although these positive values do not represent a constructive issue, as extra material is later machined.

4. Discussion

In conclusion, the results showed a reduction in material consumption and electric inputs for the WAAM tooling compared to the pure machining one.

As mentioned, WAAM process advantages are oriented to design and construct tailored and complex geometries, which is impossible to achieve by conventional manufacturing methods. Nevertheless, this study displays the capacity of this AM procedure to save energy and material in specific constructions.

The obtained results for this particular tooling design showed a total energy consumption of 696.228 kWh for pure machining tooling. On the other hand, the recorded data showed a combined energy consumption of 568.515 kWh for WAAM tooling, combining both WAAM and hybrid machining. Based on the data obtained, a significant reduction in energy consumption (18%) was achieved in the WAAM tooling for pure machining tooling.

It must be highlighted that, in a high percentage, the weight difference between the final tools developed by the two differentiated manufacturing processes is primarily due to their design differences. These differences are the consequences of the specifications of each manufacturing process, as named in Section 3.1.1, Tooling Differences. The adequacy of the procedure is closely related to the complexity of the final design. In cases such as the current design, its complexity lies in the ability to decrease its mass, thereby reducing its thermal inertia. Since it is a press-forming tooling, it is desirable to minimise the thermal cycles.

In this specific design, the internal hollows of the WAAM tooling significantly reduce its weight concerning the pure machining tooling. In this case, WAAM-produced tooling weight represents a 41% reduction regarding the pure machining tooling. This final weight reduction could be defined as a design-dependent property, the percentage of which can vary widely depending on the final design.

On the other hand, the material discarded shows the relation between the raw material input and the final material used, displaying an almost equal material utilisation percentage in both toolings. Nevertheless, the difference in the final weight between the two toolings means that, although the percentage of material utilisation is very similar, the amount of discarded material is much higher in pure machining tooling.

The difference in the construction time of the tooling should be discussed. In the case of pure machining tooling, the entire procedure is carried out on the same NC machine. This represents a significant time saving compared to the WAAM process, where the manufacturing has two steps: an AM process and a machining process. In addition, the transport of the raw tooling printed by WAAM to the NC machine should be mentioned; nevertheless, in this case, it has been omitted as it is of negligible value.

With all these specifications, we obtained a total manufacturing time for the pure machining tooling of 9.7 h for the whole procedure. In contrast, for the WAAM tooling, we first had an AM process that lasted 42.07 h (combining 37.48 h of the pure WAAM process with 4.58 h of downtime) followed by a machining process of 4.3 h, adding up to a total of 41.8 h.

The results also conclude that the WAAM process is four times more time-consuming than pure machining for this tooling design. This characteristic of AM processes makes their use in BAAM processes unfeasible when large batches of parts are to be created in short periods of time.

Based on the theoretical analysis performed for different design over-thicknesses for the WAAM-process-adapted CAD, there is an opportunity for a further reduction in energy and material costs. Once the metrological analysis was concluded, the results supported that a decrease in the over-thickness from 10 mm to 3 mm for the WAAM-process-adapted CAD would be optimal. The reduction in the design over-thickness linearly decreases both parameters, as well as the manufacturing time, achieving savings of 43.8% in total energy expenditure and 56.3% in raw material compared to the pure machining tooling. On the other hand, although the total manufacturing time of the theoretical WAAM tooling also following a decreasing trend with the reduction in design over-thicknesses, this most

favourable case still requires a total manufacturing time three times longer than pure machining tooling.

It should also be noted that this study is focused on the manufacturing processes, thus limiting this particular case to a gate-to-gate study. Future lines of research in this field should focus on the complete analysis of the whole life cycle of the manufactured part, conducting a cradle-to-grave study.

5. Conclusions

In summary and conclusion, the suitability of the WAAM manufacturing process for producing large-sized tooling was demonstrated. For the specific case analysed, the reduction in electrical and material consumption was 18% and 41%, respectively, compared with pure machining tooling. This weight reduction also minimised the thermal inertia in the process, increasing its productivity. Although this study was gate-to-gate, focusing on the energy needed for the additive and subtractive manufacturing process of the tooling, it did not consider the energy needed to produce the raw block, welding wire, and shielding gas.

On the other hand, the manufacturing time employed in WAAM tooling is higher than that required by pure machining tooling. However, since WAAM tooling printing is a continuous process, it only requires surface-finishing operations, being less time-consuming. In contrast, pure machining tooling requires complex positioning processes to perform challenging operations, such as thermal channels. These operations can significantly increase the manufacturing time, minimising the difference in the manufacturing time.

In addition, the metrological analysis of the WAAM tooling revealed an optimisation capacity at the design and manufacturing level. In the most favourable case, a theoretical reduction in energy and material consumption of 44% and 56%, respectively, could be obtained compared with the pure machining tooling. This theoretical approach will be studied in future constructions.

In this study, a gate-to-gate manufacturing process was analysed for two aeronautical toolings designed to manufacture limited batches. The study of the durability of both tooling and its comparison was not contemplated due to their reduced productivity. This WAAM tooling durability is considered a possible line of future research, in relating this characteristic to the mechanical properties of the WAAM tooling. In this context, an interesting line of research is the analysis of the life cycle of the WAAM tooling, not limited to its production phase, but to a cradle-to-grave analysis.

As discussed throughout the article, the data obtained depend on the final part design. However, the procedures mentioned are common for tools manufactured by additive manufacturing procedures, so although it is not possible to create a rule regarding the proportionality between manufacturing times, it serves as a guideline.

Author Contributions: Conceptualisation, J.A.D.; methodology, A.L.; software, I.M.; validation, A.M. and J.A.D.; formal analysis, I.M.; investigation, A.M.; resources, A.L.; data curation, I.M.; writing—original draft preparation, A.M.; writing—review and editing, C.J. and D.E.; visualisation, C.J. and D.E.; supervision, C.J. and D.E.; project administration, J.A.D.; funding acquisition, J.A.D. All authors have read and agreed to the published version of the manuscript.

Funding: This research was funded under the European Health and Digital executive agency (HADEA): 101057049 framework through BIO-UPTAKE project, Grant Number 101057049. This study was performed by members of the I + AITIIP (DGAT08 20R) research group of the FEDER 2014-2020 'Building Europe from Aragón'.

Institutional Review Board Statement: Not applicable.

Informed Consent Statement: Not applicable.

Data Availability Statement: The data supporting the findings of this study are available from the corresponding author upon reasonable request.

Conflicts of Interest: The authors declare no conflicts of interest.

Appendix A

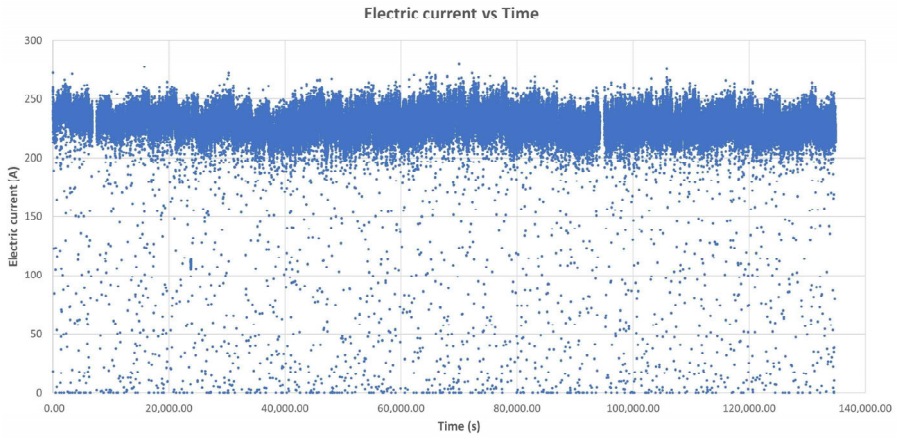

Figure A1. Electric current over time. The blue dots represent electric current data collected every 0.1 s throughout the entire WAAM manufacturing process.

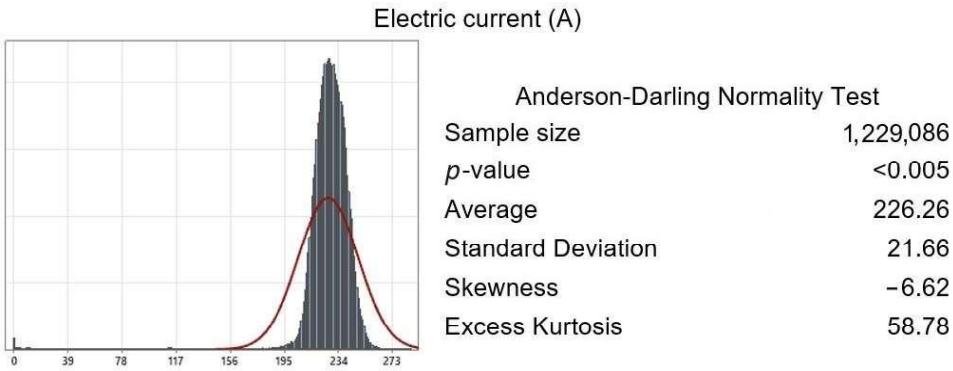

Figure A2. Anderson–Darling normality test applied to electric current data collected every 0.1 s throughout the WAAM manufacturing process. The p-value < 0.05 shows that the acquired data follow a normal distribution.

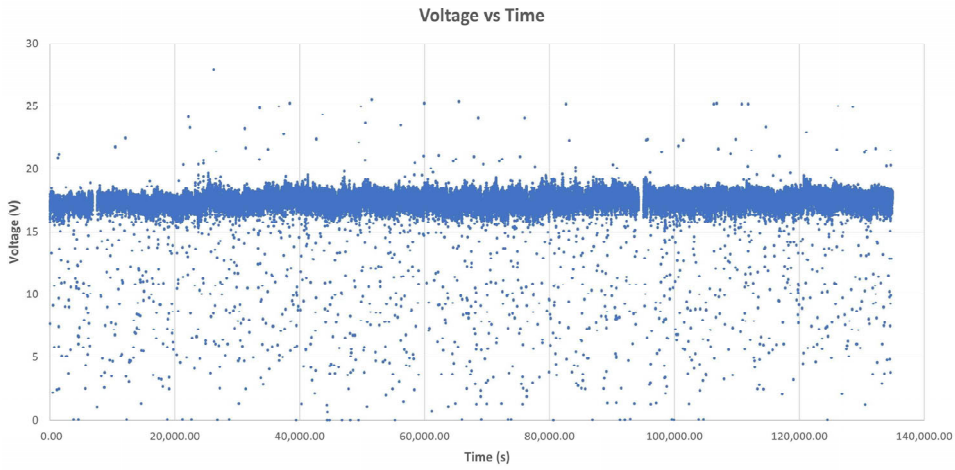

Figure A3. Voltage over time. The blue dots represent voltage data collected every 0.1 s throughout the entire WAAM manufacturing process.

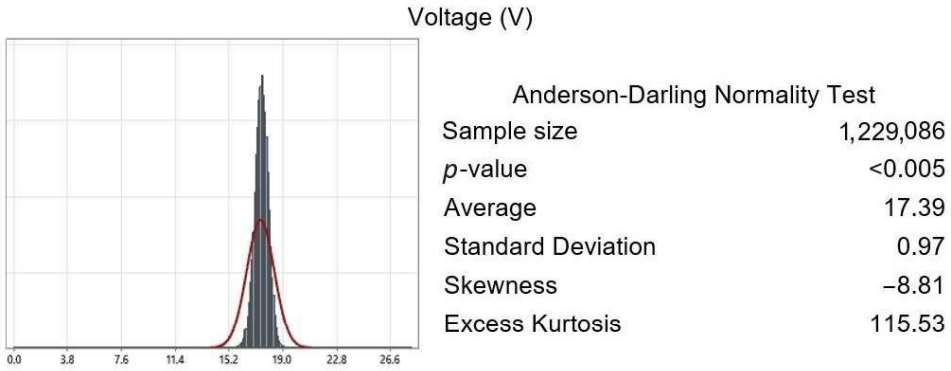

Figure A4. Anderson–Darling normality test applied to voltage data collected every 0.1 s throughout the WAAM manufacturing process. The p-value < 0.05 shows that the acquired data follow a normal distribution.

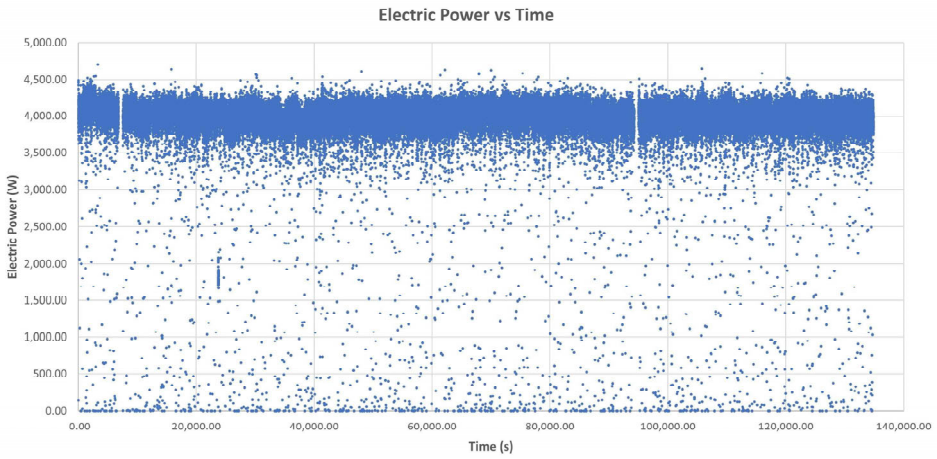

Figure A5. Electric power over time. The blue dots represent electric power data collected every 0.1 s throughout the entire WAAM manufacturing process.

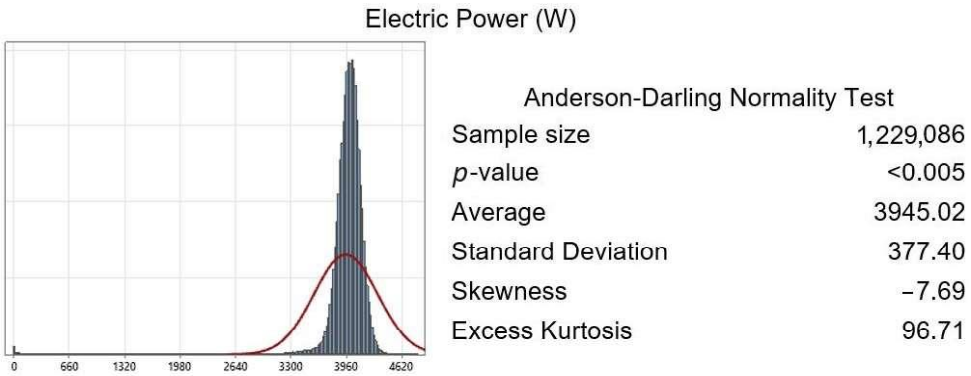

Figure A6. Anderson–Darling normality test applied to electric power data collected every 0.1 s throughout the WAAM manufacturing process. The p-value < 0.05 shows that the acquired data follows a normal distribution.

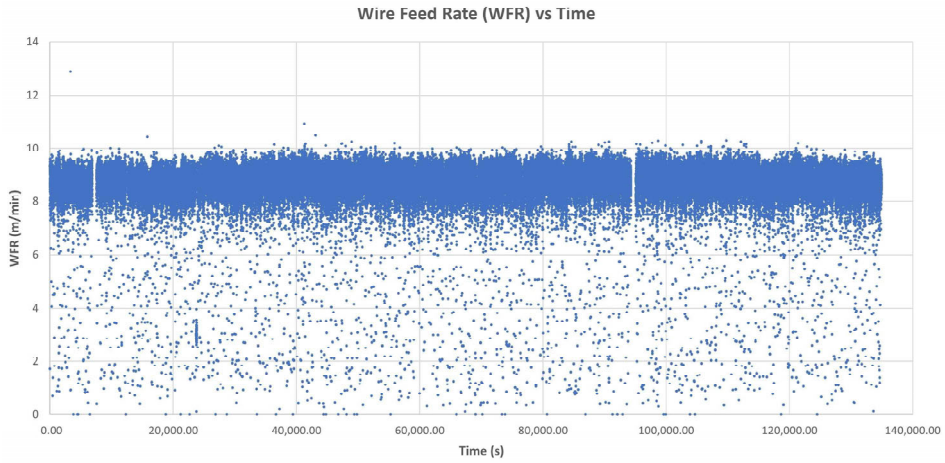

Figure A7. Wire feed rate over time. The blue dots represent WFR data collected every 0.1 s throughout the entire WAAM manufacturing process.

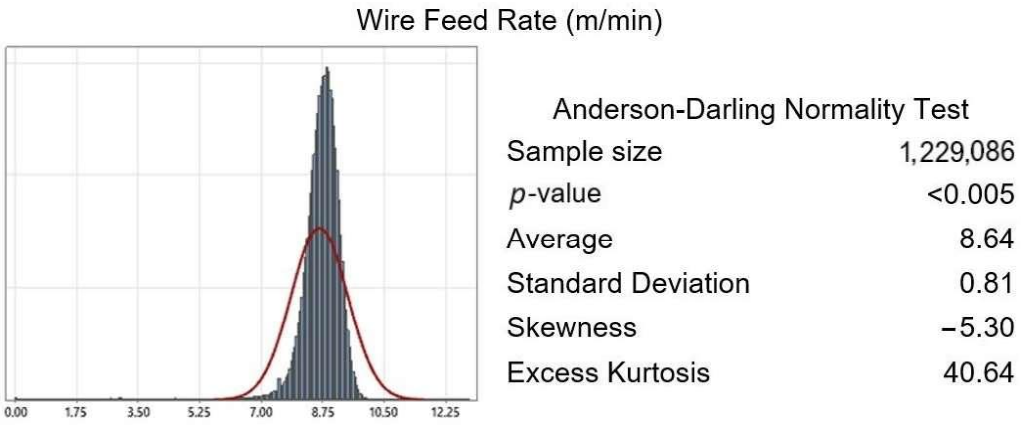

Figure A8. Anderson–Darling normality test applied to WFR data collected every 0.1 s throughout the WAAM manufacturing process. The p-value < 0.05 shows that the acquired data follow a normal distribution.

References

1. Melnychuk, O.; Rachner, J.; Kaven, L.; Göppert, A.; Schmitt, R.H.; Tolio, T. Evaluation of Material Shortage Effect on Assembly Systems Considering Flexibility Levels. *Procedia CIRP* **2022**, *107*, 966–971. [CrossRef]
2. Carvalho, H.; Naghshineh, B.; Govindan, K.; Cruz-Machado, V. The Resilience of On-Time Delivery to Capacity and Material Shortages: An Empirical Investigation in the Automotive Supply Chain. *Comput. Ind. Eng.* **2022**, *171*, 108375. [CrossRef]
3. Jadhav, A.; Jadhav, V.S. A Review on 3D Printing: An Additive Manufacturing Technology. *Mater. Today Proc.* **2022**, *62*, 2094–2099. [CrossRef]
4. Kannan, D.; Shankar, K.M.; Gholipour, P. Paving the Way for a Green Transition through Mitigation of Green Manufacturing Challenges: A Systematic Literature Review. *J. Clean. Prod.* **2022**, *368*, 132578. [CrossRef]
5. Sharma, K.; Arora, R.; Nangia, R.; Singel, R.; Dharmveer; Dixit, S. Effects of Green Manufacturing and Technological Innovations on Sustainable Development. *Mater. Today Proc.* **2022**, *69*, 266–270. [CrossRef]
6. Prakash, A.; Arora, M.; Mittal, A.; Kampani, S.; Dixit, S. Green Manufacturing: Related Literature over the Past Decade. *Mater. Today Proc.* **2022**, *69*, 468–472. [CrossRef]
7. Ahn, D.-G. Direct Metal Additive Manufacturing Processes and Their Sustainable Applications for Green Technology: A Review. *Int. J. Precis. Eng. Manuf.—Green Technol.* **2016**, *3*, 381–395. [CrossRef]
8. Roberts, T.; Bartkova, B. *Additive Manufacturing Trend Report 2021: 3D Printing Market Growth in the Year of the COVID-19*; Hubs BV: Amsterdam, The Netherlands, 2021; pp. 1–16.
9. Derekar, K.S. A Review of Wire Arc Additive Manufacturing and Advances in Wire Arc Additive Manufacturing of Aluminium. *Mater. Sci. Technol.* **2018**, *34*, 895–916. [CrossRef]
10. Paolini, A.; Kollmannsberger, S.; Rank, E. Additive Manufacturing in Construction: A Review on Processes, Applications, and Digital Planning Methods. *Addit. Manuf.* **2019**, *30*, 100894. [CrossRef]

11. Singh, S.; Sharma, S.K.; Rathod, D.W. A Review on Process Planning Strategies and Challenges of WAAM. *Mater. Today Proc.* **2021**, *47*, 6564–6575. [CrossRef]
12. Betzler, B.R. Additive Manufacturing in the Nuclear Reactor Industry. *Encycl. Nucl. Energy* **2021**, *1*, 851–863. [CrossRef]
13. Li, Y.; Wu, S.; Wang, J.; Wang, H.; Kong, W.; Cheng, F. Microstructure Homogeneity and Strength-Toughness Balance in Submerged Arc Additive Manufactured Mn-Ni-Mo High-Strength Steel by Unique Intrinsic Heat Treatment. *J. Mater. Process. Technol.* **2022**, *307*, 117682. [CrossRef]
14. Evans, S.I.; Wang, J.; Qin, J.; He, Y.; Shepherd, P.; Ding, J. A Review of WAAM for Steel Construction—Manufacturing, Material and Geometric Properties, Design, and Future Directions. *Structures* **2022**, *44*, 1506–1522. [CrossRef]
15. Zhang, J.; Zhao, T.; Yi, Y.; An, Q.; Yanagimoto, J. Additive Manufacturing Assisted Fabrication of Octet Truss Structures Using Continuous Carbon Fibre Composites and the Resulting Mechanical Responses. *J. Mater. Process. Technol.* **2023**, *319*, 118089. [CrossRef]
16. Toth, A.D.; Padayachee, J.; Mahlatji, T.; Vilakazi, S. Report on Case Studies of Additive Manufacturing in the South African Railway Industry. *Sci. Afr.* **2022**, *16*, e01219. [CrossRef]
17. Busachi, A.; Erkoyuncu, J.; Colegrove, P.; Martina, F.; Ding, J. Designing a WAAM Based Manufacturing System for Defence Applications. *Procedia CIRP* **2015**, *37*, 48–53. [CrossRef]
18. Anand, M.; Bishwakarma, H.; Kumar, N.; Ujjwal, K.; Das, A.K. Fabrication of Multilayer Thin Wall by WAAM Technique and Investigation of Its Microstructure and Mechanical Properties. *Mater. Today Proc.* **2022**, *56*, 927–930. [CrossRef]
19. Al-Nabulsi, Z.; Mottram, J.T.; Gillie, M.; Kourra, N.; Williams, M.A. Mechanical and X Ray Computed Tomography Characterisation of a WAAM 3D Printed Steel Plate for Structural Engineering Applications. *Constr. Build. Mater.* **2021**, *274*, 121700. [CrossRef]
20. Vora, J.; Parmar, H.; Chaudhari, R.; Khanna, S.; Doshi, M.; Patel, V. Experimental Investigations on Mechanical Properties of Multi-Layered Structure Fabricated by GMAW-Based WAAM of SS316L. *J. Mater. Res. Technol.* **2022**, *20*, 2748–2757. [CrossRef]
21. Su, G.; Shi, Y.; Li, G.; Zhang, G.; Xu, Y. Improving the Deposition Efficiency and Mechanical Properties of Additive Manufactured Inconel 625 through Hot Wire Laser Metal Deposition. *J. Mater. Process. Technol.* **2023**, *322*, 118175. [CrossRef]
22. Jackson, M.A.; Van Asten, A.; Morrow, J.D.; Min, S.; Pfefferkorn, F.E. A Comparison of Energy Consumption in Wire-Based and Powder-Based Additive-Subtractive Manufacturing. *Procedia Manuf.* **2016**, *5*, 989–1005. [CrossRef]
23. Singh, S.R.; Khanna, P. Wire Arc Additive Manufacturing (WAAM): A New Process to Shape Engineering Materials. *Mater. Today Proceed.* **2021**, *44*, 118–128. [CrossRef]
24. Martina, F.; Mehnen, J.; Williams, S.W.; Colegrove, P.; Wang, F. Investigation of the Benefits of Plasma Deposition for the Additive Layer Manufacture of Ti-6Al-4V. *J. Mater. Process. Technol.* **2012**, *212*, 1377–1386. [CrossRef]
25. Roschli, A.; Gaul, K.T.; Boulger, A.M.; Post, B.K.; Chesser, P.C.; Love, L.J.; Blue, F.; Borish, M. Designing for Big Area Additive Manufacturing. *Addit. Manuf.* **2019**, *25*, 275–285. [CrossRef]
26. Brackett, J.; Yan, Y.; Cauthen, D.; Kishore, V.; Lindahl, J.; Smith, T.; Sudbury, Z.; Ning, H.; Kunc, V.; Duty, C. Characterizing Material Transitions in Large-Scale Additive Manufacturing. *Addit. Manuf.* **2021**, *38*, 101750. [CrossRef]
27. Kampker, A.; Triebs, J.; Kawollek, S.; Ayvaz, P.; Hohenstein, S. Review on Machine Designs of Material Extrusion Based Additive Manufacturing (AM) Systems—Status-Quo and Potential Analysis for Future AM Systems. *Procedia CIRP* **2019**, *81*, 815–819. [CrossRef]
28. Robles Poblete, F.; Ireland, M.; Slattery, L.; Davids, W.G.; Lopez-Anido, R.A. In Situ, Real-Time Temperature Mapping and Thermal FE Simulations of Large-Format 3D Printed PETG/CF Vertical Wall. *Materials* **2023**, *16*, 6486. [CrossRef] [PubMed]
29. Paranthaman, M.P.; Yildirim, V.; Lamichhane, T.N.; Begley, B.A.; Post, B.K.; Hassen, A.A.; Sales, B.C.; Gandha, K.; Nlebedim, I.C. Additive Manufacturing of Isotropic NdFeB PPS Bonded Permanent Magnets. *Materials* **2020**, *13*, 3319. [CrossRef]
30. Kawalkar, R.; Dubey, H.K.; Lokhande, S.P. Wire Arc Additive Manufacturing: A Brief Review on Advancements in Addressing Industrial Challenges Incurred with Processing Metallic Alloys. *Mater. Today Proc.* **2022**, *50*, 1971–1978. [CrossRef]
31. Nurhudan, A.I.; Supriadi, S.; Whulanza, Y.; Saragih, A.S. Additive Manufacturing of Metallic Based on Extrusion Process: A Review. *J. Manuf. Process.* **2021**, *66*, 228–237. [CrossRef]
32. Clare, A.T.; Mishra, R.S.; Merklein, M.; Tan, H.; Todd, I.; Chechik, L.; Li, J.; Bambach, M. Alloy Design and Adaptation for Additive Manufacture. *J. Mater. Process. Technol.* **2022**, *299*, 117358. [CrossRef]
33. Sun, J.; Ye, D.; Zou, J.; Chen, X.; Wang, Y.; Yuan, J.; Liang, H.; Qu, H.; Binner, J.; Bai, J. A Review on Additive Manufacturing of Ceramic Matrix Composites. *J. Mater. Sci. Technol.* **2023**, *138*, 1–16. [CrossRef]
34. Li, J.; Durandet, Y.; Huang, X.; Sun, G.; Ruan, D. Additively Manufactured Fiber-Reinforced Composites: A Review of Mechanical Behavior and Opportunities. *J. Mater. Sci. Technol.* **2022**, *119*, 219–244. [CrossRef]
35. Riquelme, A.; Sánchez de Rojas Candela, C.; Rodrigo, P.; Rams, J. Influence of Process Parameters in Additive Manufacturing of Highly Reinforced 316L/SiCp Composites. *J. Mater. Process. Technol.* **2022**, *299*, 117325. [CrossRef]
36. Gregor-Svetec, D.; Leskovšek, M.; Vrabič Brodnjak, U.; Stankovič Elesini, U.; Muck, D.; Urbas, R. Characteristics of HDPE/Cardboard Dust 3D Printable Composite Filaments. *J. Mater. Process. Technol.* **2020**, *276*, 116379. [CrossRef]
37. Cacace, S.; Furlan, V.; Sorci, R.; Semeraro, Q.; Boccadoro, M. Using Recycled Material to Produce Gas-Atomized Metal Powders for Additive Manufacturing Processes. *J. Clean. Prod.* **2020**, *268*, 122218. [CrossRef]
38. Hart, K.R.; Frketic, J.B.; Brown, J.R. Recycling Meal-Ready-to-Eat (MRE) Pouches into Polymer Filament for Material Extrusion Additive Manufacturing. *Addit. Manuf.* **2018**, *21*, 536–543. [CrossRef]

39. Dritsas, S.; Fernandez, J.G. Towards Sustainable Additive Manufacturing Using Fungus-like Adhesive Materials. *Mater. Today Proc.* **2022**, *70*, 418–424. [CrossRef]
40. Ren, L.; Wang, Z.; Ren, L.; Han, Z.; Liu, Q.; Song, Z. Graded Biological Materials and Additive Manufacturing Technologies for Producing Bioinspired Graded Materials: An Overview. *Compos. Part B Eng.* **2022**, *242*, 110086. [CrossRef]
41. *ASTM ISO/ASTM52900-15*; Standard Terminology for Additive Manufacturing—General Principles—Terminology. ASTM International: West Conshohocken, PA, USA, 2015.
42. Ahn, D.-G. Directed Energy Deposition (DED) Process: State of the Art. *Int. J. Precis. Eng. Manuf.-Green Technol.* **2021**, *8*, 703–742. [CrossRef]
43. Chaturvedi, M.; Scutelnicu, E.; Rusu, C.C.; Mistodie, L.R.; Mihailescu, D.; Vendan, S.A. Wire Arc Additive Manufacturing: Review on Recent Findings and Challenges in Industrial Applications and Materials Characterization. *Metals* **2021**, *11*, 939. [CrossRef]
44. Rodríguez-González, P.; Ruiz-Navas, E.M.; Gordo, E. Wire Arc Additive Manufacturing (WAAM) for Aluminum-Lithium Alloys: A Review. *Materials* **2023**, *16*, 1375. [CrossRef] [PubMed]
45. Jiang, D.; Ning, F. Physical-Mechanical Behaviors of Stainless Steel Plate-Lattice Built by Material Extrusion Additive Manufacturing. *J. Mater. Process. Technol.* **2022**, *309*, 117739. [CrossRef]
46. Li, Y.; Han, Q.; Horváth, I.; Zhang, G. Repairing Surface Defects of Metal Parts by Groove Machining and Wire + Arc Based Filling. *J. Mater. Process. Technol.* **2019**, *274*, 116268. [CrossRef]
47. Liu, W.; Deng, K.; Wei, H.; Zhao, P.; Li, J.; Zhang, Y. A Decision-Making Model for Comparing the Energy Demand of Additive-Subtractive Hybrid Manufacturing and Conventional Subtractive Manufacturing Based on Life Cycle Method. *J. Clean. Prod.* **2021**, *311*, 127795. [CrossRef]
48. Priarone, P.C.; Ingarao, G. Towards Criteria for Sustainable Process Selection: On the Modelling of Pure Subtractive versus Additive/Subtractive Integrated Manufacturing Approaches. *J. Clean. Prod.* **2017**, *144*, 57–68. [CrossRef]
49. Lu, X.; Li, M.V.; Yang, H. Comparison of Wire-Arc and Powder-Laser Additive Manufacturing for IN718 Superalloy: Unified Consideration for Selecting Process Parameters Based on Volumetric Energy Density. *Int. J. Adv. Manuf. Technol.* **2021**, *114*, 1517–1531. [CrossRef]
50. Campatelli, G.; Montevecchi, F.; Venturini, G.; Ingarao, G.; Priarone, P.C. Integrated WAAM-Subtractive Versus Pure Subtractive Manufacturing Approaches: An Energy Efficiency Comparison. *Int. J. Precis. Eng. Manuf.-Green Technol.* **2020**, *7*, 1–11. [CrossRef]
51. Tanabi, N.; Silva, A.M.; Pessoa, M.A.O.; Tsuzuki, M.S.G. Robust Algorithm Software for NACA 4-Digit Airfoil Shape Optimization Using the Adjoint Method. *Appl. Sci.* **2023**, *13*, 4269. [CrossRef]
52. González, J.; Rodríguez, I.; Prado-Cerqueira, J.L.; Diéguez, J.L.; Pereira, A. Additive Manufacturing with GMAW Welding and CMT Technology. *Procedia Manuf.* **2017**, *13*, 840–847. [CrossRef]
53. Ramarao, M.; King, M.F.L.; Sivakumar, A.; Manikandan, V.; Vijayakumar, M.; Subbiah, R. Optimizing GMAW Parameters to Achieve High Impact Strength of the Dissimilar Weld Joints Using Taguchi Approach. *Mater. Today Proc.* **2022**, *50*, 861–866. [CrossRef]
54. Ding, J.; Colegrove, P.; Martina, F.; Williams, S.; Wiktorowicz, R.; Palt, M.R. Development of a Laminar Flow Local Shielding Device for Wire + Arc Additive Manufacture. *J. Mater. Process. Technol.* **2015**, *226*, 99–105. [CrossRef]
55. Wang, Z.; Zimmer-Chevret, S.; Léonard, F.; Abba, G. Improvement Strategy for the Geometric Accuracy of Bead's Beginning and End Parts in Wire-Arc Additive Manufacturing (WAAM). *Int. J. Adv. Manuf. Technol.* **2022**, *118*, 2139–2151. [CrossRef]
56. Xiong, J.; Li, Y.; Li, R.; Yin, Z. Influences of Process Parameters on Surface Roughness of Multi-Layer Single-Pass Thin-Walled Parts in GMAW-Based Additive Manufacturing. *J. Mater. Process. Technol.* **2018**, *252*, 128–136. [CrossRef]
57. Williams, S.; Martina, F.; Wood, D.; Colomo, A.G. A Comparison Framework to Support the Selection of the Best Additive Manufacturing Process for Specific Aerospace Applications. *Int. J. Rapid Manuf.* **2020**, *9*, 194–211. [CrossRef]
58. Liu, Z.Y.; Li, C.; Fang, X.Y.; Guo, Y.B. Energy Consumption in Additive Manufacturing of Metal Parts. *Procedia Manuf.* **2018**, *26*, 834–845. [CrossRef]
59. Campatelli, G.; Campanella, D.; Barcellona, A.; Fratini, L.; Grossi, N.; Ingarao, G. Microstructural, Mechanical and Energy Demand Characterization of Alternative WAAM Techniques for Al-Alloy Parts Production. *CIRP J. Manuf. Sci. Technol.* **2020**, *31*, 492–499. [CrossRef]
60. Warsi, R.; Kazmi, K.H.; Chandra, M. Mechanical Properties of Wire and Arc Additive Manufactured Component Deposited by a CNC Controlled GMAW. *Mater. Today Proc.* **2022**, *56*, 2818–2825. [CrossRef]
61. Chernovol, N.; Sharma, A.; Tjahjowidodo, T.; Lauwers, B.; Rymenant, P. Van Machinability of Wire and Arc Additive Manufactured Components. *CIRP J. Manuf. Sci. Technol.* **2021**, *35*, 379–389. [CrossRef]
62. Bociaga, E. Effect of Mould Temperature and Injection Speed on Selected Properties of Polyethylene Mouldings. *Int. Polym. Sci. Technol.* **2001**, *28*, 96–102. [CrossRef]
63. Lopes, J.G.; Machado, C.M.; Duarte, V.R.; Rodrigues, T.A.; Santos, T.G.; Oliveira, J.P. Effect of Milling Parameters on HSLA Steel Parts Produced by Wire and Arc Additive Manufacturing (WAAM). *J. Manuf. Process.* **2020**, *59*, 739–749. [CrossRef]
64. Dinovitzer, M.; Chen, X.; Laliberte, J.; Huang, X.; Frei, H. Effect of Wire and Arc Additive Manufacturing (WAAM) Process Parameters on Bead Geometry and Microstructure. *Addit. Manuf.* **2019**, *26*, 138–146. [CrossRef]
65. Nagasai, B.P.; Malarvizhi, S.; Balasubramanian, V. Effect of Welding Processes on Mechanical and Metallurgical Characteristics of Carbon Steel Cylindrical Components Made by Wire Arc Additive Manufacturing (WAAM) Technique. *CIRP J. Manuf. Sci. Technol.* **2022**, *36*, 100–116. [CrossRef]

66. Zhang, C.; Shen, C.; Hua, X.; Li, F.; Zhang, Y.; Zhu, Y. Influence of Wire-Arc Additive Manufacturing Path Planning Strategy on the Residual Stress Status in One Single Buildup Layer. *Int. J. Adv. Manuf. Technol.* **2020**, *111*, 797–806. [CrossRef]
67. Wang, X.; Wang, A.; Li, Y. A Sequential Path-Planning Methodology for Wire and Arc Additive Manufacturing Based on a Water-Pouring Rule. *Int. J. Adv. Manuf. Technol.* **2019**, *103*, 3813–3830. [CrossRef]
68. Chen, X.; Kong, F.; Fu, Y.; Zhao, X.; Li, R.; Wang, G.; Zhang, H. A Review on Wire-Arc Additive Manufacturing: Typical Defects, Detection Approaches, and Multisensor Data Fusion-Based Model. *Int. J. Adv. Manuf. Technol.* **2021**, *117*, 707–727. [CrossRef]
69. Thien, A.; Saldana, C.; Kurfess, T. The Effect of WAAM Process Parameters on Process Conditions and Production Metrics in the Fabrication of Single-Pass Multi-Layer Wall Artifacts. *Int. J. Adv. Manuf. Technol.* **2022**, *119*, 531–547. [CrossRef]
70. Zhang, H.; Liu, W.; Zhao, X.; Zhang, X.; Chen, C. Improvement in Microstructure and Properties of 304 Steel Wire Arc Additive Manufacturing by the Micro-Control Deposition Trajectory. *Materials* **2024**, *17*, 1170. [CrossRef]
71. Garaigordobil, A.; Ansola, R.; Veguería, E.; Fernandez, I. Overhang Constraint for Topology Optimization of Self-Supported Compliant Mechanisms Considering Additive Manufacturing. *CAD Comput. Aided Des.* **2019**, *109*, 33–48. [CrossRef]
72. Doubrovski, Z.; Verlinden, J.C.; Geraedts, J.M.P. Optimal Design for Additive Manufacturing: Opportunities and Challenges. In *Volume 9: 23rd International Conference on Design Theory and Methodology; 16th Design for Manufacturing and the Life Cycle Conference; ASMEDC, Proceedings of the 23rd International Conference on Design Theory and Methodology, Washington, DC, USA, 28–31 August 2011*; ASME: New York, NY, USA, 2011; pp. 635–646.
73. Zhang, J.; Cao, Q.; Lu, W.F. A Review on Design and Removal of Support Structures in Metal Additive Manufacturing. *Mater. Today Proc.* **2022**, *70*, 407–411. [CrossRef]
74. Li, Y.; Huang, X.; Horváth, I.; Zhang, G. GMAW-Based Additive Manufacturing of Inclined Multi-Layer Multi-Bead Parts with Flat-Position Deposition. *J. Mater. Process. Technol.* **2018**, *262*, 359–371. [CrossRef]
75. Xu, T.; Cui, Y.; Ma, S.; Wang, J.; Liu, C. Exploring the Inclined Angle Limit of Fabricating Unsupported Rods Structures by Pulse Hot-Wire Arc Additive Manufacturing. *J. Mater. Process. Technol.* **2021**, *295*, 117160. [CrossRef]
76. Liu, B.; Shen, H.; Zhou, Z.; Jin, J.; Fu, J. Research on Support-Free WAAM Based on Surface/Interior Separation and Surface Segmentation. *J. Mater. Process. Technol.* **2021**, *297*, 117240. [CrossRef]
77. Circutor Circutor C-80 System Analyser. Balanced Three-Phase Portable Power Analyzer 2005. Available online: https://circutor.com/productos/analizadores-de-redes-portatiles/analizadores-de-red-portatiles/analizador-de-redes-portatil-monofasico-o-trifasico-equilibrado/product/M80120./ (accessed on 8 June 2024).
78. AITIIP FUNDATION. Hybrid Automated Machine Integrating Concurrent Manufacturing Processes, Increasing the Production Volume of Functional on-Demand Using High Multi-Material Deposition Rates Fact Sheet Project Information 2019. Available online: https://cordis.europa.eu/project/id/723759/reporting (accessed on 8 June 2024).
79. COMAU COMAU NJ130. 6-Axes Collaborative Robotic Arm 2010. Available online: https://www.comau.com/en/competencies/robotics-automation/robot-team/nj-130-2-0/ (accessed on 8 June 2024).
80. Open Mind Technologies. *HyperMILL CAD/CAM Software*, (version 2023) Windows; Open Mind Technologies: Weßling, Germany, 2023.
81. Ultimaker. *UltiMaker Cura 2023*, v. 5.6.0; Ultimaker: Utrecht, The Netherlands, 2023.
82. Fronius Fronius TPS 400i. MIG/MAG Welding System 2018. Available online: https://www.fronius.com/es-es/spain/tecnologia-de-soldadura/productos/soldadura-manual/migmag/tpsi/tpsi/tps-400i (accessed on 8 June 2024).
83. Keyence CMOS Multi-Function Analogue Laser Sensor. Laser Differentiation Displacement Sensor 2010. Available online: https://www.keyence.com/products/sensor/positioning/il/ (accessed on 8 June 2024).
84. OPTRIS OPTRIS—3MH CF. Micro Size Infrared Thermometer for Precise Temperature Measurement of Metal from 50 to 600 °C 2018. Available online: https://www.optris.com/es/producto/termometros-infrarrojos/serie-ct/ct-3m/ (accessed on 8 June 2024).
85. Fundacion Tekniker. Development of Thermoplastic Press-Forming Tool for Advanced Rear End Closing Frame Prototype and Tooling 4.0 for Assembly and Transportation of the Advanced Rear End Prototype 2022. Available online: https://cordis.europa.eu/project/id/886491 (accessed on 8 June 2024).
86. Khalid, M.Y.; Arif, Z.U.; Rashid, A. Al Investigation of Tensile and Flexural Behavior of Green Composites along with Their Impact Response at Different Energies. *Int. J. Precis. Eng. Manuf.-Green Technol.* **2022**, *9*, 1399–1410. [CrossRef]
87. Choi, J.Y.; Jeon, J.H.; Lyu, J.H.; Park, J.; Kim, G.Y.; Chey, S.Y.; Quan, Y.-J.; Bhandari, B.; Prusty, B.G.; Ahn, S.-H. Current Applications and Development of Composite Manufacturing Processes for Future Mobility. *Int. J. Precis. Eng. Manuf.-Green Technol.* **2022**, *10*, 269–291. [CrossRef]
88. Li, X.-P.; Zhao, G.-Q.; Guan, Y.-J.; Ma, M.-X. Optimal Design of Heating Channels for Rapid Heating Cycle Injection Mold Based on Response Surface and Genetic Algorithm. *Mater. Des.* **2009**, *30*, 4317–4323. [CrossRef]
89. HEXAGON Leica T-Scan 5 2015. Available online: https://hexagon.com/products/leica-t-scan-5 (accessed on 8 June 2024).
90. *ISO 14175:2008*; Welding Consumables—Gases and Gas Mixtures for Fusion Welding and Allied Processes. International Organization for Standardization: Geneva, Switzerland, 2008.

Artículo 2

Improvements in Injection Moulds Cooling and Manufacturing Efficiency Achieved by Wire Arc Additive Manufacturing Using Conformal Cooling Concept

Alejandro Marqués, Jose Antonio Dieste, Iván Monzón, Alberto Laguía, Pascual Gracia, Carlos Javierre, Isabel Clavería y Daniel Elduque. (2024).

Polymers 2024, 16(21), 3057

DOI: 10.3390/polym16213057

Impact Factor: 4.700 (JCR 2023); Q1. Polymer science.

Este artículo examina las capacidades de la tecnología WAAM para fabricar elementos complejos de gran tamaño, centrándose en el diseño y la fabricación de un molde macho para inyección de plástico. Este molde requiere de canales térmicos internos para su funcionamiento. Dichos canales se han diseñado bajo el concepto *Conformal Cooling.* Este enfoque permite que los canales se adapten a la geometría de la superficie a inyectar, optimizando el proceso de enfriamiento y mejorando la calidad de las piezas obtenidas.

El diseño avanzado de los canales térmicos fue posible gracias a las capacidades únicas de la tecnología WAAM para fabricar geometrías complejas. Con este diseño, se fabricó el utillaje, monitorizando sus parámetros de proceso. Paralelamente, se diseñó un molde teórico alternativo, basado en las limitaciones de los métodos de fabricación convencionales, con el objetivo de comparar el rendimiento de ambos utillajes. Este molde presentó canales térmicos de diseño simplificado y centrado, alejados de la geometría de la pieza, debido a las restricciones técnicas de las tecnologías tradicionales de fabricación.

Para evaluar el rendimiento de ambos moldes, se utilizó el software CADMOULD v16, realizando un análisis comparativo del ciclo de enfriamiento. Los resultados mostraron que el molde WAAM ofreció ventajas significativas, incluyendo un mayor calor extraído durante el ciclo (derivando en una mejora del tiempo de ciclo) y una mayor homogeneidad térmica lograda.

Por último, se realizó un estudio sobre la sostenibilidad del proceso WAAM, centrado en el consumo de material. Los datos recogidos del proceso aditivo se compararon con una estimación teórica del material requerido por el método convencional. Este análisis destacó la eficiencia del proceso WAAM, con una notable reducción tanto en el material total utilizado, como en el material descartado. Estos resultados subrayan las ventajas de la tecnología WAAM en términos de sostenibilidad y eficiencia productiva.

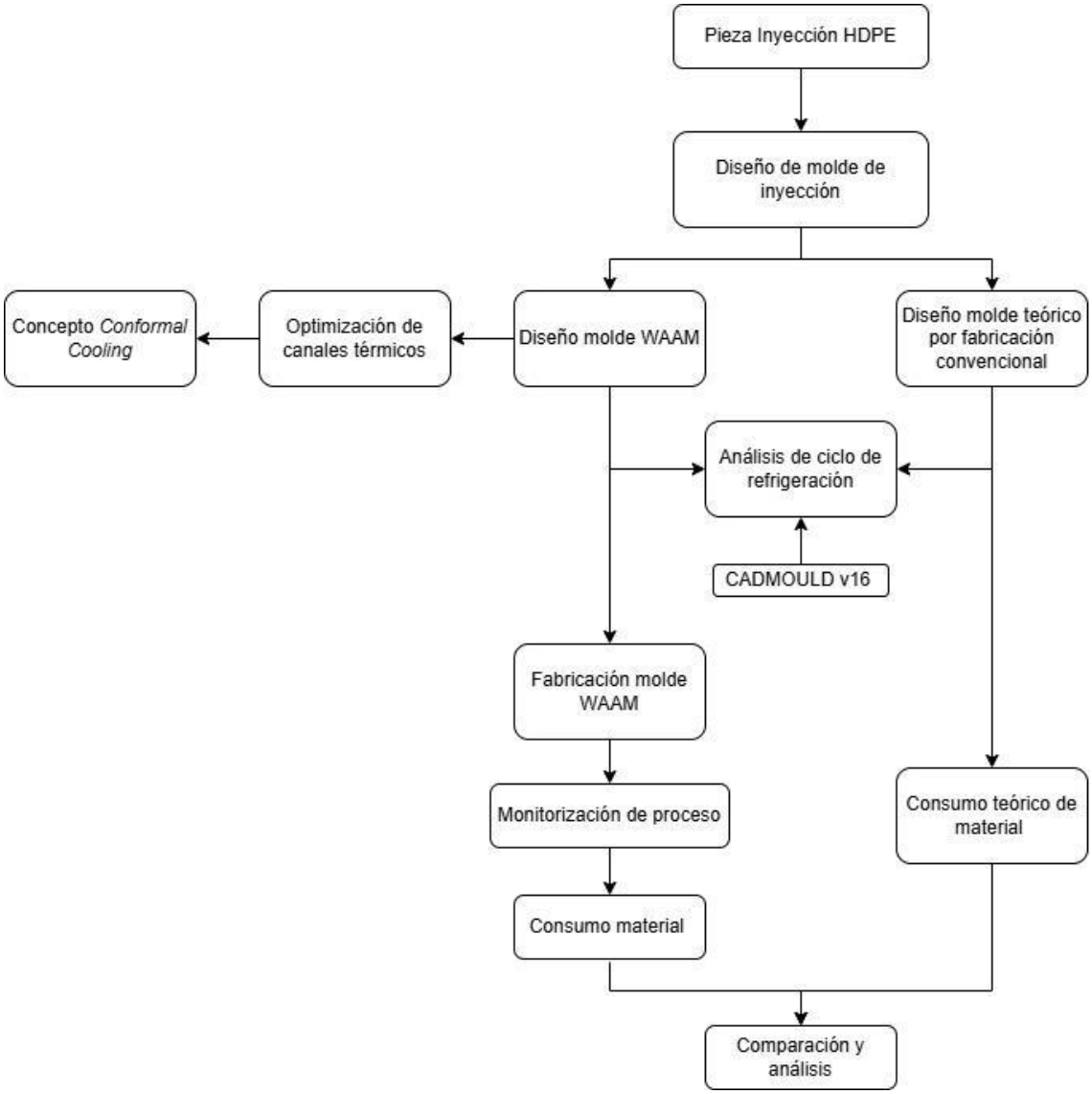

Ilustración 18 Esquema de los trabajos realizados en el artículo 2 pata la optimización canales térmicos internos en molde de inyección WAAM y su comparación con un molde teórico realizado por métodos de fabricación convencionales

polymers

MDPI

Article

Improvements in Injection Moulds Cooling and Manufacturing Efficiency Achieved by Wire Arc Additive Manufacturing Using Conformal Cooling Concept

Alejandro Marqués [1,*], Jose Antonio Dieste [1], Iván Monzón [1], Alberto Laguía [1], Pascual Gracia [1], Carlos Javierre [2], Isabel Clavería [2] and Daniel Elduque [2]

[1] R&D Department, Aitiip Fundation, Empresarium Industrial Site, C/Romero, No. 12, 50720 Zaragoza, Spain; joseantonio.dieste@aitiip.com (J.A.D.); ivan.monzon@aitiip.com (I.M.); alberto.laguia@aitiip.com (A.L.); pascual.gracia@aitiip.com (P.G.)

[2] Department of Mechanical Engineering, University of Zaragoza, C/María de Luna, 50720 Zaragoza, Spain; carlos.javierre@unizar.es (C.J.); iclaver@unizar.es (I.C.); delduque@unizar.es (D.E.)

* Correspondence: alejandro.marques@aitiip.com

Abstract: The plastic injection moulding industry is a constantly developing industrial field. This industrial process requires the manufacturing of metal moulds using complex heating and cooling systems. The purpose of this research is to optimize both the plastic injection moulding process and the mould manufacturing process itself by combining practices in this industry with current additive manufacturing technologies, specifically Wire Arc Additive Manufacturing (WAAM) technology. A mould punch was manufactured by using both WAAM technology, whose internal cooling system has been designed under the concept of Conformal Cooling, and conventional cooling channel designs and manufacturing techniques in order to carry out a comparative analysis. Theoretical results obtained by CAE methods showed an improvement in heat extraction in the WAAM mould. In addition, the WAAM mould was able to achieve better temperature homogeneity in the final part, minimizing deformations in the final part after extraction. Finally, the WAAM manufacturing process was proven to be more efficient in terms of material consumption than the conventional mould, reducing the buy-to-fly ratio of the part by 5.11.

Keywords: additive manufacturing; big area additive manufacturing; injection moulding; wire arc additive manufacturing; conformal cooling

Citation: Marqués, A.; Dieste, J.A.; Monzón, I.; Laguía, A.; Gracia, P.; Javierre, C.; Clavería, I.; Elduque, D. Improvements in Injection Moulds Cooling and Manufacturing Efficiency Achieved by Wire Arc Additive Manufacturing Using Conformal Cooling Concept. *Polymers* **2024**, *16*, 3057. https://doi.org/10.3390/polym16213057

Academic Editor: Andrea Sorrentino

Received: 23 September 2024
Revised: 24 October 2024
Accepted: 29 October 2024
Published: 30 October 2024

1. Introduction

Today's industry trends demand large batches of identical parts in a short time and at minimal cost. This situation has led to the development of the injection moulding industry. This industry has not stopped growing year by year, with an estimated market size of $261.8 billion in 2021, and an estimated growth of 4.8% by 2030 according to the Grand View Research database [1].

Plastic injection moulding leads the market due to its capacity to produce large batches of parts, as mentioned, as well as the ability of this process to maintain high standards of precision, its customization capabilities, and the outstanding final quality this technology offers [2]. Moreover, thanks to the high optimization of this process [3–5], plastic has replaced other conventional materials such as metal, ceramic, or glass in certain industries [6,7].

Plastics Europe reports that, out of all the types of plastics available, the thermoplastic variations [8], namely polypropylene (PP), low-density polyethylene (LDPE), and high-density polyethylene (HDPE), are the most sought after. HDPE, in particular, accounts for 12% of the overall plastic demand in Europe [9]. This polymer is enormously

versatile, and it is suited to a wide range of applications. The producer or converter can modify the impact and tear resistance, transparency, tactility, flexibility, formability, and the coating/laminating/printing capability of polyethylene by adjusting its formulation and thickness [10]. HDPE can be recycled, and many products, including bin bags, agricultural films, park benches, bollards, and waste bins, use recycled polyethylene [11,12]. Moreover, due to its high calorific value, this thermoplastic is also an excellent candidate for energy recovery through clean incineration [13,14]. These properties make HDPE quite a common material in various industries, such as packaging [15], construction [16,17], agriculture [18,19], healthcare [20,21] and automobility [22].

Focusing on the injection moulding process, it can be broken down into five stages: mould filling, packing, cooling, plasticizing, and ejection of the finished product [23]. Regarding mould filling, this process is conducted in toolings in which, by means of temperature and pressure, the geometry of the part is formed, the so-called moulds, consisting of two parts, the punch and the cavity. One of the key issues in this process is the design and optimization of the heating and cooling channels for the injected material, with the cooling process being the most influential in terms of total cycle time, representing between 50% and 70% of it [24]. In addition, throughout the cooling cycle of the injected part, the temperature distribution in the mould and its cooling rate are critical for the quality of the injected part. Insufficient or non-uniform cooling can affect the part geometry, shrinking or deforming it [25,26]. In addition, a non-uniform temperature distribution may also cause undesirable effects on the part, which can be observed in its surface finish (such as poor surface finish areas or the appearance of shiny spots) [27].

Conventional cooling methods, based on drilling or the use of bubblers, baffles, and isobars on the mould, are producible by conventional manufacturing methods. This procedure is suitable for simple final part geometries; however, it is not appropriate when the part to be injected is geometrically complex [28]. With an emphasis on the cooling cycle of the final parts, the concept of Conformal Cooling (CC) was developed. Based on this concept, the cooling channels of the moulds are designed to follow the shape of the final part [29–32], seeking to minimize the distance between the cooling source and the plastic injected part. This optimization results in enhanced heat transfer with the final part, which in turn improves cycle time [33–35]. In addition, several studies have shown significant improvements in heat distribution across the tooling [36,37], a reduction in the process temperature obtained through channel optimization [38], and a reduction in final part deformation [39]. However, in larger moulds, the manufacturing of these channels is usually complex due to the limitations of the machining processes themselves [40]. For this reason, a mould whose cooling system is based on the CC concept requires, in most instances, advanced manufacturing methods. As common manufacturing methods only allow for straight holes to be drilled, adapting the channels to the shape of complex geometries requires intricate successions of straight holes, which demands multiple secondary operations, like plugging the channels, polishing the plug area, etc. Another method of fabrication would be to design inserts for the areas of the channels where their geometry does not allow straight holes to be drilled. These inserts could consist of several pieces, separately machined and installed in the indicated area of the mould. This method has the disadvantage of adding secondary parts to the mould, which must be adjusted after installation, making the system even more complex. For both cases, an added problem is the increased possibility of leaks, as the number of areas requiring a perfect seal increases. For these reasons, Conformal Cooling designed channels generally cannot be achieved by conventional machining methods, making it necessary to resort to technologies such as additive manufacturing (AM) [41]. It should be noted that the CC concept is applicable to any manufacturing process involving a thermal cycle of heating and cooling by means of fluid, such as injection moulding (as in the case of the current study), thermoforming, press-forming, etc.

The industrial use of additive manufacturing has become increasingly important, and it has already demonstrated its full applicability in the plastic injection moulding field

[42–44]. AM is being utilized to manufacture efficiently functioning metallic parts, and its use is becoming more widespread in several industries. This technology is highly researched due to its ability to produce complex geometries while maintaining high mechanical properties [45–47]. In addition, it has the potential to save both materials and energy compared to traditional manufacturing methods [48–50]. One notable aspect of AM is the procedure known as BAAM (Big Area Additive Manufacturing), which is a dimensional specification of AM processes. BAAM includes additive manufacturing machines that can create larger dimensions than standard 3D printers (400 × 400 × 200 mm) and produce printed volumes of several cubic meters [51–53].

AM is a widely used manufacturing process in several industries, and it has the advantage of working with different materials, among other benefits. Focusing on the plastic injection moulding process, due to the high mechanical and thermal requirements of the moulds, as well as their need for manufacturing large parts, the possibilities for AM in terms of filler materials are restricted to the use of metallic materials. This technology is known as Metallic Additive Manufacturing (MAM) [54,55]. Regarding MAM technologies, depending on the filler material used, we can name two main groups: powder-feed technologies and wire-feed technologies [56,57]. For the specific case of large toolings, the printing area limitations of powder-feed technologies (limited to maximum dimensions of 300 × 300 mm for the printing bed, with part heights of less than 500 mm) make them unfeasible.

On the other hand, wire-feed technologies are capable of manufacturing large metal parts by the superposition of welding layers [58]. This process can be performed by a collaborative robot adapted to the additive process, eliminating the size limitation of the printing base [59]. Wire Arc Additive Manufacturing (WAAM) is the most representative technology within this group. It can be defined as a manufacturing process which involves the use of an electric arc to melt the apported electrode, creating layers with the deposited material. In this study, the chosen WAAM method has been Gas Metal Arc Welding (GMAW) [60]. In this welding process, an electric arc is generated between a consumable electrode and the workpiece, generating high temperatures that melt the upper surface layers of the base metal and the tip of the electrode. At this point, the electrode molten metal is deposited onto the upper molten surface layer of the workpiece, creating a unique metallic part. An inert gas-protected atmosphere, wire feed, and welding current are the main inputs required by the system [61,62]. This process presents several advantages, such as a high deposition rate, low equipment costs, and a small amount of residues. On the other hand, it should be noted that this process is relatively young and is therefore not developed to the same level as conventional manufacturing systems. In addition, another sensitive point to consider is the limited quality of the printed surfaces, making a post-processing of the surfaces with precision finishing requirements indispensable [63,64]. The consequence of these circumstances is the need to design a specific CAD (computer-aided design) for AM, removing certain features such as threads or small holes that should be manufactured in the second-stage post-processing. In addition, due to the necessity of removing material to achieve a high-quality final part, this AM specific design must have a design that includes over-thickness on the outer surface, which will then be machined [65–67]. This over-thickness also serves as a safety element in the event of a failure of the printing process. Another circumstance that must be considered during the design stage is the process temperature of the WAAM system. During this additive process, the material reaches temperatures of up to 450 °C, expanding the geometry. To compensate for this expansion, the part must be designed taking into account this shrinkage, so that the cold tooling accomplishes the target geometry. This specific CAD has been named WAAM-process-adapted CAD.

Based on the information presented, there is a lack of literature regarding large-size tooling designed according to the CC concept. The use of Metal Additive Manufacturing is shown to be the most suitable for the fabrication of these tools. However, the scale restrictions imposed by contemporary technologies have prevented this phenomenon from

being fully developed. Therefore, the objective of this paper will be the study of a large punch mould manufactured by WAAM technology, designed according to the CC concept. The manufacturing parameters of this mould, as well as the performance of its cooling system, will be compared with those of an identical theoretical mould, with a conventional cooling system, machined by conventional manufacturing techniques.

2. Materials and Methods

As introduced, the aim of this article is the manufacturing comparison of two similar large-dimension moulds (Figure 1), with sizes of approximately 820 × 1510 × 512 mm, in terms of manufacturing parameters and cooling performance.

The first mould is based on the concept of Conformal Cooling, for which cooling channels adapted to the shape of the final part have been designed. This mould has been manufactured by Metal Additive Manufacturing, specifically by WAAM technology, due to the complexity of the design, which is not achievable by conventional manufacturing methods. This mould is henceforth named the WAAM mould for easy identification. On the other hand, the second mould, which will be called the Conventional mould, was used as a reference to compare with the WAAM mould. This Conventional mould was designed to be completely manufacturable by conventional manufacturing processes; therefore, its cooling channels were simplified, moving away from the concept of Conformal Cooling.

First, a comparison was made at the design level, emphasizing the differences between the two moulds derived from the manufacturing point of view.

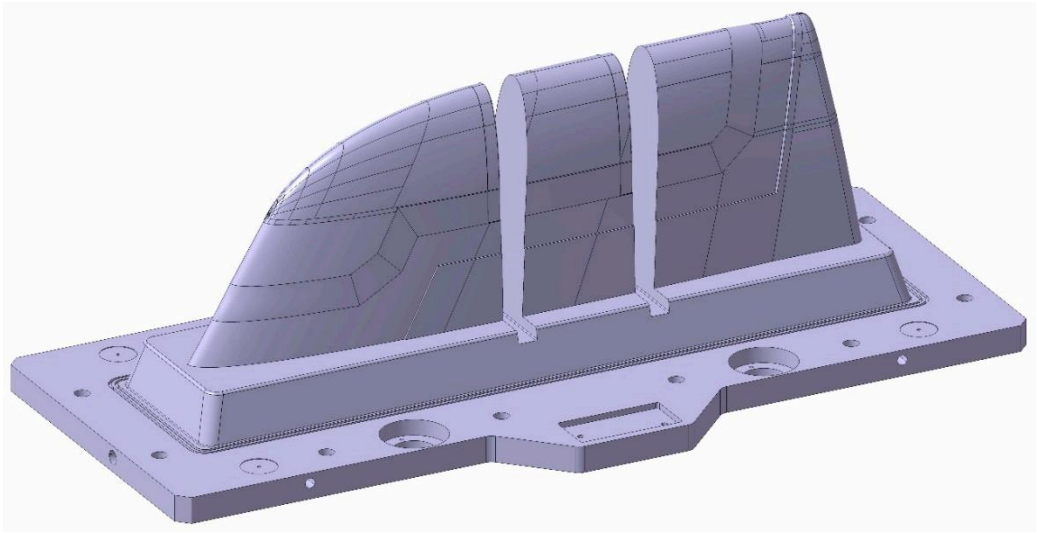

Figure 1. Final mould design CAD.

Based on the initial design analysis, a comparison was made between the manufacturing processes of the Conventional mould and the WAAM mould. For this purpose, emphasis was placed on the design differences depending on the manufacturing process, as well as on the material consumptions in both processes.

It should be mentioned that the total mould assembly has two parts: punch and cavity. The study is based on the design and manufacturing of the mould punch, as it is the most suitable to be manufactured by additive manufacturing methods; therefore, we always refer to this part of the mould in this article. Regarding the mould cavity, its design and manufacturing were carried out following conventional manufacturing criteria. This decision was based on two main reasons:

- The main concept to be analyzed during this manufacturing study was the ability of the WAAM system to manufacture internal channels according to the Conformal Cooling concept. In the case of the cavity mould, this type of design strategy could

be achieved by conventional manufacturing methods with few geometrical constraints and therefore was not of interest for the study.

- During the study, only one WAAM manufacturing system was available. Consequently, the simultaneous fabrication of both parts of the mould was not possible and would have taken excessive manufacturing time.

The design of the cavity mould is shown in Figure 2, with its internal circuitry highlighted in violet. The Channel diameter is 15 mm.

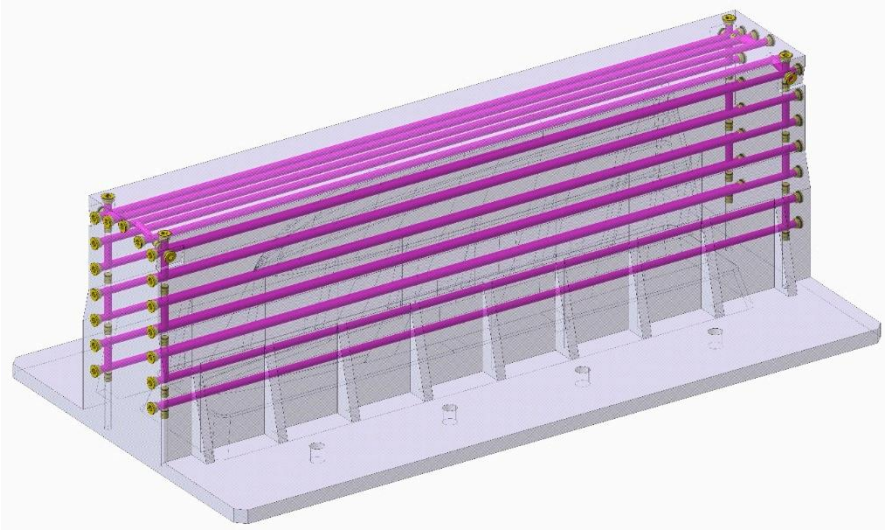

Figure 2. Cavity mould CAD. Cooling channels are highlighted in purple.

It should be noted that, along with the study, the displayed images of the mould only include the figure's footprints parts (punch and cavity), leaving out the casting elements of the system for a better visualization of the mould' s characteristics.

Regarding the WAAM mould manufacturing process, two different steps should be differentiated: the WAAM process and the second-stage post-processing.

1. The WAAM process was performed by the welding system Fronius 400i [68]. This device was assembled over a collaborative robotic arm Yaskawa GP50 [69], allowing 6 degrees of freedom in the robot's welding header (Figure 3). This welding system has been tested in the literature previously [70], as well as on multiple occasions at Aitia's facilities. In terms of software, the movements of the robot are programmed directly from a CAM software (Hyper MILL CAD/CAM 2023) [71], which automatically guides the robot's path. The resulting movements are post-processed into ISO G-Code language. The resulting file is then simulated in an Off-line Programming Software (Ultimaker Cura 2023) [72] to prevent collisions and ensure that all the movements are within the robot's range.

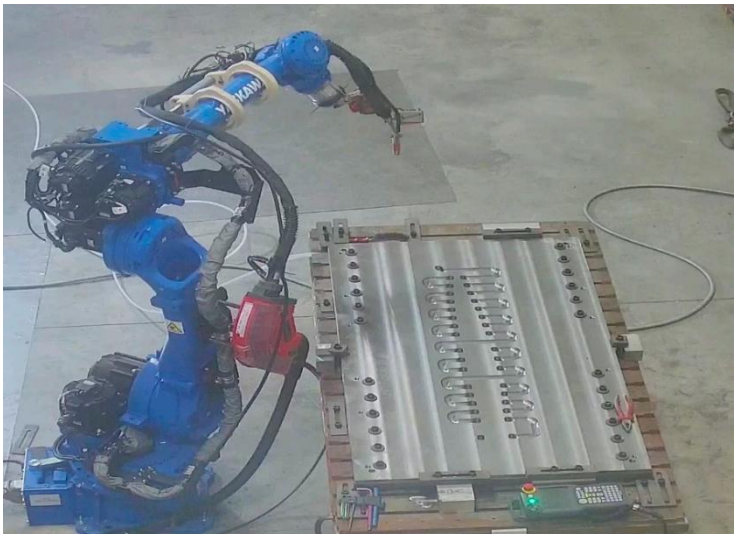

Figure 3. WAAM manufacturing system with mould base Photograph taken at the facilities of Fundación Aitiip.

2. The post-processing process is the machining process needed to achieve the final dimensional requirements, as well as to perform specific features such as drills, threads, etc. In our specific case, it was carried out by a CME FCM400 5 axis machining center, as shown in Figure 4.

Figure 4. The 5-Axis NC machine, CME FCM 400. Photograph taken at the facilities of Fundación Aitiip. (Reprinted from ref. [50]).

Finally, the cooling cycles proposed for both moulds were simulated. This simulation compared the effect of the designed internal channels on mould cooling cycle performance in both moulds.

The above-described methodology will be used for the study of the fabrication and performance of a punch mould designed according to the CC concept. This large-size tooling has been manufactured by the WAAM process in order to achieve the design specifications, constituting a unique specimen in terms of size and complexity for metallic additive manufacturing. The methodology of the study is based on the diagram shown in Figure 5, and its applications can be found in Section 3. It shows the comparative analyses carried out between the two moulds, as well as the previous steps carried out.

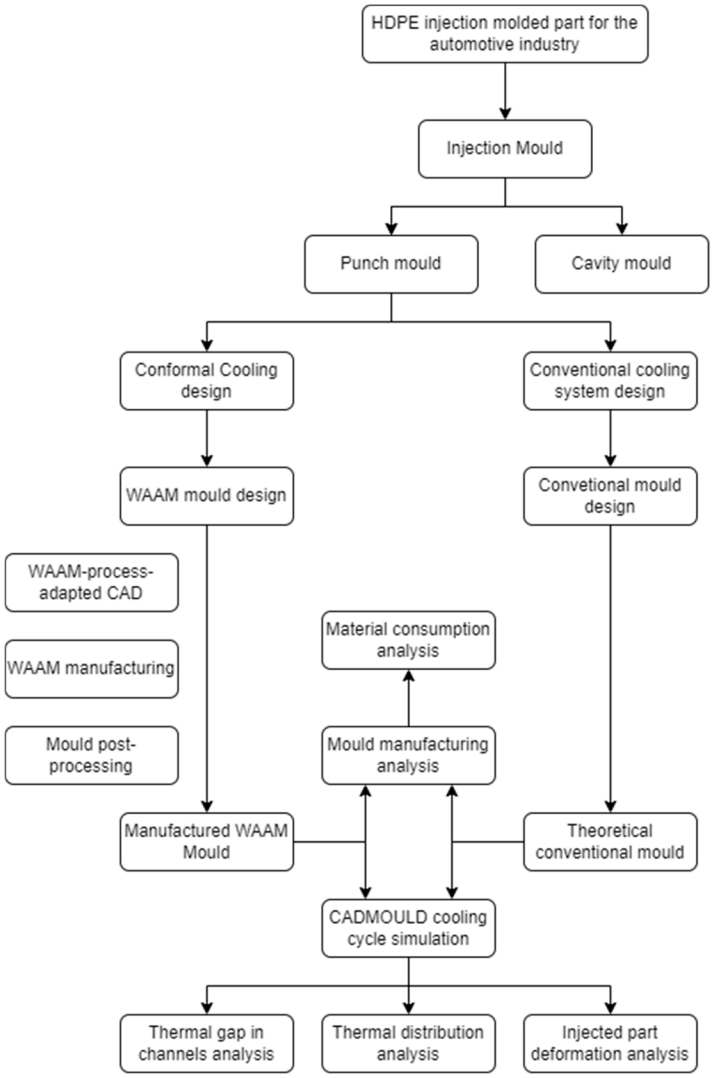

Figure 5. Schematic diagram of the study methodology.

3. Case Study

In this study, an automotive mould designed for the manufacture of injection-moulded HDPE parts was analyzed. From this premise, the concept of Conformal Cooling was developed for the WAAM mould. In order to compare the cooling process, the Conventional mould was designed. The cooling circuits of the Conventional mould were adapted, as far as possible, to the difficult part geometry, while complying with the limitations of conventional manufacturing methods. For its design, a baffle system was used to create the cooling circuits.

To get a broader perspective of the differences between the two toolings, as mentioned above, a comparison of the material consumption across the manufacturing process of both moulds was performed. The WAAM process material consumption data was based on the welding wire consumption, whose specific parameter is called Wire Feed Rate (WFR). This is a direct input of the welding device used. On the other hand, the material consumption in the Conventional mould was calculated according to the tooling machining requirements and based on tooling design experience.

As previously stated, the final part to be injected was an exterior trim for the automotive industry (Figure 6). As it is a part that does not have high mechanical requirements, the injection material is high-density polyethylene, which is commonly used in the automotive industry [73].

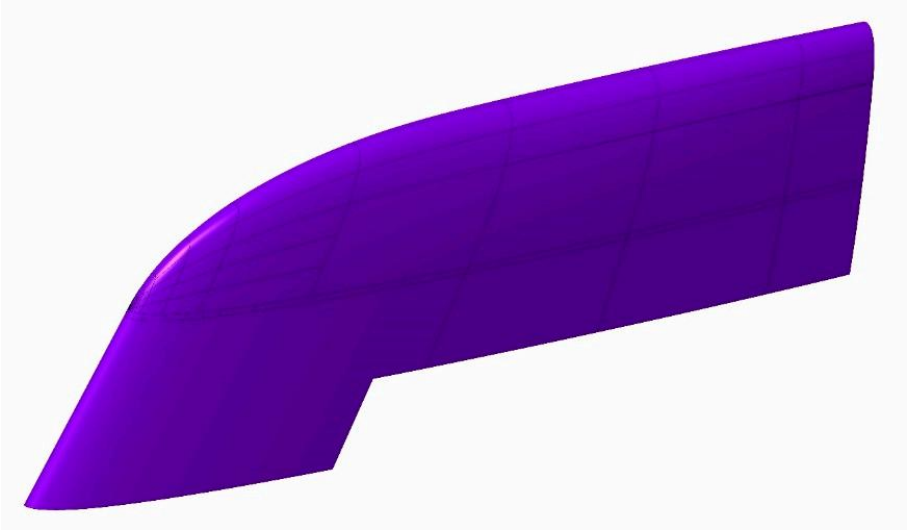

Figure 6. Automotive injection-moulded part CAD.

For this study, a thermal and deformation analysis of the final part was performed considering the effect of the internal channels designed and manufactured for the WAAM mould. To this effect, the performance of the CC concept-designed channels was compared with that of the Conventional mould previously presented. The outer geometry of these toolings was identical; however, the distance between the internal channels and the outer surface of the tooling varied considerably. The cooling cycle analyses were carried out by means of the CADMOULD V16 [74] software. CADMOULD is a professional plastic injection moulding simulation software fully integrated in the industry and used in various research articles related to plastic injection moulding [75].

3.1. Mould Design Differences

Regarding the WAAM mould, for the design and fabrication of the channels, two different design strategies were differentiated, depending on the printing area. The design premise was to maintain the channel section constant throughout the mould, an objective that was considered to be achieved by maintaining section differences of approximately 10% throughout the tooling. This difference is in response to the slight collapse of the horizontal channel geometry in its upper zone, as shown in Figure 7a. This collapse decreases the area of the channel by approximately 10%, according to the tests carried out. For this reason, the vertical channels were designed with a 10% reduction in this area to maintain a constant area along the internal channels. For horizontal channels, whose first circular half is machined on the flat plate on which the impression is made, the upper part of the channel must be closed. For this manufacturing operation, the cantilever angle printed for closing such a channel should be at 20° maximum. This value for the maximum cantilever angle has been obtained based on both own experiments and the existing literature [76,77]. It should be noted that this is a conservative value, aiming to minimize possible collapse errors during construction. As for the channels growing vertically, a geometry easily adaptable to the lower channels was chosen. It should be noted that the cantilever angle of these "vertical" channels is between 5° and 8°. Both channels' geometries are visualized with their respective dimensions in Figure 7. As for the design cross-section, the channel geometry manages to maintain a reasonably constant cross-section of 0.092 m^2 in the horizontal channels and 0.098 m^2 in the vertical channels.

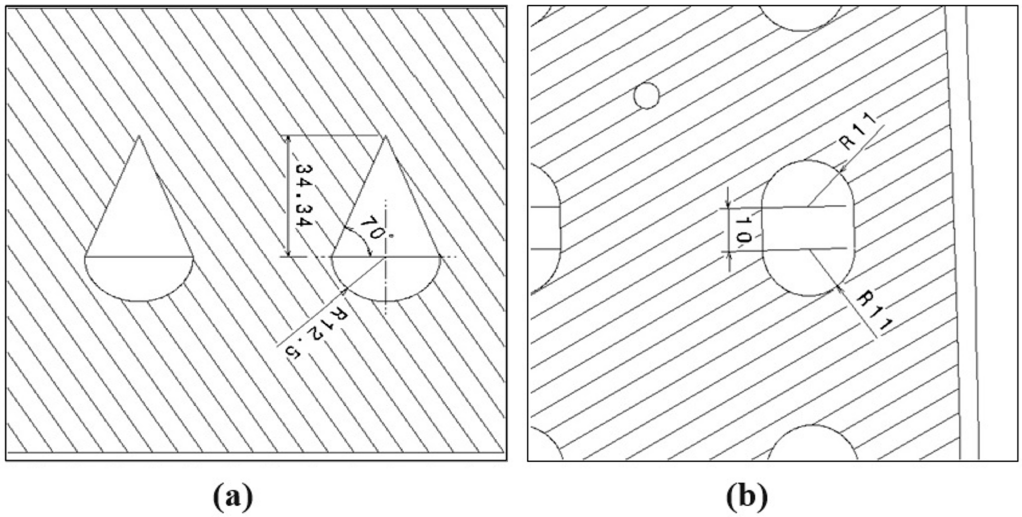

Figure 7. Dimensioned mould drawing. (**a**) Horizontal channel section detail and (**b**) Vertical channel section detail.

As explained before, the WAAM process is a near- to-shape process. The WAAM fabrication process involves the overlapping of weld seams, which generates irregular side surfaces on the outer surfaces of the geometry. To prevent these irregularities from affecting the final shape of the part [78,79], a specific WAAM-process-adapted CAD was designed, adding over-thickness for safety on the external surfaces to be machined and eliminating elements that were machined later, such as threaded holes, housings, etc. Regarding the inner channels, they have their own printing and design specifications. Inner channels should accomplish a minimum 25 mm security distance from the outer printing surface. Concerning the channels themselves, it is recommended to increase their design dimensions with a theoretical offset of 7.5 mm. The reason is that these areas are heat accumulation zones during the additive process; thus, the material flows more during the welding process. This issue creates wider than normal beads in these print areas. The WAAM tooling cooling channel design is displayed at Figure 8.

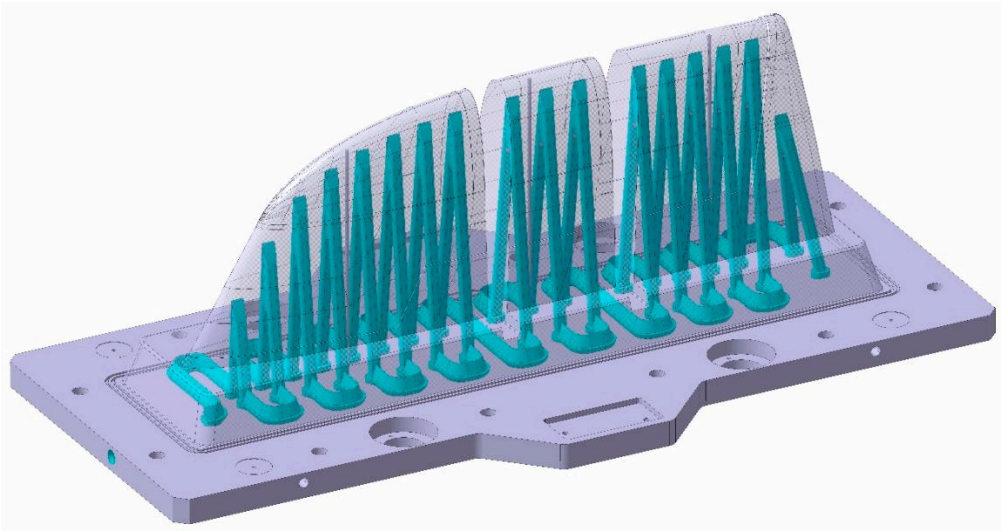

Figure 8. Conformal tooling concept WAAM mould. Inner cooling channels highlighted in blue.

The so-called Conventional mould was based on the mentioned baffle heating and cooling system (Figure 9). The baffles are a dividing element capable of creating two circuits from a single hole. Thanks to this element, a cooling system is achieved whose channels coincide in the horizontal plane with the channels designed under the concept of

Conformal Cooling; however, they are not adapted to the geometry of the final part but positioned in the central area of the mould.

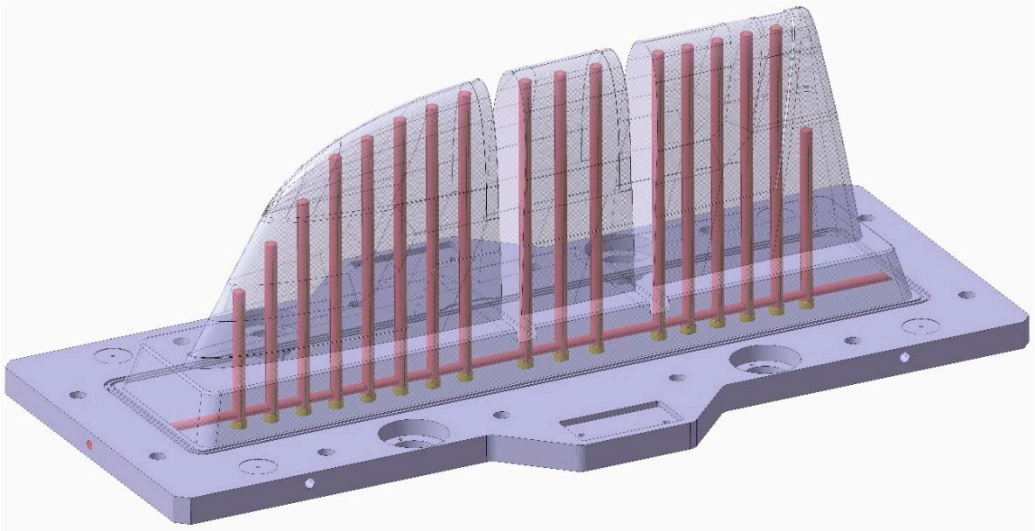

Figure 9. Conventional mould CAD design. Inner cooling channels highlighted in orange**.**

Regarding the complexity of the manufacturing of both moulds, it should be noted that the WAAM process requires only two phases: the additive manufacturing phase and the second-step machining phase. In this sense, the manufacturing process is significantly simplified with respect to the manufacturing of the Conventional mould, since, in order to for it to have the required cooling channels, it would be necessary to drill deep boreholes, which require specific machinery for their execution, being difficult to perform on a technical level [80]. In addition, the Conventional mould requires a system of baffles and plugs, which make up the thermal circuit. The installation of these peripherals greatly increases the complexity of assembly compared to the WAAM mould.

With the aim of testing the distance of the cooling channels to the workpiece injection surface, a distance analysis was performed. As can be observed, in the case of the Conventional mould (Figures 10 and 11), the cooling channels were mostly at separation distances from the outer surface of about 30 mm. However, the WAAM mould (Figure 11) achieved much smaller clearances, reaching distances close to 5 mm in its best-optimized areas. It should be noted that only the injection area of the tooling has been included in these clearance graphs.

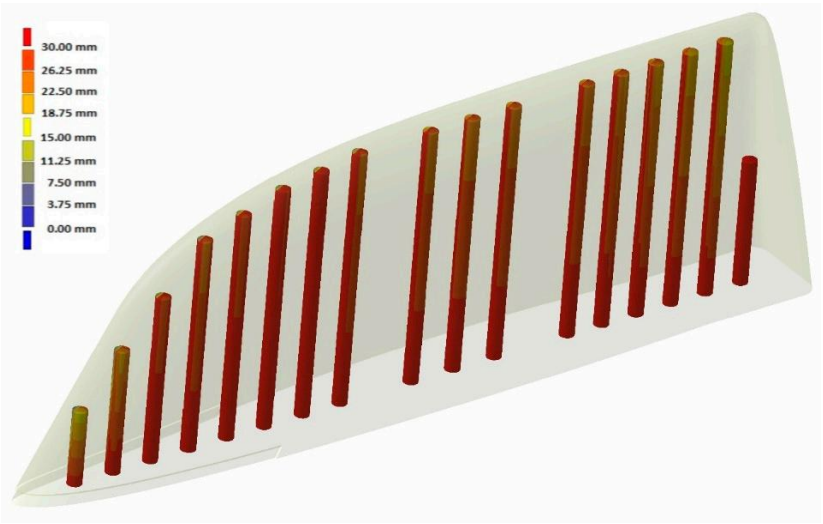

Figure 10. Conventional mould: distance between cooling channels and outer surface.

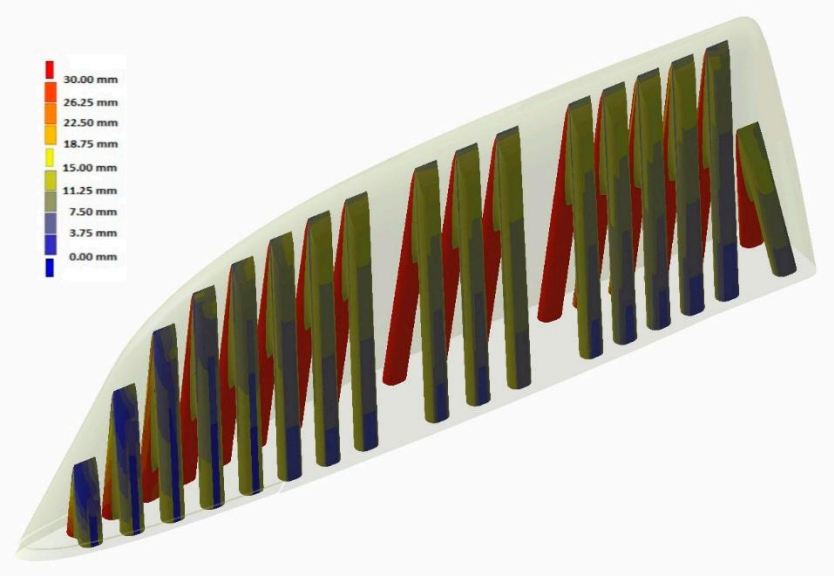

Figure 11. WAAM mould: distance between cooling channels and outer surface.

3.2. Material Comsumption Description

3.2.1. Conventional Mould Manufacturing

For the concept of the Conventional mould, the design premise involved making the entire punch mould in one piece. Therefore, the selected raw steel block should accomplish nominal dimensions, plus 5 mm of extra growth. This extra growth was selected according to machining experience, being the minimum growth required to ensure the dimensions of the final mould. The final dimensions of the raw steel block were 825 × 1515 × 517 mm, and its density was 7860 kg/m^3. Figure 12 displays the Conventional mould design integrated in its raw steel block.

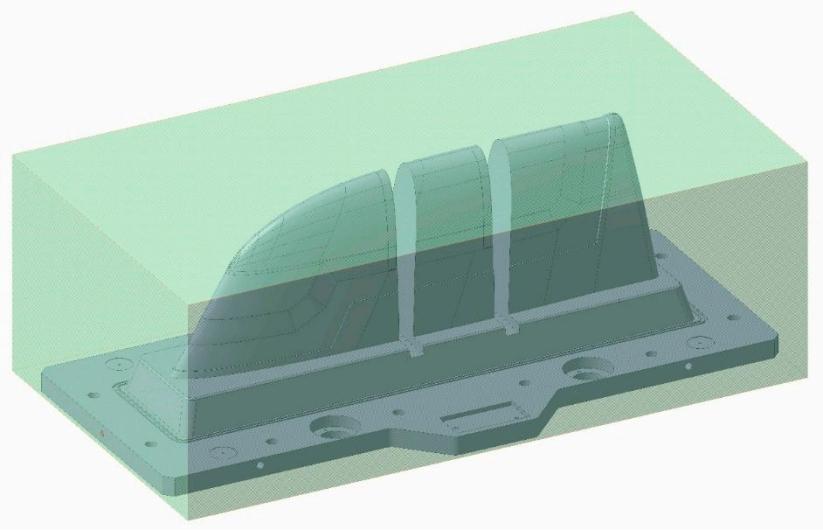

Figure 12. Conventional mould design integrated in its raw steel block.

3.2.2. WAAM Mould Manufacturing

In order to optimize the manufacturing process of the mould as much as possible, hybrid production of the tooling was carried out. For this purpose, the WAAM process was performed on the previously machined mould base. As mentioned above, the additive manufacturing process is optimal for complex designs; however, it is not advantageous for the manufacture of the mould base, as it is a flat plate. Therefore, the mould base

was manufactured from a steel plate, on which the corresponding areas of the cooling channels were machined, as well as the different forms required (Figure 13). For the manufacturing of this part, a steel block of 50 mm thickness and dimensions of 825 × 1515 mm was used. These dimensions corresponded to the nominal dimensions of the part, to which an extra thickness of 5 mm has was added for subsequent machining.

Moreover, the WAAM process requires a metallic base on which to weld its first layer. Both this plate and the first welded layers are considered as sacrificial and are removed during second-step machining in a standard WAAM manufacturing operation. In our case, we used the mould base plate to start printing, so that we did not waste any material.

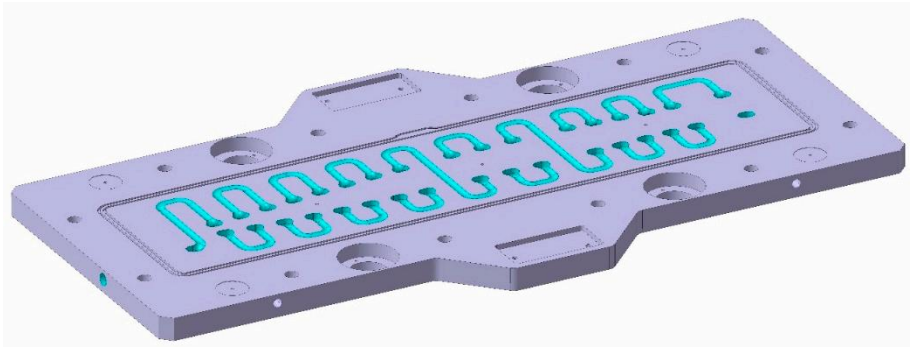

Figure 13. Machined mould base CAD. Manufactured inner cooling channels highlighted in blue.

The over-thickness of the WAAM-process-adapted CAD (highlighted in green) is displayed in Figure 14 over the final CAD design. A design over-thickness of 10 mm was chosen for this construction, based on previous tests in the same environment. Considering the manufacturing time and material required, this more conservative over-thickness value was chosen to avoid possible errors due to lack of material during the printing and machining process.

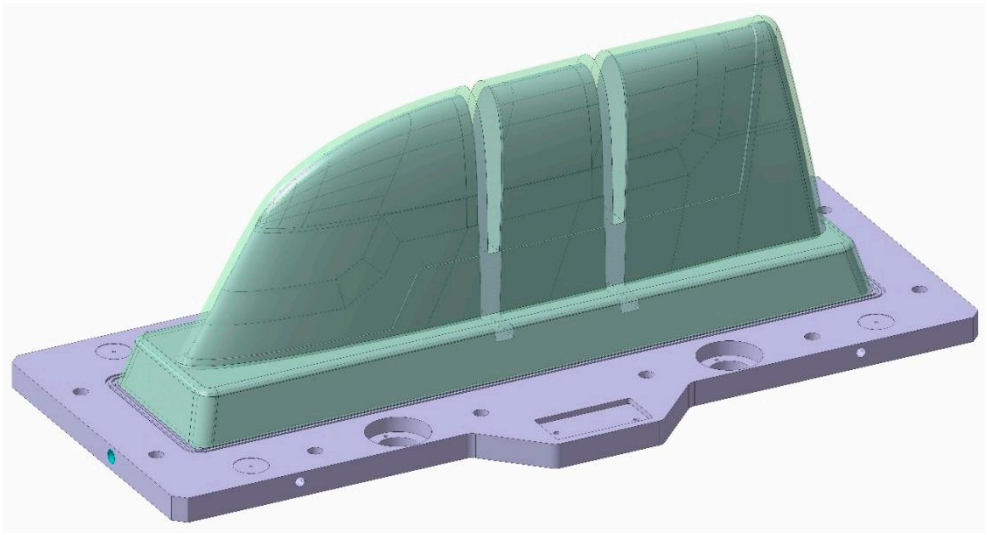

Figure 14. Over-thickness WAAM-process-adapted CAD (green) over final design (grey).

Initially, the selection of the input material for the AM process is crucial. The chosen wire material was G42 4 M21 3Si1 (ISO specification) [81], which is a carbon steel electrode known for its outstanding weldability and high content of deoxidizing elements. This makes it suitable for welding applications where stringent cleaning practices may not be feasible.

Regarding the printing strategy, it followed the following criteria:

- The solid internal area of the mould was printed. This zone is called the filling zone.

- The outer contour of the internal cooling channels was printed.
- The outer contour of the mould was printed.
- The subsequent layer was initiated from a randomly chosen point on the surface to prevent localized heat concentrations in specific areas.

This strategy of printing the infill areas first and the contours afterward allowed us to define the exteriors of the construction. The defined shape of the weld seam in these areas allowed the printing of cantilevered seams. These beads complied with the maximum cantilever angle of 20° [72,73].

The WAAM process manufacturing timelapse is shown in Figure 15.

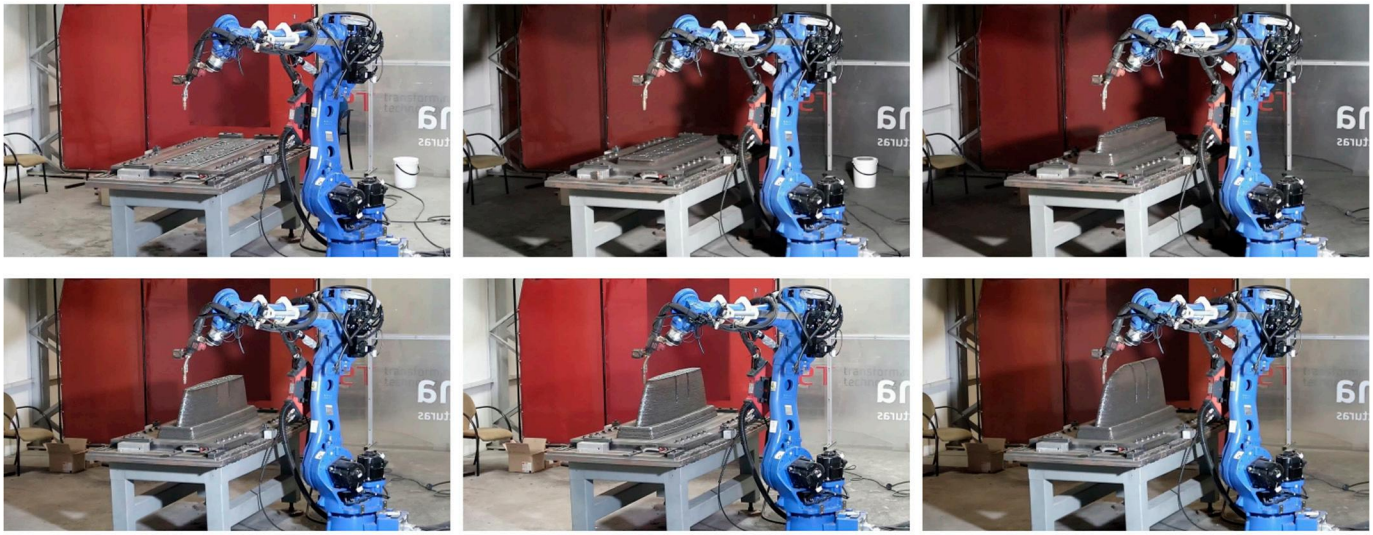

Figure 15. WAAM process manufacturing timelapse.

Regarding the WAAM process, its parameters are shown in Table 1.

Table 1. Process parameters for WAAM deposition (courtesy of AITIIP).

Process Parameters	Details	Value
Speed	Welding speed	0.06 m/s
	Wire feed rate	8.64 ± 0.81 m/min
	Deposition rate	0.077 kg/min
Distance and angle	Layer height	1.2 mm
	Electrode to layer angle	90°
Wire	Wire grade	ISO G42 4 M21 3Si1 [81]
	Wire diameter	1.2 mm
	Wire material density	7816.17 kg/m^3
Shield gas	Shield gas type	ISO 14175-M20-ArC-8 [81] (CO_2 8% Ar 92%)
	Shield gas flow rate	15 L/min

For the specific case of the WAAM tooling, the total weight of the additive construction was calculated based on the WFR parameter instead of based on the theoretical weight of the over-thickness WAAM-process-adapted CAD fabrication. This parameter shows the actual material consumption, since it includes unexpected material wastes, such as repetitions or printing layer jumps. These anomalies occur when the system sensor detects a growth of the printed piece different from the theoretical one, so the print control loop repeats the printed layer or skips the following one. Another possible anomaly that occurs during the process is the appearance of spatter during

welding, which is not reflected in the final weight of the printed tooling but reflected in the consumption of wire.

3.3. Cooling Cycle Description

Before the thermal analysis of the process, we must emphasize the final part to be injected. The final geometry, as shown in Figure 16, has a variable thickness between 1.6 and 3 mm. HDPE was the material used for both injection moulding simulations (the WAAM mould and Conventional mould). The injection strategy was a three-point injection. Each injection point is marked as a green arrow in Figure 16.

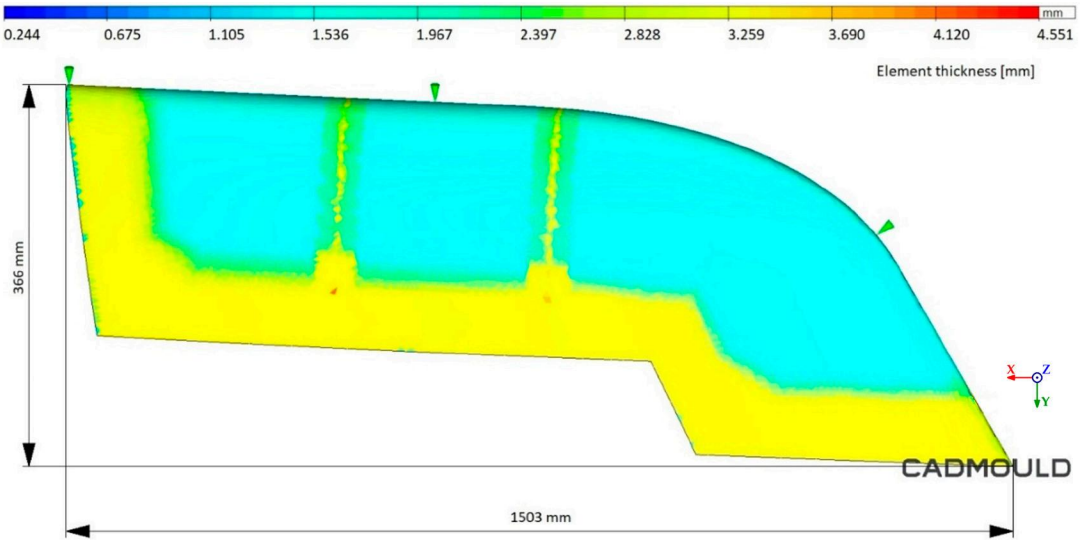

Figure 16. Injected part thickness analysis.

For the cooling cycle analysis, the following aspects were taken into account:

- The cavity mould, as discussed, is common for both moulds.
- Both moulds have two inserts for part extraction, which have not been taken into account in the previous sections but can be identified in the part as transverse areas of less thickness.
- The simulation was performed with the same parameters for both mould designs, with identical simulation times. The objective is that the results are comparable for both moulds.

The cooling system simulation environment comparison for both moulds is shown in Figures 17 and 18, where blue arrows refer to inlet coolant and red arrows the outlet coolant.

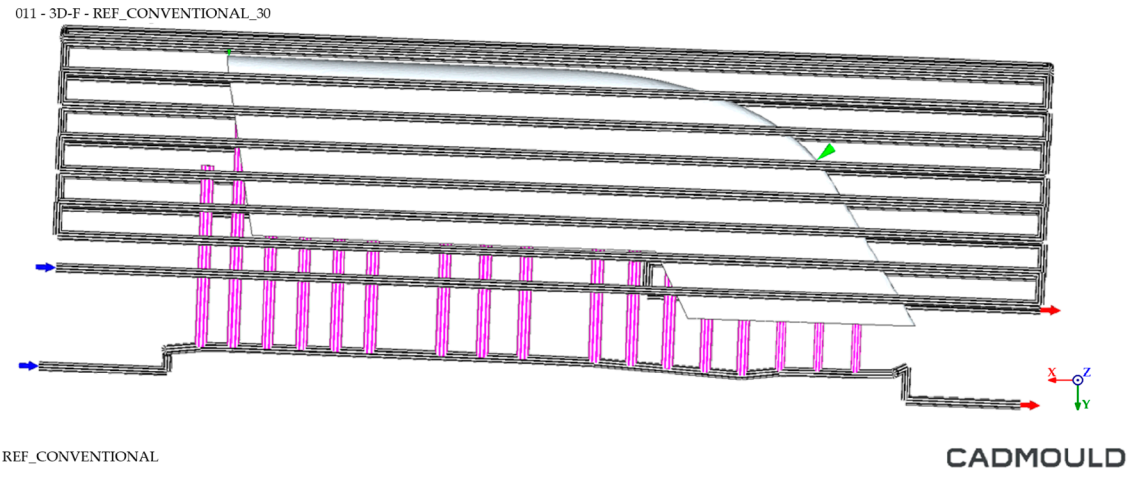

Figure 17. Cooling system simulation environment for Conventional mould.

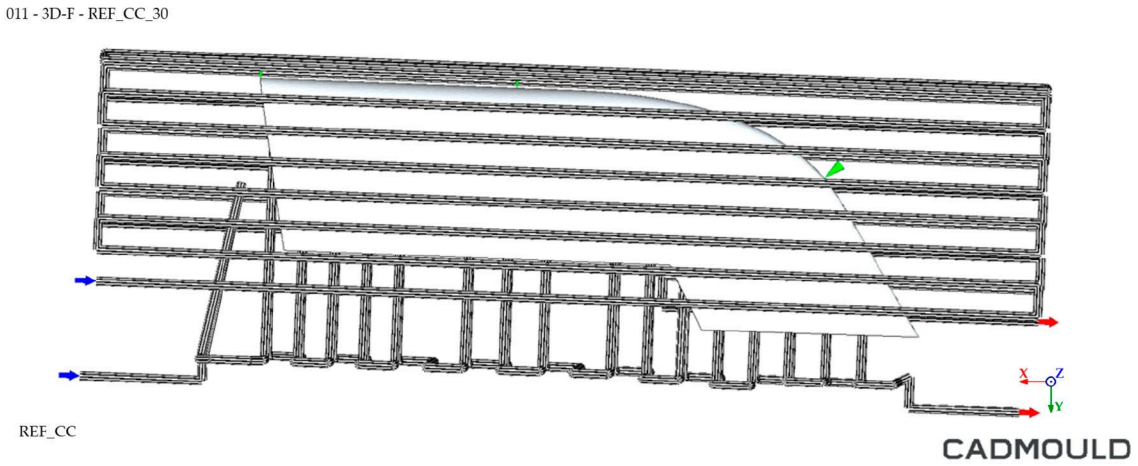

Figure 18. Cooling system simulation environment for WAAM mould.

Regarding the injection process, the parameters used for the simulation are shown in Table 2. It should be noted that the injected part properties were not only dependent on the cooling process analysis in the study but were also highly dependent on the injection parameters and strategy [82–84]. However, by using the same theoretical injection strategy for both simulations, the results were not dependent on these conditions.

One of the most important characteristics of HDPE injection moulding parts is their tendency to shrink during cooling [85]. This process can be controlled and minimized by optimizing the process parameters. The most influential parameters for shrinkage are mould draw temperature and cooling homogeneity. The final part deformation after the cooling cycle was also analyzed.

Table 2. Simulated injection parameters.

Simulated Injection Parameters	
Injection Temperature	245 °C
Injection time	2.6 s
Compaction pressure	400 bar
Compaction time	10 s
Coolant inlet temperature (water)	15 °C
Cooling time (additional to compaction time)	10 s

The following parameters were tested and studied in the analysis:

- The thermal gap in the cooling channels.
- The temperature of the injected part on its inner and outer walls.
- The final deformation of the injected part

4. Discussion

4.1. Material Consumption Analysis

It should be noted that, as mentioned in the 3.2.2 WAAM mould manufacturing section, the WAAM mold consists of two parts: base and additive manufacturing material. Due to this fact, material consumption was calculated not considering the material consumptions of each of its parts separately, but the final mould as a whole. Table 3 shows the raw material consumption data for both moulds. Emphasis is placed on the material utilization for both moulds, defined as the percentage of material consumed during the manufacturing process that remains in the final part. The extractable results were as follows:

- The amount of material unloaded for each tooling, shown in terms of mass.
- The percentage of material used in relation to the material consumed.
- The buy-to-fly ratio.

This last concept is defined as the ratio of the weight of raw material used to manufacture the part to the weight of the final part and is used to easily compare material usage in manufacturing parts.

Table 3. Mould weight output comparative.

Mould Punch		Raw Material Weight (kg)	Final Weight (kg)	Discarded Weight (kg)	Discarded Weight (%)	Buy-to-Fly Ratio
WAAM Mould	AM	492.38	446.24	212.05	21.56%	1.27
	Plate	491.20	325.30			
Conventional mould	-	5079.02	796.11	4282.91	84.33%	6.38

Certain information that is not in Table 3 should be highlighted, such as the total raw material mass required for the manufacturing of each of the toolings. As can be seen, the amount of raw material required for the manufacturing of the theoretical tooling was much higher than that of the WAAM tooling (983.58 kg). As for the final weight of the tooling, calculated using the design software, the weight difference was minimal, with the Conventional mould being 24.58 kg heavier than the WAAM mould. This fact is due to the designed internal channels, which in the case of the WAAM tooling represent a larger volume.

The final WAAM mould, once the second-stage machining was completed, is shown in the Figure 19.

Figure 19. Final WAAM tooling.

The WAAM additive manufacturing process used to manufacture the punch mould should be highlighted. This system makes it possible to manufacture a mould with water-tight internal channels adapted to the geometry of the final part, according to the concept of Conformal Cooling. In addition, it should be noted that in our state-of-the-art review, a mould manufactured in MAM, following the concept of Conformal Cooling design and larger than 300 × 300 × 500 mm, was not found. The tooling presented in this study exceeds these dimensions by a clear margin (820 × 1510 × 512 mm).

4.2. Cooling Cycle Analysis

It should be noted that the cooling analysis was made supposing the same initial injection conditions for both moulds, since the cooling cycle was the main feature to be analyzed.

4.2.1. Thermal Gap in Cooling Channels Analysis

First, the results of the thermal gaps in the cooling channel systems were analyzed. Figures 20 and 21 show the comparison between both cooling channel systems. As can be observed in Figure 20, the thermal jump in the Conventional mould channel system was lower, reaching a thermal difference of 3.7 °C compared to the 4.4 °C thermal difference of the Conformal Cooling channel system (WAAM mould), as displayed in Figure 21. This thermal difference showed that the Conformal Cooling system was able to extract more heat from the part and therefore the cooling water was heated further by 0.7 °C. It should be noted that the thermal jump was high in both cases.

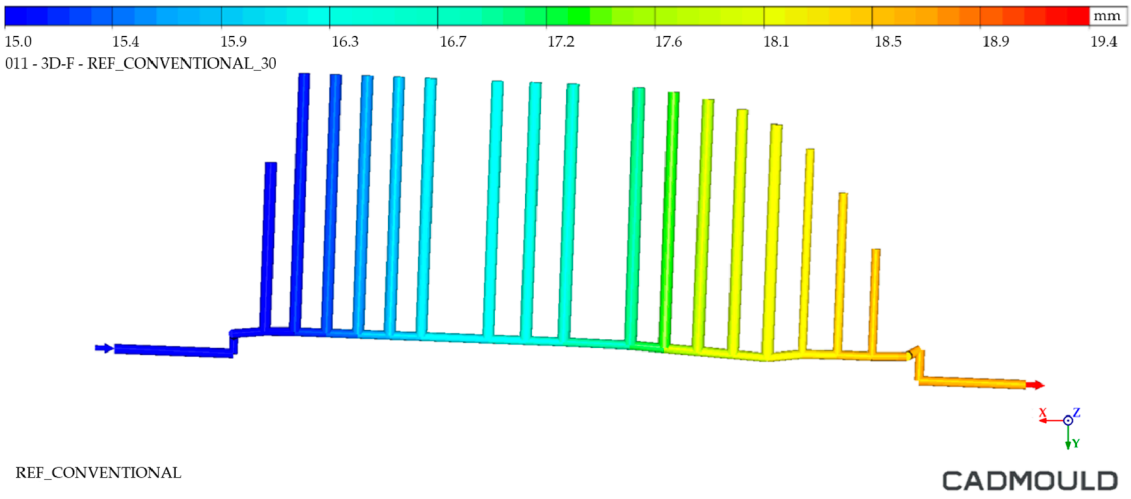

Figure 20. Thermal gap in channels—Conventional mould.

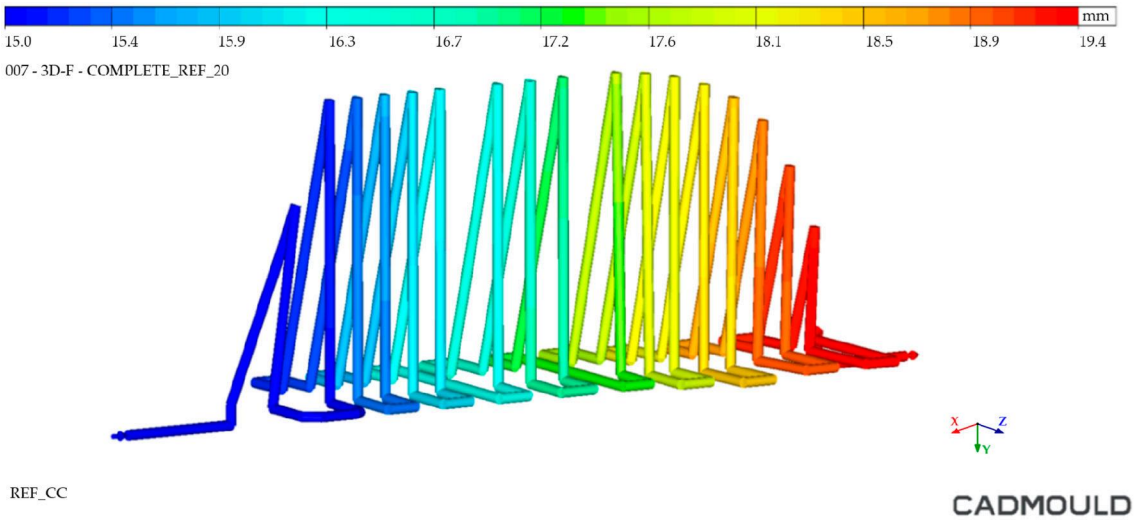

Figure 21. Thermal gap in channels—WAMM mould.

4.2.2. Thermal Distribution on Mould Walls Analysis

The analysis of the internal and external walls of the injected part after the cooling cycle provided information about the mould surface in these areas. Regarding inner mould walls, Figures 22 and 23 display a temperature comparison for both moulds. As

can be seen, the inner wall temperature of the Conventional mould injected part was higher, reaching temperatures up to 87 °C in its most unfavorable zone and 65 °C in its coldest zone. As for the inner wall of the WAAM mould injected part, we observed a maximum temperature of 80 °C and a minimum temperature of 57 °C. When analyzing the temperature distribution, it was observed that the greatest temperature differences were located in the inferior area of the injected part. This is due to the fact that, in the inferior area, the channels of the Conventional mould cooling channels were drilled with a greater distance from the mould walls. In the case of the WAAM mould, its channels' adaptation to the part geometry provided the benefit of a uniform temperature distribution in the part, in addition to extracting more heat from it.

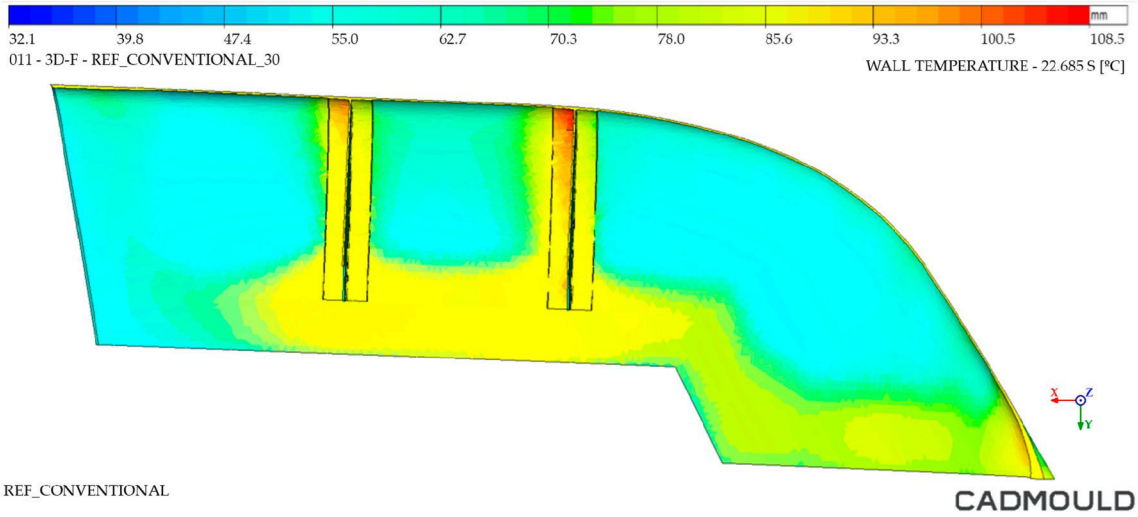

Figure 22. Thermal distribution on inner walls of Conventional mould.

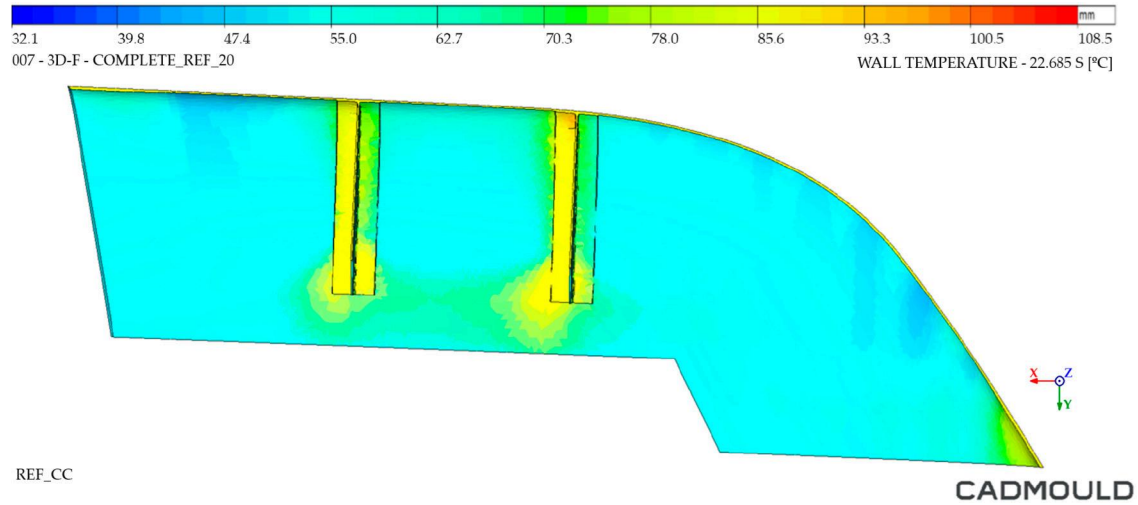

Figure 23. Thermal distribution on inner walls of WAAM mould.

As for the analysis of the outer walls of the part, shown in Figures 24 and 25, there was a slight difference in the lower area of the injected component. Its maximum temperature on the WAAM mould reached 65 °C, 5 °C less than that corresponding to the Conventional mould. This temperature difference was located in the lower zone of the component, also the most unfavorable for the previous analysis. It should be noted that the temperature distribution in the part was quite uniform. In this analysis, a common cavity mould design was used, with the same distribution of cooling channels. For this reason, these thermal differences must be directly related to the heat extraction achieved in the WAAM mould by means of the Conformal Cooling concept.

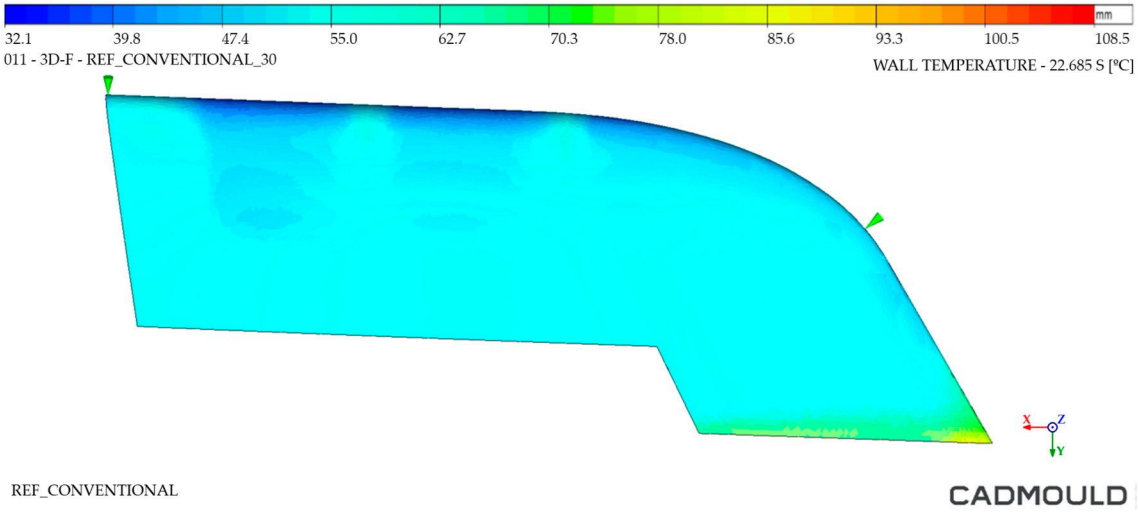

Figure 24. Thermal distribution on outer walls of Conventional mould.

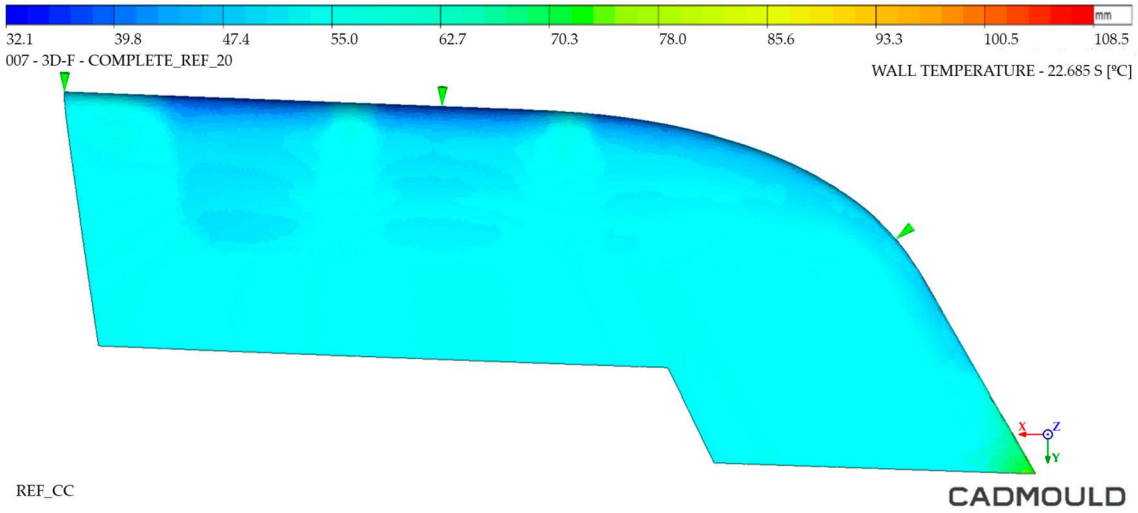

Figure 25. Thermal distribution on outer walls of WAAM mould.

4.2.3. Injected Part Deformation Analysis

Finally, an analysis of the deformations of the injected part was performed. In this analysis, the deformations that the injected part would undergo when it was removed from the mould at the end of the calculated cooling time (10 s for both moulds in this case) were studied. For an optimal result, a minimum part temperature with uniform distribution across the part should be sought. High draw temperatures lead to higher out-of-mould shrinkage, deforming the injected part. In addition, non-homogeneous temperature distribution in the part can result in surface anomalies such as shininess or marks.

Figure 26, corresponding to the Conventional mould, displays an important deformation zone in its lower open area. It is worth noting that this is one of the most unfavorable zones for deformation purposes, since HDPE tends to shrink during cooling and these zones have geometric freedom for it, since they do not have internal reinforcements. This same deformation was found in the WAAM mould (Figure 27) but much reduced (35% lower). In addition, it can be seen how the temperature distribution was much more homogeneous in the injected part extracted from the WAAM mould. It should be noted that the deformations at the graphic level have been enlarged in both named figures to facilitate their visualization.

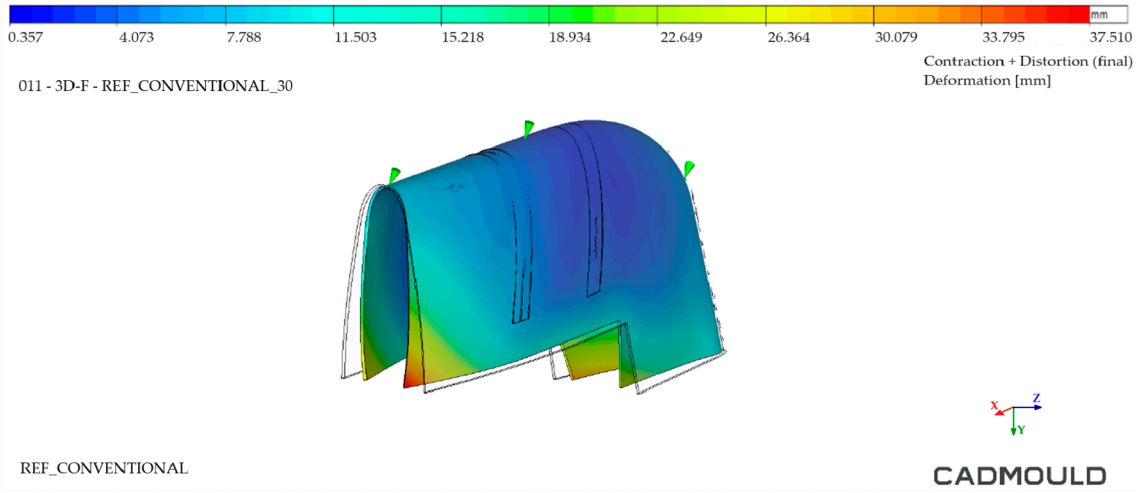

Figure 26. Injected part deformation analysis—Conventional mould.

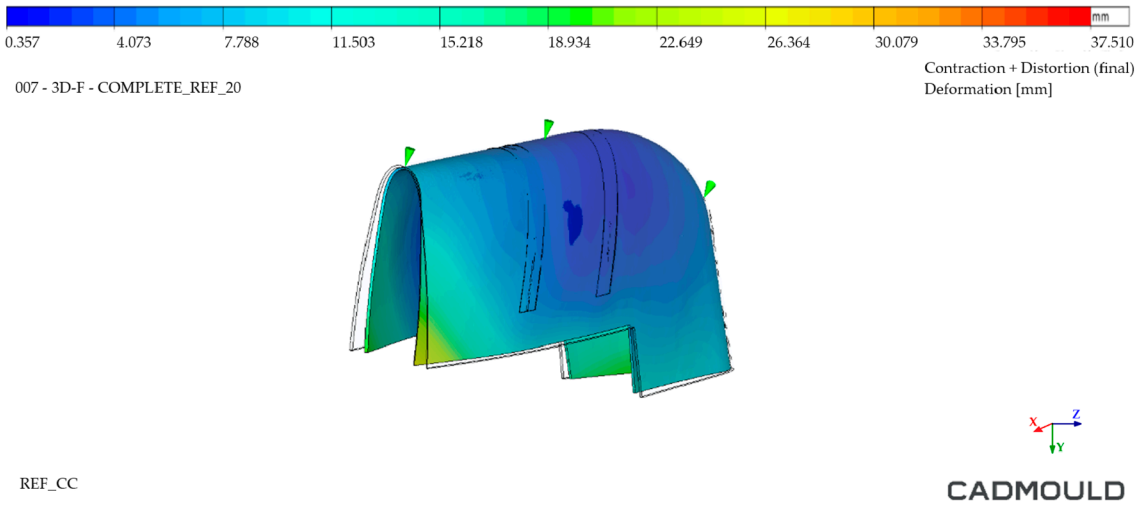

Figure 27. Injected part deformation analysis—WAAM mould.

The results obtained through the analysis of the cooling cycle revealed extremely promising improvements in terms of increased homogeneity in the WAAM mould, as well as a significant increase in the amount of heat extracted. This translates into reduced deformation of the final part, thereby reducing distortions to levels comparable to the current state-of-the-art methods. In addition, the higher heat extracted from the WAAM mould can be interpreted as an improvement in the cooling cycle time. It should be noted that the analyses were performed under the assumption of a uniform cooling cycle time for both moulds.

The originality of this study relies on the fact that a real large-dimension mould was manufactured, thanks to WAAM. It was carried out on a physically fabricated large mould, instead of being limited to theoretical simulations. This makes it a relevant case within the state of the art, where previous studies were mainly focused on tools of considerably smaller dimensions or, for the most part, on theoretical tools that have not been produced.

5. Conclusions

In conclusion, this article shows the significant suitability of the integration of WAAM technology for the manufacturing of injection moulds. The advantages in terms of material consumption and injection process optimization are evidenced throughout the study.

First of all, the CC-designed WAAM mould was compared with an identical theoretical mould, designed to be produced by conventional manufacturing methods. This conventional mould required a system of baffles as thermal channels, increasing its complexity by requiring auxiliary systems and compromising its watertightness.

A study of the material consumption for the manufacturing of both moulds was carried out. The results showed, for the WAAM mould, a remarkable decrease in the material consumed for manufacturing. The amount of material required for the manufacturing of the WAAM mould was 920.58 kg, which was 4095.44 kg lower than for the conventional mould. Consequently, the percentage of material discarded in the WAAM tooling was 21.56%, and improvement compared to the 84.33% discarded in the conventional mould. This is remarkable because the base plate was a common element in both moulds, with a significant percentage of material utilization. This means the fundamental difference in material savings was that corresponding to the WAAM construction, whose percentage of discarded material was only 9.37%. Finally, the buy-to-fly ratio obtained by the WAAM tooling was only 1.27, compared to the 6.38 of the conventional mould.

Finally, an HDPE injection process simulation and its corresponding thermal analysis for both cooling systems were carried out. As a result, we obtained a greater thermal gap in the inner channel system of the WAAM mould. This data verifies that, for the same period, the CC-based system extracted 0.7 °C more than the system designed in the Conventional mould. This represents an increase of 18.92%. In addition, the analysis of both the outer and lower surfaces of the part showed not only a lower part temperature at the end of the cycle for the WAAM mould, but also a more homogeneous temperature distribution.

In the case of the internal area of the injected part, coincident with the punch mould subject of the study, the difference is more remarkable. The maximum and minimum temperature of this area decreased by 8 °C in the WAAM mould injected part compared to the Conventional mould injected part. Moreover, as the channels of the WAAM mould adapted much better to the geometry of the lower zone of the injected component, the cooling of the part remained homogeneous. In the case of the Conventional mould, in addition to the temperature increase, the influence of the greater distance of the cooling channels from the surface in the lower area of the mould created a high temperature zone.

On the other hand, the results of the analysis of the outer area of the part, corresponding to the mould cavity, show a great similarity. This is because the simulated outer cavity was common for both moulds. However, for the WAAM mould, a lower maximum temperature at the inferior area of the injected part was observed.

As the last element of the study, the deformations of the injected part after the cooling cycle were compared. As in the previous cases, the WAAM mould injected part was found to be superior to the part extracted from the Conventional mould. The deformations of the part injected in the WAAM mould were 26.48% lower in its higher temperature zones. In addition, the temperature distribution was more homogeneous. This homogeneity is desirable to avoid surface defects on the part.

In conclusion, the capabilities of the WAAM process for the manufacturing of large tooling were studied in present research. This study has shown the advantages of the AM process over traditional machining methods in terms of design, manufacturing, and final performance of the manufactured mould. It should be noted that these advantages are situational, depending on the geometry to be manufactured, and should not be taken as a rule when choosing the most appropriate manufacturing method. However, they can serve as a fabrication guideline applicable to future tooling.

Author Contributions: Conceptualization, J.A.D.; Data curation, I.M.; Formal analysis, I.M. and I.C.; Funding acquisition, J.A.D.; Investigation, A.M.; Methodology, A.L. and P.G.; Project administration, J.A.D.; Resources, A.L. and P.G.; Software, I.M. and I.C.; Supervision, C.J. and D.E.; Validation, A.M.

and J.A.D.; Visualization, C.J. and D.E.; Writing—original draft, A.M.; Writing—review & editing, C.J. and D.E. All authors have read and agreed to the published version of the manuscript.

Funding: This research was funded under the European Commission within the HORIZON-CL4-2023-TWIN-TRANSITION-01-04 framework through the COMPASS project, Grant Number 101136940. This study was performed by members of the I + AITIIP (DGAT08 20R) research group of the FEDER 2014-2020 'Building Europe from Aragón'.

Institutional Review Board Statement: Not applicable.

Consent Statement: Not applicable.

Data Availability Statement: The data supporting the findings of this study are available from the corresponding author upon reasonable request.

Conflicts of Interest: The authors declare no conflicts of interest.

References

1. Grand View Research. *Injection Molding Market Size, Share & Trends Analysis Report by Material (Plastics, Metals), by Application (Packaging, Medical), by Region (North America, Europe, APAC, CSA, MEA), and Segment Forecasts, 2022–2030*; Grand View Research: San Francisco, CA, USA, 2020.
2. Gim, J.; Turng, L.-S. A Review of Current Advancements in High Surface Quality Injection Molding: Measurement, Influencing Factors, Prediction, and Control. *Polym. Test.* **2022**, *115*, 107718. https://doi.org/10.1016/j.polymertesting.2022.107718.
3. Wang, H.S.; Wang, Y.N.; Wang, Y.C. Cost Estimation of Plastic Injection Molding Parts through Integration of PSO and BP Neural Network. *Expert Syst. Appl.* **2013**, *40*, 418–428. https://doi.org/10.1016/j.eswa.2012.01.166.
4. Cheng, C.-D.; Liao, Y.-L.; Tsai, H.-H. Investigation of the Warpage of a High-Density Polyethylene Pallet by Plastic Injection Compression Molding: Part I—Numerical Approach. *Polymers* **2022**, *14*, 1437. https://doi.org/10.3390/polym14071437.
5. Minh, P.S.; Nguyen, V.-T.; Uyen, T.M.T.; Huy, V.Q.; Le Dang, H.N.; Nguyen, V.T.T. Enhancing Amplification in Compliant Mechanisms: Optimization of Plastic Types and Injection Conditions. *Polymers* **2024**, *16*, 394. https://doi.org/10.3390/polym16030394.
6. Sogancioglu, M.; Yel, E.; Ahmetli, G. Pyrolysis of Waste High Density Polyethylene (HDPE) and Low Density Polyethylene (LDPE) Plastics and Production of Epoxy Composites with Their Pyrolysis Chars. *J. Clean Prod.* **2017**, *165*, 369–381. https://doi.org/10.1016/j.jclepro.2017.07.157.
7. Wong, S.L.; Ngadi, N.; Abdullah, T.A.T.; Inuwa, I.M. Current State and Future Prospects of Plastic Waste as Source of Fuel: A Review. *Renew. Sustain. Energy Rev.* **2015**, *50*, 1167–1180. https://doi.org/10.1016/j.rser.2015.04.063.
8. Elsheikhi, S.A.; Benyounis, K.Y. Review of recent developments in injection molding process for polymeric materials. In *Reference Module in Materials Science and Materials Engineering*; Elsevier: Amsterdam, The Netherlands, 2016.
9. PlasticsEurope, E. *Plastics—The Facts 2019. An Analysis of European Plastics Production, Demand and Waste Data*; Plastic Europe: Brussels, Belgium, 2019.
10. Amjadi, M.; Fatemi, A. Creep and Fatigue Behaviors of High-Density Polyethylene (HDPE): Effects of Temperature, Mean Stress, Frequency, and Processing Technique. *Int. J. Fatigue* **2020**, *141*, 105871. https://doi.org/10.1016/j.ijfatigue.2020.105871.
11. Elduque, A.; Elduque, D.; Javierre, C.; Fernández, Á.; Santolaria, J. Environmental Impact Analysis of the Injection Molding Process: Analysis of the Processing of High-Density Polyethylene Parts. *J. Clean. Prod.* **2015**, *108*, 80–89. https://doi.org/10.1016/J.JCLEPRO.2015.07.119.
12. Tareen, A.; Saeed, S.; Iqbal, A.; Batool, R.; Jamil, N. Biodeterioration of Microplastics: A Promising Step towards Plastics Waste Management. *Polymers* **2022**, *14*, 2275. https://doi.org/10.3390/polym14112275.
13. Foolmaun, R.K.; Ramjeawon, T. Life Cycle Sustainability Assessments (LCSA) of Four Disposal Scenarios for Used Polyethylene Terephthalate (PET) Bottles in Mauritius. *Environ. Dev. Sustain.* **2013**, *15*, 783–806. https://doi.org/10.1007/s10668-012-9406-0.
14. Singh, P.; Déparrois, N.; Burra, K.G.; Bhattacharya, S.; Gupta, A.K. Energy Recovery from Cross-Linked Polyethylene Wastes Using Pyrolysis and CO_2 Assisted Gasification. *Appl. Energy* **2019**, *254*, 113722. https://doi.org/10.1016/j.apenergy.2019.113722.
15. Ojha, A.; Sharma, A.; Sihag, M.; Ojha, S. Food Packaging—Materials and Sustainability-A Review. *Agric. Rev.* **2015**, *36*, 241. https://doi.org/10.5958/0976-0741.2015.00028.8.
16. Sangwan, K.S.; Bhakar, V. Life Cycle Analysis of HDPE Pipe Manufacturing—A Case Study from an Indian Industry. *Procedia CIRP* **2017**, *61*, 738–743. https://doi.org/10.1016/j.procir.2016.11.193.
17. Pešić, N.; Živanović, S.; Garcia, R.; Papastergiou, P. Mechanical Properties of Concrete Reinforced with Recycled HDPE Plastic Fibres. *Constr. Build. Mater.* **2016**, *115*, 362–370. https://doi.org/10.1016/j.conbuildmat.2016.04.050.
18. Liu, J.; Yu, H.; Zhang, L.; Zhang, G.; Qu, J.; Lv, H. Effect of Greenhouse Environment on Organics Migrating from Agricultural High-Density Polyethylene (HDPE) Pipes. *Sens. Lett.* **2013**, *11*, 1293–1297. https://doi.org/10.1166/sl.2013.2868.
19. Rijal, K.P. High Density Polyethylene (HDP) Pipe as a Lining Material in Hilly Regions of Nepal. *Hydro Nepal J. Water Energy Environ.* **2016**, *18*, 25–29. https://doi.org/10.3126/hn.v18i0.14640.
20. Jaime, S.B.M.; Alves, R.M.V.; Bócoli, P.F.J. Moisture and Oxygen Barrier Properties of Glass, PET and HDPE Bottles for Pharmaceutical Products. *J. Drug Deliv. Sci. Technol.* **2022**, *71*, 103330. https://doi.org/10.1016/j.jddst.2022.103330

21. Hou, Z.; Cao, X.; Bai, Y.; Jiao, X.; He, X.; Dai, Y.; Xu, F. SEBS Effect on 60Co Radiation Resistance Behavior of PP/HDPE Matrix for Medical Device Applications. *Radiat. Phys. Chem.* **2021**, *184*, 109442. https://doi.org/10.1016/j.radphyschem.2021.109442.
22. Girijappa, Y.G.T.; Ayyappan, V.; Puttegowda, M.; Rangappa, S.M.; Parameswaranpillai, J.; Siengchin, S. Plastics in automotive applications. In *Encyclopedia of Materials: Plastics and Polymers*; Elsevier: Amsterdam, The Netherlands, 2022; pp. 103–113.
23. Groover, M.P. *Fundamentals of Modern Manufacturing: Materials, Processes, and Systems*; John Wiley & Sons: Hoboken, NJ, USA, 2020.
24. Sun, Y.F.; Lee, K.S.; Nee, A.Y.C. Design and FEM Analysis of the Milled Groove Insert Method for Cooling of Plastic Injection Moulds. *Int. J. Adv. Manuf. Technol.* **2004**, *24*, 715–726. https://doi.org/10.1007/s00170-003-1755-2.
25. Karagöz, İ.; Tuna, Ö. Effect of Melt Temperature on Product Properties of Injection-Molded High-Density Polyethylene. *Polym. Bull.* **2021**, *78*, 6073–6091. https://doi.org/10.1007/s00289-021-03695-w.
26. Wenzel, M.; Raisch, S.R.; Schmitz, M.; Hopmann, C. Comparison of Hybrid Machine Learning Approaches for Surrogate Modeling Part Shrinkage in Injection Molding. *Polymers* **2024**, *16*, 2465. https://doi.org/10.3390/polym16172465.
27. White, J.L.; Dee, H.B. Flow Visualization for Injection Molding of Polyethylene and Polystyrene Melts. *Polym. Eng. Sci.* **1974**, *14*, 212–222. https://doi.org/10.1002/pen.760140310.
28. Tang, S.H.; Kong, Y.M.; Sapuan, S.M.; Samin, R.; Sulaiman, S. Design and Thermal Analysis of Plastic Injection Mould. *J. Mater. Process. Technol.* **2006**, *171*, 259–267. https://doi.org/10.1016/j.jmatprotec.2005.06.075.
29. Barbeiro, S.; Enguiça, R.; Lobo, D. Automatic Generation of Conformal Cooling Channels in Injection Moulding. *Comput. -Aided Des.* **2022**, *150*, 103312. https://doi.org/10.1016/J.CAD.2022.103312.
30. Li, Z.; Wang, X.; Gu, J.; Ruan, S.; Shen, C.; Lyu, Y.; Zhao, Y. Topology Optimization for the Design of Conformal Cooling System in Thin-Wall Injection Molding Based on BEM. *Int. J. Adv. Manuf. Technol.* **2018**, *94*, 1041–1059. https://doi.org/10.1007/s00170-017-0901-1.
31. Feng, S.; Kamat, A.M.; Pei, Y. Design and Fabrication of Conformal Cooling Channels in Molds: Review and Progress Updates. *Int. J. Heat Mass Transf.* **2021**, *171*, 121082. https://doi.org/10.1016/j.ijheatmasstransfer.2021.121082.
32. Gao, Z.; Dong, G.; Tang, Y.; Zhao, Y.F. Machine Learning Aided Design of Conformal Cooling Channels for Injection Molding. *J. Intell. Manuf.* **2023**, *34*, 1183–1201. https://doi.org/10.1007/s10845-021-01841-9.
33. Deepika, S.S.; Patil, B.T.; Shaikh, V.A. Plastic Injection Molded Door Handle Cooling Time Reduction Investigation Using Conformal Cooling Channels. *Mater. Today Proc.* **2020**, *27*, 519–523. https://doi.org/10.1016/j.matpr.2019.11.316.
34. Wahl, J.P.; Niedermeyer, J.; Bernhard, R.; Hermsdorf, J.; Kaierle, S. Design of Additively Manufacturable Injection Molds with Conformal Cooling. *Procedia CIRP* **2022**, *111*, 97–100. https://doi.org/10.1016/j.procir.2022.08.146.
35. Torres-Alba, A.; Mercado-Colmenero, J.M.; Caballero-Garcia, J.D.D.; Martin-Doñate, C. A Hybrid Cooling Model Based on the Use of Newly Designed Fluted Conformal Cooling Channels and Fastcool Inserts for Green Molds. *Polymers* **2021**, *13*, 3115. https://doi.org/10.3390/polym13183115.
36. Mercado-Colmenero, J.M.; Torres-Alba, A.; Catalan-Requena, J.; Martin-Doñate, C. A New Conformal Cooling System for Plastic Collimators Based on the Use of Complex Geometries and Optimization of Temperature Profiles. *Polymers* **2021**, *13*, 2744. https://doi.org/10.3390/polym13162744.
37. Vargas-Isaza, C.; Benitez-Lozano, A.; Rodriguez, J. Evaluating the Cooling Efficiency of Polymer Injection Molds by Computer Simulation Using Conformal Channels. *Polymers* **2023**, *15*, 4044. https://doi.org/10.3390/polym15204044.
38. Rosa, N.; Costa, J.; Lopes, A.G. CFD Study of Transient Heating and Cooling of a Blank Mould with a Conformal Cooling Channel for Manufacturing Glass Containers. *Results Eng.* **2023**, *17*, 100932. https://doi.org/10.1016/J.RINENG.2023.100932.
39. Torres-Alba, A.; Mercado-Colmenero, J.M.; Caballero-Garcia, J.d.D.; Martin-Doñate, C. Application of New Triple Hook-Shaped Conformal Cooling Channels for Cores and Sliders in Injection Molding to Reduce Residual Stress and Warping in Complex Plastic Optical Parts. *Polymers* **2021**, *13*, 2944. https://doi.org/10.3390/polym13172944.
40. Ma, Y.-S.; Tong, T. Associative Feature Modeling for Concurrent Engineering Integration. *Comput. Ind.* **2003**, *51*, 51–71. https://doi.org/10.1016/S0166-3615(03)00025-3.
41. Kanbur, B.B.; Suping, S.; Duan, F. Design and Optimization of Conformal Cooling Channels for Injection Molding: A Review. *Int. J. Adv. Manuf. Technol.* **2020**, *106*, 3253–3271. https://doi.org/10.1007/s00170-019-04697-9.
42. Derekar, K.S. A Review of Wire Arc Additive Manufacturing and Advances in Wire Arc Additive Manufacturing of Aluminium. *Mater. Sci. Technol.* **2018**, *34*, 895–916. https://doi.org/10.1080/02670836.2018.1455012.
43. Veiga, F.; Bhujangrao, T.; Suárez, A.; Aldalur, E.; Goenaga, I.; Gil-Hernandez, D. Validation of the Mechanical Behavior of an Aeronautical Fixing Turret Produced by a Design for Additive Manufacturing (DfAM). *Polymers* **2022**, *14*, 2177. https://doi.org/10.3390/polym14112177.
44. Pelin, G.; Sonmez, M.; Pelin, C.-E. The Use of Additive Manufacturing Techniques in the Development of Polymeric Molds: A Review. *Polymers (Basel)* **2024**, *16*, 1055. https://doi.org/10.3390/polym16081055.
45. Anand, M.; Bishwakarma, H.; Kumar, N.; Ujjwal, K.; Das, A.K. Fabrication of Multilayer Thin Wall by WAAM Technique and Investigation of Its Microstructure and Mechanical Properties. *Mater Today Proc* **2022**, *56*, 927–930. https://doi.org/10.1016/J.MATPR.2022.02.542.
46. Al-Nabulsi, Z.; Mottram, J.T.; Gillie, M.; Kourra, N.; Williams, M.A. Mechanical and X Ray Computed Tomography Characterisation of a WAAM 3D Printed Steel Plate for Structural Engineering Applications. *Constr. Build. Mater.* **2021**, *274*, 121700. https://doi.org/10.1016/J.CONBUILDMAT.2020.121700.

47. Vora, J.; Parmar, H.; Chaudhari, R.; Khanna, S.; Doshi, M.; Patel, V. Experimental Investigations on Mechanical Properties of Multi-Layered Structure Fabricated by GMAW-Based WAAM of SS316L. *J. Mater. Res. Technol.* **2022**, *20*, 2748–2757. https://doi.org/10.1016/J.JMRT.2022.08.074.
48. Jackson, M.A.; Van Asten, A.; Morrow, J.D.; Min, S.; Pfefferkorn, F.E. A Comparison of Energy Consumption in Wire-Based and Powder-Based Additive-Subtractive Manufacturing. *Procedia Manuf.* **2016**, *5*, 989–1005.
49. Singh, S.; Sharma, S.K.; Rathod, D.W. A Review on Process Planning Strategies and Challenges of WAAM. *Mater. Today Proc.* **2021**, *47*, 6564–6575. https://doi.org/10.1016/J.MATPR.2021.02.632.
50. Marqués, A.; Dieste, J.A.; Monzón, I.; Laguía, A.; Javierre, C.; Elduque, D. Analysis of Energy and Material Consumption for the Manufacturing of an Aeronautical Tooling: An Experimental Comparison between Pure Machining and Big Area Additive Manufacturing. *Materials* **2024**, *17*, 3066. https://doi.org/10.3390/ma17133066.
51. Roschli, A.; Gaul, K.T.; Boulger, A.M.; Post, B.K.; Chesser, P.C.; Love, L.J.; Blue, F.; Borish, M. Designing for Big Area Additive Manufacturing. *Addit. Manuf.* **2019**, *25*, 275–285. https://doi.org/10.1016/j.addma.2018.11.006.
52. Brackett, J.; Yan, Y.; Cauthen, D.; Kishore, V.; Lindahl, J.; Smith, T.; Sudbury, Z.; Ning, H.; Kunc, V.; Duty, C. Characterizing Material Transitions in Large-Scale Additive Manufacturing. *Addit. Manuf.* **2021**, *38*, 101750. https://doi.org/10.1016/j.addma.2020.101750.
53. Kampker, A.; Triebs, J.; Kawollek, S.; Ayvaz, P.; Hohenstein, S. Review on Machine Designs of Material Extrusion Based Additive Manufacturing (AM) Systems—Status-Quo and Potential Analysis for Future AM Systems. *Procedia CIRP* **2019**, *81*, 815–819.
54. Kawalkar, R.; Dubey, H.K.; Lokhande, S.P. Wire Arc Additive Manufacturing: A Brief Review on Advancements in Addressing Industrial Challenges Incurred with Processing Metallic Alloys. *Mater. Today Proc.* **2022**, *50*, 1971–1978. https://doi.org/10.1016/j.matpr.2021.09.329.
55. Nurhudan, A.I.; Supriadi, S.; Whulanza, Y.; Saragih, A.S. Additive Manufacturing of Metallic Based on Extrusion Process: A Review. *J. Manuf. Process.* **2021**, *66*, 228–237. https://doi.org/10.1016/j.jmapro.2021.04.018.
56. Zhang, Y.; Wu, L.; Guo, X.; Kane, S.; Deng, Y.; Jung, Y.-G.; Lee, J.-H.; Zhang, J. Additive Manufacturing of Metallic Materials: A Review. *J. Mater. Eng. Perform.* **2018**, *27*, 1–13. https://doi.org/10.1007/s11665-017-2747-y.
57. Vayre, B.; Vignat, F.; Villeneuve, F. Metallic Additive Manufacturing: State-of-the-Art Review and Prospects. *Mech. Ind.* **2012**, *13*, 89–96. https://doi.org/10.1051/meca/2012003.
58. Singh, S.R.; Khanna, P. Wire Arc Additive Manufacturing (WAAM): A New Process to Shape Engineering Materials. *Mater. Today Proc.* **2021**, *44*, 118–128. https://doi.org/10.1016/j.matpr.2020.08.030.
59. Ding, D.; Pan, Z.; Cuiuri, D.; Li, H. A Multi-Bead Overlapping Model for Robotic Wire and Arc Additive Manufacturing (WAAM). *Robot. Comput. Integr. Manuf.* **2015**, *31*, 101–110. https://doi.org/10.1016/j.rcim.2014.08.008.
60. González, J.; Rodríguez, I.; Prado-Cerqueira, J.L.; Diéguez, J.L.; Pereira, A. Additive Manufacturing with GMAW Welding and CMT Technology. *Procedia Manuf.* **2017**, *13*, 840–847. https://doi.org/10.1016/J.PROMFG.2017.09.189.
61. Ramarao, M.; King, M.F.L.; Sivakumar, A.; Manikandan, V.; Vijayakumar, M.; Subbiah, R. Optimizing GMAW Parameters to Achieve High Impact Strength of the Dissimilar Weld Joints Using Taguchi Approach. *Mater Today Proc* **2022**, *50*, 861–866. https://doi.org/10.1016/J.MATPR.2021.06.137.
62. Jing, C.; Mao, H.; Xu, T.; Guo, Y.; Lu, J.; Liang, X.; Liu, C. Impact of Process Parameters on Forming Quality and Deposition Efficiency of Unsupported Rods in Wire Arc Additive Manufacturing. *J Manuf. Process.* **2024**, *124*, 12–23. https://doi.org/10.1016/j.jmapro.2024.06.001.
63. Wang, Z.; Zimmer-Chevret, S.; Léonard, F.; Abba, G. Improvement Strategy for the Geometric Accuracy of Bead's Beginning and End Parts in Wire-Arc Additive Manufacturing (WAAM). *Int. J. Adv. Manuf. Technol.* **2022**, *118*, 2139–2151. https://doi.org/10.1007/s00170-021-08037-8.
64. Lopes, J.G.; Machado, C.M.; Duarte, V.R.; Rodrigues, T.A.; Santos, T.G.; Oliveira, J.P. Effect of Milling Parameters on HSLA Steel Parts Produced by Wire and Arc Additive Manufacturing (WAAM). *J. Manuf. Process.* **2020**, *59*, 739–749. https://doi.org/10.1016/j.jmapro.2020.10.007.
65. Chernovol, N.; Sharma, A.; Tjahjowidodo, T.; Lauwers, B.; Rymenant, P. Van Machinability of Wire and Arc Additive Manufactured Components. *CIRP J. Manuf. Sci. Technol.* **2021**, *35*, 379–389. https://doi.org/10.1016/j.cirpj.2021.06.022.
66. Laghi, V.; Palermo, M.; Gasparini, G.; Veljkovic, M.; Trombetti, T. Assessment of Design Mechanical Parameters and Partial Safety Factors for Wire-and-Arc Additive Manufactured Stainless Steel. *Eng. Struct.* **2020**, *225*, 111314. https://doi.org/10.1016/J.ENGSTRUCT.2020.111314.
67. Kerber, E.; Knitt, H.; Fahrendholz-Heiermann, J.L.; Ergin, E.; Brell-Cokcan, S.; Dewald, P.; Sharma, R.; Reisgen, U. Variable Layer Heights in Wire Arc Additive Manufacturing and WAAM Information Models. *Machines* **2024**, *12*, 432. https://doi.org/10.3390/machines12070432.
68. Fronius International. *Fronius Fronius TPS 400i. MIG/MAG Welding System;* Fronius International: Wels, Austria, 2018.
69. Yaskawa Motoman. *Gp50. Multi-Purpose Handling Robot with 50 kg Payload 2020*; Yaskawa: Miamisburg, OH, USA.
70. Li, H.; Shi, X.; Wu, B.; Corradi, D.R.; Pan, Z.; Li, H. Wire Arc Additive Manufacturing: A Review on Digital Twinning and Visualization Process. *J. Manuf. Process.* **2024**, *116*, 293–305. https://doi.org/10.1016/j.jmapro.2024.03.001.
71. OPEN MIND Technologies. *HyperMILL CAD/CAM Software 2023*; OPEN MIND Technologies: Needham, MA, USA.
72. UltiMaker. *UltiMaker Cura;* UltiMaker: Utrecht, Netherlands, 2023.

73. Patil, A.; Patel, A.; Purohit, R. An Overview of Polymeric Materials for Automotive Applications. *Mater. Today Proc.* **2017**, *4*, 3807–3815. https://doi.org/10.1016/j.matpr.2017.02.278.
74. SIMCON CADMOULD. *Plastic Injection Molding Simulation Software;* SIMCON: Wuerselen, Germany, 1989.
75. Mańko, P.; Majewski, Ł. Design of the Optimal Geometry of the Moulded Piece Based on Numerical Analyses in Cadmould 3D-F. *Adv. Sci. Technol. Res. J.* **2020**, *14*, 96–106. https://doi.org/10.12913/22998624/114961.
76. Tomar, B.; Shiva, S.; Nath, T. A Review on Wire Arc Additive Manufacturing: Processing Parameters, Defects, Quality Improvement and Recent Advances. *Mater. Today Commun.* **2022**, *31*, 103739. https://doi.org/10.1016/j.mtcomm.2022.103739.
77. Liu, B.; Shen, H.; Zhou, Z.; Jin, J.; Fu, J. Research on Support-Free WAAM Based on Surface/Interior Separation and Surface Segmentation. *J. Mater. Process. Technol.* **2021**, *297*, 117240. https://doi.org/10.1016/j.jmatprotec.2021.117240.
78. Garaigordobil, A.; Ansola, R.; Veguería, E.; Fernandez, I. Overhang Constraint for Topology Optimization of Self-Supported Compliant Mechanisms Considering Additive Manufacturing. *CAD Comput. Aided Des.* **2019**, *109*, 33–48. https://doi.org/10.1016/j.cad.2018.12.006.
79. Zhang, J.; Cao, Q.; Lu, W.F. A Review on Design and Removal of Support Structures in Metal Additive Manufacturing. *Mater Today Proc* **2022**, *70*, 407–411. https://doi.org/10.1016/j.matpr.2022.09.277.
80. Sandén, T.; Nilsson, U.; Johannesson, L.E.; Hagman, P.; Nilsson, G. *Sealing of Investigation Boreholes*; SKB: Stockholm, Sweden, 2011.
81. *ISO 14175:2008*; Welding Consumables—Gases and Gas Mixtures for Fusion Welding and Allied Processes. International Organization for Standardization: Geneva, Switzerland, 2008.
82. Bociaga, E.; Palutkiewicz, P. The Influence of Injection Molding Parameters and Blowing Agent Addition on Selected Properties, Surface State, and Structure of HDPE Parts. *Polym. Eng. Sci.* **2013**, *53*, 780–791. https://doi.org/10.1002/pen.23316.
83. Pervez, H.; Mozumder, M.; Mourad, A.-H. Optimization of Injection Molding Parameters for HDPE/TiO2 Nanocomposites Fabrication with Multiple Performance Characteristics Using the Taguchi Method and Grey Relational Analysis. *Materials* **2016**, *9*, 710. https://doi.org/10.3390/ma9080710.
84. Azad, R.; Shahrajabian, H. Experimental Study of Warpage and Shrinkage in Injection Molding of HDPE/RPET/Wood Composites with Multiobjective Optimization. *Mater. Manuf. Process.* **2019**, *34*, 274–282. https://doi.org/10.1080/10426914.2018.1512123.
85. Abdul, R.; Guo, G.; Chen, J.C.; Yoo, J.J.-W. Shrinkage Prediction of Injection Molded High Density Polyethylene Parts with Taguchi/Artificial Neural Network Hybrid Experimental Design. *Int. J. Interact. Des. Manuf. (IJIDeM)* **2020**, *14*, 345–357. https://doi.org/10.1007/s12008-019-00593-4.

Artículo 3

Tubular Sandwich Cross-Sections Fabricated with Wire Arc Additive Manufacturing for Jumbo Structural Members

Lidiana Arrè, Vittoria Laghi, Alejandro Marqués y Michele Palermo (2024).

Structures, 67, 106689

DOI: 10.1016/j.istruc.2024.106689

Impact Factor: 3.900 (JCR 2023); Q1 Structural engineering.

El tercer artículo se centró en el diseño de una estructura final de gran tamaño mediante proceso aditivo WAAM. El sector de la construcción mostró ser un campo en el que la tecnología WAAM podría resultar conveniente creando estructuras tubulares optimizadas de gran tamaño. Con esta premisa se plantearon dos casos de estudio.

En primer lugar, se creó un catálogo de configuraciones de secciones tubulares auto-reforzadas de gran tamaño, centrándose principalmente en los principios de diseño, la elección de los algoritmos de optimización y las limitaciones de fabricación. Estas estructuras auto-reforzadas se generaron mediante diseño computacional, mediante la optimización de los siguientes parámetros de diseño: diámetro exterior (D_{ext}), diámetro interior (D_{int}), número de refuerzos (N_w) y espesor de pared (t). La fabricación de dos especímenes del catálogo, denominados como TSSU_280–240-12–8 y TSSU_240–160-12–4, verificaron las premisas de fabricación de estas estructuras tubulares.

En segundo lugar, tras verificar la hipótesis inicial de diseño y fabricación de estructuras de gran tamaño por método WAAM, se exploró un segundo escenario enfocado en diseñar elementos tubulares auto-reforzados con alta resistencia a la presión radial. Estas estructuras estarían destinadas a aplicaciones offshore, donde la presión del agua ejerce un esfuerzo radial muy importante. La peculiaridad de este diseño residía en el grosor no uniforme de las estructuras diseñadas. Las simulaciones numéricas de pandeo no lineal, que consideraron las propiedades del acero WAAM y las imperfecciones geométricas, demostraron que los diseños WAAM ofrecen prestaciones estructurales significativamente superiores a las de estructuras comerciales equivalentes. Incluso bajo condiciones adversas con grandes imperfecciones geométricas, los diseños WAAM destacaron por su rendimiento, consolidando su viabilidad como solución eficiente e innovadora.

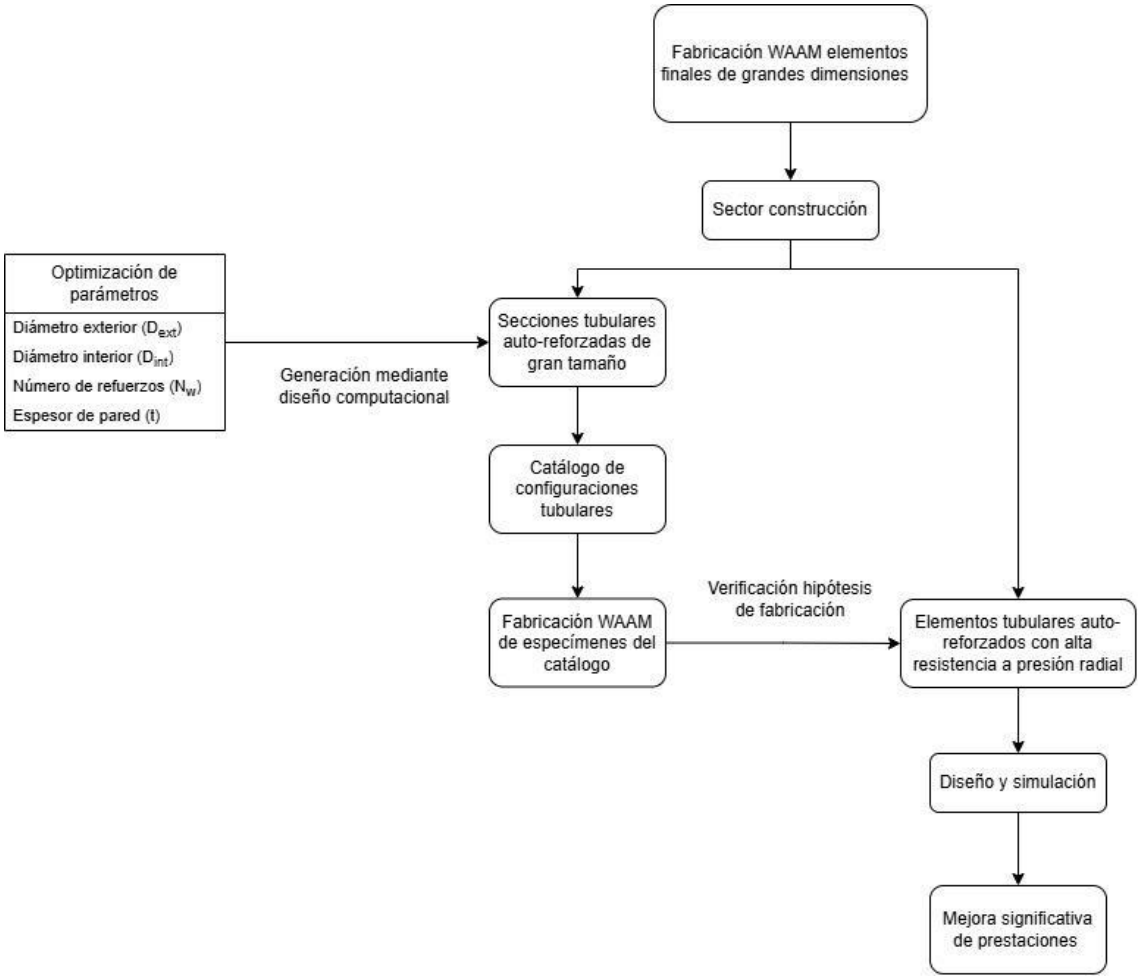

Ilustración 19 Esquema de los trabajos realizados en el artículo 3 para la generación de un catálogo optimizado de secciones tubulares auto reforzadas fabricadas por tecnología WAAM y diseño y simulación de una estructura tubular auto-reforzada de alta resistencia a presión radial.

Structures 67 (2024) 106689

Contents lists available at ScienceDirect

Structures

journal homepage: www.elsevier.com/locate/structures

Tubular sandwich cross-sections fabricated with Wire Arc Additive Manufacturing for jumbo structural members

Lidiana Arrè [a,*], Vittoria Laghi [a], Alejandro Marqués Paola [b], Michele Palermo [a]

[a] Department of Civil, Chemical, Environmental and Materials Engineering (DICAM) - University of Bologna, Viale del Risorgimento, 2, 40136 Bologna, Italy
[b] AITIIP Centro Tecnológico, Romero 12, 50720 Zaragoza, Spain

ARTICLE INFO

Keywords:
Computational design
Design for additive manufacturing
Digital fabrication
Directed Energy Deposition
Offshore engineering

ABSTRACT

Innovations in the field of robotics and production processes have led to the exploration of new manufacturing techniques, offering greater freedom in size and shape of metal additively manufactured (AM) components. This has opened the doors to the design of customized complex-shaped elements. Among these metal AM processes, Wire Arc Additive Manufacturing (WAAM) stands out, enabling the fabrication of complex large-scale structural elements, which are essential for applications in the construction sector. Within offshore engineering applications, submerged steel members of offshore jacket structures, exposed to significant compressive radial pressure, are typically made by Circular Hollow Section (CHS) tubular members. In this regard, the present work focuses on the initial investigations of new geometrical shapes for jumbo tubular cross-sections of steel members, referred to as Tubular Sandwich Sections (TSS), for structural engineering applications requiring high resistance against buckling failure. In detail, the engineered geometrical shape of TSSs offers higher freedom to structural designers able to optimize the design based on different target structural performances. However, to properly account for the specific manufacturing constraints, computational design approaches and advanced numerical simulations should assist the designer towards a feasible structural solution. The present study aims at exploring the potential capabilities of TSSs. First, the geometrical properties and potential structural performances of TSSs are investigated. Then, two different case studies are presented to illustrate different target structural performances. The first one illustrates the application of a parametric approach to design efficient TSSs of uniform thickness leading to the creation of a first catalogue of uniform TSSs. The first proof of concept of uniform TSS is provided by the manufacturing of two samples realized with WAAM technology. The second case study investigates the structural behaviour of non-uniform TSS member specifically designed to resist to high radial compressions. For this aim, linear and non-linear finite element buckling analyses are carried out also considering the effect of initial geometrical irregularities. The structural performances of the TSS member are compared with those of an equivalent CHS member, demonstrating a significant increase in the critical pressure of TSS, even when considering geometrical irregularities.

1. Introduction

In the 21st century, the advancements in software for Computer-Aided Design (CAD), three-dimensional modelling and digital fabrication methods have opened up possibilities for exploring complex and innovative structural forms, including free-form designs, shells and lattice structures [1,2]. The use of these software tools have enabled designers to employ computational methods in the exploration of new structural solutions [3]. However, when adopting Additive Manufacturing (AM) processes to realize these novel designs, it is essential to consider the printing strategy and manufacturing constraints proper of the specific process, that should be integrated within the computational design approach.

Among the AM processes, Wire Arc Additive Manufacturing (WAAM) is an emerging metal AM technology that shows high potential for structural engineering applications [4–6]. It offers benefits like reduced material consumption, design freedom, and the ability to strengthen and repair components [7,8]. Researchers have studied geometrical, mechanical, and microstructural features of WAAM metals [9,10] such as stainless steel [11–13], carbon steel [14,15], and aluminium alloys [16,

* Corresponding author.
E-mail address: lidiana.arre2@unibo.it (L. Arrè).

https://doi.org/10.1016/j.istruc.2024.106689
Received 1 September 2023; Received in revised form 9 March 2024; Accepted 31 May 2024
Available online 19 July 2024

Fig. 1. Potential structural application of TSS members for tree-like structures.

17].

WAAM has been employed in some pilot projects for construction purposes, such as the MX3D Bridge in Amsterdam and the AM Bridge at TU Darmstadt [8,18]. However, the material and structural behaviour of WAAM elements differ from conventionally-produced elements, as proved by several experimental investigations [9,11–15,17,19–23]. This discrepancy requires further research to thoroughly comprehend the microstructural and mechanical properties of WAAM material, thereby enabling the use of WAAM technology in real construction projects. Such research is pivotal for expanding WAAM's application in the construction sector and ensuring the required structural performances and safety levels as prescribed by current design codes for steel constructions [24]. Therefore, further investigation is required to fully grasp the structural performances at the element scale, as data on this aspect remain limited.

Moreover, WAAM process parameters have been investigated to understand how they affect the geometrical quality and mechanical behaviour of the printed outcomes. Consequently, there is a need to integrate the current WAAM limitations into the optimization approach, aiming to design complex-shaped geometries that can be validated in advance for the manufacturing stage [25].

The starting point of this research is represented by conventional Circular Hollow Section (CHS) members, which offer advantages due to their compact and bi-symmetrical cross-sectional shape as compared to other typical cross-sections currently employed for steel structures, such as those based on thin plates (I, C, omega, cruciform,…). These advantages include, among others: (1) high strength-to-weight ratio due to large moment of inertia over cross-sectional area, (2) equal strength against lateral actions applied along any direction, (3) high strength due to lateral-torsional buckling, (4) good buoyancy and hydrodynamic performances. All these features make CHS members ideal for structures subjected to high axial loads and lateral pressures. Examples of possible use include tree-like structural members for large-span pavilions or infrastructures, mega braces for high-rise buildings, and tubular members for offshore jacket structures. For the last, in particular, high resistance to lateral radial pressure induced by hydrostatic loads is required. However, welding is traditionally employed for their fabrication and cast iron-made solutions are often preferred for the joints. Additionally, tree-like structural elements also require complex welding to connect the branches to the trunk (see e.g. Fig. 1), and the construction of mega frames for high-rise steel buildings requires jumbo cross-sections with large-thickness walls.

The initial investigations into new WAAM structural elements that overcome complex welding challenges were conducted by Imperial College London, see [26,27]. They examined WAAM plain Square Hollow Sections (SHS) and strengthened SHS, demonstrating that the latter exhibited improved structural efficiency in terms of load-carrying and deformation capacity.

The present work aims to explore the potential of a novel Tubular Sandwich Section (TSS) for tubular members of enhanced structural performances by merging the good properties of conventional CHS with the possibility offered by WAAM technology to make stronger and stiffer cross-sections [19,26,27], also reducing material waste for more efficient and sustainable structural elements [28]. The novel TSS offers greater geometrical freedom to structural designers for creating structurally efficient and optimized elements. In the case of complex cross-sections, like the proposed TSS, WAAM demonstrates advantages in the fabrication process. Conventional manufacturing technologies would require welding together the cross-sectional components to construct the elements [9]. The large geometrical freedom of WAAM opens new possibilities for the structural design of tubular members characterized by tailored structural performances that can be exploited by different design approaches, such as novel computational design methods based on topology optimization algorithms. On the other hand, the specific fabrication constraints proper of WAAM should be accounted in the design phase to deploy solutions that can be efficiently manufactured. In this regard, the authors recently proposed a conceptual design framework, referred to as "blended" approach [25] to efficiently merge the conceptual structural design with the possibilities offered by optimization algorithms and manufacturing constraints.

The specific objective of this first study is to illustrate the geometrical properties, some potential structural features and the manufacturing feasibility of WAAM-produced TSS. First, the main advantages and potential issues related to the use of WAAM for the fabrication of TSS members are discussed. Then, the "blended" structural design approach is introduced for the design of TSS members. The main geometrical and structural properties of TSS members are illustrated to provide an overview of their potential performances. Two selected scenarios are considered, each one presenting specific properties of TSS members: the first case study focuses on uniform thickness TSS members to develop a structural catalogue for professional designers, while the second case study explores the structural performances of a non-uniform thickness TSS member designed to withstand high radial pressure.

2. Wire Arc Additive Manufacturing

2.1. WAAM technology for the construction sector

Among AM processes, WAAM resulted to be the most suitable technology to realize large-scale metal elements for the construction sector. The main advantages of this technology for large-scale elements are: (i) the possibility to print "out of the box", thus allowing to print complex geometrical shapes, such as those proposed in this work, properly accounting for the main geometrical constraints (such as overhangs, wall thickness) [9,29,30], and (ii) the high deposition rate (2–9.5 kg/h) when compared to other metal AM technologies, while still maintaining good mechanical performances [31]. The typical WAAM set-up adopts an arc welder as power source and welding wire as feedstock to realize the 3D-printed outcome, using either a robotic system or a computer numerically-controlled gantry as motion system.

In the last few years, research efforts have been focused on the assessment of the microstructural and mechanical features of different WAAM metals, such as steels, titanium and aluminium alloys [16,17,32,33]. Research on WAAM investigated the following main aspects: (i) anisotropic behaviour of the 3D-printed specimens, (ii) geometrical characterization, (iii) mechanical characterization, (iv) quality control, (v) development of new forms for structural elements [9]. Nevertheless, there are still challenges and aspects to be explored. Previous studies on the mechanical response of metal WAAM outcomes showed different mechanical properties from the ones of the corresponding wrought material. Therefore, further research is still required to completely characterize the geometrical and mechanical features of WAAM parts, as well as the influence of the process parameters and the reproducibility of their response to draw ad-hoc structural design guidelines.

WAAM elements can be realized by making use of one of the two known printing deposition strategies: (i) the continuous printing, consisting of a layer-by-layer deposition strategy, suitable to realize planar elements by deposition of a layer of molten metal on successive layers, see e.g. [7,14,21,34], (ii) the alternative single-cycle deposition strategy (also referred to as dot-by-dot deposition), consisting of the deposition of subsequent droplets, suitable to realize rod-like elements and lattice structures [13,15]. The first example of large-scale application of WAAM in construction with continuous printing is represented by the MX3D Bridge [35], the first 3D-printed steel pedestrian bridge, which demonstrated that metal 3D printing is suitable for the real-scale applications in the construction sector. The first example of dot-by-dot printing for structural elements is the half-scaled diagrid column realized by AMAC research group at University of Bologna in collaboration with MX3D, designed to achieve the optimal shape of a structural element subjected to compression [5]. In recent years, an increasing interest in dot-by-dot WAAM strategy has emerged, enabling the fabrication of lattice structures and reinforcement for innovative 3D-printed concrete structures [36,37].

2.2. Limitations and advantages of WAAM in the design and manufacturing of TSS

The present section first briefly reviews of the main characteristics of WAAM-produced plates and CHS/SHS elements in terms of mechanical and geometrical properties. Then, it identifies some potential advantages of the WAAM technology in manufacturing complex cross-sections, such as the TSS members introduced here and described in detail in Section 4.

An open issue that requires further study is the influence of the printing process parameters and cooling strategies on both the geometrical and mechanical properties, including surface roughness, lack of straightness, microstructural properties, porosities, cracks, anisotropy, and fatigue-induced effects [10,22,23,38]. Consequently, these features must be addressed when designing and fabricating WAAM-produced members such as TSSs, where post-processing is impractical due to the large-scale of the parts.

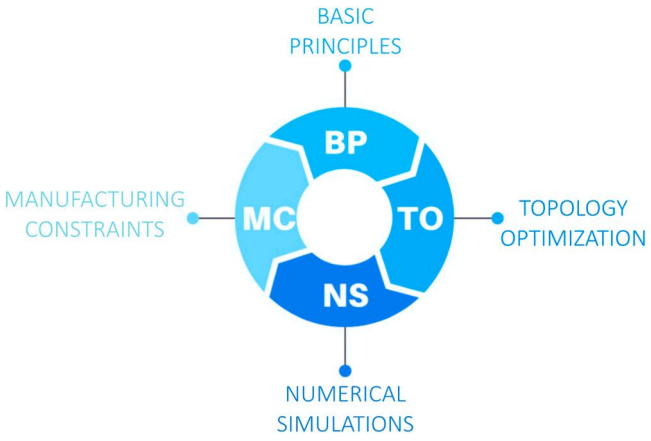

Fig. 2. Fundamental aspects of the blended structural optimization approach. Adapted from [25].

Previous research has explored correlations between the geometrical and mechanical properties of planar WAAM elements, emphasizing inherent geometrical irregularities proper of the layer-by-layer printing process that affect the mechanical response of as-built components [12]. In this context, the maximum peak and pit heights associated with the surface roughness were estimated to reach up to 0.85 mm. The non-linear behaviour of WAAM material was also investigated in previous research carried out by the authors, focusing on thick carbon steel plates (see e.g. [19]). The plates were fabricated using the same WAAM setup, parameters and feedstock as the TSSs studied in this work. The geometrical irregularities of WAAM planar elements, as well as CHS and SHS members, were analyzed to assess their influence on mechanical response [11,12,19,27,39–41]. In particular, CHS members showed out-of-roundness values (O(%)) of approximately 3 % [41], while SHS members exhibited local imperfection amplitude values (e_{max}/t) around 1.0 [27].

On the other hand, recent studies demonstrated the feasibility of strengthening conventional SHS with WAAM through longitudinal stiffeners, fabricated to enhance the local buckling resistance [26]. The limitations and possibilities offered by the WAAM technology, as summarized above, will be accounted for in this work to explore the potential of the novel TSS.

3. Integrated design approaches for Wire Arc Additive Manufacturing in construction

3.1. The blended design approach and its previous applications

In recent years, the use of computational design algorithms allowed the exploration of new structural solutions and the development of novel design ideas. Within the computational design framework, different approaches were proposed. Generative design was used by Wang et al. [42] in an integrated method to create joints for tree-like columns to be realized in AM. Alternatively, topology optimization algorithms were implemented to consider the features proper of AM process. Kanyilmaz et al. [43] proposed innovative steel tubular joints designed by making use of topology optimization and metal AM techniques by mimicking features present in nature. Recently, an automated end-to-end framework for the generation of high-performance AM structures was implemented to integrate AM techniques into the construction of optimized members [6].

With the aim of integrating the capabilities of optimization procedures in terms of new structural shapes with the current limitations of WAAM technology (i.e. manufacturing constraints, printing precision and material properties) together with the robustness and reliability of

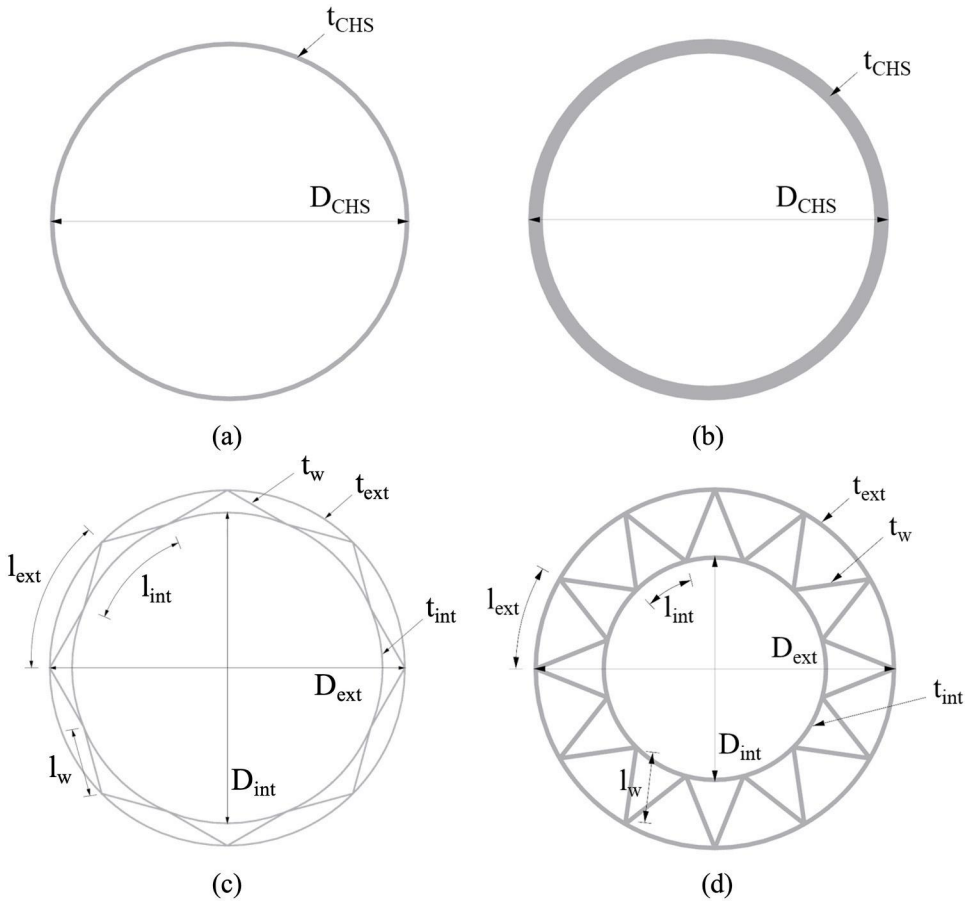

Fig. 3. Main geometrical parameters of: conventional thin (a) and compact (b) CHS, thin (c) and compact (d) TSS.

structural design principles, a so-called "blended" structural optimization approach was recently proposed by the authors [25]. The approach is graphically represented in Fig. 2, which illustrates its main aspects, namely the basic principles, manufacturing constraints, topology optimization algorithms and numerical simulations to verify the structural performances. Indeed, the approach is intended to "blend" a stiffness-based topology optimization approach, suitably tailored for WAAM in terms of manufacturing constraints and material properties, with basic principles of structural design in terms of conceptual design and structural solutions to conceive an initial design. Structural robustness and reliability methods are used to verify the obtained structural performances and guide the designer from the purely mathematically-optimized solutions towards the final design.

The "blended" structural optimization approach may be conveniently used to investigate the potential structural performances of novel structural solutions in an efficient way. The interested reader may find additional information in [25,44,45]. The rationale behind the blended approach was employed to conceive the proposed TSS members, as detailed in the next section.

3.2. The blended design approach for the design of TSS

The concept behind the proposed TSS, which will be illustrated hereafter, was initially conceived by considering all the main aspects of the blended approach as discussed in Section 3.1. The conceptual design phase of TSSs starts with the establishment of their main geometrical parameters and the identification of their main influence on the structural behaviour. Therefore, the design is guided to achieve the target performance criteria in terms of structural behaviour, through a topologically optimized cross-section configuration. The main geometrical properties of TSS are illustrated in Section 4.1, while the general concepts related to the expected structural performances of TSS are discussed in Section 4.2. The main aspects of the blended design are then investigated in detail through two different scenarios, dealing with uniform and non-uniform TSS configurations and presented in Sections 5.1 and 5.2, respectively.

The first case study, detailed in Section 5.1, involves the development of a structural catalogue of uniform TSS configurations, primarily focusing on the design principles, the choice of the optimization algorithms and manufacturing constraints, while the detailed verification of the achieved structural performance is left for future work. The computational design is achieved through the implementation of generative design algorithms to explore various geometrical properties and cross-section classifications of the generated TSSs. WAAM manufacturing constraints are considered in terms of admissible values of wall thickness (t_{int}, t_{ext}, t_w), number of spokes (N_w) and internal and external diameters (D_{int}, D_{ext}), tailored to the current printing limitations of WAAM.

The second case study, outlined in Section 5.2, focuses on a non-uniform thickness TSS configuration designed to exhibit high strength against radial pressure. The conceptual design is guided by the desired buckling mode shape to prevent global cross-section ovalization, thus reducing the free buckling length of the external cylindrical wall directly exposed to radial compression. To achieve this goal, the wall thickness was varied along the cross-section for different components, accounting for the fabrication constraints proper of WAAM. The principles of the conceptual design are then verified by focusing on a specific TSS configuration, which is analysed through numerical buckling simulations. The structural performances are assessed by considering material and geometrical non-linearities and including initial geometrical

imperfections.

4. WAAM tubular sandwich sections for jumbo structural members

4.1. Main geometrical properties of TSSs

The present section introduces the main geometrical and mechanical features of the novel TSS for steel structural members fabricated using WAAM. The geometry of the TSS consists of two thin cylindrical walls connected by several thin spokes with equal length and arranged in triangles, as shown in Fig. 3c-d. For comparison purposes, Fig. 3a-b illustrate conventional CHSs, characterized by a cylindrical wall defined by the external diameter (D_{CHS}) and the thickness (t_{CHS}). The CHS exhibits a quite limited number of degrees of freedom, and its structural performances are mainly governed by the diameter-to-thickness ratio (D_{CHS} / t_{CHS}). Therefore, the typical structural performance that is optimized when using CHS is the area centrifugation which leads to high moment of inertia-to-cross-sectional area ratio. This property allows to obtain larger bending capacity with reduced material usage. On the other hand, as the D_{CHS} / t_{CHS} value increases, it also significantly reduces both the ductility and rotational capacity of the member. Further increases in the D_{CHS} / t_{CHS} values make it prone to local buckling failure, resulting in reduced structural performances with brittle modes of failure. This gradual transition corresponds, in practical design applications, to the progressive change of cross-sectional class from 1 to 4.

Fig. 3c-d illustrate the geometrical parameters of TSSs, namely: the diameter (D_{ext}) and thickness (t_{ext}) of the outer cylindrical wall, the diameter (D_{int}) and thickness (t_{int}) of the inner cylindrical wall, the length (l_w), thickness (t_w) and number of spokes (N_w) connecting the outer and inner cylindrical walls, the free length of the outer cylinder (l_{ext}) defined as the outer circumference (C_{ext}) divided by half number of spokes (l_{ext}=2 C_{ext}/N_w), the free length of the inner cylinder (l_{int}) defined as the inner circumference (C_{int}) divided by half number of spokes (l_{int}=2 C_{int}/N_w). The ranges of variability of the main geometrical parameters (i.e. D_{ext}, t_{ext}, D_{int}, t_{int}, l_w, N_w, t_w, l_{ext}, l_{int}) depend on the adopted WAAM technology, in terms of manufacturing constraints, printing precision and material properties. Based on the current state of development of WAAM, the single-layer wall thickness could be set in the range of 4 to 10 mm, approximately. Generally speaking, the external-to-internal diameters ratio (D_{ext} / D_{int}) and the number of spokes mainly govern the hollowness of the cross-section, while free lengths-to-thickness ratios (l/t) of the walls govern the cross-section slenderness. Therefore, the choice of large D_{ext} / D_{int} ratios coupled with small l/t ratios should lead to ductile compact cross-sections, while small D_{ext} / D_{int} ratios coupled with large l/t ratios should lead to slender cross-sections. Similarly, a low number of spokes coupled with small wall thickness should lead to cross-sections prone to local buckling. Compact cross-sections could be preferred when the main objective is to achieve high ductility under axial forces and bending moments, regardless of their structural efficiency in terms of optimal material use. On the other hand, slender cross-sections could be preferred to achieve more resource-efficient structures in terms of optimal material use, as for the case of lightweight secondary structural elements.

As a result, the large number of parameters describing the TSS geometry offers new possibilities for the structural designer in terms of design freedom. However, effectively designing such new TSS structural cross-section requires a deep comprehension of the relationship between geometrical properties and structural performances. To achieve this goal, several approaches could be pursued, including analytical investigations based on parametric analysis, computational design methods using optimization algorithms, and numerical simulations based on Finite Element (FE) models.

4.2. Mechanical and structural properties of TSSs

As mentioned in the previous sections, the structural design of TSS steel members requires the assessment of their maximum strengths associated with the following failure modes: (i) axial tension, (ii) bending, (iii) buckling under axial compression, and (iv) buckling under radial pressure. In the case of slender steel structural members subjected to high axial compression loading, one of the primary failure mechanisms is buckling. Buckling failure can either involve the entire element (global buckling) or a small portion of it (local buckling). In the first case, the global buckling mode is characterized by a buckling length of the order of magnitude of the element length. In the latter case, the local buckling mode is characterized by buckling lengths of the same order of magnitude of the cross-sectional main dimensions (e.g. the diameter).

This work focuses on TSS members subjected to vertical load and radial pressure, comparing their buckling behaviour with those of CHS members. It is important to recognize that the CHS members are characterized by two cross-sectional geometrical parameters only (i.e. D_{CHS} and t_{CHS}) that govern their structural response. In this regard, the CHS can be seen as an optimized cross-section with respect to the moment of inertia, exhibiting high values when compared with the cross-sectional area. Consequently, CHS members are characterized by large global buckling strength resulting from the high moment of inertia-to-cross-sectional area ratio leading to small slenderness (defined as the ratio between the effective buckling length and the radius of gyration). On the other hand, when the diameter-to-thickness ratio becomes too large, the local buckling failure mode occurs at a stress value smaller than the stress leading to global buckling, and the full global buckling capacity cannot be achieved. Thus, for practical design purposes, high D_{CHS} / t_{CHS} values cannot be used, and specific thresholds are provided by current European codes such as the EC3 in form of tables summarizing the rules for cross-sectional classification (see Table 5.2 of EN 1993–1-1 [24]). In detail, the classification of CHS cross-section is made in terms of D_{CHS} / t_{CHS} values, with the class 4 occurring for D_{CHS} / t_{CHS} values higher than 90 ε^2 ($\varepsilon = \sqrt{235/f_y}$ with f_y being the material yield strength). A further possible buckling failure for CHS may be caused by excessive lateral radial pressure resulting in a form of local buckling characterized by cross-section ovalization. This mode of failure could be particularly relevant for submerged tubular members like the ones adopted in offshore jacket structures.

The same concepts and requirements outlined in EC3 for conventional cross-sections, such as CHS, can be applied to evaluate the strengths of the proposed TSS. These members are characterized by a large number of degrees of freedom, which affect the main geometrical cross-sectional properties. According to EC3, the classification of a generic cross-section may be conducted by evaluating the width (e.g., the free buckling lengths)-to-thickness ratios of all walls that could potentially buckle (e.g., the cross-section portions not restrained by other walls). According to this classification criterion, the buckling stress leading to local buckling is reached in the wall having the maximum width-to-thickness ratio. Similarly, the free buckling length of the external cylinder will trigger the buckling mode under radial compression, with the remaining infill walls acting as restraints. In general, the free buckling length of a TSS member is significantly smaller than the one of a CHS members having the same external diameter and wall thickness. Therefore, TSS members could potentially offer higher buckling strength against both axial compression and radial compression.

The above observations allow to clarify some important general aspects related to the potential advantages of using TSS members, enabling the design of cross-sections with optimized structural properties tailored to the specific applications and load cases. Some of these aspects will be analysed in detail in Section 5.

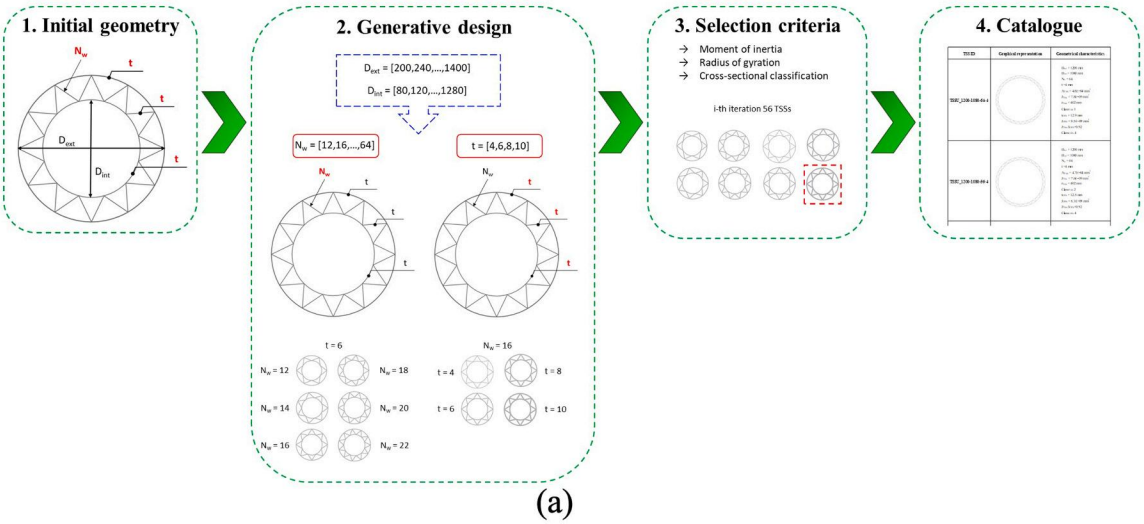

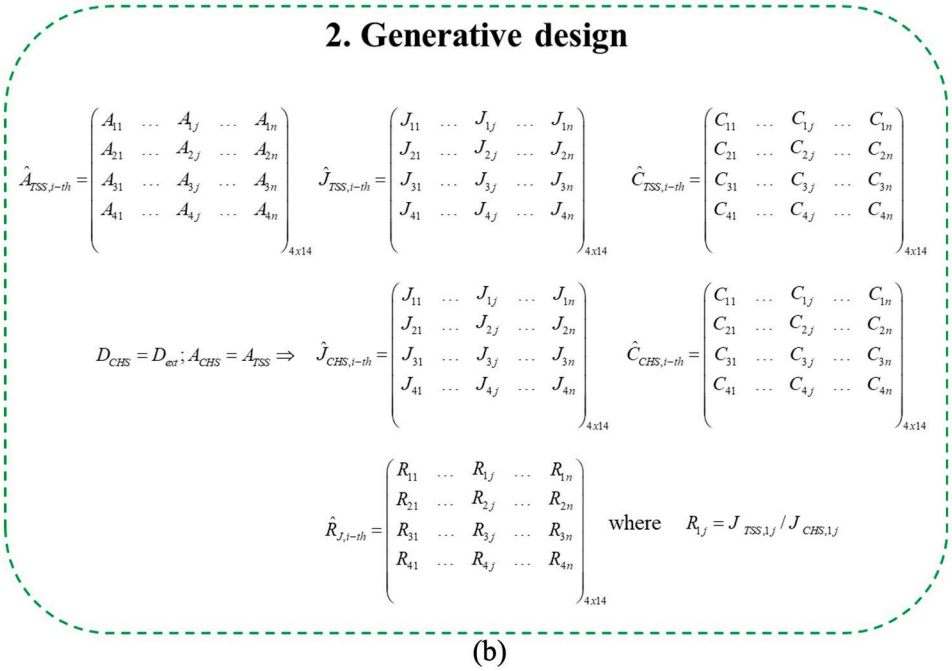

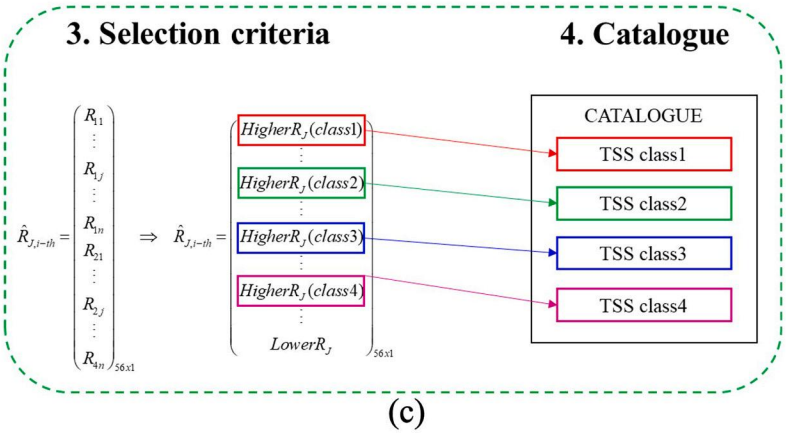

Fig. 4. (a) Computational design flowchart for uniform thickness TSSs. Illustration of the actions implemented in step2 (b) and steps3–4 (c).

Table 1
TSS independent geometrical parameters with their ranges of variability and steps.

Parameters	D_{ext} [mm]	D_{int} [mm]	N_w [-]	t [mm]
Range and step	200-1400 (40)	80-1280 (40)	12-64 (4)	4-10 (2)

5. Application scenarios

5.1. Uniform thickness TSS under bending

5.1.1. Computational design and first catalogue of uniform thickness TSS

The applicative case illustrated in this section focuses on TSS with uniform wall thickness with the main objective of defining a structural catalogue of the so-called "uniform TSS", offering the structural designer with some practical tools for the design of TSS members. The structural catalogue contains information regarding the geometrical properties (such as cross-sectional area, moment of inertia and radius of gyration) and the cross-section classification according to EC3.

For this aim, a computational design procedure is developed through a generative algorithm within Grasshopper graphical algorithm integrated with Rhino 3D modelling tools [46]. The flowchart of the computational design procedure is articulated into four main steps (as illustrated in Fig. 4). The starting point is the geometrical parametrization of the cross-section (step 1), followed by the automatic generation of the TSS configurations through generative design algorithm (step 2). The next step is the implementation of the selection criteria based on the comparison with respect to the equivalent CHS configurations (step 3), ending with the creation of the structural catalogue (step 4). The catalogue of uniform TSS encompasses a wide range of cross-section types, from very stocky to very slender, thus fitting with various civil engineering applications.

In step 1, the TSS geometry is parametrized in terms of the following set of minimum independent parameters: the diameter (D_{ext}) of the outer cylindrical wall, the diameter (D_{int}) of the inner cylindrical wall, the number (N_w) of spokes, and uniform thicknesses ($t_{ext} = t_{int} = t_w = t$), whose ranges of variability are reported in Table 1 based on the current WAAM manufacturing constraints. The physical combinations of D_{ext} and D_{int} are selected imposing the condition $D_{ext} > D_{int}$.

In step 2, the generative design is developed through an iterative process during which, for each generic *i-th* iteration, D_{ext} and D_{int} are kept constant, while all possible physical combinations of N_w and t are generated. The resulting 56 geometrical configurations are organized in a matrix of 4 rows and 14 columns. Similarly, their cross-sectional areas and moment of inertia are organized in matrices, e.g. $\widehat{A}_{TSS,i-th}$ and $\widehat{J}_{TSS,i-th}$. The matrices are graphically illustrated in Fig. 4b. Then, the generative algorithm is repeated for all the physical combinations of external and internal diameters (Table 1). At the generic *i-th* combination, the matrices of the corresponding equivalent CHS configurations are generated by imposing the conditions of equal external diameter D_{CHS}=D_{ext} and equal cross-sectional area A_{CHS}=A_{TSS} for the 56 configurations. Then, the moment of inertia matrix containing the 56 configurations of the equivalent CHS ($\widehat{J}_{CHS,i-th}$) is generated (Fig. 4b), and the 56 ratios between the TSS and corresponding CHS moments of inertia are computed and stored in the matrix $\widehat{R}_{J,i-th}$ (Fig. 4b). The selection criteria are implemented by comparing the moment of inertia and the cross-sectional class of the TSSs and the corresponding equivalent CHSs. For this aim, for each *i-th* combination, the 56 TSS and corresponding equivalent CHS configurations are classified according to EC3 and the cross-sectional classes are collected in the corresponding matrices $\widehat{C}_{TSS,i-th}$ and $\widehat{C}_{CHS,i-th}$.

In step 3, the selection is performed according to the following criteria. First, the values of the matrix ratio $\widehat{R}_{J,i-th}$ are rearranged in a vector with values ranked from the highest to the lowest, keeping track of the geometrical parameters (diameters, spokes and wall thickness) and cross-section class (Fig. 4c).

Finally, in step 4, the selected configurations are inserted into four different parts of the catalogue, each one containing only sections of a specific class, thus obtaining part 1 (containing class 1 TSSs), part 2 (containing class 2 TSSs), part 3 (containing class 3 TSSs), part 4 (containing class 4 TSSs). In the first catalogue release, one cross-section is selected (for each catalogue part, each combination of D_{ext} and D_{int} and each thickness value) considering the selection criterion based on the higher-ranked J_{TSS} / J_{CHS} value. This selection allows to encompass different desired performances, such as large ductility capacity (leading to stocky profiles) or reduced weight (leading to slender profiles). The full catalogue is generated by implementing the selection criterion for all the considered combinations of D_{ext} and D_{int}. To summarize, the first catalogue of uniform TSS provides their main geometrical characteristics and properties (i.e. D_{ext}, D_{int}, t, N_w, A_{TSS}, J_{TSS}, r_{TSS}) as well as the cross-sectional classification according to EC3 for a S235 steel grade [47].

The generic TSS entry of the catalogue is identified using a nomenclature characterized by the following specifications organized as follows: (i) the section type identifier *TSSU* indicating uniform TSS, (ii) the dimension of the outer cylindrical wall D_{ext} in mm, (iii) the dimension of the inner cylindrical wall D_{int} in mm, (iv) the number of spokes N_w, (v) the dimension of the uniform wall thickness in mm indicating a uniform thickness value t for all walls. As an example, the cross-section TSSU_1200–1080-64–4 indicates a uniform TSS with an outer cylindrical wall diameter of 1200 mm, an inner cylindrical wall diameter of 1080 mm, 64 spokes, and 4-mm thickness for all the cross-sectional components.

For illustrative purpose, Fig. 5 presents some selected entries of the uniform TSS catalogue. The table provides the following information: the cross-section identifier (TSS ID), the graphical representation of the cross-section geometry, the main geometrical properties. It also provides a comparison with respect to the equivalent CHS in terms of moment of inertia ratio and cross-sectional class. The following observations may be given. The TSSs show a decrease of the moment of inertia with respect to the equivalent CHS of 8 %. However, despite the TSSs exhibit reduced moment of inertia, they belong to a class higher than the corresponding equivalent CHS (class 4). Therefore, it is expected that TSSs may exhibit larger ductility and rotational capacities. These aspects will be assessed in future work through ad-hoc experimental tests and numerical simulations.

5.1.2. Fabrication of TSS specimens as a first proof of concept

The proof of concept for the proposed computational design approach to generate a wide range of TSSs was demonstrated by successfully producing two sample members at the AITIIP WAAM facilities in Zaragoza, Spain (Fig. 6) [48]. The two TSS demonstrators, identified as TSSU_280–240-12–8 and TSSU_240–160-12–4), were selected from the catalogue. They were fabricated using carbon steel wire with the following WAAM setup: (i) Fronius TPS 500i as welding machine equipped with Fronius WF 60i ROBOCTA DRIVE CMT welding torch mounted on a Yaskawa GP50, (ii) SplitBox SB 60i R as buffer, (iii) ER70S-6 wire as feedstock, and (iv) SanSrc8 welding gas, a mixture of Ar and CO_2. The WAAM process parameters adopted to fabricate the demonstrators are summarized in Table 2. The TSS members, whose dimensions are provided in Table 3, were manufactured using a continuous (layer-by-layer) deposition strategy.

The detailed presentation of the manufacturing process adopted to produce the specimens and their geometrical, microstructural and mechanical characterization (including, for instance, tensile, compression, and fatigue strengths as well as local weaknesses at the connection zones) will be the objective of future work.

TSS ID	Graphical representation	Geometrical characteristics
TSSU_1200-1080-64-4	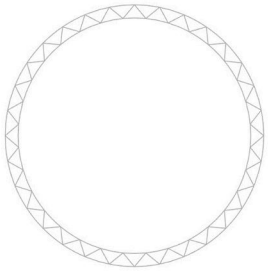	D_{ext} = 1200 mm D_{int} = 1080 mm N_w = 64 t = 4 mm A_{TSS} = 4.8E+04 mm^2 J_{TSS} = 7.8E+09 mm^4 r_{TSS} = 402 mm $Class_{TSS}$ 1 t_{CHS} = 12.9 mm J_{CHS} = 8.5E+09 mm^4 J_{TSS}/J_{CHS}=0.92 $Class_{CHS}$ 4
TSSU_1200-1080-56-4	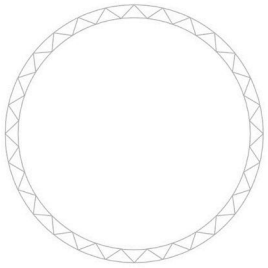	D_{ext} = 1200 mm D_{int} = 1080 mm N_w = 56 t = 4 mm A_{TSS} = 4.7E+04 mm^2 J_{TSS} = 7.6E+09 mm^4 r_{TSS} = 402 mm $Class_{TSS}$ 2 t_{CHS} = 12.5 mm J_{CHS} = 8.3E+09 mm^4 J_{TSS}/J_{CHS}=0.92 $Class_{CHS}$ 4
TSSU_1200-1080-48-4	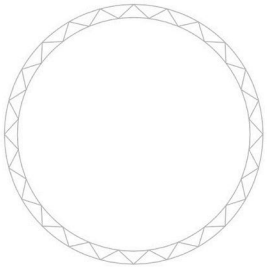	D_{ext} = 1200 mm D_{int} = 1080 mm N_w = 48 t = 4 mm A_{TSS} = 4.6E+04 mm^2 J_{TSS} = 7.4E+09 mm^4 r_{TSS} = 402 mm $Class_{TSS}$ 3 t_{CHS} = 12.2 mm J_{CHS} = 8.1E+09 mm^4 J_{TSS}/J_{CHS}=0.92 $Class_{CHS}$ 4
TSSU_1200-1080-36-4	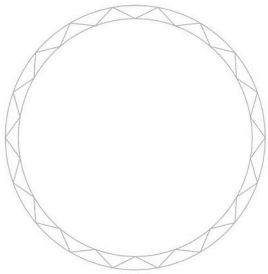	D_{ext} = 1200 mm D_{int} = 1080 mm N_w = 36 t = 4 mm A_{TSS} = 4.4E+04 mm^2 J_{TSS} = 7.1E+09 mm^4 r_{TSS} = 402 mm $Class_{TSS}$ 4 t_{CHS} = 11.8 mm J_{CHS} = 7.8E+09 mm^4 J_{TSS}/J_{CHS}=0.92 $Class_{CHS}$ 4

Fig. 5. Graphical representation and geometrical characteristics of selected TSSs extracted from the TSS structural catalogue.

5.2. *Non-uniform thickness TSS subjected to radial pressure*

5.2.1. *Design principles based on the desired buckling failure mode*

As anticipated in Section 4, CHS members exhibit a desired structural response under combined axial loads, biaxial lateral loads and hydrostatic pressure, resulting to be the most suited choice for structural members of offshore steel jacket structures. Despite this fact, their fabrication requires complex welding with particular care for the

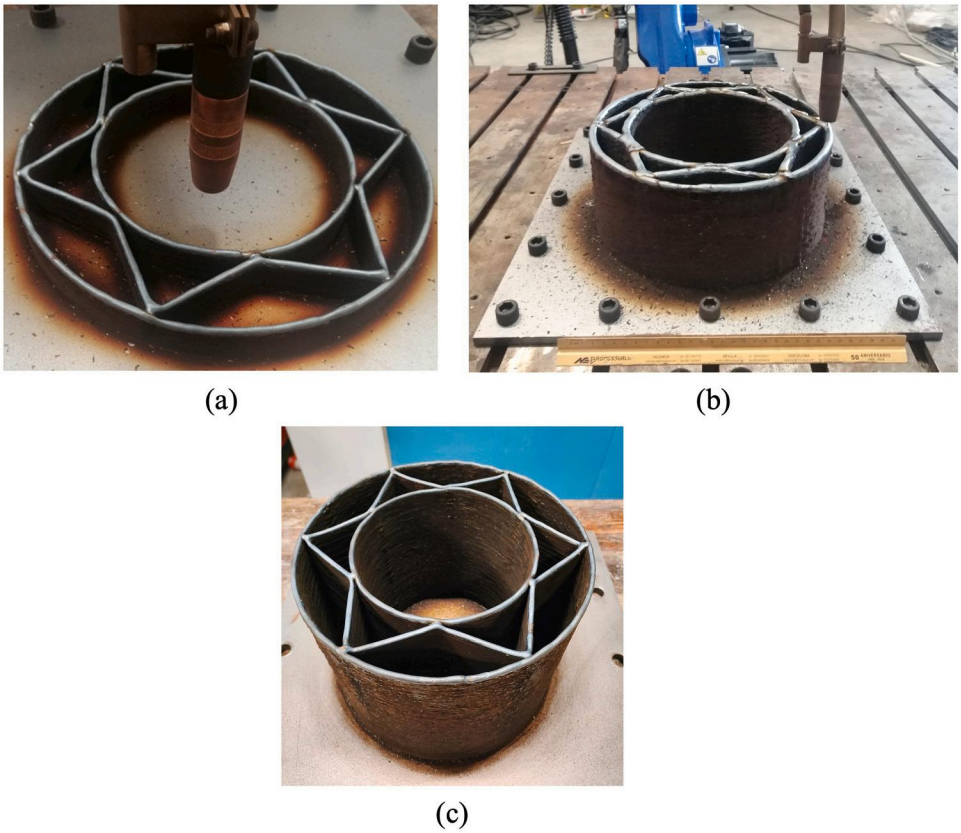

Fig. 6. (a) WAAM torch during the fabrication of the demonstrators by AITIIP company [48]. TSS sample members: (b) 8-mm thickness, (c) 4-mm thickness.

Table 2
WAAM process parameters adopted by AITIIP to fabricate the two demonstrators [48].

WAAM process parameter	
Wire feed rate	7.5 m/min
Layer height	2.25 mm
Robot printing velocity	0.018 m/s
Robot travel velocity	0.06 m/s
Current	238 A
Voltage	16.34 V
Gas flow rate	15 l/min

tubular joint parts that are subjected to a critical stress state and become very prone to stress concentration and fatigue issues [49]. In light of this, TSS can be considered an improved cross-section for tubular members in offshore structures. In fact, submerged members of offshore jacket structures need to withstand large compressive hydrostatic pressure. Hence, the proper design of TSS may optimize their behaviour, leveraging their advantages associated with the freedom of the geometric configuration and the possibility of using variable thicknesses for different walls.

For this aim, this second applicative study investigates the behaviour of a TSS steel member under axial compression and radial compression as compared with the corresponding equivalent CHS steel member having the same external diameter and cross-sectional area. According to the standards adopted for the structural design of offshore steel tubular members [50], CHS members characterized by a very large D/t ratio may experience buckling failure under hydrostatic pressure, leading to the whole cross-section ovalization (see Fig. 7a), making them unsuitable for such applications.

TSS can be designed to mitigate this disadvantage. Based on simple considerations dealing with the desired buckling mode shape under radial compression (see Fig. 7b), the TSS geometrical configuration should be designed to effectively constrain the external stiff cylinder by the spokes then connected to the inner cylinder. Therefore, a larger thickness needs to be assigned to the external cylinder which is directly subjected to the lateral radial pressure. Consequently, a smaller thickness can be allocated to the spokes and inner cylinder since their main function is only to provide an effective restraint for the external cylindrical wall.

To demonstrate the expected behaviour, a specific TSS member is designed according to the principles illustrated above, with the particular goal to improve the behaviour under radial compression. In detail, the diameter (D_{ext}) and thickness (t_{ext}) of the outer cylindrical wall are equal to 300 mm and 2 mm, respectively, the diameter of the inner cylindrical wall (D_{int}) is equal to 200 mm, the number of spokes (N_w) is equal to 24, while the wall thickness of the inner cylinder (t_{int}) and spokes (t_w) is set equal to 0.75 mm. The member is designed considering a cantilever condition with a length equal to 4.8 m. The corresponding equivalent CHS has a diameter D_{CHS}=D_{ext} and a wall thickness (t_{CHS}) of 3.6 mm. Table 4 provides a summary of the key geometrical parameters

Table 3
Geometrical properties of the TSS demonstrators.

TSS Demonstrator	TSS ID	D_{ext} [mm]	D_{int} [mm]	t_{ext} [mm]	t_{int} [mm]	t_w [mm]	N_w [-]
t = 8 mm	TSSU_280-240-12-8	280	240	8	8	8	12
t = 4 mm	TSSU_240-160-12-4	240	160	4	4	4	12

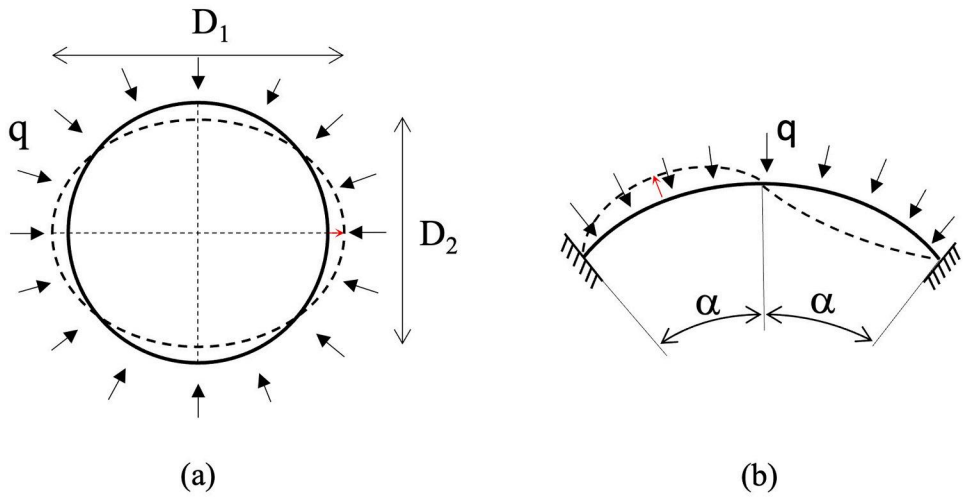

Fig. 7. Graphical representation of buckled deformed configurations: (a) buckled ovalized shape of CHS under radial pressure; (b) buckled shape of a circular arch sector with hinged ends under radial pressure, representing the portion of the external circumference of the TSS effectively restrained by the spokes and the internal circunference.

Table 4
Geometrical and mechanical properties of CHS and TSS members.

	CHS	TSS
Geometrical		
D_{ext}, D_{int} [mm]	/	300, 200
t_{ext}, t_{int}, t_w [mm]	/	2, 0.75, 0.75
N_w [-]	/	24
D_{CHS} [mm]	300	/
t_{CHS} [mm]	3.6	/
A [mm^2]	3352	3368
J [mm^4]	3.68E+07	3.10E+07
r [mm]	105	96
L [mm]	4800	4800
Mechanical		
E [MPa]	205000	205000
f_y [MPa]	332	332

Table 5
Structural performances of CHS and TSS members with element lengths of 4.8 m.

Predicted strengths	CHS	TSS
Axial load [kN]	1113	1118
Yielding moment [kN m]	81	69
Global Euler buckling [kN]	828	680
Critical pressure [MPa]	0.8	1.6

of the TSS and the corresponding equivalent CHS member.

The main expected structural performances of the TSS and corresponding equivalent CHS were initially estimated considering the values of the geometrical and material parameters reported in Table 4 according to the formulations reported below and graphically illustrated in Fig. 7. Then, the CHS and TSS structural performances are summarized in Table 5.

- Axial yield strength [51]: $N_{pl} = Af_y$;
- Yielding bending moment strength [51]: $M_y = W_{el}f_y$, with $W_{el} = \frac{J}{(D_{ext}/2)}$ being the strength modulus;
- Global Euler buckling strength [52]: $N_{cr,E} = \frac{\pi^2 EJ}{(\beta L)^2}$, assuming an effective length factor $\beta = 2$ (cantilever configuration);
- Critical radial pressure [52]: (i) for the CHS the critical pressure is evaluated according to the formulation valid for circular arches: $q_{cr} = \frac{2E}{(1-\nu^2)}\left(\frac{t}{D}\right)^3$ (in this case the buckled deformed shape is ovalized, as depicted in Fig. 7a); (ii) for the TSS the critical pressure is evaluated according to the formulation valid for a sector of a circular arch described by a central angle equal to 2α: $q_{cr} = \frac{2}{3}\frac{E}{(1-\nu^2)}\left(\frac{t}{D}\right)^3\left(\frac{\pi^2}{\alpha^2} - 1\right)$ (with $\alpha = 60^\circ$ corresponding to the central angle between two spokes, see Fig. 7b).

It can be noted that the expected elastic critical pressure for the TSS is twice the one expected for the corresponding equivalent CHS, thus confirming the basic design principles outlined in this section (see Table 5). On the other hand, given that the CHS has a higher moment of inertia and wall thickness, it is consequently characterized by a higher yielding moment strength and a higher Euler buckling load. Moreover, since the wall thickness of the CHS is greater than that of the spokes of the TSS, it follows that the local buckling stress under compression of the CHS is much higher than that of the TSS.

5.2.2. *Numerical modelling*

The TSS and CHS members were numerically analysed by means of Finite Element Analysis (FEA). For this aim, both linear elastic buckling analysis and non-linear buckling analysis were developed considering the influence of mechanical and geometrical irregularities (GMNIA) [53]. The analyses were carried out employing the FE software ABAQUS [54]. The small thickness of the walls allow the use of shell models made of 4-node linear quadrilateral shell elements (designated as S4R in the ABAQUS element library). The nominal size of the mesh was selected through a mesh sensitivity analysis as discussed in Section 5.2.3.

The analyses were carried out on both CHS and TSS members with two different member lengths, i.e. 0.5 m (stub members) and 4.8 m (slender members). Both axial compression and radial pressure load cases were analysed. Then, the non-linear GMNIA were carried out considering only the radial pressure load, as the TSS was designed primarily to withstand high radial compression. The linear buckling analysis allowed for the evaluation of the first elastic critical loads and the corresponding buckling mode shape, which were then used to model the initial geometrical imperfections for the GMNIA. Fig. 8a-b display the mesh of the FE models of TSS and CHS members, while Fig. 8c-d provide a graphical illustration of the applied loads and boundary conditions.

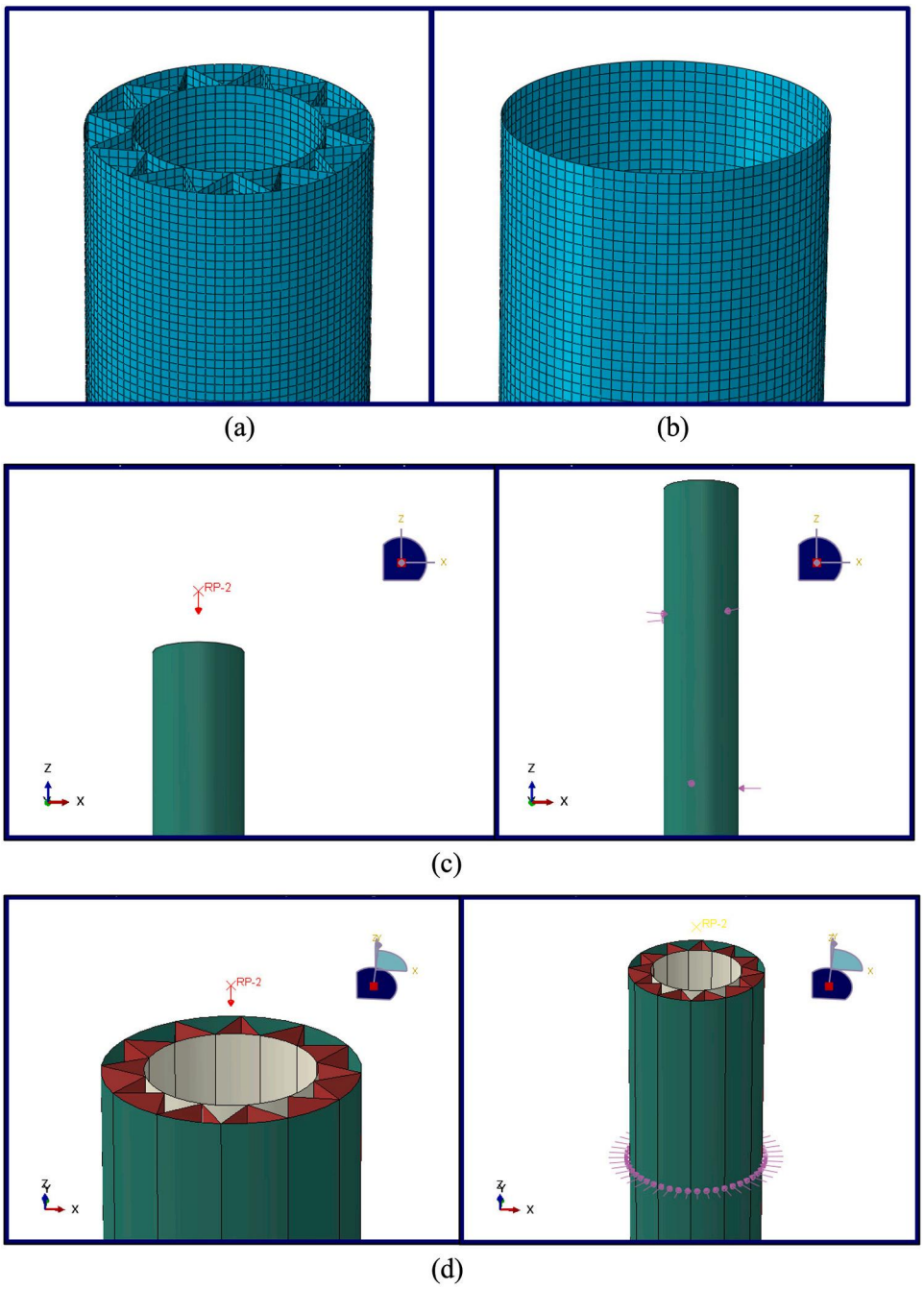

Fig. 8. FE models of TSS and CHS members: (a-b) mesh of TSS and CHS, respectively; (c-d) load cases for axial compression (on the left) and lateral radial pressure (on the right) of CHS and TSS, respectively.

The boundary and loading conditions were set using two reference points (RP) defined by a set of coordinates. One reference point (RP-1) was set at the bottom end of the member to simulate a fixed support, while the other reference point (RP-2) located at the top end of the member was not constrained thus leading to a cantilever structural scheme. The second reference point (RP-2) was used to apply the vertical load. The radial pressure is applied by imposing a uniform distribution of radial compression to the outer face of the external cylindrical wall.

For the linear elastic buckling analysis, the steel material is modelled according to the Hook's law, while for the GMNIA the steel material is modelled according to an elasto-plastic with hardening stress-strain curve (Fig. 9a). The key mechanical parameters of both linear and non-linear constitutive material models are based on the results of previous tests on layer-by-layer steel WAAM-produced plates manufactured by the same producer using ER70S-6 welding wire as feedstock [19]. The Young's modulus is set equal to 205 GPa, the yield stress and strain are set equal to 332 MPa and 0.16 %, respectively, while the ultimate stress and strain are set equal to 455 MPa and 23 %, respectively. In particular, ABAQUS requires a stress-strain curve defined in terms of true stress and log plastic strain, which was implemented to perform the FE simulations according to [55].

The non-linear buckling analyses under lateral radial pressure were conducted employing the Riks method available on ABAQUS to efficiently deal with the geometrical and material non-linearities [56]. The magnitude of the initial imperfections is assumed to encompass a range similar to the intrinsic imperfections obtained from the geometrical characterization of WAAM CHS members, as discussed in [12,41] and schematically illustrated in Fig. 9b.

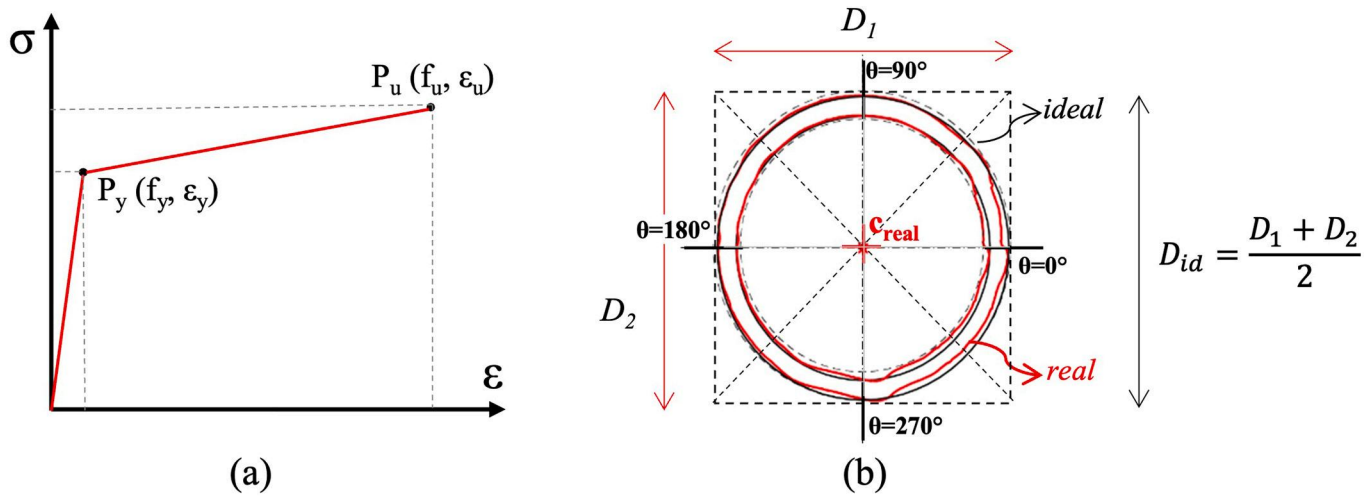

Fig. 9. (a) Elasto-plastic with hardening stress-strain curve. (b) Real CHS printed using WAAM, and evaluation of an ideal CHS with a specified outer diameter (D_{id}) Adapted from [41].

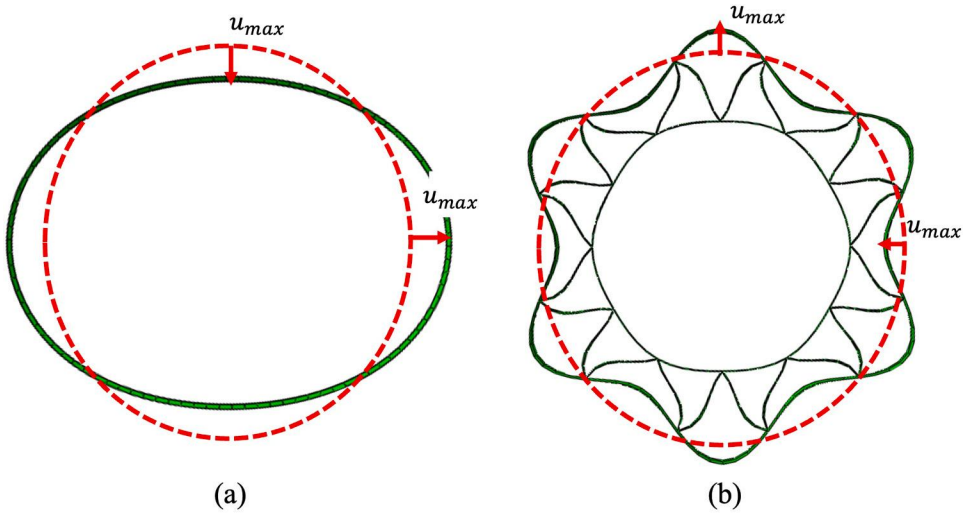

Fig. 10. Buckled shape under lateral radial pressure highlighting the maximum amplitude of initial imperfections for (a) CHS member and (b) TSS member.

The TSS and CHS geometrical shapes with imperfections were set as the deformed shape of the first buckling mode obtained from the linear buckling analysis, as also discussed in [55]. To quantify the influence of the geometrical imperfections on the critical pressure, the maximum amplitudes of the local imperfections (represented with red arrows in Fig. 10) were set equal to 0.5 mm, 1 mm, 2 mm, and 3 mm, corresponding to a CHS out-of-roundness (i.e. $O(\%) = \frac{|D_2 - D_1|}{D_n} \cdot 100$ [41]) of 0.67 %, 1.33 %, 2.67 % and 4.00 %, respectively. These out-of-roundness values are in line with the maximum admissible tolerances as provided by typical standards adopted by CHS members. Specifically, industry standards specify a maximum out-of-roundness tolerance of 2 % for traditionally cold-formed welded CHS according to EN 10219–2 [57], increased to 3 % for tubular members of fixed steel offshore structures according to ISO 19902 [50]. Additionally, the assumed out-of-roundness values are also in agreement with the maximum out-of-roundness value of 3.2 % measured for WAAM CHSs [41]. The maximum amplitude of local imperfections defined for CHS members is also imposed on TSS members (as represented in Fig. 10b), for which standards are not currently available. In addition, to assess the sensitivity of both CHS and TSS when subjected to the same maximum local imperfections, it is convenient to compare the imperfection amplitude with the wall thickness. For the considered case, the maximum imperfections range from 0.25t to 4t for the TSS (whose wall thickness t varies from 0.75 mm to 2 mm), and from 0.14t to 0.93t for CHS (having a constant thickness t of 3.6 mm) [55,58]. Based on this comparison, the TSS would experience a much higher sensitivity to the same absolute imperfections with respect to CHS.

5.2.3. *Results from the linear buckling analysis*

The choice of mesh size plays a pivotal role in achieving accurate and efficient numerical results. Thus, a mesh sensitivity analysis was conducted with the aim of balancing the required level of accuracy from structural engineering perspective with affordable computational cost. The mesh sensitivity analysis was performed on a portion of 0.5 m-long tubular member (the reduced length allows to substantially reduce the computational effort). Two separate load cases were considered including axial compression and lateral radial compression. In each analysis the mesh size was varied considering six different models (M_1, M_2, M_3, M_4, M_5, M_6) and varying the nominal element size from 25 mm (for M_1), 22 mm (for M_2), 20 mm (for M_3), 15 mm (for M_4), 10 mm (for M_5), up to 9 mm (for M_6) while monitoring its effect on the resulting first buckling load. To further validate the results of the numerical simulations, comparisons were also made considering the predicted values according to the analytical formulations discussed in Section 5.2.1. For

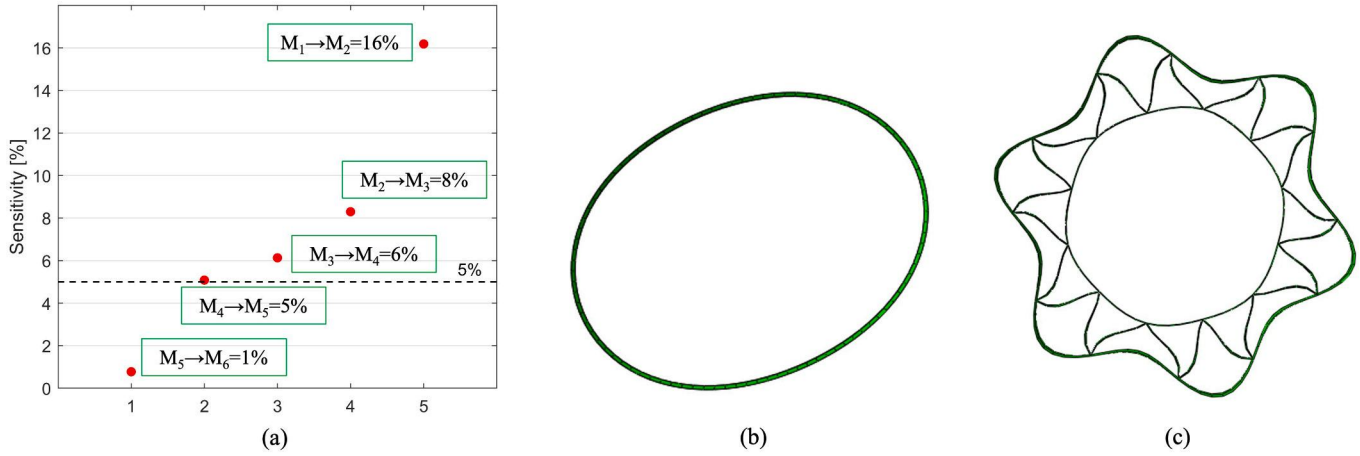

Fig. 11. Results from linear buckling analyses on CHS and TSS members: (a) sensitivity analysis performed on stub TSS member under lateral radial pressure. (b) Ovalization of slender CHS member under radial pressure. (c) Buckled shape of slender TSS member under radial pressure.

Table 6
Structural performances comparison between slender TSS and conventional CHS members.

	CHS		TSS	
	Analytical	**Numerical**	**Analytical**	**Numerical**
Global Euler buckling [kN]	828	751	680	631
Critical pressure [MPa]	0.78	0.80	1.56	1.92

illustrative purposes, Fig. 11a shows the results of the sensitivity analysis conducted on the TSS member as subjected to radial pressure. The graph displays the relative error (indicated as sensitivity [%]) in the estimation of the first buckling load as computed comparing model M_i and M_{i+1} (the comparison is indicated with the following notation, M_i => M_{i+1}). It can be noted that the relative error drastically reduces from 16 % when comparing M_1 with M_2 up to 1 % when comparing M_5 and M_6. Assuming a threshold for admissible error of 5 %, it leads to the selection of an optimal mesh size of 10 mm (e.g. model M_5), which provides the required good balance between precision and computational cost.

Fig. 11b-c display the deformed shapes of the first buckling modes of both TSS and CHS members under radial compression. The deformed shapes confirm the expected buckling modes based on the theoretical formulations mentioned in Section 5.2.1. Furthermore, the values of the first buckling modes from the FEA, summarized in Table 6, are consistent with the analytical predictions. The numerical simulations confirm that the TSS has an elastic critical pressure almost twice the one of the corresponding equivalent CHS.

The enhanced buckling strength of the TSS member is attributed to the effective constraints provided by the spokes and the inner cylinder, reducing the free buckling length corresponding to the arch sector between two consecutive spokes, as illustrated by the buckled shape shown in Fig. 11c. On the contrary, the buckled shape of the CHS member involves the full cylinder, leading to a global cross-section ovalization, see Fig. 11b, according to the theoretical formulation reported in Section 5.2.1.

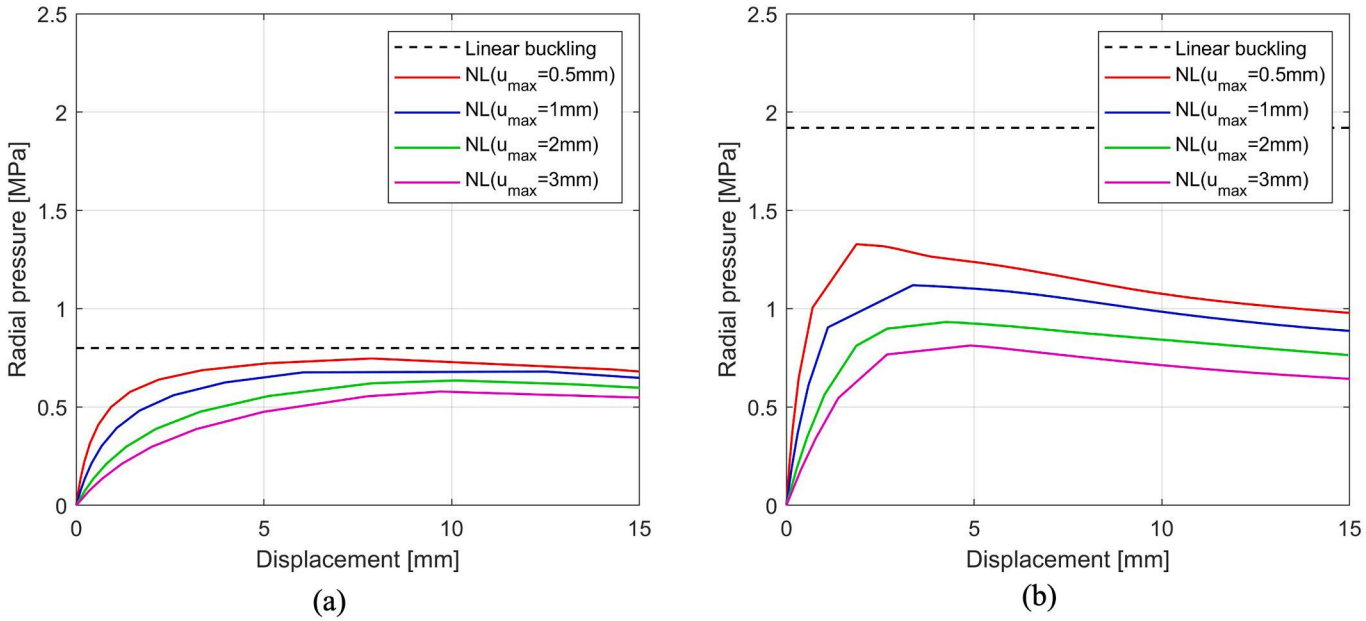

Fig. 12. Non-linear analyses on members with initial imperfections (imposing a maximum amplitude of 0.5 mm, 1 mm, 2 mm, 3 mm) under lateral radial pressure: (a-b) slender CHS and TSS members, respectively.

Table 7
Results from non-linear analyses: critical pressures for both TSS and CHS slender members, and their ratios.

		Critical pressure			
		CHS [MPa]	TSS [MPa]	TSS GMNIA/TSS linear [-]	TSS/CHS [-]
Linear Buckling Analysis		0.80	1.92	-	2.40
GMNIA	u_{max}= 0.5 mm	0.75	1.33	0.69	1.77
	u_{max}= 1.0 mm	0.68	1.12	0.58	1.65
	u_{max}= 2.0 mm	0.63	0.93	0.49	1.48
	u_{max}= 3.0 mm	0.58	0.81	0.42	1.40

5.2.4. Results from GMNIA

The global results from the non-linear static analyses with material and geometrical imperfections (GMNIA) are represented in Fig. 12a,b in terms of buckling curves showing the radial pressure vs maximum local imperfection, e.g. the cross-section ovalization for the CHS and the maximum deflection reached at the crest points for the TSS, as illustrated in Fig. 10. The peak values of the radial pressure shown in the buckling curves represent the critical pressure values q_{cr} and are collected in Table 7, which also provides the ratios between the critical pressure achieved by the TSS and the corresponding equivalent CHS.

It can be noted that the TSS critical pressure decreases from 1.92 to 0.81 MPa, while a smaller reduction is observed when considering the CHS, since the critical pressure reduces from 0.80 to 0.58 MPa. The reduction of the critical pressure in presence of imperfections can be expressed in terms of ratio between the results from the non-linear (GMNIA) and linear analyses, whose minimum value is equal to 0.42 for TSS, as reported in Table 7. These results confirm the expected higher sensitivity of the TSS members to local imperfections as compared to the CHS members subjected to the same maximum local imperfection. The critical pressure ratio between TSS and CHS decreases from 2.40 (when considering the results of the linear buckling analysis) to 1.40 (when considering the results of the non-linear GMNIA). This finding indicates that, despite the higher sensitivity of the TSS to the initial imperfections, even in presence of very large initial imperfections, it still exhibits a significantly higher buckling capacity (+40% of that of the equivalent CHS). Such increase can be also expressed in terms of increment of the hydrostatic load which can be withstood by the TSS member. The increase in water column depth exhibited by TSS when compared to CHS varies between 20 m (for GMNIA with u_{max}=3 mm) up to 110 m (for linear buckling analysis). Those considerations, even though based on very preliminary results, clearly show the high potential of TSS for offshore applications.

6. Conclusions

The present work aims at providing the first insights on a new class of tubular cross-sections for steel members, referred to as Tubular Sandwich Section (TSS). TSS offers several advantages to the designers related to the increased degrees of freedom of its geometrical configuration, allowing for a wider range of structural requirements to be met and ensuring flexibility in the design phase. In this respect, they are particularly suitable to exploit the high potential offered by Additive Manufacturing (AM) technologies, novel computational design and topology optimization algorithms. One recent design approach proposed by the authors was specifically developed to blend the conceptual design of new efficient structural forms with computational design algorithms, accounting for AM constraints and advanced simulation tools for the final verification of the structural performances. This paper sheds light on the conceptual design of TSSs and the application of the blended design approach through the illustration of two specific scenarios dealing with uniform and non-uniform thickness TSS members.

The focus of the first scenario was on uniform thickness TSS to develop a first structural catalogue of uniform TSSs providing their main geometrical properties and cross-sectional classification. The catalogue is organized into four parts, each one including cross-sections characterized by the same class. This approach ensures that the catalogue offers a broad spectrum of solutions to the industry and structural designers, ranging from compact class 1 cross-sections with thick walls to slender class 4 cross-sections with thin walls. The feasibility of the concept was demonstrated through the successful manufacturing of two prototypes of uniform thickness TSSs (i.e. 4 mm and 8 mm) using WAAM technology, allowing the production of optimized large-scale structural elements.

In the second scenario, the focus was shifted to the design of non-uniform TSS members with high strength against radial pressure, which could be particularly suitable for applications in the offshore sector. The structural performances of a specific slender TSS were evaluated through numerical non-linear buckling simulations accounting for the non-linear behaviour of WAAM steel material and initial geometrical imperfections. The comparison with the performances of the equivalent slender CHS member of the same external diameter and cross-sectional area demonstrated that the TSS may lead to significantly improved structural performances, with an increase in the elastic critical pressure of 140%. Even when high geometrical imperfections are considered, the TSS performances are still superior to that of the equivalent CHS, with an increased critical pressure of 40%. Such increases in critical pressure correspond to a water column depth ranging between 20 m and 110 m (ranging from GMNIA with u_{max}=3 mm to linear buckling analysis). The higher sensitivity to geometrical imperfections of TSS is related to the thinner wall thickness, less than one-third of that of the equivalent CHS.

Overall, the obtained results indicate that TSS represents a very promising solution for optimized tubular steel members capable of fulfilling a wide range of structural performances. The next steps of the research will focus on the development, verification and validation of new TSS designs, exploring, for example, the possibility of considering all available geometrical degrees of freedom. The validation will include the development of a wide experimental testing campaign to assess the microstructural, geometrical and mechanical performances of the optimized TSS members. Moreover, future research will delve deeper into the manufacturing process, therefore facilitating considerations for cost-effective and time-efficient solutions tailored to specific industrial applications.

Declaration of Competing Interest

The authors declare that they have no known competing financial interests or personal relationships that could have appeared to influence the work reported in this paper.

Acknowledgements

The authors gratefully acknowledge AITIIP Centro Tecnologico held in Zaragoza (Spain) for the fabrication of the demonstrators.

References

[1] Li Z, Ye J, Gao B, Wang Q, Quan G, Shepherd P. Digital and automatic design of free-form single-layer grid structures. Autom Constr 2022;133. https://doi.org/10.1016/J.AUTCON.2021.104025.

[2] Xie YM. Generalized topology optimization for architectural design. Archit Intell 2022;1. https://doi.org/10.1007/s44223-022-00003-y.

[3] Rong Y, Zhao ZL, Feng XQ, Xie YM. Structural topology optimization with an adaptive design domain. Comput Methods Appl Mech Eng 2022;389. https://doi.org/10.1016/J.CMA.2021.114382.

[4] Feucht T, Lange J, Waldschmitt B, Schudlich AK, Klein M, Oechsner M. Welding process for the additive manufacturing of cantilevered components with the waam. Adv Struct Mater 2020;125:67–78. https://doi.org/10.1007/978-981-15-2957-3_5/COVER.

[5] Laghi V, Palermo M, Gasparini G, Trombetti T. Computational design and manufacturing of a half-scaled 3D-printed stainless steel diagrid column. Addit Manuf 2020;36. https://doi.org/10.1016/j.addma.2020.101505.

[6] Ye J, Kyvelou P, Gilardi F, Lu H, Gilbert M, Gardner L. An End-to-End Framework for the Additive Manufacture of Optimized Tubular Structures. IEEE Access 2021;9:165476–89. https://doi.org/10.1109/ACCESS.2021.3132797.

[7] Kloft H, Schmitz LP, Müller C, Laghi V, Babovic N, Baghdadi A. Experimental application of robotic wire-and-arc additive manufacturing technique for strengthening the I-beam profiles. Buildings 2023;13:366. https://doi.org/10.3390/buildings13020366.

[8] Feucht T, Lange J. 3-d-printing with steel: additive manufacturing of connection elements. Adv Eng Mater, Struct Syst: Innov, Mech Appl - Proc 7th Int Conf Struct Eng, Mech Comput 2019;2019:419–24. https://doi.org/10.1201/9780429426506-75/3-PRINTING-STEEL-ADDITIVE-MANUFACTURING-CONNECTION-ELEMENTS-FEUCHT-LANGE.

[9] Gardner L. Metal additive manufacturing in structural engineering – review, advances, opportunities and outlook. Structures 2023;47:2178–93. https://doi.org/10.1016/j.istruc.2022.12.039.

[10] Mao H, Jing C, Kong F, Xu T, Xiao X, Li K, Ling X, Liu C. Improve the manufacturing efficiency of steel bars by using hot-wire pulse arc additive manufacturing. J Manuf Process 2023;89:430–43. https://doi.org/10.1016/j.jmapro.2023.01.074.

[11] Hadjipantelis N, Weber B, Buchanan C, Gardner L. Description of anisotropic material response of wire and arc additively manufactured thin-walled stainless steel elements. Thin-Walled Struct 2022;171. https://doi.org/10.1016/j.tws.2021.108634.

[12] Laghi V, Palermo M, Gasparini G, Girelli VA, Trombetti T. On the influence of the geometrical irregularities in the mechanical response of Wire-and-Arc Additively Manufactured planar elements. J Constr Steel Res 2021;178. https://doi.org/10.1016/j.jcsr.2020.106490.

[13] Laghi V, Palermo M, Tonelli L, Gasparini G, Girelli VA, Ceschini L, Trombetti T. Mechanical response of dot-by-dot wire-and-arc additively manufactured 304L stainless steel bars under tensile loading. Constr Build Mater 2022;318. https://doi.org/10.1016/j.conbuildmat.2021.125925.

[14] Huang C, Kyvelou P, Zhang R, Ben Britton T, Gardner L. Mechanical testing and microstructural analysis of wire arc additively manufactured steels. Mater Des 2022;216. https://doi.org/10.1016/j.matdes.2022.110544.

[15] Silvestru VA, Ariza I, Taras A. Structural behaviour of point-by-point wire arc additively manufactured steel bars under compressive loading. J Constr Steel Res 2023;207. https://doi.org/10.1016/j.jcsr.2023.107982.

[16] Anaz Khan M, Latheef A. Metal additive manufacturing of alloy structures in architecture: a review on achievements and challenges. Mater Today Proc 2023. https://doi.org/10.1016/j.matpr.2023.05.192.

[17] Dinovitzer M, Chen X, Laliberte J, Huang X, Frei H. Effect of wire and arc additive manufacturing (WAAM) process parameters on bead geometry and microstructure. Addit Manuf 2019;26:138–46. https://doi.org/10.1016/J.ADDMA.2018.12.013.

[18] Gardner L, Kyvelou P, Herbert G, Buchanan C. Testing and initial verification of the world's first metal 3D printed bridge. J Constr Steel Res 2020;172. https://doi.org/10.1016/j.jcsr.2020.106233.

[19] Laghi V, Arrè L, Tonelli L, Di Egidio G, Ceschini L, Monzón I, Laguía A, Dieste JA, Palermo M. Mechanical and microstructural features of wire-and-arc additively manufactured carbon steel thick plates. Int J Adv Manuf Technol 2023;127:1391–405. https://doi.org/10.1007/S00170-023-11538-3/FIGURES/11.

[20] Rodrigues TA, Duarte V, Miranda RM, Santos TG, Oliveira JP. Current status and perspectives on wire and arc additive manufacturing (WAAM). Materials 2019;12. https://doi.org/10.3390/ma12071121.

[21] Tripathi U, Saini N, Mulik RS, Mahapatra MM. Effect of build direction on the microstructure evolution and their mechanical properties using GTAW based wire arc additive manufacturing. CIRP J Manuf Sci Technol 2022;37:103–9. https://doi.org/10.1016/j.cirpj.2022.01.010.

[22] Huang C, Li L, Pichler N, Ghafoori E, Susmel L, Gardner L. Fatigue testing and analysis of steel plates manufactured by wire-arc directed energy deposition. Addit Manuf 2023;73:103696. https://doi.org/10.1016/J.ADDMA.2023.103696.

[23] Huang C, Zheng Y, Chen T, Ghafoori E, Gardner L. Fatigue crack growth behaviour of wire arc additively manufactured steels. Int J Fatigue 2023;173:107705. https://doi.org/10.1016/J.IJFATIGUE.2023.107705.

[24] European Committee for Standardization (CEN), EN 1993 1–4: Eurocode 3 - Design of steel structures, part 1–4: General rules, supplementary rules for stainless steel, (2015).

[25] Laghi V, Palermo M, Bruggi M, Gasparini G, Trombetti T. Blended structural optimization for wire-and-arc additively manufactured beams. Prog Addit Manuf 2022. https://doi.org/10.1007/s40964-022-00335-1.

[26] Meng X, Weber B, Nitawaki M, Gardner L. Optimisation and testing of wire arc additively manufactured steel stub columns. Thin-Walled Struct 2023;189:110857. https://doi.org/10.1016/J.TWS.2023.110857.

[27] Kyvelou P, Huang C, Gardner L, Buchanan C. Structural testing and design of wire arc additively manufactured square hollow sections. J Struct Eng 2021;147:04021218. https://doi.org/10.1061/(ASCE)ST.1943-541X.0003188/ASSET/D40B28F4-795D-4643-8B66-117DE1E555B7/ASSETS/IMAGES/LARGE/FIGURE31.JPG.

[28] Shah IH, Hadjipantelis N, Walter L, Myers RJ, Gardner L. Environmental life cycle assessment of wire arc additively manufactured steel structural components. J Clean Prod 2023;389:136071. https://doi.org/10.1016/J.JCLEPRO.2023.136071.

[29] Rodrigues TA, Duarte V, Avila JA, Santos TG, Miranda RM, Oliveira JP. Wire and arc additive manufacturing of HSLA steel: effect of thermal cycles on microstructure and mechanical properties. Addit Manuf 2019;27:440–50. https://doi.org/10.1016/J.ADDMA.2019.03.029.

[30] Cunningham CR, Flynn JM, Shokrani A, Dhokia V, Newman ST. Invited review article: strategies and processes for high quality wire arc additive manufacturing. Addit Manuf 2018;22:672–86. https://doi.org/10.1016/J.ADDMA.2018.06.020.

[31] Martina F, Ding J, Williams S, Caballero A, Pardal G, Quintino L. Tandem metal inert gas process for high productivity wire arc additive manufacturing in stainless steel. Addit Manuf 2019;25:545–50. https://doi.org/10.1016/J.ADDMA.2018.11.022.

[32] Veiga F, Suárez A, Aldalur E, Goenaga I, Amondarain J. Wire arc additive manufacturing process for topologically optimized aeronautical fixtures. 3D Print Addit Manuf 2023;10:23–33. https://doi.org/10.1089/3dp.2021.0008.

[33] Evans SI, Wang J, Qin J, He Y, Shepherd P, Ding J. A review of WAAM for steel construction – Manufacturing, material and geometric properties, design, and future directions. Structures 2022;44:1506–22. https://doi.org/10.1016/J.ISTRUC.2022.08.084.

[34] Evans SI, Xu F, Wang J. Material properties and local stability of WAAM stainless steel equal angle sections. Eng Struct 2023;287. https://doi.org/10.1016/j.engstruct.2023.116160.

[35] MX3D, ⟨www.mx3d.com⟩, (n.d.).

[36] Dörrie R, Laghi V, Arrè L, Kienbaum G, Babovic N, Hack N, Kloft H. Combined additive manufacturing techniques for adaptive coastline protection structures. Buildings 2022;12:1806. https://doi.org/10.3390/buildings12111806.

[37] Abe T, Sasahara H. Layer geometry control for the fabrication of lattice structures by wire and arc additive manufacturing. Addit Manuf 2019;28:639–48. https://doi.org/10.1016/j.addma.2019.06.010.

[38] Tonelli L, Sola R, Laghi V, Palermo M, Trombetti T, Ceschini L. Influence of interlayer forced air cooling on microstructure and mechanical properties of wire arc additively manufactured 304l austenitic stainless steel. Steel Res Int 2021;92:2100175. https://doi.org/10.1002/SRIN.202100175.

[39] Huang C, Meng X, Gardner L. Cross-sectional behaviour of wire arc additively manufactured tubular beams. Eng Struct 2022;272:114922. https://doi.org/10.1016/J.ENGSTRUCT.2022.114922.

[40] Laghi V, Tonelli L, Palermo M, Bruggi M, Sola R, Ceschini L, Trombetti T. Experimentally-validated orthotropic elastic model for wire-and-arc additively manufactured stainless steel. Addit Manuf 2021;42. https://doi.org/10.1016/j.addma.2021.101999.

[41] Laghi V, Palermo M, Gasparini G, Girelli VA, Trombetti T. Experimental results for structural design of wire-and-arc additive manufactured stainless steel members. J Constr Steel Res 2020;167. https://doi.org/10.1016/j.jcsr.2019.105858.

[42] Wang H, Du W, Zhao Y, Wang Y, Hao R, Yang M. Joints for treelike column structures based on generative design and additive manufacturing. J Constr Steel Res 2021;184:106794. https://doi.org/10.1016/J.JCSR.2021.106794.

[43] Kanyilmaz A, Berto F. Robustness-oriented topology optimization for steel tubular joints mimicking bamboo structures, Material Design \& Processing. Communications 2019;1:e43.

[44] Laghi V, Gasparini G. Explorations of efficient design solutions for Wire-and-Arc Additive manufacturing in construction. Structures 2023;56:104883. https://doi.org/10.1016/J.ISTRUC.2023.104883.

[45] Laghi V, Babovic N, Benvenuti E, Kloft H. Blended structural optimization of steel joints for Wire-and-Arc Additive Manufacturing. Eng Struct 2024;300:117141. https://doi.org/10.1016/J.ENGSTRUCT.2023.117141.

[46] Grasshopper3D, ⟨www.grasshopper3d.com⟩, (n.d.).

[47] B. Standard, Eurocode 3—Design of steel structures—, BS EN 1993–1 1 (2006) 2005.

[48] ⟨https://www.aitiip.com/en/⟩, (n.d.).

[49] B.W. Marshall, A.A. Toprac, Basis for Tubular Joint Design Design criteria of the codes that govern construction of offshore drilling platforms are analyzed and evaluated, (n.d.).

[50] International Standard Organization (ISO), ISO 19902, Petroleum and Natural Gas Industries e Fixed Steel Offshore Structures, 2007., (n.d.).

[51] The Behaviour and Design of Steel Structures to EC3 - N.S. Trahair, M.A. Bradford, David Nethercot, Leroy Gardner - Google Libri, (n.d.). https://books.google.it/books?hl=it&lr=&id=KDsPEAAAQBAJ&oi=fnd&pg=PP1&dq=Trahair,+N.+S.,+Bradford,+M.+A.,+Nethercot,+D.,+%26+Gardner,+L.+(2017).+The+behaviour+and+design+of+steel+structures+to+EC3.+CRC+Press&ots=ZGc8ggbZ8V&sig=Re_DEqx3mhhp3Wge3NdESMgKR00&redir_esc=y#v=onepage&q=Trahair%2C%20N.%20S.%2C%20Bradford%2C%20M.%20A.%2C%20Nethercot%2C%20D.%2C%20%26%20Gardner%2C%20L.%20(2017).%20The%20behaviour%20and%20design%20of%20steel%20structures%20to%20EC3.%20CRC%20Press&f=false (accessed March 3, 2024).

[52] Timoshenko S, Gere JM. Theory of Elasticity Stability. McGraw,; 1961.

[53] Müller A, Toffolon A, Taras A. Experimental and numerical data from stub-column, short beam-column and long beam-column tests on the local and global buckling behavior of RHS/SHS under N–M interaction. Data Brief 2024;53:110162. https://doi.org/10.1016/J.DIB.2024.110162.
[54] Dassault Systemes, Abaqus CAE, (2016).
[55] Gardner L, Nethercot DA. Numerical modeling of stainless steel structural componentsA consistent approach. J Struct Eng 2004;130:1586–601. https://doi.org/10.1061/(ASCE)0733-9445(2004)130:10(1586).
[56] Ramm E. Strategies for tracing the nonlinear response near limit points. Nonlinear Finite Elem Anal Struct Mech 1981:63–89. https://doi.org/10.1007/978-3-642-81589-8_5.
[57] European Committee for Standardization (CEN), EN 10219–2, Cold Formed Welded Structural Hollow Sections of Non-Alloy and Fine Grains Steels-Part 2: tolerances, Dimensions and Sectional Properties, 2006., (n.d.).
[58] Pastor MM, Casafont M, Bonada J, Roure F. Imperfection amplitudes for nonlinear analysis of open thin-walled steel cross-sections used in rack column uprights. Thin-Walled Struct 2014;76:28–41. https://doi.org/10.1016/J.TWS.2013.10.025.

Artículo 4

rCF LM PAEK press-moulding process optimization through the introduction of a WAAM mould core

Alejandro Marqués, José Antonio Dieste, Iván Monzón, Carlos Javierre y Daniel Elduque. (2024).

Materiales Compuestos 2024, Vol. 08 - COMUNICACIONES MATCOMP21 (2022) Y MATCOMP23 (2023)

Link: https://www.scipedia.com/public/Marques*_et_al_2024a

Artículo publicado en los proceding del congreso MATCOMP23, tras su revisión por pares

Este estudio se basa en los desarrollos previamente detallados en el Artículo 1, centrando su objetivo en verificar las prestaciones de los utillajes diseñados para el proceso de *press-forming*. Este método de fabricación se utilizó para conformar piezas a partir de laminados LM PAEK reforzados con fibra de carbono mediante estampación rápida a alta temperatura. El ciclo de trabajo del proceso consta de los siguientes pasos:

1. El sistema de calentamiento de aceite eleva la temperatura del molde por encima de la temperatura de transición vítrea (T_g) del composite termoplástico.
2. La placa de composite termoplástico consolidada se coloca en un marco diseñado para facilitar su calentamiento mediante lámparas de infrarrojos (IR) y mantener la tracción en zonas críticas durante todo el proceso.
3. La placa en el marco es transferida al utillaje de prensado, donde las lámparas IR elevan su temperatura hasta alcanzar la temperatura de fusión (T_m).
4. Al alcanzar la T_m, las lámparas se retiran, permitiendo el cierre del sistema de moldeo por inyección en cuestión de segundos.
5. Se aplica presión para mantener una distribución térmica homogénea en la pieza, seguido del ciclo de refrigeración del utillaje.
6. Cuando la temperatura del sistema desciende por debajo de la T_g, el molde se abre y la pieza conformada se extrae.

El análisis comparativo del ciclo térmico en ambos utillajes mostró que el diseño WAAM redujo el tiempo de ciclo térmico en un 20 %, atribuible a su menor peso y optimización geométrica derivada de este método de fabricación. Por otro lado, no se observaron diferencias significativas en los resultados metrológicos de las piezas obtenidas con ambos utillajes (tradicional y WAAM). Esto refuerza el potencial de la tecnología WAAM como una alternativa eficiente y sostenible a los procesos tradicionales de fabricación, que ha demostrado su capacidad para procesos de altos requerimientos mecánicos.

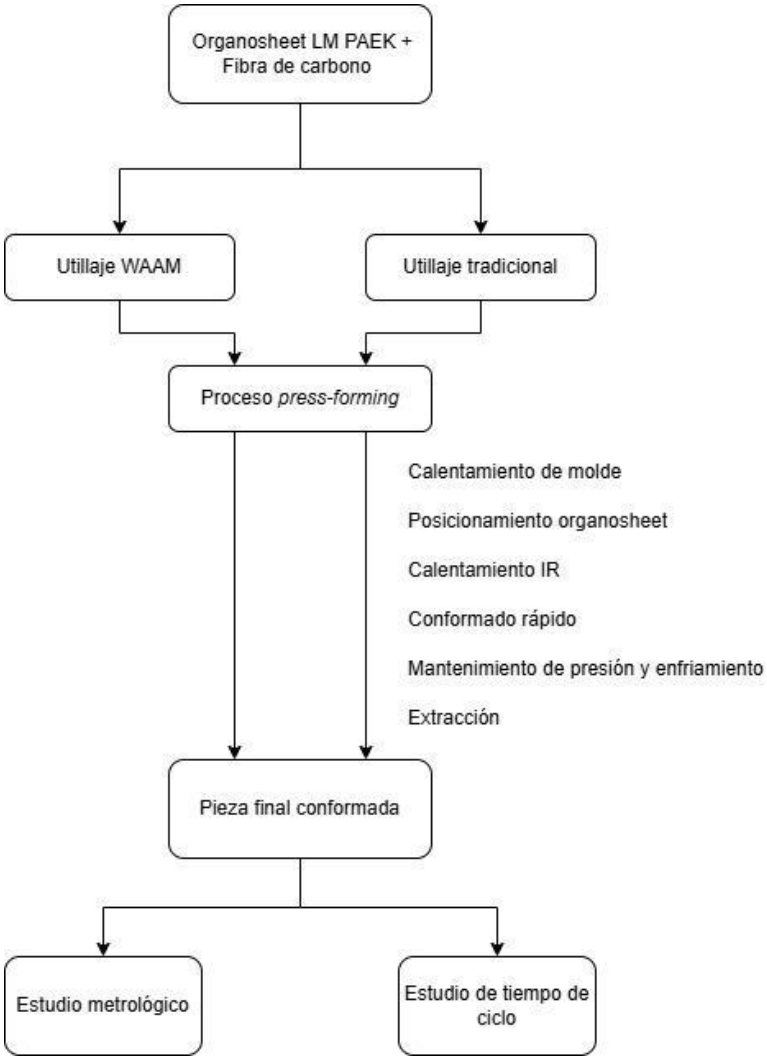

Ilustración 20 Ilustración 21 Esquema de los trabajos realizados en el artículo 4 para la verificación de rendimiento de utillaje WAAM respecto a utillaje tradicional en proceso press-forming

SCIPEDIA Revista de Materiales Compuestos

rCF LM PAEK PRESS-MOULDING PROCESS OPTIMIZATION THROUGH THE INTRODUCTION OF A WAAM MOULD CORE

A. Marqués*, J. A. Dieste, I. Monzón, C. Javierre, D. Elduque

Abstract

Carbon fibre matrix composites are consolidated in high-demanding industries such as aeronautics and aerospace. Nowadays, thermoset composites are fully integrated on several new aircrafts in production. However, thermoplastic composites are progressively emerging as a better solution due to their end-of-life recyclability and optimized manufacturing process. One of the processes used to manufacture final parts from thermoplastic composite materials is press-moulding, in which a high-temperature heating system is combined with the application of pressure at high speeds. This article studies the optimization of press-moulding process in combination with an Additive Manufacturing (AM) produced metallic mould core. The aim of this study is the manufacturing of a thermoplastic aeronautical part, that would be submitted to real-world performance test. For the press-moulding process, a high-temperature infrared heating system was designed, supported by thermal oil mould heating, this heating system was combined with a mould-pressing process by integrating the system in a commercial injection machine. Regarding the AM tooling, produced by Wire Arc Additive Manufacturing (WAAM) process, was designed to reduce tooling weight, and optimise thermal cycle. Moreover, manufacturing data from WAAM tooling was recorded and compared with that obtained from a symmetrical conventional manufacturing made mould. The analysis shows savings in terms of material and energy consumption, as well as cycle times reduction. The final part metrology study shows indistinguishable results between the press-moulding process carried out using the WAAM tooling and that manufactured through conventional methods.

OPEN ACCESS

Published: 26/09/2024

Accepted: 01/04/2024

Submitted: 15/05/2023

DOI: 10.23967/r.matcomp.2024.06.01

Keywords:
additive manufacturing
wire arc additive manufacturing
thermoplastic
LM PAEK
press moulding
fabricación aditiva
composites termoplásticos
Impresión 3D

Introduction

Composite materials have become one of the pillars of today's aeronautics industry. It could be verified the use of composite materials on aviation since first flight of the Wright Brothers' Flyer 1 on December 17, 1903, nevertheless, it was not until 1960 that these materials began to be definitively integrated into the industry [1]. Airbus used for the first-time composite materials on the vertical stabilizer of the A300 aircraft more than 50 years ago, and nowadays the A350 model use lightweight composite materials on critical structural components [2]. This significant increase in the use of composite materials not only leads to further research into the uses of these materials, but also to the development of manufacturing techniques for parts made from them.

Nowadays, thermosetting composites, based on carbon fibre high-performance reinforcements held together by polymer resin, are the most common composite materials used in the aircraft industry [3]. Despite their superior characteristics compare to metallic materials (superior specific strength and stiffness, along with improved corrosion and fatigue resistance) [4], the development of new thermoplastic composite materials will lead to their substitution in future applications. Thermoplastic composite materials present similar mechanical properties than thermoset materials [5]–[7], however, their its advantages in terms of energy and process time savings during manufacture, its recyclability and reusability [8] position thermoplastic composites as a promising alternative to thermoset materials.

It should be noted that most of these composite materials are not final products, but rather intermediate products that are converted into final products by advanced manufacturing methods. This is the case, for example, of 3D printing [9] or press-forming processes [10].

Regarding the press-forming process, which will be the one developed in the article, is based on the following steps and summarize at Figure 1:

1. A consolidated rCF thermoplastic composite plate is positioned on the press-forming system.
2. The plate is heated up until it reaches its processing temperature (T_m), also called melt temperature. At this temperature, the thermoplastic matrix is fluid enough to adapt to the mould's final geometry.
3. Once this temperature is reached, the composite plate is placed on the press-forming mould (already heated). At this point, the system rapidly closes, exerting high pressure to the composite plate.
4. After the mould closing and stabilization cycle, the cooling system starts decreasing the temperature of the whole. The system should reach a temperature lower than the material glass transition temperature (T_g). At this temperature the polymer that makes up the composite undergoes a transition from rubbery state to glassy state.
5. At this point, the final conformed part is ready to be extracted from the system.

Correspondence: A. Marqués* (alejandro.marques@aitiip.com), J. A. Dieste (joseantonio.dieste@aitiip.com), I. Monzón (ivan.monzon@aitiip.com), C. Javierre (sabicjl@unizar.es), D. Elduque (delduque@unizar.es).

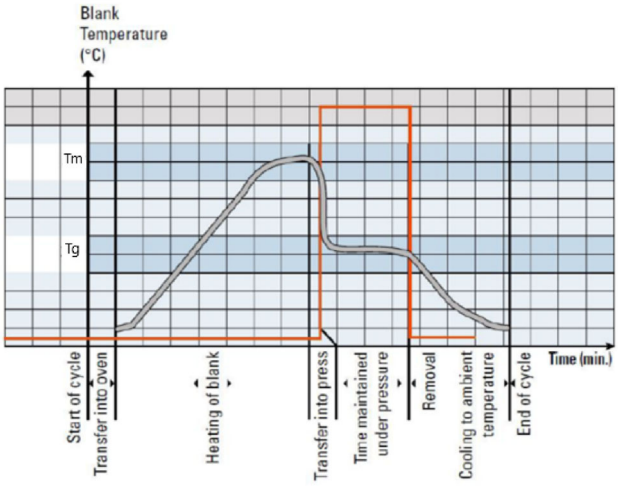

Figure 1 Press-forming cycle graph

Regarding the explained press-forming process, the performing toolings function conceptually as a mould. In terms of this mould manufacturing, concepts such as thermal expansion or spring-back [11] are taken into consideration during the design stage. In addition, the mould will be heated by means of thermal oil (a fluid capable of reaching high temperatures), which will run through the mould via channels designed for this purpose. This channels optimization should theoretically be adapted to the surfaces of the final geometry, so that the temperature behaves homogeneously throughout the part. This objective is hard to achieve during tooling manufacture process using traditional methods, due to system restrictions. However, new manufacturing models, such as Additive Manufacturing (AM), propose novel solutions to this problem. For this reason and taking into account other properties of the AM processes such as possible energy and material savings, the core of the forming tool was manufactured by metal additive manufacturing (MAM).

The MAM technology chosen was Wire Arc Additive Manufacturing (WAAM), which is a fusion AM process in which the heat energy of an electric arc is employed for melting the electrodes and depositing material layers for wall formation or for simultaneously cladding two materials to form a composite structure [12]. This technology allows the creation of large metallic toolings following geometries impossible to achieve by conventional manufacturing methods. Moreover, due to the large size of the tooling manufactured, this construction would be considered as a Big Area Additive Manufacturing (BAAM) product [13]. Based on the data obtained from the tooling manufacturing and performance, not only the press-forming process would be tested, but the availability of an AM tooling to carry out this process.

This article looks forward to describing an experimental thermoplastic composite material forming process, performed by a mould partly made by additive manufacturing (tie part). The aim of the article is not only validating the press-forming manufacturing process for the rCF thermoplastic material tested, but the operability of a tooling made by WAAM technology.

Methods/Case study

All test performed for this article were made under INNOTOOL project [14], on Clean Sky 2 program, within the Horizon 2020 framework, whose objective is the development of a rCF thermoplastic press-forming tool for advanced rear end closing frame prototype. The rCF thermoplastic material used was LM PAEK reinforced by carbon fibre with quasi-tropical disposition (45°/135°/90°/0°). Should be mentioned that the significant thickness of this part was one of the critical points of the process. As aforementioned, both the press-forming manufacturing process and the WAAM tooling performance would be tested. Moreover, 2 symmetrical toolings were required for this project, allowing the comparison of material and energy consumption between the core produced by WAAM process and the symmetrical one produced by conventional machining.

This article would be divided in 2 differentiated parts:

- AM tooling description, encompassing its design and manufacturing processes.
- Press-forming process description and performance

It should be mentioned that both the material and the press-moulding process have been tested experimentally beforehand. Therefore, the scaling of the system has been done based on the results obtained in these tests.

AM tooling

As mentioned, press-forming tooling designed concept could be assimilated to that of a mould. For this project, only the die part of the mould was performed by WAAM, therefore, this article would focus on this WAAM tooling core. Should be highlighted that, as WAAM process is based on the superposition of material layers, the final printed geometry shows an uneven finish. For this reason, WAAM technology is consider a Near-to-Net-Shape technology, which requires from a second-stage machining process before being considered finalised [15], [16]. This second-stage machining will be also measured, and the results will be presented. Should be mentioned that the selected wire material was ER70S-6 (carbon steel electrode), and the shield gas was SANARC 8 (CO_2 8% Ar 92%).

Regarding the WAAM core design, thanks to the design possibilities of the technology, several optimizations could be performed compared to the symmetrical core manufactured by conventional methods, emphasizing the following two:

- Internal heating channels could be directly performed adapting to the final geometry.
- Tooling inner part was designed empty in order to reduce tooling weight and therefore, thermal inertia.

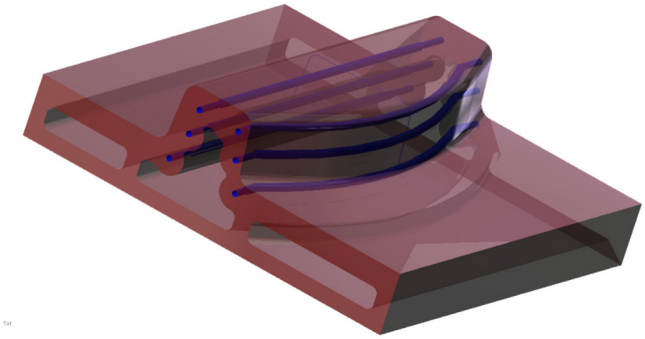

Figure 2 CAD design comparison between a) Pure machining core and b) WAAM core.

Figure 2 displays inner channels disposition, highlighted in blue.

Across both the WAAM process and second-stage machining process, material and energy consumption were analysed. Also, the symmetrical tooling conventional machining manufacturing process was analysed, allowing a direct comparison of the above-mentioned consumptions, as well the total time of the

processes.

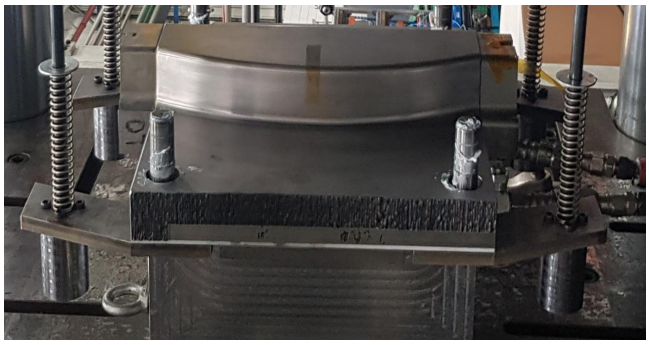

Figure 3 WAAM tooling after second-stage machining

The results show an important reduction in terms of energy consumption, being the amount of energy needed for the 2 combined manufacturing processes (WAAM process + Second-stage machining) 20% lower than the single process traditional manufacturing. Also, tooling weight is 40% reduced. Regarding the material save, this reduction is even much favourable, decreasing the amount of material consumed by 40%. Nevertheless, the WAAM manufacturing process carries an important increase in total process time, being the total process time 4 times longer than in the case of tooling made by conventional methods.

Press-forming process

The aforementioned explained press-forming system was adapted to the dimensions and characteristics of an injection machine (Billion 750) in such a way as to take advantage of both its closing speed and operating pressure. The clamping force of the press was set at 300 tonnes, affecting the surface of the rCF thermoplastic material by approximately 100 bar thanks to the compression stops designed for the tooling.

Regarding the thermal cycle, material T_m is in the range of 400 ºC, which is a thermal requirement that is difficult to achieve with conventional heating systems such as electric heaters or thermal oil. For this reason, infrared radiation heating was chosen. Infrared radiation heating system was based on 2 lamp grills filled by infrared radiation screens (Figure 4). These screens are medium-wave emitters that allow the transfer of thermal energy from one body to another without the need for any intermediate support and without the sensitive absorption of the energy emitted by the medium that separates them, which is usually air. Should be mentioned that the lamp grill system was designed to ensure that it could be rapidly removed from the press during the process. The temperature must be controlled during this thermal process, as an unbridled temperature rise could degrade the material.

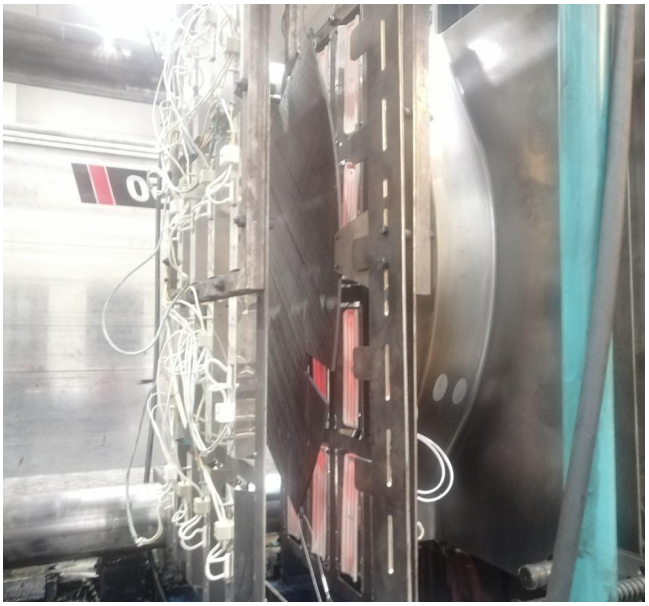

Figure 4 IR lamp grill

It should be noted that the rCF thermoplastic plate was adapted in geometry to the subsequent process devised, for this reason, areas with different amounts of extra material were designed. This material was used both as a clamping area for the thermoplastic plate and as a back-up material to ensure that, after a trimming process, the final part complies with the required dimensions.

Regarding the moulding system, process temperature requirement is less restricted, requiring process temperatures slightly superior to the LM PAEK T_g, around 200 ºC. This temperature is achievable by an industrial oil heating system, which performs not only heating cycle, but also the cooling cycle.

The rCF thermoplastic part press-forming process, based on the explained cycle at Introduction section, is broken down as follows:

1. The WAAM mould oil heating system is initiated, heating up the mould until a temperature superior to thermoplastic T_g. This process would last between 3 to 4 hours.

2. The consolidated rCF thermoplastic plate is placed on the positioning framework. This framework is developed to allow the IR heating while positioning the plate. Its design also allows the plate to be strategically clamped, maintaining the necessary traction in critical areas across the process.

3. The positioning framework is placed at the press-moulding tooling, where it is heated up by the aforementioned IR lamp grills until the T_m is reached. IR heating is shown at Figure 5. This IR heating process is relatively fast regarding the high temperatures achieves, lasting approximately 30 min.

4. At this point, the IR lamp grill is removed, allowing the press-moulding system to close. Taking advance of the injection mould system, a rapid confinement of the rCF thermoplastic plate is achieved in seconds.

5. The moulding system pressure is maintained until the conformed rCF thermoplastic part is stabilized, ensuring the whole part maintains a homogeneous temperature. This process takes around 20 min. After this stabilization time, cooling system refrigerates the whole tooling.

6. When the temperature of the system decreases below the T_g, the mould opens, and the conformed part is retrieved. This cooling process last around 2 hours.

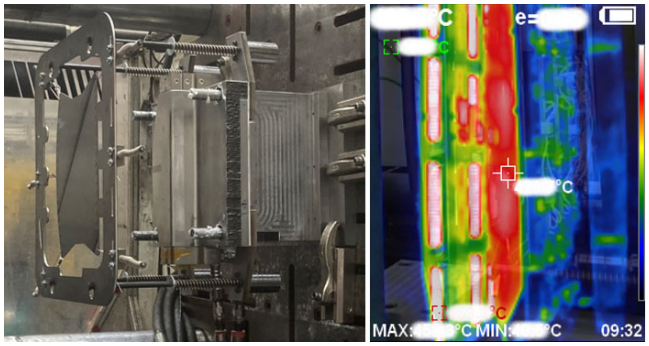

Figure 5 Press-moulding process images

The rCF thermoplastic part obtained from this process was subjected to a trimming post-process, using a positioning and cutting tooling for this purpose. After this process, the part was subjected to a metrological studio (Figure 6). It should be noted that the tolerances of this part, being a first R&D process in development, are not very restrictive, being ±2 mm in these first tests.

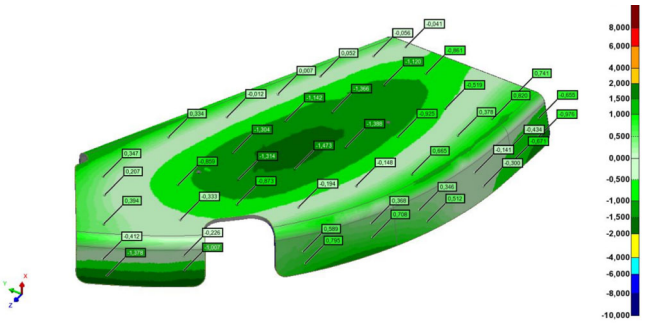

Figure 6 Final CFRP part meteorological studio

Results/Conclusions

As stated in the Introduction section, the objective of this study is the validation of both the AM process for mould manufacture and the press-forming process for the manufacture of CFRP parts. This combination of process aims not only to perform the forming process of large rCF thermoplastic materials quickly, but also to take advantage of the possibilities of AM process to produce complex structures in order to accelerate manufacturing cycles.

Regarding to the additive process (WAAM), the optimisation of the mould allows significant energy and material savings compared to conventional production. Moreover, in direct process terms, the possibility of adapting the thermal heating channels to the geometry of the part and the reduction in the mass of the tooling reduces the thermal cycle time, and, thus, the production cycle. It is important to note that the optimisation of tooling manufacturing by additive manufacturing is directly dependent on the geometry of the final tooling, so the data cannot be extrapolated as valid for any design, but nevertheless show a very favourable trend for AM processes based on WAAM technology. For these reasons, this study verifies this process as suitable for a press-moulding process with rCF thermoplastic materials.

Also, thanks to the core mould weight reduction achieved by the WAAM process, thermal inertia was reduced. This optimisation can be seen in the cycle times, which are reduced by 20% compared to those measured with conventional manufacturing made mould. However, it is estimated that the manufacture of the female mould using the WAAM process would be able to further optimise cycle times. This solution will be evaluated for future applications.

As for the press-moulding process for rCF thermoplastic parts, several innovations were incorporated. Firstly, the design and cutting of the CFRP fabric was optimised to fit correctly on the tooling. Also, the IR lamp grill system was designed as a removable tooling, which can be taken out of the press station during the process, avoiding the need to transport the CFRP plate from the infrared heating station to the press station. This feature prevents the heat loss that this entails. Finally, Process parameters obtained from previous tests and subsequently scaled for this study proved to be valid in view of the results.

On the other hand, it should be noted that the accuracies achieved, despite being within the framework of validity of the project as it is an R&D process, are much higher than those commonly used in the aeronautical industry. In this direction, studies on the thermal shrinkage and spring-back processes of the part should be carried out.

Acknowledgment

Author Contributions: All co-authors have covered all tasks of this research.

Funding: The authors gratefully acknowledge the European commission for support through the financial aid under the framework HORIZON-CL4-2021-TWIN-TRANSITION-01- 5 program through the project BIO-UPTAKE (PN:101057049 DOI: 10.3030/101057049) This study has been performed by members of the I+AITIIP (DGAT08 23R) research group recognised by the Administration of the Community of Aragon for the period 2023-2025 (Order CUS/1638/2022, of 8 November).

Conflicts of Interest: The authors declare no conflict of interest.

Bibliography

[1] C. Soutis, “Fibre reinforced composites in aircraft construction,” *Progress in Aerospace Sciences*, vol. 41, no. 2, pp. 143–151, Feb. 2005, doi: 10.1016/J.PAEROSCI.2005.02.004.

[2] O. Memon, “How Composite Materials Make The Airbus A350 A Gamechanger,” *Simply Flying*, Jan. 04, 2023. https://simpleflying.com/composite-materials-airbus-a350-gamechanger/ (accessed Jan. 30, 2023).

[3] C. Soutis, “Carbon fiber reinforced plastics in aircraft construction,” *Materials Science and Engineering: A*, vol. 412, no. 1–2, pp. 171–176, Dec. 2005, doi: 10.1016/j.msea.2005.08.064.

[4] B. G. Falzon and R. S. Pierce, “Thermosetting Composite Materials in Aerostructures,” in *Revolutionizing Aircraft Materials and Processes*, Cham: Springer International Publishing, 2020, pp. 57–86. doi: 10.1007/978-3-030-35346-9_3.

[5] A. Sudhin, M. Remanan, G. Ajeesh, and K. Jayanarayanan, “Comparison of Properties of Carbon Fiber Reinforced Thermoplastic and Thermosetting Composites for Aerospace Applications,” *Mater Today Proc*, vol. 24, pp. 453–462, 2020, doi: 10.1016/j.matpr.2020.04.297.

[6] T. Gobikannan *et al.*, “Flexural properties and failure mechanisms of infusible thermoplastic- and thermosetting based composite materials for marine applications,” *Compos Struct*, vol. 273, p. 114276, Oct. 2021, doi: 10.1016/j.compstruct.2021.114276.

[7] R. E. Murray *et al.*, "Structural validation of a thermoplastic composite wind turbine blade with comparison to a thermoset composite blade," *Renew Energy*, vol. 164, pp. 1100–1107, Feb. 2021, doi: 10.1016/j.renene.2020.10.040.

[8] W. S. Khan, E. Asmatulu, Md. N. Uddin, and R. Asmatulu, "Recycling and reusing of thermoplastic and thermoset composites," in *Recycling and Reusing of Engineering Materials*, Elsevier, 2022, pp. 141–161. doi: 10.1016/B978-0-12-822461-8.00001-2.

[9] B. Barış Vatandaş *et al.*, "Additive manufacturing of PEEK-based continuous fiber reinforced thermoplastic composites with high mechanical properties," *Compos Part A Appl Sci Manuf*, vol. 167, p. 107434, Apr. 2023, doi: 10.1016/J.COMPOSITESA.2023.107434.

[10] D. Tatsuno, T. Yoneyama, K. Kawamoto, and M. Okamoto, "Hot press forming of thermoplastic CFRP sheets," *Procedia Manuf*, vol. 15, pp. 1730–1737, Jan. 2018, doi: 10.1016/J.PROMFG.2018.07.254.

[11] M. J. Donough, Shafaq, N. A. St John, A. W. Philips, and B. Gangadhara Prusty, "Process modelling of In-situ consolidated thermoplastic composite by automated fibre placement – A review," *Compos Part A Appl Sci Manuf*, vol. 163, p. 107179, Dec. 2022, doi: 10.1016/J.COMPOSITESA.2022.107179.

[12] M. Chaturvedi, E. Scutelnicu, C. C. Rusu, L. R. Mistodie, D. Mihailescu, and S. A. Vendan, "Wire arc additive manufacturing: Review on recent findings and challenges in industrial applications and materials characterization," *Metals (Basel)*, vol. 11, no. 6, 2021, doi: 10.3390/met11060939.

[13] A. Roschli *et al.*, "Designing for Big Area Additive Manufacturing," *Addit Manuf*, vol. 25, 2019, doi: 10.1016/j.addma.2018.11.006.

[14] AITIIP FUNDATION, "Hybrid automated machine integrating concurrent manufacturing processes, increasing the production volume of functional on-demand using high multi-material deposition rates Fact Sheet Project Information." 2019. doi: 10.3030/723759.

[15] R. Warsi, K. H. Kazmi, and M. Chandra, "Mechanical properties of wire and arc additive manufactured component deposited by a CNC controlled GMAW," *Mater Today Proc*, vol. 56, pp. 2818–2825, Jan. 2022, doi: 10.1016/J.MATPR.2021.10.114.

[16] N. Chernovol, A. Sharma, T. Tjahjowidodo, B. Lauwers, and P. Van Rymenant, "Machinability of wire and arc additive manufactured components," *CIRP J Manuf Sci Technol*, vol. 35, 2021, doi: 10.1016/j.cirpj.2021.06.022.

Discusión de resultados

Con el propósito de analizar las ventajas y limitaciones del proceso WAAM en la producción de piezas de grandes dimensiones, el trabajo inicial se centró en el diseño y fabricación de utillajes específicos para procesos de moldeo. El primer paso fue evaluar las capacidades constructivas del sistema KRAKEN, el cual emplea un robot colaborativo COMAU NJ130 [108], instalado sobre la estructura de pórtico escrita, permitiendo trabajar en seis ejes de movimiento. Los movimientos del sistema fueron programados a través del software CAM HyperMILL CAD/CAM 2023 [109], cuyos códigos fueron posteriormente postprocesados en lenguaje ISO G-Code.

Antes de la ejecución, los archivos fueron simulados en un software de programación offline (Ultimaker Cura 2023) [110] para identificar posibles colisiones, evitar singularidades y garantizar que todos los movimientos estuvieran dentro del rango operativo del robot colaborativo. En cuanto al sistema de soldadura utilizado para el proceso WAAM, se empleó el Fronius TPS 400i [111].

En el marco del proyecto Innotool [112], se llevó a cabo la primera fabricación WAAM de gran tamaño, enfocada en la producción de dos utillajes simétricos para *press-forming*. Como parte del diseño experimental, uno de los utillajes se fabricó mediante procesos convencionales, mientras que el segundo fue optimizado en la etapa de diseño y producido utilizando el proceso WAAM. El utillaje fabricado mediante proceso WAAM se muestra en la Ilustración 21.

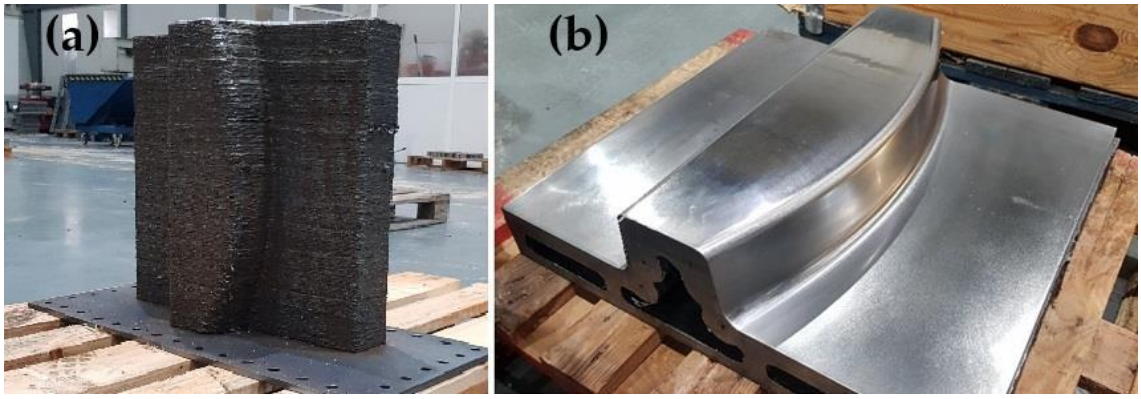

Ilustración 21 Comparación entre (a) utillaje WAAM impreso sobre placa y (b) utillaje tras eliminación de base de sacrificio y segunda fase de postprocesado

Este enfoque permitió recopilar datos relevantes de ambos métodos, lo que facilitó una comparación directa en términos de consumo eléctrico y de material. Los resultados obtenidos se muestran en la Tabla 1. Estos respaldaron la sostenibilidad del proceso WAAM frente a la fabricación tradicional, mostrando una reducción del 41% en el material total consumido y de un 18% en la energía. Además, se destacaron importantes ventajas del enfoque aditivo, como la reducción del peso del componente (41% de reducción) gracias a la optimización geométrica, y una primera evaluación de la viabilidad para integrar canales internos según el concepto de *Conformal Cooling*.

Tabla 1 Consumos eléctricos y de material durante los procesos de fabricación de utillajes simétricos para press-forming

		Utillaje convencional	Utillaje WAAM
Consumo material	Materia prima consumida	291.345 kg	173.091 kg
	Peso final de utillaje	152.747 kg	90.960 kg
	Material descartado	47.57%	47.45%
Consumo eléctrico	Proceso WAAM	-	311.365 kWh
	Proceso de mecanizado	696.228 kWh	257.15 kWh
	Total	696.228 kWh	568.515 kWh

Una vez fabricada la pieza WAAM, se realizó un estudio metrológico para el estudio del parámetro de sobre-espesor seleccionado. En este caso, como se especifica en el apartado Diseño, se establece en 10 mm. Los resultados de estos estudios, como el representado en la Ilustración 22, revelan una considerable variabilidad en la cantidad de material depositado, identificándose áreas con espesores que superan en más de 10 mm el sobre-espesor de diseño. Esto se traduce en un consumo adicional de material y un aumento significativo del consumo energético durante el mecanizado necesario para eliminar dicho excedente.

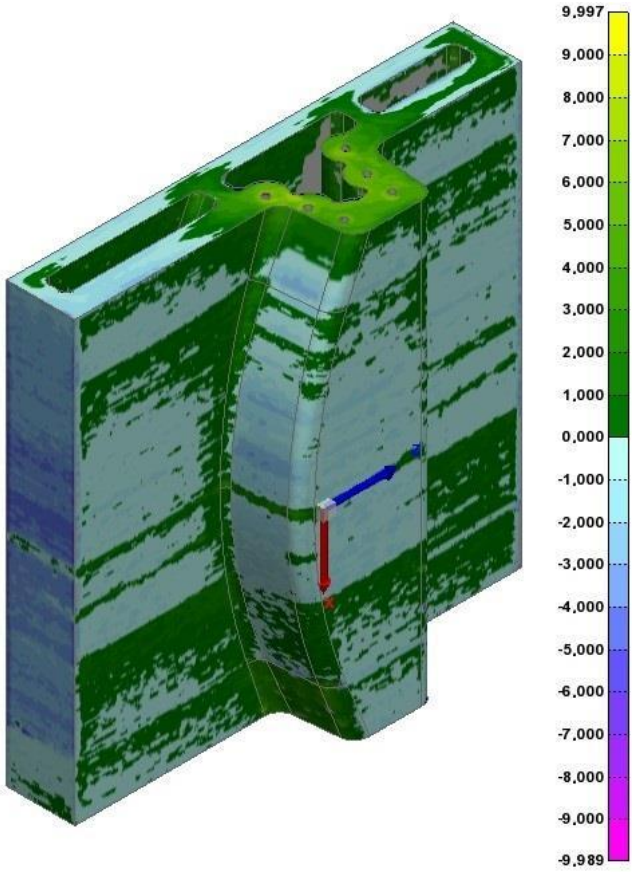

Ilustración 22 estudio metrológico de construcción WAAM respecto a CAD adaptado al proceso WAAM con 10 mm de sobre-espesor

Los resultados evidencian zonas diferenciadas donde se alternan capas con exceso de espesor y otras con espesores inferiores al valor teórico. Esta distribución es consecuencia de la dilatación térmica del material durante la impresión, ya que el proceso WAAM deposita material a altas temperaturas, generando expansión térmica que se corrige al enfriarse.

Cuando se producen pausas prolongadas durante la impresión, la pieza se contrae al enfriarse, desplazando su geometría respecto a la ruta de impresión. Al reanudar el proceso, las capas impresas se desalinean, aumentando el ancho y reduciendo la altura en las nuevas deposiciones. Este efecto no es crítico, ya que las capas sobrantes se eliminarán durante el mecanizado posterior.

El análisis adquiere especial relevancia en las regiones donde el material depositado queda por debajo de la cota teórica, ya que imposibilita que la pieza final alcance las dimensiones tras el proceso de mecanizado híbrido de segunda fase. Según este análisis, un sobre espesor mínimo de 3 mm podría ser implementado, reduciendo 70% el consumo de material impreso por cada metro de perímetro de pieza.

Una vez fabricados y sometidos a verificación metrológica, los utillajes fueron utilizados en un innovador proceso de *press-forming* diseñado para conformar piezas en LM PAEK reforzado con fibra de carbono. Este proceso, caracterizado por sus elevados requerimientos mecánicos, implica una estampación rápida a alta temperatura. Los resultados obtenidos fueron satisfactorios en ambos casos: tanto el utillaje fabricado mediante WAAM como el producido de manera convencional mostraron un desempeño equivalente, sin diferencias significativas en las piezas obtenidas con cada molde.

Es importante destacar que este proceso de fabricación de componentes en LM PAEK reforzado con fibra de carbono ha sido protegido mediante patente (EP4400292A1), subrayando su carácter innovador y su potencial industrial [113].

Establecidas las bases para la fabricación aditiva WAAM en piezas de gran tamaño y comprobado su desempeño en condiciones industriales reales, se propuso aplicar esta tecnología para fabricar un nuevo molde industrial destinado a la inyección de plástico. En concreto, se diseñó el molde macho del conjunto, con la peculiaridad de requerir canales internos de refrigeración. Dado que estos canales, debido a la geometría de la pieza, debían mecanizarse en posiciones centralizadas con una distancia considerable desde la base hasta las paredes laterales, se aprovechó la capacidad de la tecnología WAAM para crear diseños complejos. Cabe resaltar que la placa base de fabricación en este caso se integró en el diseño final, siendo mecanizada para dar continuidad a los canales internos diseñados.

El molde fue diseñado siguiendo estrictamente el concepto de *Conformal Cooling*, optimizando la disposición de los canales internos para una refrigeración eficiente. Estos canales se analizaron utilizando el software CADMould [114], comparándolos con un diseño teórico adaptado a métodos de mecanizado convencional. La Ilustración 23

permite observar las diferencias entre ambos enfoques. Además, se llevó a cabo un estudio comparativo del consumo de material entre el proceso WAAM y el consumo teórico asociado al molde fabricado por métodos convencionales, destacando las ventajas de sostenibilidad de la fabricación aditiva. Las fases de fabricación del utillaje estudiado pueden apreciarse en la Ilustración 24.

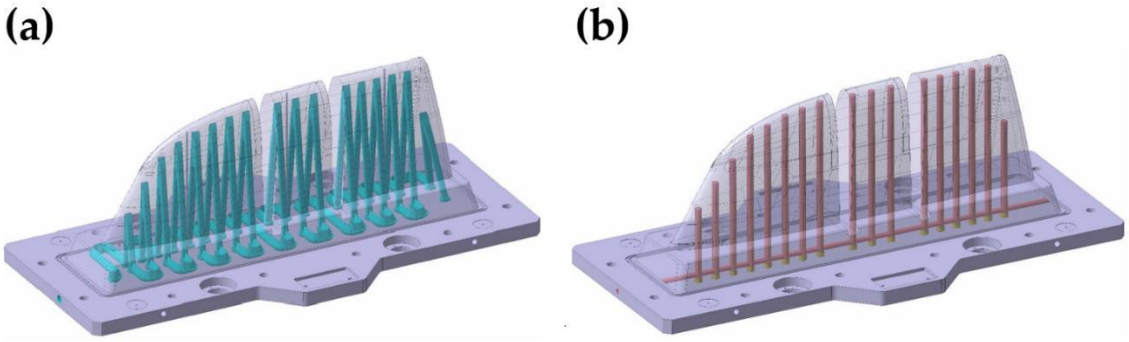

Ilustración 23 Comparación de diseño de moldes de inyección (a) para fabricación por proceso WAAM diseñado según el concepto de Conformal Cooling y (b) para fabricación convencional

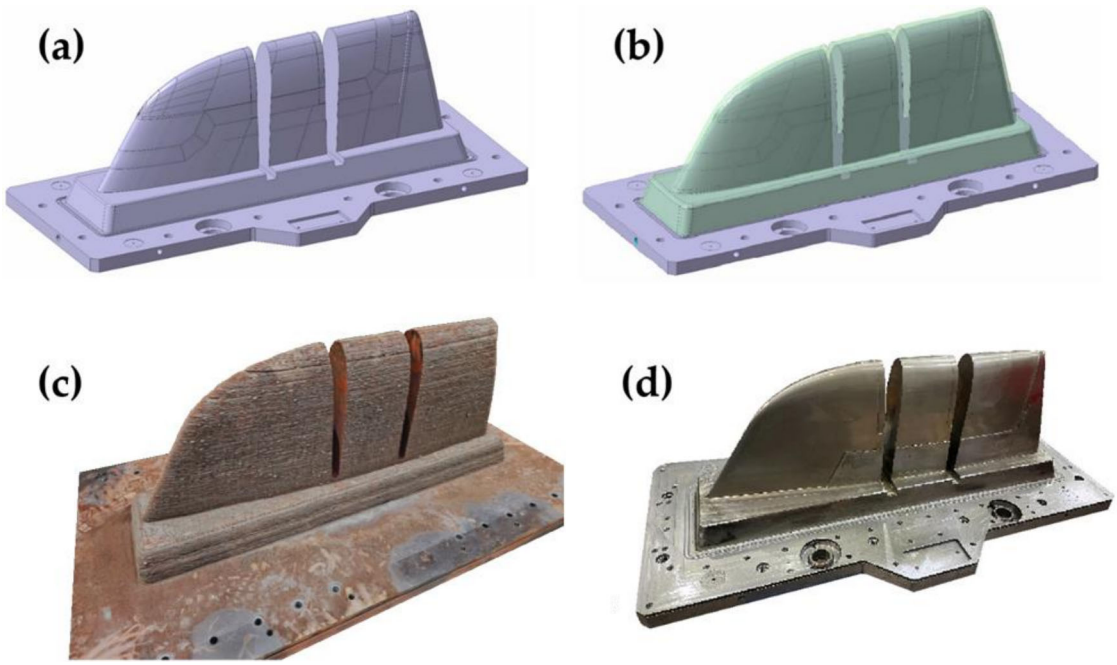

Ilustración 24 Estados en la fabricación de una pieza por tecnología WAAM. (a) Diseño final de la pieza. (b) CAD adaptado al proceso WAAM con sobre-espesor de 10 mm. (c) Pieza WAAM producida. (d) Pieza final tras segunda fase de postprocesado.

El estudio de refrigeración del molde fabricado mediante tecnología WAAM evidenció mejoras notables en comparación con el diseño teórico adaptado para métodos convencionales de fabricación. Entre los principales beneficios destacan la reducción significativa en los tiempos del ciclo de enfriamiento. La simulación mostró un aumento del 18.92% en la extracción de calor en el molde WAAM, siendo este parámetro aplicable al tiempo de ciclo inversamente.

Por otro lado, los resultados mostraron una distribución más homogénea de la temperatura. Este hecho impacta positivamente en la disminución de las deformaciones finales de la pieza moldeada. Las deformaciones simuladas en la pieza final para el molde WAAM se reducen un 26.48% respecto de su análoga realizada en su molde tradicional simulado.

Además, en línea con los hallazgos previos sobre la fabricación aditiva WAAM, este utillaje demostró una considerable reducción tanto en el consumo total de material como en los desperdicios generados, en contraste con su equivalente diseñado para técnicas de fabricación tradicionales, como se evidencia en la Tabla 2. Los resultados muestran una reducción de 4095.44 kg en el consumo total de materia prima para el utillaje WAAM, repercutiendo en una reducción del material descartado de un 62% respecto al molde teórico diseñado para su fabricación mediante técnicas de fabricación convencionales. Cabe resaltar que en el molde WAAM, la placa base mecanizada integrada en el diseño (nombrada como "base de soldadura") se ha sido realizada mediante procesos de fabricación tradicional, por lo que sus datos de consumo se han comentado de manera específica en la Tabla 2.

Tabla 2 Análisis de consumo de material en molde WAAM de inyección respecto a molde análogo teórico diseñado para su fabricación mediante técnicas de fabricación convencionales

	Utillaje convencional	Utillaje WAAM	
	-	Base de soldadura	Fabricación aditiva
Materia prima consumida	5079.02 kg	491.20 kg	492.38 kg
Peso final de utillaje	796.11 kg	446.24 kg	325.30 kg
Material descartado	84.33%	21.56%	

Tras analizar los consumos de material en los dos primeros estudios de esta tesis, resulta pertinente introducir el concepto de *Buy-to-Fly* (BTF). Este indicador se define como la relación entre la masa inicial del material en bruto y la masa de la pieza final acabada. Su utilidad radica en evaluar el aprovechamiento de materia prima durante un proceso de fabricación.

En el caso del primer utillaje fabricado, descrito en el Artículo 1, el BTF del utillaje producido mediante tecnología WAAM es de 1,90, comparado con un BTF de 1,91 del utillaje fabricado por métodos convencionales. Si bien la diferencia entre ambos procesos en términos de aprovechamiento de material es insignificante, cabe destacar que el consumo total de materia prima en el proceso convencional es un 168% mayor que en el proceso WAAM.

En el segundo utillaje analizado, descrito en el Artículo 2, el impacto del BTF es significativamente mayor. El utillaje fabricado mediante tecnología WAAM presenta un BTF de 1,27, en comparación con un 6,38 del utillaje teórico diseñado basado en métodos tradicionales de fabricación. Este dato evidencia una notable ventaja de la tecnología WAAM en el aprovechamiento de material.

Aunque el BTF es un parámetro relativo al diseño final de cada pieza, estos resultados reflejan una tendencia clara hacia un mayor aprovechamiento de la materia prima en los procesos de fabricación aditiva WAAM, frente a sus equivalentes en la fabricación convencional. Esto refuerza la viabilidad de la tecnología WAAM como una solución eficiente y sostenible en términos de consumo de material.

Una vez testeadas y confirmadas las capacidades de fabricación de diseños complejos optimizados de la tecnología WAAM en el campo de la industria del moldeo, se planteó la utilización del proceso para la fabricación de elementos finales. Por ello, se tomó un nuevo enfoque hacia la industria de la construcción. En este caso, la estructura fabricada no sería un medio para obtener una pieza final, como en el caso de la industria del molde, sino un producto acabado. Por ello, se planteó el diseño y fabricación de prototipos estructurales de gran tamaño.

Estas estructuras de diseño tubular fueron diseñadas mediante la optimización de los parámetros de diámetro exterior (D_{ext}), diámetro interior (D_{int}), número de refuerzos (N_w) y espesor de pared (t). Como resultado, se generó un catálogo de diseños optimizados, del cual se fabricaron demostradores (Ilustración 25) para verificar la viabilidad del proceso.

Ilustración 25 De mostrador de estructura tubular reforzada. Identificador TSSU_280–240-12–8

Tras la verificación de la hipótesis inicial del estudio, se planteó un segundo escenario. En él, la atención se centró en el diseño de elementos tubulares reforzados con alta resistencia frente a la presión radial, que podrían ser especialmente adecuados para aplicaciones en el sector de alta mar. Las prestaciones de estas estructuras auto-reforzadas fueron evaluadas mediante simulaciones numéricas de pandeo no lineal, que incorporaron tanto el comportamiento del acero WAAM como las imperfecciones geométricas iniciales.

Los resultados de las simulaciones revelaron que los diseños WAAM superan significativamente en prestaciones estructurales a estructuras tubulares comerciales equivalentes, considerando el mismo diámetro exterior y área de sección transversal. La estructura WAAM alcanza unas prestaciones estructurales significativamente mejores, con un aumento de la presión crítica elástica del 140%. Incluso en los escenarios más

desfavorables, con valores elevados de imperfecciones geométricas simuladas, las estructuras WAAM demostraron un rendimiento notablemente superior (40% mayor en comparación con sus análogos comerciales), consolidando su potencial como solución innovadora y eficiente.

A lo largo de este estudio, la tecnología WAAM ha sido evaluada exhaustivamente, abarcando desde su etapa de diseño inicial hasta la fabricación final. Se ha analizado su viabilidad y sus ventajas en comparación con los métodos de fabricación convencionales, siguiendo un enfoque progresivo que partió de hipótesis de diseño aplicadas a productos simples, aumentando gradualmente la complejidad y los requisitos funcionales.

Los resultados obtenidos destacan importantes mejoras tanto en el rendimiento estructural de las piezas fabricadas como en los procesos de producción, incluyendo un factor clave de sostenibilidad. Este estudio ha demostrado reducciones significativas en el consumo de material y energía en los casos evaluados, lo que refuerza la eficiencia del proceso WAAM. Estas evidencias consolidan la idoneidad de esta tecnología para su adopción en entornos industriales, ofreciendo soluciones innovadoras y sostenibles a los desafíos actuales de fabricación.

Contribuciones a la transferencia tecnológica: Patentes

En el marco de las investigaciones realizadas durante el desarrollo de esta tesis doctoral, se han generado dos patentes que ofrecen soluciones innovadoras a los desafíos técnicos y científicos identificados. Estas patentes protegen los desarrollos realizados en colaboración con el entorno empresarial privado, aportando no solo originalidad al conocimiento existente, sino también un alto potencial para aplicaciones prácticas. Su utilidad y capacidad de impacto destacan especialmente en el sector de la fabricación.

En este apartado se describen las características más relevantes de cada patente, incluyendo un resumen de su contenido y el modo en que este trabajo ha contribuido a su desarrollo. Este esfuerzo de protección y formalización de los resultados de la investigación pone de manifiesto su importancia y asegura una transferencia efectiva tanto al ámbito académico como al industrial.

A continuación, se detallan las patentes publicadas, junto con su número, fecha de publicación y área de aplicación.

- Patente Europea EP4400243A1 publicada el 17-07-2024.
- Patente Europea EP4400292A1 publicada el 17-07-2024.

Patente EP4400243A1

Título

Método de fabricación aditiva para fabricar moldes y sistema de fabricación

Aplicantes

FUNDACIÓN AITIIP

Inventores

MONZÓN CATALÁN, Iván; LAGUÍA PÉREZ, Alberto; **MARQUÉS PAOLA, Alejandro**; GONZALVO BAS, Berta; DIESTE MARCIAL, José Antonio; GRACIA ARANEGA, Pascual

Prioridades y aplicación

EP23382012A·2023-01-11

Publicación y fecha

EP4400243A1·2024-07-17

Resumen. La invención se centra en la fabricación aditiva mediante tecnología DED WAAM para la optimización de moldes metálicos. Utiliza un modelo computacional que define estratégicamente la disposición de las capas de material, evita deformaciones y mantiene parámetros óptimos del proceso. Incluye trayectorias específicas de arco y un diseño optimizado para moldes con geometrías complejas y canales internos de refrigeración. El sistema abarca desde el modelado 3D hasta el control en bucle cerrado del proceso de impresión.

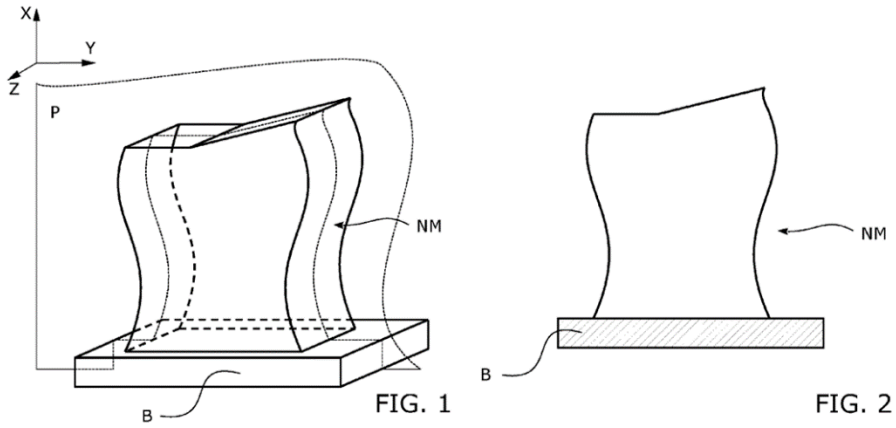

Ilustración 26 Método de fabricación aditiva para fabricar moldes y sistema de fabricación. Patente EP4400243A1 [115]

Este método permite fabricar moldes eficientes, ligeros y con alto rendimiento térmico, adecuados para procesos como inyección, soplado, RTM y compresión de materiales. Ofrece ventajas frente a técnicas tradicionales, como reducción de mecanizado, costes, peso y consumo de material, además de facilitar diseños complejos y sostenibles.

Contribución de la tesis.

El proceso de fabricación WAAM ha sido evaluado y optimizado a lo largo de esta tesis. Los ensayos de fabricación previos y los utillajes finales producidos mencionados en este documento sirvieron como base para el desarrollo del modelo computacional patentado. La correcta parametrización de los modelos y la optimización previa del diseño de las estructuras han permitido agilizar y aumentar la eficiencia del proceso, mejorando su competitividad frente a los métodos de fabricación tradicionales.

Patente EP4400292A1

Título

Un sistema y un método de fabricación de piezas moldeadas

Aplicantes

FUNDACIÓN AITIIP

Inventores

MARQUÉS PAOLA, Alejandro; LAGUÍA PÉREZ, Alberto; MONZÓN CATALÁN, Iván; GONZALVO BAS, Berta; DIESTE MARCIAL, José Antonio; GRACIA ARANEGA, Pascual

Prioridades y aplicación

EP23382013A·2023-01-11

Publicación y fecha

EP4400292A1·2024-07-17

Resumen La presente patente describe un sistema y método innovador para fabricar piezas moldeadas, especialmente fabricadas de materiales termo-formables, como el LMPAEK, utilizado en componentes aeronáuticos. Este proceso aborda el desafío de controlar con precisión la posición y deformación de la placa durante el moldeo, un problema común que afecta la calidad final. La invención incluye una máquina equipada con guías precisas para el movimiento de la placa, un sistema de calentamiento que garantiza la temperatura óptima antes del moldeo, y elementos elásticos que tensan la placa para evitar arrugas y deformaciones.

El método abarca desde la instalación de la placa en un marco de sujeción hasta la extracción de la pieza moldeada final. Además, el diseño optimizado del molde mejora los procesos de calentamiento y enfriamiento, aumentando la eficiencia

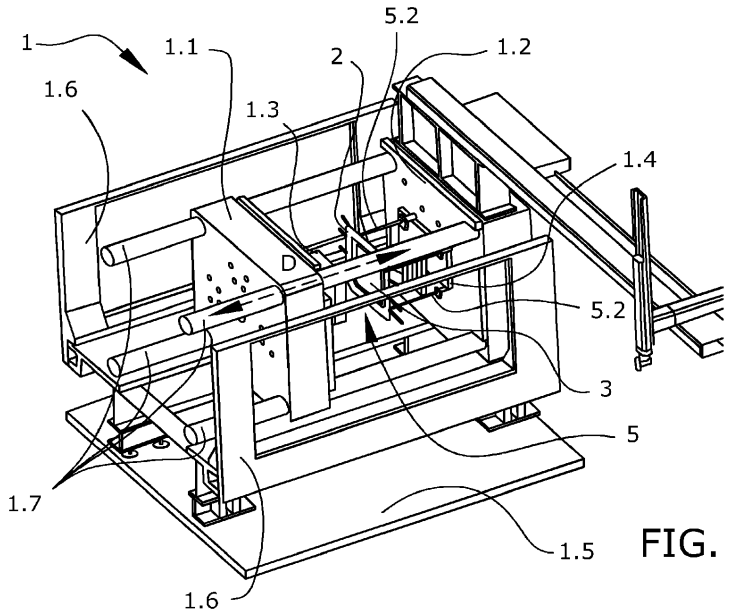

Ilustración 27 Un sistema y un método de fabricación de piezas moldeadas. Patente EP4400292A1[113]

Entre sus ventajas destacan un mayor control de la posición y la deformación de la placa, lo que asegura piezas de alta calidad, y una mejora en la eficiencia y precisión en comparación con métodos tradicionales. Las innovaciones presentadas tienen el potencial de mejorar significativamente los procesos de moldeo en diversas industrias.

Contribución de la tesis. El sistema descrito en la patente emplea como moldes de termoformado los utillajes detallados en el Artículo 1. Además, este proceso fue implementado para validar el desempeño de dicho utillaje fabricado mediante tecnología WAAM, tal como se detalla en el Artículo 4. Por ello, se puede afirmar que la patente nace de los desarrollos realizados durante los mencionados artículos de la tesis.

Contribuciones científicas: Congresos

En esta sección se detallan las actividades de difusión realizadas en el marco de esta tesis, destacando las conferencias y seminarios impartidos, los cuales han abordado de manera específica las temáticas principales del estudio.

Conferencia: Metromeet 2021

Título

"Development of innovative smart 4.0 tooling set for the manufacturing and assembly of the advanced rear end product"

Fecha de participación

25-03-2021

Congreso

"Intelligent metrology for a sustainable and efficient digital factory"

Autores

Alejandro Marqués, Jose Antonio Dieste, Iván Monzón

Resumen. Durante esta conferencia se presentó el concepto del proceso de *press-forming* para materiales termoplásticos de altas prestaciones, específicamente LM-PAEK. La exposición incluyó tanto el desarrollo del proceso como los principios de fabricación de utillajes mediante tecnología aditiva WAAM. Asimismo, se planteó la fabricación de un conjunto macho-hembra para molde optimizados para reducir el peso del conjunto y por tanto mejorar el ciclo de fabricación

Contribución de la tesis. En este congreso se introdujeron los fundamentos del proceso de *press-forming*, posteriormente sometido a pruebas, validación y patentado, junto con la optimización y fabricación de utillajes mediante tecnología WAAM. Ambos conceptos planteados y demostrados a raíz de la investigación realizada durante la presente tesis.

Conferencia: Additive manufacturing in the automotive industry

Título

"*AM boost in Automotive Sector"*

Fecha de participación

22-04-2021

Congreso

"Additive manufacturing in the automotive industry"

Autores

Alejandro Marqués, Jose Antonio Dieste

Resumen. Durante esta conferencia se expusieron diversas propuestas para la implementación de tecnologías aditivas en la industria automotriz. Entre ellas, se destacaron soluciones estéticas basadas en fabricación mediante tecnología FDM, como un salpicadero multi-material intercambiable que ofrece acabados personalizados, propiedades antimicrobianas y aromas específicos. Asimismo, se presentó una demostración de fabricación aditiva metálica, en la que se integraron estructuras metálicas directamente sobre el chasis de un modelo deportivo de Alfa Romeo, evidenciando el potencial de estas tecnologías para aplicaciones funcionales y estructurales en el sector.

Contribución de la tesis. En este congreso se expusieron diversas aplicaciones de las tecnologías aditivas orientadas a la fabricación de piezas finales para uso industrial. En particular, se destacaron soluciones basadas en materiales de aporte metálicos utilizando tecnología WAAM, demostrando su versatilidad y potencial en el sector automovilístico. Además, la fabricación de moldes metálicos mediante tecnología WAAM fue presentada como una innovadora alternativa para su implementación en la industria automovilística, un concepto desarrollado a partir del primer artículo de esta tesis.

Conferencia: Advanced Manufacturing Madrid 2023

Título

"*HELACS - Procesos avanzados de desmantelamiento y valorización de materiales compuestos aeronáuticos*"

Fecha de participación

24-11-2023

Congreso

"Advanced Manufacturing Madrid 2023"

Autor

Alejandro Marqués

Resumen. Presentación de un sistema de desmantelamiento novedoso por imitación, basado en un sistema de *Digital Twin*, aplicado en este caso específico al desmantelamiento y revalorización de material compuesto aeronáutico. Dicho sistema de programación se presentó también para una variedad de aplicaciones, como serían operaciones de corte, taladrado y soldadura. Esta última aplicación a los procesos de soldadura utiliza el mismo sistema GMAW integrado en el proceso de fabricación aditiva WAAM, lo que permite utilizar el sistema de programación también como ruteado de impresión WAAM.

Contribución de la tesis. El sistema *Digital Twin* de programación por imitación incorpora la capacidad de ser aplicado a procesos aditivos WAAM, facilitando la impresión 3D metálica in situ. Esta innovación representa un avance significativo al posibilitar la integración de la tecnología WAAM en el ámbito de la fabricación de manera disruptiva y novedosa. Los avances logrados en el proceso de fabricación aditiva WAAM durante esta tesis permiten adaptar dicha tecnología a la implementación in situ planteada por el sistema.

Seminario: Towards a Greener Aviation

Título

"*Integración de la colaboración humano-robot en los procedimientos de desmantelamiento de composites en su fin de vida"*

Fecha de participación

28-02-2024

Congreso

"Towards a Greener Aviation"

Autor

Alejandro Marqués

Resumen. Presentación de un sistema novedoso de desmantelamiento robótico de aeronaves mediante un sistema de programación por imitación, basado en el concepto *Digital Twin*. Este sistema, ya presentado en la Conferencia: Advanced Manufacturing Madrid 2023, es aplicable a diversos procesos de mecanizado o fabricación aditiva, como ya se ha comentado. Además, se presentaron mejoras en el software del sistema y en la interfaz de usuario.

Contribución de la tesis. Tal como se expuso en la contribución de la conferencia anterior, el sistema *Digital Twin* de programación por imitación integra la capacidad de aplicación en procesos aditivos WAAM, permitiendo la impresión 3D metálica *in situ*. Los avances alcanzados en el proceso de fabricación aditiva WAAM durante esta tesis permiten su adaptación tanto para la implementación in situ propuesta por el sistema como para su aplicación en reparaciones de componentes metálicos.

Colaboración en proyectos de investigación

La ejecución y los resultados de esta tesis han estado vinculados a distintos proyectos de investigación, tanto con financiación pública, como con financiación privada. A continuación, se realizará un resumen de los proyectos más relevantes en los que la ha participado el doctorando, remarcando su relación con la presente tesis.

Proyecto KRAKEN

Nombre extendido

"Hybrid automated machine integrating concurrent manufacturing processes, increasing the production volume of functional on-demand using high multi-material deposition rates"

Programa, expediente y financiación

H2020-FOF-2016No7237595.947.836€

Socios

Coordinador: Fundación AITIIP. **Participantes:** TWI, CSEM, ACCIONA, CRF, Pininfarina, Teamnet Group. Leica Geosystems, Vero Software, Arasol Industrial, VBC, Alchemie, Espace2001 y Autonomous Systems.

Resumen. KRAKEN es un proyecto financiado por el programa europeo Horizon2020, desarrollado entre octubre de 2016 y septiembre de 2019. Su objetivo principal fue la creación de una máquina de fabricación híbrida de grandes dimensiones (20x6x3 m), que combina tecnologías sustractivas y avanzadas tecnologías aditivas para trabajar en amplias áreas sin requerimientos de espacio adicional en el suelo. Además, el proyecto buscó proporcionar a empresas de diferentes tamaños una solución "todo en uno" asequible, diseñada para producir componentes personalizados, integrando procesos de fabricación, reparación y control de calidad de piezas funcionales.

El consorcio de KRAKEN, permitió vincular resultados de investigación con necesidades tecnológicas en áreas clave como software, monitorización, automatización, materiales, estandarización y usuarios finales, consolidando así la cadena de valor de la fabricación híbrida. Durante el proyecto, se validaron nuevas tecnologías aditivas para la producción de grandes componentes multimateriales, tanto en entornos de laboratorio como en escenarios industriales de alta relevancia, y se integraron para su demostración en aplicaciones reales.

Contribución de la tesis. El proyecto KRAKEN es el germen del que parte esta tesis, siendo el punto inicial del desarrollo de la tecnología aditiva WAAM. A partir de los desarrollos iniciales testeados y validados en KRAKEN se realizaron las primeras pruebas de fabricación aditiva metálica, incluyendo las pruebas conceptuales de diseño adaptado al proceso, optimizaciones de patrón de impresión y parametrización del proceso. Por ello, la presente tesis resultó la validación de los procesos de fabricación aditiva metálica planteados durante el proyecto.

Proyecto INNOTOOL

Nombre extendido

"Development of Thermoplastic press-forming Tool for Advanced Rear End Closing Frame Prototype and Tooling 4.0 for Assembly and transportation of the Advanced Rear End Prototype"

Programa, expediente y financiación

H2020-CS2-CFP10-2019-01No886491715.952€

Socios

Coordinador: Tekniker. **Participantes:** Fundación AITIIP. **Topic Manager:** Airbus Operations

Resumen. El proyecto INNOTOOL, cofinanciado a través del programa Horizon2020, específicamente en el área de CleanSky2, se desarrolló en AITIIP entre mayo de 2020 y junio de 2022. Este proyecto tuvo como objetivo principal el diseño de utillajes innovadores para la fabricación y ensamblaje de componentes de altas prestaciones basados en LM-PAEK (termoplástico reforzado con fibra de carbono).

El papel de AITIIP en el proyecto se centró en la creación de un utillaje avanzado para el proceso de conformado por prensa, integrando la consolidación de refuerzos y el conformado de materiales termoplásticos con espesores variables. La innovación de este enfoque radica en la incorporación de tecnologías de fabricación aditiva, el diseño modular de los componentes y la implementación de estrategias de control térmico optimizado durante el proceso de prensado.

Contribuciones de la tesis. Dentro de este proyecto se enmarcan los artículos 1 y 4 presentados dentro del compendio, además del desarrollo de la patente EP4400292A1. Por ello, la presente tesis fue esencial para el desarrollo del proyecto, específicamente para la fabricación aditiva WAAM aplicada a moldes de gran tamaño, englobando la optimización de diseño, el análisis comparativo de la sostenibilidad del proceso y finalmente su validación industrial.

Proyecto AGRIAM

Nombre extendido

"DED-arc manufacturing of highly customized functional injection moulds, to produce thermoplastic parts for agricultural machinery, optimising for weight reduction and forest fire prevention"

Programa y financiación

3DP PAN EU40.000€

Socios

Coordinador: MOSES. **Participantes:** Fundación AITIIP, TECOS y UNIBO

Resumen. Los proyectos bajo el programa 3DP PAN, están destinados a PYMES, tratando de acercar las tecnologías de fabricación aditiva a los procesos industriales de estas compañías. En este proyecto, la empresa MOSES desarrolló piezas termoplásticas personalizadas para maquinaria agrícola, buscando la reducción de peso y el riesgo de incendios. Usando la tecnología WAAM, se fabricaron moldes metálicos para procesos de inyección de plásticos, optimizando el peso y diseño de los canales de refrigeración de éstos. El proyecto validó la cadena de valor, demostrando que este proceso es viable para producir moldes funcionales con alta calidad y en menor tiempo.

Contribución de la tesis. A partir de los desarrollos de fabricación aditiva WAAM estudiados en loa presente tesis, fue posible validar los procesos de fabricación aditiva metálica en entornos industriales de alta exigencia, como es el caso de la industria de inyección de plástico. Se fabricó un molde de inyección de plástico mediante la tecnología DED WAAM, el cual, fue testeado y validado en una máquina de inyección de plástico.

Proyecto WELDER

Nombre extendido

"Welding Equipment for optimised, fast and accurate LongituDinal barrEl joint closuRe"

Programa, expediente y financiación

H2020-CS2-CFP11-2020-011010078141.592.062€

Socios

Coordinador: CT Ingenieros **Participantes:** Fundación AITIIP, DUKANE IAS y AIMEN Centro Tecnológico

Resumen. Los equipos de soldadura de precisión son un componente esencial de la fabricación aeroespacial de alta calidad. El proyecto WELDER, con el objetivo de situarse a la vanguardia de la estrategia para la adopción de termoplásticos en la industria aeroespacial, desarrolló y demostró diferentes métodos de soldadura de fuselajes aeronáuticos. Para ello, se diseñaron, desarrollaron e implementaron dos equipos de soldadura robótica modulares, flexibles y totalmente operativos, proporcionando un sistema de control y supervisión en línea para la gestión del ciclo de vida al completo.

Además, los elementos termoplásticos a soldar fueron desarrollados dentro del marco del proyecto, mediante un innovador sistema de *press-forming* llevado a cabo por Aitiip Centro tecnológico.

Contribución de la tesis. Durante este proyecto se desarrolló el sistema de *press-forming* utilizado previamente para la validación de utillajes desarrollados en el proyecto *Innotool*. Por lo tanto, los conocimientos y las enseñanzas obtenidos en el desarrollo de los artículos 1 y 4 de esta tesis fueron esenciales para el desarrollo del proyecto.

Capítulo 4

Conclusiones y aportaciones originales

En este capítulo final, se presentan las conclusiones del trabajo de investigación desarrollado en el marco de la tesis doctoral del doctorando Alejandro Marqués. Se resumen los resultados obtenidos y se destacan las principales claves para una integración efectiva de la tecnología aditiva metálica en los sectores industriales más relevantes.

La investigación concluye reafirmando que la optimización de procesos industriales actuales es viable mediante la incorporación de la fabricación aditiva metálica de gran escala. Esta tecnología no solo permite mejorar los procesos intermedios, sino que, desde una perspectiva de sostenibilidad, ofrece importantes ventajas en términos de ahorro de material y energía en comparación con los métodos de fabricación convencionales. Sin embargo, la tecnología aditiva metálica continúa teniendo niveles de TRL inferiores a los procesos de fabricación consolidados, lo que implica desafíos significativos, especialmente en la estandarización de procesos y la reducción de tiempos de fabricación. La evolución de los criterios de diseño y fabricación específicos para la fabricación aditiva sigue siendo un aspecto crucial para su consolidación.

El objetivo principal de esta tesis ha sido avanzar hacia la integración completa de esta tecnología en la industria, generando una base de conocimiento sólida y resultados prometedores.

Asimismo, este capítulo incluye propuestas para futuras líneas de investigación relacionadas con los estudios realizados. Algunas de estas investigaciones, ya vinculadas a la actividad profesional del doctorando, buscan extender el impacto de los resultados obtenidos en la tesis, promoviendo la adopción progresiva de procesos aditivos metálicos en las operaciones industriales cotidianas. Estas perspectivas refuerzan la relevancia del trabajo realizado y su potencial para transformar los paradigmas actuales de fabricación industrial.

Conclusiones

La fabricación aditiva se posiciona como uno de los pilares fundamentales de la cuarta revolución industrial, abriendo nuevas posibilidades para la manufactura gracias a su capacidad de trabajar con materiales diversos y producir diseños complejos que resultan inalcanzables mediante procesos tradicionales. Aunque esta tecnología ya se encuentra plenamente implementada en la industria para aplicaciones de prototipado rápido, el objetivo de este estudio ha sido evaluar su capacidad para una integración total en procesos industriales reales, con altos requerimientos mecánicos, optimizando tanto el rendimiento de los procesos como su sostenibilidad.

Durante esta tesis se han investigado los procesos de diseño, fabricación e implementación de la tecnología aditiva, específicamente WAAM, en sectores como el moldeo y la construcción. Los resultados obtenidos han sido muy prometedores, demostrando el potencial de esta tecnología en la fabricación de utillajes intermedios para la industria del moldeo y de estructuras finales para la construcción.

Las conclusiones extraídas del estudio pueden resumirse en las siguientes conclusiones, que serán desarrolladas posteriormente:

- Se ha validado la excepcional capacidad de la tecnología de fabricación aditiva metálica WAAM para la optimización de diseños y fabricación de estructuras complejas con altos requerimientos mecánicos.
- Se han demostrado mejoras procesos de inyección, mediante la optimización del diseño del circuito de refrigeración del molde utilizando tecnología WAAM.
- Se ha mostrado la capacidad para fabricar estructuras auto-reforzadas destinadas a la construcción, diseñadas específicamente para cumplir con requisitos mecánicos avanzados, y con propiedades superiores en comparación con sus equivalentes convencionales.
- Se ha evidenciado una reducción significativa en el consumo de materia prima durante la fabricación WAAM en comparación con tecnologías convencionales, incluyendo una notable disminución del material descartado.
- Se ha analizado y validado la optimización de los parámetros de diseño y fabricación, en procesos WAAM, específicamente mediante la reducción del sobre-espesor de diseño, para minimizar aún más el consumo de material.
- Se ha mostrado el ahorro energético logrado con el método de fabricación WAAM, frente a los métodos tradicionales, gracias a sus capacidades de diseño, y al concepto de fabricación *Near to Net Shape*.
- Se ha validado el proceso WAAM para la fabricación de utillajes destinados al moldeo, mediante su aplicación exitosa en un proceso de *press-forming* que exige altos estándares mecánicos.

En primer lugar, uno de los aspectos más destacados del estudio ha sido la capacidad de la tecnología WAAM para la optimización de diseños, con un impacto directo en la mejora de los procesos industriales. Durante el primer artículo presentado, la tecnología WAAM permitió la optimización del diseño del utillaje a estudiar, permitiendo una reducción de peso del 41% respecto a su homólogo realizado por métodos de fabricación convencional, lo que disminuyó la inercia térmica y reduciendo los ciclos de fabricación en un 20%, impactando en una mejora del tiempo de ciclo. Además, esta tecnología posibilitó la incorporación de canales térmicos internos complejos diseñados bajo el concepto de *Conformal Cooling*, aumentando significativamente la transferencia de calor entre el molde y la pieza. En un segundo caso de estudio, los canales térmicos optimizados mejoraron la extracción de calor en un 18% y redujeron las deformaciones de la pieza final en un 26%.

En relación con la implementación de la tecnología WAAM en la fabricación de estructuras destinadas a la industria de la construcción, se desarrolló un catálogo de estructuras tubulares auto-reforzadas, cuya fabricación sería inviable mediante métodos convencionales. Cada estructura del catálogo fue diseñada con configuraciones específicas en términos de diámetro exterior, diámetro interior, número de refuerzos y espesor de pared, permitiendo una adaptación precisa a los requerimientos estructurales de cada proyecto de construcción. Esta versatilidad no solo responde a las necesidades específicas de la industria, sino que también contribuye a una significativa optimización en el uso del material.

En términos de desempeño estructural, se evaluó la optimización de diseño de las estructuras auto-reforzadas en comparación con una estructura equivalente sometida a condiciones de aplicaciones *off-shore*. Los resultados demostraron una mejora del 140% en la presión crítica elástica, destacando el notable potencial de la tecnología WAAM para optimizar tanto el diseño como las propiedades finales de las estructuras fabricadas. En este sentido, se concluye que WAAM no solo facilita la implementación de diseños avanzados, sino que también aporta importantes beneficios en la mejora de procesos industriales y en el rendimiento estructural de los productos finales.

El estudio también ha puesto de manifiesto el impacto positivo de la tecnología WAAM en términos de sostenibilidad, tanto en el proceso de fabricación como en la operatividad de los diseños. En el caso de la sostenibilidad en el funcionamiento de los diseños fabricados, esta es inherente a las optimizaciones de proceso mencionadas. Como se ha comentado, la capacidad del proceso de fabricar estructuras complejas ha permitido reducir los ciclos de fabricación en los procesos de moldeo testeados, repercutiendo en una optimización del proceso.

Por otra parte, en relación con los procesos de fabricación WAAM realizados, se ha monitorizado el consumo de material durante los estudios realizados, mostrando una importante reducción del consumo total de material respecto a las construcciones análogas realizadas por métodos de fabricación convencional. En los casos analizados,

el consumo de material se redujo considerablemente, alcanzando un 41% y el 80% respectivamente al primer y segundo artículo. Además, se ha mostrado una importante capacidad de optimización de la materia prima aportada, específicamente en el segundo utillaje impreso, correspondiente al artículo 2. En este utillaje, el BTF ratio del utillaje WAAM se redujo en 5,11 puntos respecto a su homólogo diseñado para fabricación convencional.

Como se evidencia en el primer artículo, el proceso de diseño específico para la fabricación mediante tecnología WAAM aún presenta oportunidades de mejora, particularmente en la optimización del término de sobre espesor de diseño. Este valor, concebido como un margen de seguridad para garantizar la integridad geométrica del perímetro de la pieza, se estableció inicialmente en 10 mm. Sin embargo, los resultados del estudio metrológico indican que este sobre espesor puede reducirse a 3 mm, lo que implica una disminución significativa en el material de aporte consumido, así como en el consumo energético asociado al mecanizado posterior.

En cuanto al proceso de mecanizado subsiguiente, la naturaleza *Near to Net Shape* de la fabricación WAAM elimina la necesidad de una etapa de desbaste en la pieza. Esto permite limitar el mecanizado posterior a las fases de pre-acabado y acabado, que son menos intensivas en términos de consumo energético, junto con los procesos de taladrado y roscado necesarios. Esta característica del proceso WAAM conlleva una reducción en el consumo eléctrico en comparación con los métodos convencionales de fabricación. En el contexto específico del estudio, esta disminución en el consumo energético ha alcanzado un 18%, evidenciando el potencial de la tecnología WAAM para optimizar tanto los recursos materiales como energéticos en la fabricación industrial.

El cuarto artículo del compendio validó la aplicación de utillajes WAAM en un proceso industrial de alta exigencia mecánica, como es el *press-forming* de piezas termoplásticas de altas prestaciones. Este logro confirma la capacidad de la tecnología WAAM para adaptarse a procedimientos industriales avanzados y satisfacer requerimientos complejos.

No obstante, la tecnología WAAM, siendo más joven que otros procesos de fabricación tradicionales, enfrenta desafíos como tiempos de producción más largos y restricciones específicas de diseño. Estas limitaciones reflejan un menor grado de madurez tecnológica, aunque los beneficios demostrados en esta investigación respaldan su integración progresiva en la industria. Además, la estandarización de los criterios de diseño y fabricación para WAAM será crucial para su adopción generalizada, especialmente en lo que respecta a la reducción del sobre-espesor de diseño, lo que podría disminuir aún más el consumo de material y energía.

En conclusión, esta tesis doctoral ha demostrado que la tecnología WAAM no solo ofrece una solución eficaz para la optimización de procesos industriales existentes, sino que

también abre nuevas posibilidades en el diseño y fabricación de componentes. Su contribución a la sostenibilidad y eficiencia de la fabricación moderna posiciona a WAAM como una herramienta clave en la transformación industrial hacia modelos más sostenibles y avanzados.

Aportaciones originales e innovaciones técnico-científicas

La presente tesis doctoral, desarrollada por el doctorando Alejandro Marqués, ha tenido como eje central la identificación de estrategias óptimas para la integración de procesos de fabricación aditiva metálica de grandes dimensiones en la industria contemporánea. Este enfoque ha buscado aprovechar las ventajas inherentes de esta tecnología, tales como la posibilidad de realizar diseños complejos y su contribución a la sostenibilidad, demostrando de manera efectiva su viabilidad y beneficios. Para ello, se seleccionaron dos nichos de mercado en los que la implementación de esta tecnología podría generar resultados particularmente significativos.

En primer lugar, se exploró el diseño de utillajes complejos destinados a la industria del moldeo, maximizando las capacidades específicas de la tecnología WAAM. En este contexto, el objetivo principal fue la optimización de los procesos industriales en los que estos utillajes son empleados. Entre las mejoras introducidas destacan la reducción del peso de los utillajes y la incorporación de canales térmicos internos complejos, los cuales han demostrado un impacto directo en la mejora de los ciclos de fabricación y en la calidad de las piezas finales producidas. Este enfoque de rediseño y reinterpretación de estructuras tradicionales para su adaptación a la tecnología WAAM se extendió al sector de la construcción mediante la creación de un catálogo de elementos estructurales autoreforzados, diseñados para satisfacer las necesidades específicas de fabricación de cada proyecto.

En segundo lugar, la perspectiva de sostenibilidad ha sido un pilar fundamental de este estudio. Gracias a la capacidad de optimización de diseño inherente a la fabricación aditiva y a las características específicas del proceso WAAM, se ha demostrado una significativa reducción en el consumo de material durante los procesos de fabricación analizados. Asimismo, se logró disminuir considerablemente el material descartado, lo que conllevó una reducción proporcional en el consumo energético asociado a toda la fase de fabricación, abarcando tanto la impresión 3D como los procesos de mecanizado posteriores.

Por último, se ha validado la capacidad de un utillaje fabricado mediante WAAM para llevar a cabo procesos industriales de alta exigencia, como el press-forming, que representa hasta la fecha el desafío más riguroso al que ha sido sometido un utillaje WAAM de grandes dimensiones. Este logro no solo refuerza el potencial de esta tecnología para satisfacer los altos estándares de la industria, sino que también consolida su viabilidad como herramienta clave en la transición hacia procesos industriales más eficientes y sostenibles.

Líneas de investigación futuras

Gracias a la naturaleza de un doctorado industrial, el doctorando tiene la oportunidad de continuar las líneas de investigación iniciadas en el centro tecnológico, consolidando y ampliando los avances logrados. En este contexto, destaca la continuidad del desarrollo de la fabricación aditiva metálica mediante la tecnología WAAM, aplicada específicamente a las industrias del moldeo y la construcción. Las principales direcciones de investigación futura propuestas son las siguientes:

1. Realización de un estudio integral de LCA (*Life Cycle Assessment*) y LCC (*Life Cycle Costing*) para la fabricación de un utillaje destinado a la industria del moldeo, con el objetivo de obtener datos representativos sobre el impacto ambiental y el coste del proceso, en comparación con los métodos de fabricación tradicionales.
2. Testeo de diseños fabricados con tecnología WAAM aplicando un factor de sobre-espesor minimizado, vinculado a los resultados del primer artículo de la tesis.
3. Estudio metrológico comparativo de un utillaje fabricado mediante tecnología WAAM, sometido a condiciones industriales a lo largo de un ciclo de fabricación prolongado, en relación con su homólogo fabricado por métodos convencionales.
4. Diseño y fabricación de estructuras tubulares con configuraciones tipo árbol para el sector de la construcción, avanzando en la investigación asociada al tercer artículo de la tesis.
5. Evaluación de las posibilidades de optimización del proceso de soldadura WAAM, específicamente en parámetros como la velocidad de impresión, y los parámetros relacionados con la definición del cordón de soldadura, como son las dimensiones de altura y anchura del cordón de aporte.
6. Investigación sobre la mejora en la fabricación de estructuras en voladizo, aplicables tanto a construcciones exteriores como a elementos interiores con cavidades complejas.
7. Testeo y validación de nuevos materiales de aporte para el sistema WAAM, como aceros inoxidables y aleaciones de hierro-níquel (Invar), explorando sus potenciales aplicaciones industriales.

Estas líneas de investigación no solo permitirán profundizar en los conocimientos adquiridos durante el doctorado, sino que también contribuirán al avance y la consolidación de la tecnología WAAM en la industria.

Bibliografía

1. International Organization for Standarization ISO/ASTM 52900:2021(En). *Additive manufacturing — General principles — Fundamentals and vocabulary»* 2021.
2. AITIIP FUNDATION Hybrid Automated Machine Integrating Concurrent Manufacturing Processes, Increasing the Production Volume of Functional on-Demand Using High Multi-Material Deposition Rates Fact Sheet Project Information 2019.
3. Liu, Z.; Wang, Y.; Wu, B.; Cui, C.; Guo, Y.; Yan, C. A Critical Review of Fused Deposition Modeling 3D Printing Technology in Manufacturing Polylactic Acid Parts. *The International Journal of Advanced Manufacturing Technology* **2019**, *102*, 2877–2889, doi:10.1007/s00170-019-03332-x.
4. Zhai, Y.; Lados, D.A.; LaGoy, J.L. Additive Manufacturing: Making Imagination the Major Limitation. *JOM* **2014**, *66*, 808–816, doi:10.1007/s11837-014-0886-2.
5. Chang, K.-H. Rapid Prototyping. In *e-Design*; Elsevier, 2015; pp. 743–786.
6. Huang, S.H.; Liu, P.; Mokasdar, A.; Hou, L. Additive Manufacturing and Its Societal Impact: A Literature Review. *The International Journal of Advanced Manufacturing Technology* **2013**, *67*, 1191–1203, doi:10.1007/s00170-012-4558-5.
7. Pei, E.; Kabir, I.R.; Leutenecker-Twelsiek, B. History of AM. In; 2023; pp. 3–29.
8. Hull, C. On Stereolithography. *Virtual Phys Prototyp* **2012**, *7*, 177–177, doi:10.1080/17452759.2012.723409.
9. Su, A.; Al'Aref, S.J. History of 3D Printing. In *3D Printing Applications in Cardiovascular Medicine*; Elsevier, 2018; pp. 1–10.
10. Dilberoglu, U.M.; Gharehpapagh, B.; Yaman, U.; Dolen, M. The Role of Additive Manufacturing in the Era of Industry 4.0. *Procedia Manuf* **2017**, *11*, 545–554, doi:10.1016/j.promfg.2017.07.148.
11. Hernandez Korner, M.E.; Lambán, M.P.; Albajez, J.A.; Santolaria, J.; Ng Corrales, L. del C.; Royo, J. Systematic Literature Review: Integration of Additive Manufacturing and Industry 4.0. *Metals (Basel)* **2020**, *10*, 1061, doi:10.3390/met10081061.
12. Wong, K. V.; Hernandez, A. A Review of Additive Manufacturing. *ISRN Mechanical Engineering* **2012**, *2012*, 1–10, doi:10.5402/2012/208760.
13. UNE Normalización Española UNE-EN ISO/ASTM 52910:2020. *Fabricación aditiva. Diseño. Requisitos, directrices y recomendaciones* 2020.

14. German Institute of Standardization ISO/TC 261 Additive Manufacturing. *Addit Manuf* 2011.
15. Doubrovski, Z.; Verlinden, J.C.; Geraedts, J.M.P. Optimal Design for Additive Manufacturing: Opportunities and Challenges. In Proceedings of the Volume 9: 23rd International Conference on Design Theory and Methodology; 16th Design for Manufacturing and the Life Cycle Conference; ASMEDC, January 2011; pp. 635–646.
16. Brackett, J.; Yan, Y.; Cauthen, D.; Kishore, V.; Lindahl, J.; Smith, T.; Sudbury, Z.; Ning, H.; Kunc, V.; Duty, C. Characterizing Material Transitions in Large-Scale Additive Manufacturing. *Addit Manuf* **2021**, *38*, doi:10.1016/j.addma.2020.101750.
17. Li, J.; Durandet, Y.; Huang, X.; Sun, G.; Ruan, D. Additively Manufactured Fiber-Reinforced Composites: A Review of Mechanical Behavior and Opportunities. *J Mater Sci Technol* **2022**, *119*, 219–244, doi:10.1016/j.jmst.2021.11.063.
18. Gregor-Svetec, D.; Leskovšek, M.; Vrabič Brodnjak, U.; Stankovič Elesini, U.; Muck, D.; Urbas, R. Characteristics of HDPE/Cardboard Dust 3D Printable Composite Filaments. *J Mater Process Technol* **2020**, *276*, 116379, doi:10.1016/j.jmatprotec.2019.116379.
19. Sun, J.; Ye, D.; Zou, J.; Chen, X.; Wang, Y.; Yuan, J.; Liang, H.; Qu, H.; Binner, J.; Bai, J. A Review on Additive Manufacturing of Ceramic Matrix Composites. *J Mater Sci Technol* **2023**, *138*, 1–16, doi:10.1016/j.jmst.2022.06.039.
20. Nurhudan, A.I.; Supriadi, S.; Whulanza, Y.; Saragih, A.S. Additive Manufacturing of Metallic Based on Extrusion Process: A Review. *J Manuf Process* **2021**, *66*, 228–237, doi:10.1016/j.jmapro.2021.04.018.
21. Martina, F.; Mehnen, J.; Williams, S.W.; Colegrove, P.; Wang, F. Investigation of the Benefits of Plasma Deposition for the Additive Layer Manufacture of Ti-6Al-4V. *J Mater Process Technol* **2012**, *212*, doi:10.1016/j.jmatprotec.2012.02.002.
22. Jackson, M.A.; Asten, A. Van; Morrow, J.D.; Min, S.; Pfefferkorn, F.E. A Comparison of Energy Consumption in Wire-Based and Powder-Based Additive-Subtractive Manufacturing. In Proceedings of the Procedia Manufacturing; 2016; Vol. 5.
23. Ahn, D.-G. Directed Energy Deposition (DED) Process: State of the Art. *International Journal of Precision Engineering and Manufacturing-Green Technology* **2021**, *8*, 703–742, doi:10.1007/s40684-020-00302-7.
24. Kumar, S. Selective Laser Sintering: A Qualitative and Objective Approach. *JOM* **2003**, *55*, 43–47, doi:10.1007/s11837-003-0175-y.
25. Sefene, E.M. State-of-the-Art of Selective Laser Melting Process: A Comprehensive Review. *J Manuf Syst* **2022**, *63*, 250–274, doi:10.1016/j.jmsy.2022.04.002.
26. Galati, M.; Iuliano, L. A Literature Review of Powder-Based Electron Beam Melting Focusing on Numerical Simulations. *Addit Manuf* **2018**, *19*, 1–20, doi:10.1016/j.addma.2017.11.001.
27. Nagarajan, B.; Hu, Z.; Song, X.; Zhai, W.; Wei, J. Development of Micro Selective Laser Melting: The State of the Art and Future Perspectives. *Engineering* 2019, *5*, 702–720.

28. Chatham, C.A.; Long, T.E.; Williams, C.B. A Review of the Process Physics and Material Screening Methods for Polymer Powder Bed Fusion Additive Manufacturing. *Prog Polym Sci* **2019**, *93*, 68–95, doi:10.1016/j.progpolymsci.2019.03.003.
29. Hebert, R.J. Viewpoint: Metallurgical Aspects of Powder Bed Metal Additive Manufacturing. *J Mater Sci* **2016**, *51*, 1165–1175, doi:10.1007/s10853-015-9479-x.
30. Liu, Z.Y.; Li, C.; Fang, X.Y.; Guo, Y.B. Energy Consumption in Additive Manufacturing of Metal Parts.; 2018; Vol. 26.
31. Altıparmak, S.C.; Yardley, V.A.; Shi, Z.; Lin, J. Extrusion-Based Additive Manufacturing Technologies: State of the Art and Future Perspectives. *J Manuf Process* **2022**, *83*, 607–636, doi:10.1016/j.jmapro.2022.09.032.
32. Solomon, I.J.; Sevvel, P.; Gunasekaran, J. A Review on the Various Processing Parameters in FDM. *Mater Today Proc* **2021**, *37*, 509–514, doi:10.1016/j.matpr.2020.05.484.
33. Ates, M.; Karadag, S.; Eker, A.A.; Eker, B. Polyurethane Foam Materials and Their Industrial Applications. *Polym Int* **2022**, *71*, 1157–1163, doi:10.1002/pi.6441.
34. Karimi, A.; Rahmatabadi, D.; Baghani, M. Various FDM Mechanisms Used in the Fabrication of Continuous-Fiber Reinforced Composites: A Review. *Polymers (Basel)* 2024, *16*.
35. Karayannis, P.; Saliakas, S.; Kokkinopoulos, I.; Damilos, S.; Koumoulos, E.P.; Gkartzou, E.; Gomez, J.; Charitidis, C. Facilitating Safe FFF 3D Printing: A Prototype Material Case Study. *Sustainability* **2022**, *14*, 3046, doi:10.3390/su14053046.
36. Gonabadi, H.; Yadav, A.; Bull, S.J. The Effect of Processing Parameters on the Mechanical Characteristics of PLA Produced by a 3D FFF Printer. *The International Journal of Advanced Manufacturing Technology* **2020**, *111*, 695–709, doi:10.1007/s00170-020-06138-4.
37. Koch, C.; Van Hulle, L.; Rudolph, N. Investigation of Mechanical Anisotropy of the Fused Filament Fabrication Process via Customized Tool Path Generation. *Addit Manuf* **2017**, *16*, 138–145, doi:10.1016/j.addma.2017.06.003.
38. Roschli, A.; Gaul, K.T.; Boulger, A.M.; Post, B.K.; Chesser, P.C.; Love, L.J.; Blue, F.; Borish, M. Designing for Big Area Additive Manufacturing. *Addit Manuf* **2019**, *25*, doi:10.1016/j.addma.2018.11.006.
39. Singh, S.; Sharma, S.K.; Rathod, D.W. A Review on Process Planning Strategies and Challenges of WAAM. *Mater Today Proc* **2021**, *47*, 6564–6575, doi:10.1016/J.MATPR.2021.02.632.
40. Kawalkar, R.; Dubey, H.K.; Lokhande, S.P. Wire Arc Additive Manufacturing: A Brief Review on Advancements in Addressing Industrial Challenges Incurred with Processing Metallic Alloys. *Mater Today Proc* **2022**, *50*, 1971–1978, doi:10.1016/j.matpr.2021.09.329.
41. Zhang, Y.; Wu, L.; Guo, X.; Kane, S.; Deng, Y.; Jung, Y.-G.; Lee, J.-H.; Zhang, J. Additive Manufacturing of Metallic Materials: A Review. *J Mater Eng Perform* **2018**, *27*, 1–13, doi:10.1007/s11665-017-2747-y.

42. González, J.; Rodríguez, I.; Prado-Cerqueira, J.L.; Diéguez, J.L.; Pereira, A. Additive Manufacturing with GMAW Welding and CMT Technology. *Procedia Manuf* **2017**, *13*, 840–847, doi:10.1016/J.PROMFG.2017.09.189.
43. Ramarao, M.; King, M.F.L.; Sivakumar, A.; Manikandan, V.; Vijayakumar, M.; Subbiah, R. Optimizing GMAW Parameters to Achieve High Impact Strength of the Dissimilar Weld Joints Using Taguchi Approach. *Mater Today Proc* **2022**, *50*, 861–866, doi:10.1016/J.MATPR.2021.06.137.
44. Dinovitzer, M.; Chen, X.; Laliberte, J.; Huang, X.; Frei, H. Effect of Wire and Arc Additive Manufacturing (WAAM) Process Parameters on Bead Geometry and Microstructure. *Addit Manuf* **2019**, *26*, 138–146, doi:10.1016/j.addma.2018.12.013.
45. Warsi, R.; Kazmi, K.H.; Chandra, M. Mechanical Properties of Wire and Arc Additive Manufactured Component Deposited by a CNC Controlled GMAW. *Mater Today Proc* **2022**, *56*, 2818–2825, doi:10.1016/J.MATPR.2021.10.114.
46. Chernovol, N.; Sharma, A.; Tjahjowidodo, T.; Lauwers, B.; Rymenant, P. Van Machinability of Wire and Arc Additive Manufactured Components. *CIRP J Manuf Sci Technol* **2021**, *35*, doi:10.1016/j.cirpj.2021.06.022.
47. Bociaga, E. Effect of Mould Temperature and Injection Speed on Selected Properties of Polyethylene Mouldings. *International Polymer Science and Technology* **2001**, *28*, 96–102, doi:10.1177/0307174X0102800621.
48. Lopes, J.G.; Machado, C.M.; Duarte, V.R.; Rodrigues, T.A.; Santos, T.G.; Oliveira, J.P. Effect of Milling Parameters on HSLA Steel Parts Produced by Wire and Arc Additive Manufacturing (WAAM). *J Manuf Process* **2020**, *59*, doi:10.1016/j.jmapro.2020.10.007.
49. Nagasai, B.P.; Malarvizhi, S.; Balasubramanian, V. Effect of Welding Processes on Mechanical and Metallurgical Characteristics of Carbon Steel Cylindrical Components Made by Wire Arc Additive Manufacturing (WAAM) Technique. *CIRP J Manuf Sci Technol* **2022**, *36*, 100–116, doi:10.1016/J.CIRPJ.2021.11.005.
50. Zhang, C.; Shen, C.; Hua, X.; Li, F.; Zhang, Y.; Zhu, Y. Influence of Wire-Arc Additive Manufacturing Path Planning Strategy on the Residual Stress Status in One Single Buildup Layer. *The International Journal of Advanced Manufacturing Technology* **2020**, *111*, 797–806, doi:10.1007/s00170-020-06178-w.
51. Wang, X.; Wang, A.; Li, Y. A Sequential Path-Planning Methodology for Wire and Arc Additive Manufacturing Based on a Water-Pouring Rule. *The International Journal of Advanced Manufacturing Technology* **2019**, *103*, 3813–3830, doi:10.1007/s00170-019-03706-1.
52. Chen, X.; Kong, F.; Fu, Y.; Zhao, X.; Li, R.; Wang, G.; Zhang, H. A Review on Wire-Arc Additive Manufacturing: Typical Defects, Detection Approaches, and Multisensor Data Fusion-Based Model. *The International Journal of Advanced Manufacturing Technology* **2021**, *117*, 707–727, doi:10.1007/s00170-021-07807-8.
53. Thien, A.; Saldana, C.; Kurfess, T. The Effect of WAAM Process Parameters on Process Conditions and Production Metrics in the Fabrication of Single-Pass Multi-Layer Wall Artifacts. *The International Journal of Advanced Manufacturing Technology* **2022**, *119*, 531–547, doi:10.1007/s00170-021-08266-x.

54. Zhang, H.; Liu, W.; Zhao, X.; Zhang, X.; Chen, C. Improvement in Microstructure and Properties of 304 Steel Wire Arc Additive Manufacturing by the Micro-Control Deposition Trajectory. *Materials* **2024**, *17*, 1170, doi:10.3390/ma17051170.
55. Monzón Catalán, I. Procesos Robóticos Para La Fabricación Aditiva Metálica de Grandes Componentes, Universidad de Zaragoza: Zaragoza, 2023.
56. Kawalkar, R.; Dubey, H.K.; Lokhande, S.P. Wire Arc Additive Manufacturing: A Brief Review on Advancements in Addressing Industrial Challenges Incurred with Processing Metallic Alloys. In Proceedings of the Materials Today: Proceedings; Elsevier Ltd, 2021; Vol. 50, pp. 1971–1978.
57. Catalano, A.R.; Pagone, E.; Martina, F.; Priarone, P.C.; Settineri, L. Wire Arc Additive Manufacturing of Ti-6Al-4V Components: The Effects of the Deposition Rate on the Cradle-to-Gate Economic and Environmental Performance. In Proceedings of the Procedia CIRP; Elsevier B.V., 2023; Vol. 116, pp. 269–274.
58. Lin, Z.; Song, K.; Yu, X. A Review on Wire and Arc Additive Manufacturing of Titanium Alloy. *J Manuf Process* 2021, *70*, 24–45.
59. Carroll, B.E.; Palmer, T.A.; Beese, A.M. Anisotropic Tensile Behavior of Ti–6Al–4V Components Fabricated with Directed Energy Deposition Additive Manufacturing. *Acta Mater* **2015**, *87*, 309–320, doi:10.1016/j.actamat.2014.12.054.
60. Sarıkaya, M.; Başcıl Önler, D.; Dağlı, S.; Hartomacıoğlu, S.; Günay, M.; Królczyk, G.M. A Review on Aluminum Alloys Produced by Wire Arc Additive Manufacturing (WAAM): Applications, Benefits, Challenges and Future Trends. *Journal of Materials Research and Technology* **2024**, *33*, 5643–5670, doi:10.1016/j.jmrt.2024.10.212.
61. International Organization for Standardization UNE-EN ISO 18273. *Consumibles para el soldeo. Electrodos de alambre, alambres y varillas para el soldeo del aluminio y aleaciones de aluminio. Clasificación. (ISO 18273:2015)* 2015.
62. Srivastava, M.; Rathee, S.; Tiwari, A.; Dongre, M. Wire Arc Additive Manufacturing of Metals: A Review on Processes, Materials and Their Behaviour. *Mater Chem Phys* **2023**, *294*, doi:10.1016/j.matchemphys.2022.126988.
63. Bhuvanesh Kumar, M.; Sathiya, P.; Senthil, S.M. A Critical Review of Wire Arc Additive Manufacturing of Nickel-Based Alloys: Principles, Process Parameters, Microstructure, Mechanical Properties, Heat Treatment Effects, and Defects. *Journal of the Brazilian Society of Mechanical Sciences and Engineering* **2023**, *45*, 164, doi:10.1007/s40430-023-04077-1.
64. Jin, W.; Zhang, C.; Jin, S.; Tian, Y.; Wellmann, D.; Liu, W. Wire Arc Additive Manufacturing of Stainless Steels: A Review. *Applied Sciences (Switzerland)* 2020, *10*.
65. Busachi, A.; Erkoyuncu, J.; Colegrove, P.; Martina, F.; Ding, J. Designing a WAAM Based Manufacturing System for Defence Applications. In Proceedings of the Procedia CIRP; 2015; Vol. 37.
66. Paolini, A.; Kollmannsberger, S.; Rank, E. Additive Manufacturing in Construction: A Review on Processes, Applications, and Digital Planning Methods. *Addit Manuf* **2019**, *30*, doi:10.1016/j.addma.2019.100894.
67. Evans, S.I.; Wang, J.; Qin, J.; He, Y.; Shepherd, P.; Ding, J. A Review of WAAM for Steel Construction – Manufacturing, Material and Geometric Properties, Design,

and Future Directions. *Structures* **2022**, *44*, 1506–1522, doi:10.1016/J.ISTRUC.2022.08.084.
68. Laghi, V.; Palermo, M.; Gasparini, G.; Trombetti, T. Computational Design and Manufacturing of a Half-Scaled 3D-Printed Stainless Steel Diagrid Column. *Addit Manuf* **2020**, *36*, 101505, doi:10.1016/j.addma.2020.101505.
69. Muvunzi, R.; Mpofu, K.; Daniyan, I.; Fameso, F. Analysis of Potential Materials for Local Production of a Rail Car Component Using Additive Manufacturing. *Heliyon* **2022**, *8*, doi:10.1016/j.heliyon.2022.e09405.
70. Betzler, B.R. Additive Manufacturing in the Nuclear Reactor Industry. *Encyclopedia of Nuclear Energy* **2021**, 851–863, doi:10.1016/B978-0-12-819725-7.00106-9.
71. Laghi, V.; Arrè, L.; Tonelli, L.; Di Egidio, G.; Ceschini, L.; Monzón, I.; Laguía, A.; Dieste, J.A.; Palermo, M. Mechanical and Microstructural Features of Wire-and-Arc Additively Manufactured Carbon Steel Thick Plates. *International Journal of Advanced Manufacturing Technology* **2023**, *127*, 1391–1405, doi:10.1007/s00170-023-11538-3.
72. Haelsig, A.; Kusch, M.; Mayr, P. Calorimetric Analyses of the Comprehensive Heat Flow for Gas Metal Arc Welding. *Welding in the World* **2015**, *59*, 191–199, doi:10.1007/s40194-014-0193-0.
73. Kumar, S.; Bhaduri, S.C. Theoretical Investigation of Penetration Characteristics in Gas Metal-Arc Welding Using Finite Element Method. *Metallurgical and Materials Transactions B* **1995**, *26*, 611–624, doi:10.1007/BF02653882.
74. Wang, Z.; Zimmer-Chevret, S.; Léonard, F.; Abba, G. Improvement Strategy for the Geometric Accuracy of Bead's Beginning and End Parts in Wire-Arc Additive Manufacturing (WAAM). *The International Journal of Advanced Manufacturing Technology* **2022**, *118*, 2139–2151, doi:10.1007/s00170-021-08037-8.
75. Kerber, E.; Knitt, H.; Fahrendholz-Heiermann, J.L.; Ergin, E.; Brell-Cokcan, S.; Dewald, P.; Sharma, R.; Reisgen, U. Variable Layer Heights in Wire Arc Additive Manufacturing and WAAM Information Models. *Machines* **2024**, *12*, 432, doi:10.3390/machines12070432.
76. Laghi, V.; Palermo, M.; Gasparini, G.; Veljkovic, M.; Trombetti, T. Assessment of Design Mechanical Parameters and Partial Safety Factors for Wire-and-Arc Additive Manufactured Stainless Steel. *Eng Struct* **2020**, *225*, 111314, doi:10.1016/J.ENGSTRUCT.2020.111314.
77. Zhang, J.; Cao, Q.; Lu, W.F. A Review on Design and Removal of Support Structures in Metal Additive Manufacturing. *Mater Today Proc* **2022**, doi:10.1016/j.matpr.2022.09.277.
78. Treutler, K.; Wesling, V. The Current State of Research of Wire Arc Additive Manufacturing (WAAM): A Review. *Applied Sciences* **2021**, *11*, 8619, doi:10.3390/app11188619.
79. Li, Y.; Huang, X.; Horváth, I.; Zhang, G. GMAW-Based Additive Manufacturing of Inclined Multi-Layer Multi-Bead Parts with Flat-Position Deposition. *J Mater Process Technol* **2018**, *262*, 359–371, doi:10.1016/j.jmatprotec.2018.07.010.
80. Xu, T.; Cui, Y.; Ma, S.; Wang, J.; Liu, C. Exploring the Inclined Angle Limit of Fabricating Unsupported Rods Structures by Pulse Hot-Wire Arc Additive

Manufacturing. *J Mater Process Technol* **2021**, *295*, 117160, doi:10.1016/j.jmatprotec.2021.117160.

81. Garaigordobil, A.; Ansola, R.; Veguería, E.; Fernandez, I. Overhang Constraint for Topology Optimization of Self-Supported Compliant Mechanisms Considering Additive Manufacturing. *CAD Computer Aided Design* **2019**, *109*, 33–48, doi:10.1016/j.cad.2018.12.006.
82. Liu, B.; Shen, H.; Zhou, Z.; Jin, J.; Fu, J. Research on Support-Free WAAM Based on Surface/Interior Separation and Surface Segmentation. *J Mater Process Technol* **2021**, *297*, doi:10.1016/j.jmatprotec.2021.117240.
83. Barbeiro, S.; Enguiça, R.; Lobo, D. Automatic Generation of Conformal Cooling Channels in Injection Moulding. *Computer-Aided Design* **2022**, *150*, 103312, doi:10.1016/J.CAD.2022.103312.
84. Li, Z.; Wang, X.; Gu, J.; Ruan, S.; Shen, C.; Lyu, Y.; Zhao, Y. Topology Optimization for the Design of Conformal Cooling System in Thin-Wall Injection Molding Based on BEM. *The International Journal of Advanced Manufacturing Technology* **2018**, *94*, 1041–1059, doi:10.1007/s00170-017-0901-1.
85. Gao, Z.; Dong, G.; Tang, Y.; Zhao, Y.F. Machine Learning Aided Design of Conformal Cooling Channels for Injection Molding. *J Intell Manuf* **2023**, *34*, 1183–1201, doi:10.1007/s10845-021-01841-9.
86. Feng, S.; Kamat, A.M.; Pei, Y. Design and Fabrication of Conformal Cooling Channels in Molds: Review and Progress Updates. *Int J Heat Mass Transf* **2021**, *171*, 121082, doi:10.1016/j.ijheatmasstransfer.2021.121082.
87. Sun, Y.F.; Lee, K.S.; Nee, A.Y.C. Design and FEM Analysis of the Milled Groove Insert Method for Cooling of Plastic Injection Moulds. *The International Journal of Advanced Manufacturing Technology* **2004**, *24*, 715–726, doi:10.1007/s00170-003-1755-2.
88. Karagöz, İ.; Tuna, Ö. Effect of Melt Temperature on Product Properties of Injection-Molded High-Density Polyethylene. *Polymer Bulletin* **2021**, *78*, 6073–6091, doi:10.1007/s00289-021-03695-w.
89. Wenzel, M.; Raisch, S.R.; Schmitz, M.; Hopmann, C. Comparison of Hybrid Machine Learning Approaches for Surrogate Modeling Part Shrinkage in Injection Molding. *Polymers (Basel)* **2024**, *16*, 2465, doi:10.3390/polym16172465.
90. White, J.L.; Dee, H.B. Flow Visualization for Injection Molding of Polyethylene and Polystyrene Melts. *Polym Eng Sci* **1974**, *14*, 212–222, doi:10.1002/pen.760140310.
91. Singh, S.R.; Khanna, P. Wire Arc Additive Manufacturing (WAAM): A New Process to Shape Engineering Materials. In Proceedings of the Materials Today: Proceedings; 2021; Vol. 44.
92. Bekker, A.C.M.; Verlinden, J.C. Life Cycle Assessment of Wire + Arc Additive Manufacturing Compared to Green Sand Casting and CNC Milling in Stainless Steel. *J Clean Prod* **2018**, *177*, 438–447, doi:10.1016/j.jclepro.2017.12.148.
93. Liu, Z.Y.; Guo, Y.B.; Sealy, M.P.; Liu, Z.Q. Energy Consumption and Process Sustainability of Hard Milling with Tool Wear Progression. *J Mater Process Technol* **2016**, *229*, 305–312, doi:10.1016/j.jmatprotec.2015.09.032.

94. Santos, R.C.; Pereira, M.; Ferreira, J.C.E. Energy Consumption in Milling as a Result of Different Machining Parameters and Tool Paths. In Proceedings of the 2020 IEEE Green Technologies Conference(GreenTech); IEEE, April 1 2020; pp. 206–211.
95. Silva, F.J.G.; Martinho, R.P.; Magalhães, L.L.; Fernandes, F.; Sales-Contini, R.C.M.; Durão, L.M.; Casais, R.C.B.; Sousa, V.F.C. A Comparative Study of Different Milling Strategies on Productivity, Tool Wear, Surface Roughness, and Vibration. *Journal of Manufacturing and Materials Processing* **2024**, *8*, doi:10.3390/jmmp8030115.
96. Priarone, P.C.; Campatelli, G.; Montevecchi, F.; Venturini, G.; Settineri, L. A Modelling Framework for Comparing the Environmental and Economic Performance of WAAM-Based Integrated Manufacturing and Machining. *CIRP Annals* **2019**, *68*, 37–40, doi:10.1016/j.cirp.2019.04.005.
97. Kokare, S.; Oliveira, J.P.; Godina, R. A LCA and LCC Analysis of Pure Subtractive Manufacturing, Wire Arc Additive Manufacturing, and Selective Laser Melting Approaches. *J Manuf Process* **2023**, *101*, 67–85, doi:10.1016/j.jmapro.2023.05.102.
98. Postawa, P.; Stachowiak, T. Mould Temperature Control during Injection Moulding Process.; 2015; p. 110012.
99. Yao, D.; Chen, S.; Kim, B.H. Rapid Thermal Cycling of Injection Molds: An Overview on Technical Approaches and Applications. *Advances in Polymer Technology* **2008**, *27*, 233–255, doi:10.1002/adv.20136.
100. Xu, R.X.; Sachs, E. Rapid Thermal Cycling with Low Thermal Inertia Tools. *Polym Eng Sci* **2009**, *49*, 305–316, doi:10.1002/pen.21261.
101. Dimla, D.E.; Camilotto, M.; Miani, F. Design and Optimisation of Conformal Cooling Channels in Injection Moulding Tools. *J Mater Process Technol* **2005**, *164–165*, 1294–1300, doi:10.1016/j.jmatprotec.2005.02.162.
102. Shayfull, Z.; Sharif, S.; Zain, A.Mohd.; Ghazali, M.F.; Saad, R.M. Potential of Conformal Cooling Channels in Rapid Heat Cycle Molding: A Review. *Advances in Polymer Technology* **2014**, *33*, doi:10.1002/adv.21381.
103. Tan, C.; Wang, D.; Ma, W.; Chen, Y.; Chen, S.; Yang, Y.; Zhou, K. Design and Additive Manufacturing of Novel Conformal Cooling Molds. *Mater Des* **2020**, *196*, 109147, doi:10.1016/J.MATDES.2020.109147.
104. Li, Z.; Ye, J.; Gao, B.; Wang, Q.; Quan, G.; Shepherd, P. Digital and Automatic Design of Free-Form Single-Layer Grid Structures. *Autom Constr* **2022**, *133*, 104025, doi:10.1016/j.autcon.2021.104025.
105. Xie, Y.M. Generalized Topology Optimization for Architectural Design. *Architectural Intelligence* **2022**, *1*, 2, doi:10.1007/s44223-022-00003-y.
106. Rong, Y.; Zhao, Z.-L.; Feng, X.-Q.; Xie, Y.M. Structural Topology Optimization with an Adaptive Design Domain. *Comput Methods Appl Mech Eng* **2022**, *389*, 114382, doi:10.1016/j.cma.2021.114382.
107. Gardner, L.; Kyvelou, P.; Herbert, G.; Buchanan, C. Testing and Initial Verification of the World's First Metal 3D Printed Bridge. *J Constr Steel Res* **2020**, *172*, 106233, doi:10.1016/j.jcsr.2020.106233.
108. COMAU COMAU NJ130. *6-Axes Collaborative robotic arm* 2010.
109. OPEN MIND Technologies HyperMILL CAD/CAM Software 2023.

110. Ultimaker B.V. UltiMaker Cura. *UltiMaker Cura* 2023.
111. Fronius Fronius TPS 400i. *MIG/MAG welding system* 2018.
112. FUNDACION TEKNIKER Development of Thermoplastic Press-Forming Tool for Advanced Rear End Closing Frame Prototype and Tooling 4.0 for Assembly and Transportation of the Advanced Rear End Prototype 2022.
113. Marqués, A.; Laguía, A.; Monzón, I.; Gonzalvo, B.; Dieste, J.A.; Gracia, P. A System and a Method for Manufacturing Molded Pieces 2024.
114. SIMCON CADMOULD. *Plastic injection molding simulation software* 1989.
115. Monzón, I.; Laguía, A.; Marqués, A.; Gonzalvo, B.; Dieste, J.A.; Gracia, P. Method of Additive Manufacturing for Manufacturing Molds an Additive Manufacturing System for Manufacturing Molds 2024.

Índice de figuras

Índice de tablas

Anexos

Anexo A: Justificación de la contribución del doctorado

Todos los artículos incluidos en esta tesis doctoral se han desarrollado en el marco de diversos proyectos europeos, lo que ha permitido su elaboración en colaboración con múltiples autores, tanto internos como externos a la entidad de investigación. No obstante, el doctorando ha liderado tanto la investigación como la redacción de los cuatro artículos científicos que conforman esta tesis.

El doctorando ha desempeñado un papel clave en las tareas de diseño y optimización para la fabricación aditiva mediante tecnología WAAM, además de participar activamente en el análisis de los datos obtenidos y en las labores de redacción de los manuscritos. A continuación, se detallan las contribuciones específicas realizadas por el doctorando:

Artículo 1

Marqués, A.; Dieste, J.A.; Monzón, I.; Laguía, A.; Javierre, C.; Elduque, D. Analysis of Energy and Material Consumption for the Manufacturing of an Aeronautical Tooling: An Experimental Comparison between Pure Machining and Big Area Additive Manufacturing. *Materials* 2024, *17*, 3066, doi:10.3390/ma17133066.

Factor de impacto: 3.1; Q1 (JCR 2023)

Área temática: “Materials science and engineering”

En el primer artículo, el doctorando tuvo una participación destacada en la conceptualización y diseño de los utillajes objeto del estudio, tanto el fabricado mediante la tecnología WAAM como el producido mediante métodos tradicionales. Asimismo, contribuyó de manera significativa al análisis de los datos, incluyendo el consumo eléctrico y de material, así como la evaluación de la información metrológica asociada a los utillajes diseñados y fabricados.

Contribución CRediT: Validación, análisis y redacción – borrador original.

Artículo 2

Marqués, A.; Dieste, J.A.; Monzón, I.; Laguía, A.; Gracia, P.; Javierre, C.; Clavería, I.; Elduque, D. Improvements in Injection Moulds Cooling and Manufacturing Efficiency Achieved by Wire Arc Additive Manufacturing Using Conformal Cooling Concept. Polymers (Basel) 2024, 16, doi:10.3390/polym16213057.

Factor de impacto: 4.7; Q1 (JCR 2023)

Área temática: “Polymer science”

La investigación y el desarrollo asociados a este artículo han sido llevados a cabo de manera conjunta por todos los investigadores involucrados. No obstante, el doctorando ha asumido el rol de investigador principal, estando involucrado de manera activa en todas las etapas del estudio. Su contribución ha sido especialmente destacada en el diseño tanto del utillaje fabricado mediante tecnología WAAM como del utillaje teórico utilizado como referencia comparativa.

Contribución CRediT: Validación, análisis y redacción – borrador original

Artículo 3

Arrè, L.; Laghi, V.; Marqués, A.; Palermo, M. Tubular Sandwich Cross-Sections Fabricated with Wire Arc Additive Manufacturing for Jumbo Structural Members. *Structures* 2024, *67*, doi:10.1016/j.istruc.2024.106689.

Factor de impacto: 3.9; Q1 (JCR 2023)

Área temática: “Structural engineering”

En el desarrollo del tercer artículo, el doctorando desempeñó un rol destacado en el diseño y la fabricación de los demostradores seleccionados del catálogo de estructuras tubulares auto-reforzadas. Este trabajo incluyó la experimentación con diferentes parámetros de fabricación para alcanzar las características de cordón requeridas. Asimismo., el doctorando realizó el pertinente trabajo de redacción y validación del artículo.

Contribución CRediT: Metodología, investigación, recursos y redacción – revisión y edición.

Artículo 4

A. Marqués, J. Dieste, I. Monzón, C. Javierre and D. Elduque, rCF LM PAEK press-moulding process optimization through the introduction of a WAAM mould core, Materiales

Compuestos (2024). Vol. 08 - COMUNICACIONES MATCOMP21 (2022) Y MATCOMP23 (2023), (Núm. 6 - Fabricación y Aplicaciones Industriales), 35 URL https://www.scipedia.com/public/Marques*_et_al_2024a

Proceeding con revisión académica por pares

Área temática: “Composite Material”

En la cuarta publicación, el doctorando participó activamente en todas las fases del proceso. Su contribución abarcó el diseño de los utillajes empleados en el proceso de *press-forming* descrito en el artículo, así como en la ejecución integral de las pruebas realizadas. Esto incluyó la conceptualización, preparación y validación de los resultados obtenidos. Además, el doctorando asumió la responsabilidad de la redacción del artículo correspondiente.

Contribución CRediT: Metodología, investigación, metodología, recursos, validación y redacción – borrador original.

Anexo B: Patente EP4400243A1

Título

Método de fabricación aditiva para fabricar moldes y sistema de fabricación

Aplicantes

FUNDACIÓN AITIIP

Inventores

MONZÓN CATALÁN, Iván; LAGUÍA PÉREZ, Alberto; **MARQUÉS PAOLA, Alejandro**; GONZALVO BAS, Berta; DIESTE MARCIAL, José Antonio; GRACIA ARANEGA, Pascual

Prioridades y aplicación

EP23382012A·2023-01-11

Publicación y fecha

EP4400243A1·2024-07-17

(19) Europäisches Patentamt
European Patent Office
Office européen des brevets

(11) EP 4 400 243 A1

(12) EUROPEAN PATENT APPLICATION

(43) Date of publication:
17.07.2024 Bulletin 2024/29

(21) Application number: **23382012.5**

(22) Date of filing: **11.01.2023**

(51) International Patent Classification (IPC):
B23K 9/04 *(2006.01)* ***B23K 9/095*** *(2006.01)*
B33Y 10/00 *(2015.01)* ***B33Y 50/02*** *(2015.01)*
B33Y 80/00 *(2015.01)*

(52) Cooperative Patent Classification (CPC):
(C-Sets available)
B33Y 10/00; B23K 9/044; B23K 9/0956; B33Y 50/02; B33Y 80/00 (Cont.)

(84) Designated Contracting States:
AL AT BE BG CH CY CZ DE DK EE ES FI FR GB GR HR HU IE IS IT LI LT LU LV MC ME MK MT NL NO PL PT RO RS SE SI SK SM TR
Designated Extension States:
BA
Designated Validation States:
KH MA MD TN

(71) Applicant: **Fundación AITIIP**
50720 Zaragoza (ES)

(72) Inventors:
- **MONZÓN CATALÁN, Iván**
  E-50720 Zaragoza (ES)
- **LAGUÍA PÉREZ, Alberto**
  E-50720 Zaragoza (ES)
- **MARQUÉS PAOLA, Alejandro**
  E-50720 Zaragoza (ES)
- **GONZALVO BAS, Berta**
  E-50720 Zaragoza (ES)
- **DIESTE MARCIAL, José Antonio**
  E-50720 Zaragoza (ES)
- **GRACIA ARANEGA, Pascual**
  E-50720 Zaragoza (ES)

(74) Representative: **ABG Intellectual Property Law, S.L.**
Avenida de Burgos, 16D
Edificio Euromor
28036 Madrid (ES)

(54) METHOD OF ADDITIVE MANUFACTURING FOR MANUFACTURING MOLDS AN ADDITIVE MANUFACTURING SYSTEM FOR MANUFACTURING MOLDS

(57) The present invention is related to the field of additive manufacturing and, in particular, to wire arc additive manufacturing methods and systems for optimized metal molds. The invention is characterized by the use of a computational model that allows the definition of slices that serve as a reference for the addition or not of layers of material according to a strategy that prevents accidental contact of the arc tool with the manufactured piece, and serve to maintain some of the process parameters (stick out) in the optimized value range. According to specific aspects the method and system include strategies for defining arc trajectories to permit the correct growth without deformation of the manufactured part.

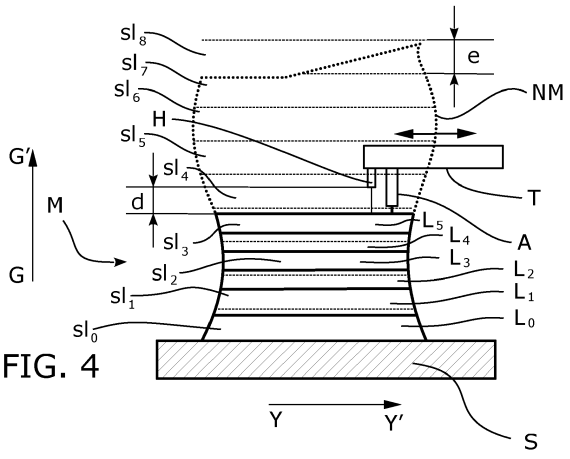

FIG. 4

EP 4 400 243 A1

(52) Cooperative Patent Classification (CPC): (Cont.)

C-Sets
B22F 2999/00, B22F 10/20, B22F 3/20;
B22F 2999/00, B22F 10/30, B22F 12/53,
B22F 12/22

Description

FIELD OF THE INVENTION

[0001] The present invention is related to the field of additive manufacturing and, in particular, to wire arc additive manufacturing methods and systems for optimized metal molds.

[0002] The invention is characterized by the use of a computational model that allows the definition of slices that serve as a reference for the addition or not of layers of material according to a strategy that prevents accidental contact of the arc tool with the manufactured piece, and serve to maintain some of the process parameters (stick out) in the optimized value range.

[0003] According to specific aspects the method and system include strategies for defining arc trajectories to permit the correct growth without deformation of the manufactured part.

PRIOR ART

[0004] Manufacturing molding processes are widely employed for producing plastic parts or components using a mold cavity for the molten material, like glass or plastics and most commonly, thermoplastic polymers. Different types of manufacturing molding processes, such as injection molding, blow molding, RTM, lay-up, compression molding, organosheet compression use a mold cavity created within a mold.

[0005] Injection machines that perform manufacturing molding processes use injection molds containing cavities that form the parts of the resulting plastic component. Melted plastic is injected into the mold, filling said cavities. The mold is continuously cooled or heated, and the parts are ejected by pins.

[0006] The mold is a key point of a manufacturing molding process. Any reference to "mold" or "injection mold" in no way limiting, as all forms or parts of a mold are contemplated, for example a mold or a counter-mold, or a fixed mold plate and a movable molt plate that close together.

[0007] Steel is the most frequently used material for the construction of a mold or a part of it. However, other materials, such as aluminum, nickel-chromium, iron-nickel or beryllium-copper alloys are also used for some mold makers mostly for prototypes and test runs. Aluminum is lighter than steel and has a better thermal conductivity than steel. The choice of one or another material is generally made based on the size of the part, the volume of parts to be manufactured and the desired quality. The type of mold material affects the product quality a lot (e.g. thermal conductivity, weight, etc.). A combination of steel and aluminum, wherein each material is used for different parts of the mold is also possible.

[0008] In reference to the steel, different types of steel material (e.g. mild steel) may be used, depending on the particular use or needs (e.g. a mold that works well in the shorter term or a longer-lasting mold with lower long term cost). On the other hand, different grades of steel material may be used.

[0009] In general, a mold is constantly receiving heat from the melted material and therefore need to be constantly cooled. It is well known to provide the molds with an inner cooling system to either cool or heat the mold or a part of said mold depending on the specific step or need of the manufacturing process. In this case, the thermal inertial is not very relevant since the heat evacuated is the heat that the mold receives from the melted material.

[0010] According to other applications with no melted material, a thermo-deformable sheet or preform is deformed by the mold at high temperature and then is cooled down before opening the mold in order to correctly set the final shape. In these cases, a mold needs to be heated before starting the manufacturing process and cooled once the process has finished. Since the mold need to be heated and cooled the time invested in a manufacturing cycle depends on the thermal inertia of the mold and therefore has to be as low as possible.

[0011] A correct design of the injection mold cooling system is, therefore, crucial since the cooling time takes more than half of injection molding cycle. Poor design of cooling system will extend molding time, increase production cost, and the injection mold temperature has great influence to the mold shrinkage, dimensional stability, deformation, internal stress and surface quality. Therefore, a well-designed cooling system can shorten the molding time and improve the productivity magnificently.

[0012] A conventional cooling inner system comprises a cooling circuit that uses a fluid (also called coolant), such as water or oil, that is selectively transmitted and passes through a plurality of cooling channels created in specific parts inside the mold for this purpose.

[0013] Said plurality of inner cooling channels are constituted as hollow spaces that are formed in specific parts of the interior of the mold body according to a determined direction depending on the geometry of the mold. The design and formation of the plurality of cooling conduits or channels inside the mold come with great challenges. There are several design aspects of cooling channels that can help achieve good channel design. These include: (a) the number of cooling channels should be as many as possible, (b) the diameter of the inner cooling channels should be as large as possible, (c) the cooling channels should be as close as possible to the thickest part of the mold cavity and (d) the cooling channels should be closely follow the specific geometry of the external mold parts to ensure a uniform thermal transfer to avoid deformation of the resulting molded part or a non-homogeneous temperature field in the mold.

[0014] One or more external mold parts are likely to have one or more curved surfaces. In those cases, as indicated in the previous paragraph, it is desirable that each cooling conduit or channel closely follows the same

specific curved trajectory than the external mold part that is placed above the inner cooling conduit or channel.

[0015] Metal molds can be produced by different types of manufacturing processes. They have traditionally been produced by casting of molten metal to generate a first part that is subsequently machined. Typical external machining operations are milling, mainly by means of numerical control machines with several degrees of freedom that allow the generation of complex shapes. For the machining of internal cavities such as cooling ducts or channel, the most common operation is drilling, imposing ducts of straight configuration. When straight ducts are to be adapted to a certain shape, one of the usual ways is to machine straight sections that are connected. A specific connection between straight sections are external chambers, for example by open chambers that allow access to the drilling tool and then closed, for example by plates.

[0016] However, the formation of the plurality of cooling channels of the metal molds or part of said molds obtained by these conventional manufacturing processes is difficult when the inner cooling channels should adapt to complex paths with one or more curvatures. The precision of design and formation of each cooling channel according to a predetermined path including one or more curvatures is critical to ensure a correct heating and cooling of the mold.

[0017] On the other hand, due to the weight of the metal, metal molds or part of such molds obtained by these conventional manufacturing processes also aim to reduce the overall weight of the mold by providing internal openings in certain parts of the mold which are devoid of material.

[0018] More recently, welding technologies for manufacturing metal parts or components, such as gas-metal arc welding (GMAW), tungsten-inert gas welding (TIG) or stick welding have been employed to produce "built-up" metal parts, pieces or components. However, metal parts, pieces or components later require significant machining to produce usable, useful parts. Instead, a relatively new manufacturing technology based on welding to produce useful metal geometries through Wire Arc Additive Manufacturing (WAAM) is gaining an increasing market share, due to their significant benefits.

[0019] WAAM is an advanced digital manufacturing process that melts a metal wire (wire feedstock) using a standard electric or plasma arc equipment as the heat source by depositing layers of metal on top of each other under the control of a program or software according to a 3D digital model, until a desired 3D metal part, piece, component or shape is created. The shape is built upon a substrate material (a base plate) that the part can be cut from once finished. The wire, when melted, is deposited in the form of a cord or bead on the substrate. As the beads stick together, they create a layer of metal material. The process is then repeated, layer-by-layer until the metal part is completed. In WAAM, components are typically deposited vertically layer-by-layer.

[0020] WAAM can generally work with a wide range of metals, provided they are in wire form. This list includes stainless steel, nickel-based alloys, titanium alloys and aluminum alloys. Any metal that can be welded can also be used with WAAM.

[0021] It would be highly desirable to find a method and system that is capable to produce an optimized metal mold suitable for being used e.g. in injection molding, blow molding, RTM, lay-up, compression molding, organosheet compression process, wherein the formed metal molds can have very complex curved external part/s (protruding or recessed parts) with an optimized design of the geometry and location of the inner cooling channels and also an optimized design of the geometry and location of other internal openings for reducing the quantity of metal, so the weight of the mold.

[0022] It would be also highly desirable to find a method and system that is capable to produce an optimized metal mold having a thermal inertia reduction and raw material consumption. Furthermore, the manufactured mold by the method and system must have no imperfections and a sufficient amount of material so that after machining the generated surface of the mold does not show voids or defects even if the deposition is by means of a bead generated by melting material that hardly generates a predictable shape.

DESCRIPTION OF THE INVENTION

[0023] The present invention provides a solution for the above mentioned issues by a method of additive manufacturing for manufacturing molds according to independent claim 1, an additive manufacturing system for manufacturing molds according to claim 13 and a computer program product according to independent claim 15. In dependent claims, preferred embodiments of the invention are defined.

[0024] In a first inventive aspect, the present invention provides a method of additive manufacturing for manufacturing molds or parts of said molds, by means of:

- *a substrate intended for supporting the generated mold or part of said mold;*
- *a wire arc device adapted for depositing metal cord according to a predetermined path over a surface in a direction perpendicular to the substrate and adapted to be movable in a plane parallel to the substrate forming a metal layer on top of each other;*
- *a sensor adapted to measure a distance between the wire arc device and a surface in a perpendicular direction to the substrate; and*
- *a computer system in communication with the wire arc device and the sensor;*

the method comprising the steps:

1. generating by the computer system a 3D numerical model of a mold or part of said mold;

2. segmenting by the computer system the 3D numerical model into a plurality of stacked slices of a predetermined thickness according to a predetermined direction;
3. iteratively, departing from the first slice until the last slice of the 3D numerical model, carrying out on each of the slices by the computer system, according to a sequential order, the following sub-steps:

a) selecting the slice of the 3D numerical model to be used for determining the path of the wire arc device to form a determined metal layer;
b) determining by the computer system, for the determined slice, a path intended to represent a trajectory of a metal cord to be deposited in respect to the slice; and
c) commanding the wire arc device by the computer system to form a determined metal layer by depositing a metal cord on top of the previously formed metal layer, or on the substrate if it is the first metal layer, following a trajectory according to the path generated by the computer system for the slice to be used;

- *wherein in step 3 the computer system further carries out a further action of checking for the selected slice the formed metal layers in comparison to the slices of the 3D numerical model, comprising the following sub-steps:*

before step c is executed, receiving from the sensor at least one measurement value of the distance and determining a representative value of the height of the formed metal layers;
if the representative value is higher than the summation of the thicknesses of the previous slices of the 3D numerical model plus the thickness of the selected slice to be used then at least c) of the currently checked slice is not executed and the computer system selects the next slice.

[0025] The following terminology is used along the whole document to describe features of the invention:

- The term "substrate" should be understood as it can be any type of support or plate intended for supporting the generated mold or the generated mold preform or part of any of them. Preferably, the substrate is a metallic substrate, for example a stainless steel. Also preferably, the substrate is flat and it is disposed in a horizontal plane. In the case where the substrate is flat and it is disposed in a horizontal plane, the direction in which the slices are generated is the direction identified during manufacture as vertical. Once the shape is built upon a substrate the substrate can be cut.
  The term "generated mold or part of said mold" should be understood in a broadly way, including a wide range of a mold or injection mold or part of said mold, e.g.: a preform of the mold that is next machined to finally obtain the final mold, a mold or a counter-mold, a fixed mold plate and a movable molt plate that close together or even a coating of a mold; wherein the mold or part of said mold is made of a material such as metal, for example steel, aluminum, nickel-chromium, iron-nickel or beryllium-copper alloys; and wherein the mold is suitable for being used in injection molding, blow molding, RTM, lay-up, compression molding, organosheet compression process or a similar manufacturing process. When the term "material" is used, it is understood as the deposition material with which the growth of the manufactured piece is obtained. The preferred material is metal or metal alloys, although the use of other resistant materials is also possible. The resulting mold or mold preform or mold part according to specific embodiments have curved external part/s or surface/s have inner cooling channels or other apertures, even for cases where the curvatures of the curved external part/s and so the curved inner cooling channels or other apertures are very complex.

- The term "steel" in no way limiting, as there are thousands of grades to choose from for each specific product. The type of material and geometry determine the choice of steel grade.

- The term "wire arc device" should be understood as it can be any wire arc device adapted for depositing a weld cord or also known as weld bead (in most cases departing from a metal wire or also known as wire feedstock) according to a predetermined path over a surface.

- In the context of the present invention, the wire arc device is at least adapted to be movable in a plane parallel to the substrate forming a plurality of cords extended along a path distributed over a certain area. Since the weld bead has a certain width, the path establishes a band that covers a portion of the area. The aim of the use of a wire arc device is at least to deposit a new layer of material, preferably metal, without leaving cavities or defects in said layer. The weld bead can cover the entire area by making use of sinuous paths or paths that at one or more points intersect. This is the case of paths that form a grid, for example triangular, by superimposing lines extending in various directions.

- Further, it should be understood that the heat source used to melt the metal cord or metal wire (wire feedstock) may be a standard electric or plasma arc equipment. The metal wire, when melted by the heat source, is deposited in the form of a cord or a bead on the substrate or the piece. As the beads stick together, they create a layer of metal material. The

weld bead not only has a certain width but, according to its cross-section, shows a curved upper surface of greater height in the central part. For this reason, once the material has been deposited by means of the wire arc device following the predetermined path, the new layer of material shows strong variations in height over the original surface, either because of the curved shape of the weld bead or because of the places where there is crossing and overlapping of weld beads or for both reasons. The growth of the part is carried out by generating a plurality of layers of material following the same strategy.

[0026] In places where a layer has irregularities in height, according to the direction of growth by deposition, the deposition of a new layer can increase these irregularities. The set of steps and features of the method allows a controlled growth of the mold even in these circumstances.

- The term "sensor" should be understood as it can be any sensor adapted to measure the distance between the wire arc device and a surface in a perpendicular direction to the substrate. When we refer to "the distance between the wire arc device and a surface in a perpendicular direction to the substrate" the reference point of the wire arc device is preferably where the material is supplied. However, the sensor can be in a different location from the point of deposition of the material but always in a fixed location with respect to the wire arc device. This makes the positional relationship between the sensor and the deposition point known. With the position relationship between the sensor and the deposition point it is possible to correct the signal directly obtained by the sensor and reference it to the desired point, in particular to the material deposition point.

[0027] In analytic geometry, the distance from a point to a plane is the shortest distance between the point and any other point in the plane. This distance corresponds to the length of the segment perpendicular to the plane that goes from the point to the plane. A possible type of sensor may be a laser sensor.

- Any reference to "part", "piece", "component" or "shape" in no way limiting, as all forms of parts are contemplated, including metal pieces or components or part of said pieces or components, such as coatings.

[0028] The present invention provides a method for manufacturing optimized metal molds or parts of said molds using Weld Arc Additive Manufacturing (WAAM), wherein the resulting formed metal mold or parts of said molds is suitable for being used, e.g., in injection molding, blow molding, RTM, lay-up, compression molding, organosheet compression, is an improvement upon existing methods of additive manufacturing using weld materials. This method allows has the advantages thatthe raw mould formed requires only a small amount of finishing, it greatly simplifies the processing procedure, avoids special tools, shortens the product manufacturing cycle, and enables customised production of a mold with a complex shape.

[0029] On the other hand, advantageously, the resulting WAAM formed metal mold or part of said mold produced through the disclosed method is capable of manufacturing complex shaped molds having curved external part/s or surface/s (protruding and/or recessed parts), even for cases where the curvatures of said curved external part/s is very pronounced.

[0030] Furthermore, advantageously, the resulting WAAM optimized metal mold or part of said mold produced through the disclosed method permit manufacturing complex shaped molds having curved external part/s or surface/s and including inner apertures, inner conduits or inner cooling channels with the same curvature as the curved external part/s with a high degree of precision and accuracy according to a predetermined curvature requirements. In particular, the plurality of inner cooling channels are constituted as hollow spaces, in specific parts of the interior of the mold body depending on the geometry of the shape of the mold. In particular, the present method makes it possible to create these cooling channels in a close position to the thickest part of the mold cavity and closely following the specific geometry of the external mold parts (even if the external mold parts are curved) to ensure uniform the thermal transfer to avoid deformation of the resulting molded part. A well-designed inner cooling channels for the coolant in the mold according to a predetermined path ensures a correct heating and cooling of the mold, which shorten the molding time and improve the productivity magnificently of the molding process. Moreover, the method and system of the present invention allow to form an optimized mold having a good design of the geometry and location of one or more internal openings or apertures. The provision of these one or more internal openings or apertures advantageously reduces the amount of metal in the mold in specific parts, thereby consequently reducing the overall weight of the mold.

[0031] The specific strategy according to claim 1 of establishing the metal deposition paths combined by the layer selection criteria depending on the result that is being measured on the generated part allows the use of a metal deposition by beads or cords that, traditionally, does not offer control over the thickness or shape adopted on a surface that is increasingly irregular. On the contrary, it has been observed that as a result, even though the generated metal part according to method claim 1 has roughness, the overlapping of beads does not generate cavities due to inadequate deposition. In addition, the claimed method guarantees the non-interference of the arc generating head with the generated metal part. This is very important since a simple contact of the head

with the generated metal part would give rise to a very high intensity discharge that would generate the undesired welding of the head itself, destroying it at least in part.

[0032] In respect to the predetermined path, according to an embodiment, it is planned according to the specific mold to be manufactured. According to an embodiment, the predetermined path of the wire arc device comprises one or a plurality of lines following the contour or part of it and a set of lines filling the inner area surrounded by the contour. The set of lines filling the inner area, according to an embodiment, are parallel lines equally spaced. According to a further embodiment, the set of lines filling the inner area comprises a first set of parallel lines equally spaced and a second set of parallel lines equally spaced and rotated a predetermined angle in respect to the first set of lines. Examples of angles are 30º, 45º, or 90. According to a further embodiment, the set of lines filling the inner area are parallel lines equally spaces that are rotates in respect to the lines of the part of the path corresponding to the inner area of the former slice.

[0033] Preferably, step 2 of the method consists of *segmenting by the computer system the 3D numerical model into a plurality of stacked slices of a predetermined thickness according to a predetermined direction, wherein said predetermined direction in which the slices are generated is perpendicular to the substrate.*

[0034] Once the 3D numerical model of a mold or part of said mold has been generated, a segmentation process generates a plurality of stacked slices of a predetermined thickness wherein the stacking direction is preferably the vertical direction to a base. Thus, if the substrate extends along a horizontal plane, the direction in which the slices are generated in the 3D numerical model is the vertical direction wherein a base of the 3D numerical model uses as a coordinate reference system the substrate position and orientation. This base of the 3D numerical model is the base representing the substrate on which the mold or piece will be manufactured. The vertical direction in respect to the base in the 3D numerical model is the same that that the vertical direction in respect to the substrate during real manufacturing of the mold. That is, the numerical model is a representation of the mold to be manufactured and the base is a representation in the 3D numerical model of the substrate.

[0035] The set of slices having a predetermined thickness are references that will be used when determining if a new layer is added to the piece being manufactured and when determining the path that the wire arc device must follow when depositing a new layer. The shape of the perimeter of each layer may vary from one layer to another and is delimited by the mold model when segmented.

[0036] The addition of layers using the wire arc device is done by applying an iterative method that runs through the set of slices of the 3D numerical model. In the execution of the method, there will be slices that do not result in a new layer deposited by the wire arc device or, there will be slices that result in the deposition of one or more layers.

[0037] The first reference slice is the first slice of the 3D numerical model, the one closest to the base and which should result in one or more layers of material on the substrate. Starting with this first slice, one slice is taken sequentially as a reference slice. From a reference slice, the path that the wire arc device will follow is established according to the shape of the slice, mainly the perimeter shape. While the segmentation of a body delimited by a curved surface by stacked slices gives rise to perimeter limits according to a curved perimeter band, the determination of the path of the wire arc device is established for a reference plane, for example either a middle plane of the slice or one of the base planes of the slice, and the perimeter limit is the intersection of the reference plane with the perimeter surface of the slice.

[0038] Once the path of the wire arc device is established, the method acts on the wire arc device so that it deposits a weld bead or cord following the path previously established on the slice of the model and deposited on the previous layer (or the substrate if it is the first layer).

[0039] Once this new layer has been deposited, a measurement of the height reached with the new layer is carried out. Although each point of the upper surface of the layer provides a different measurement due to irregularity, the method establishes a single reference value where, according to a preferred example, this reference value is taken based on a plurality of measurements taken on the surface.

[0040] When a new reference slice is selected, a check is carried out: the representative height measured on the top surface of the last layer is compared with the corresponding height in the 3D numerical model resulting from considering the sum of the thicknesses of the new reference slice and all the reference slices that have been previously used.

[0041] If the measured height is greater than the height resulting from adding the thicknesses of the slices, the used slices plus the new reference slice, then the method moves on to the next slice without carrying out the layer deposition process. That is, the reference slice becomes the next slice by rechecking if now the height provided by the 3D numerical model by stacking reference slices is greater than the height measured on the part of the piece already measured.

[0042] The technical effect of this check is not to allow the piece to grow too much, especially when the height of growth in one or more layers is greater than the thickness of the slices. Otherwise, if the part grows more than expected it could result in accidental contact of the wire arc device and the part being manufactured and this accidental contact causes the wire arc device to weld directly to the part damaging the tool.

[0043] Preferably, the distance measurement made by the sensor is taken right at the point of the wire arc device where the metal material is introduced.

[0044] In some embodiments, *after receiving from the*

sensor the measurement of the distance and determining a representative value of the height of the formed metal layers, the method further comprises the step:

- *before step a), receiving from the sensor a measurement of the distance and determining a representative value of the height of the formed metal layers and, if the representative value of the height is lower than the summation of the thicknesses of the previously used slices then steps b) and c) are executed.*

[0045] Once it has been ensured that the height reached with the deposition of a new layer does not grow excessively such as coming into contact with the tool, according to this embodiment an additional check identifies situations in which the last deposited layer has not reached the height corresponding to the sum of the thicknesses of the slices used as reference. In this case the method deposit again a new layer according to steps b) and c).

[0046] *In some embodiments of the method, the path, determined by the computer system, generated for at least one slice of the plurality of stacked slices comprises the following regions or portions:*

- *a first portion of path that corresponds to the perimeter of the slice;*
- *a second portion of path that corresponds to inner perimeter/s of one or more inner conduits, inner openings or inner cavities sectioned by the slice (if they exists); and*
- *a third portion of path that corresponds to the inner area of the slice.*

[0047] According to another embodiment of the method, the predetermined path also comprises a portion extended along the outer perimeter of the layer and the perimeter of any of the openings caused by the inner conduits sectioned by the layer. This possible form of the predetermined path is repeated for layer-by-layer accumulation to complete the production of a certain surface of the mold. This embodiment providing a path extended at least along the outer perimeter of the layer allows to avoid a growth process that has been observed to be anomalous since the addition of successive layers in practice results in the manufactured piece tilting in respect to the direction of growth. It has been observed that increasing the material deposition specifically in the perimeter zone avoids this anomalous behavior.

[0048] *In other embodiments of the method, the path, determined by the computer system, generated for at least one slice of the plurality of stacked slices, additionally to the previous three steps, further comprises:*

- *a forth portion of path that corresponds to inner perimeter/s of one or more inner cooling ducts or channels sectioned by the slice.*

[0049] A similar effect is observed in the inner openings or inner cavities sectioned by the slice. The wire arc device add material but these specific regions close to the inner perimeters show a lower height and adding the second portion of path that corresponds to inner perimeter/s increase the amount of material avoiding deformations of the whole mold parts close to the existence of inner cooling ducts or channels.

[0050] *In some embodiments of the method, two sensor measurements are taken:*

- *a first measurement at a location corresponding to the inner area of the slice determining a representative value of the height at said location and,*
- *a second measurement at a location corresponding to a perimeter of the second portion or the third portion or both portions determining a representative value of the height at said location;*

wherein the step c) is executed over the second portion, the third portion or both portions if the absolute value of the difference between the representative value of the height of the first measurement and the representative value of the height of the second measurement is higher than a predetermined threshold.

[0051] Although it has been observed that the manufactured pieces by layered deposition using a wire arc device give rise to deformations that are compensated by the inclusion of a portion of the perimeter path, this perimeter deposition does not necessarily correspond to a deposition of material in the inner area of the slice.

[0052] According to this embodiment, two independent measurements are carried out, one representative of the height reached inside the deposited layer and the other representative of the height reached in the perimeter area. The difference, if it exceeds a predetermined threshold value assesses whether the degree of growth in the perimeter zone and the inner zone is different. In particular, when the growth of the inner zone is greater than the perimeter zone exceeding the predetermined threshold value then a deposition is established only along a path in the third portion; that is, in the perimeter zone causing a compensation effect of the heights obtained in the manufactured piece.

[0053] *In some embodiments of the method, the generated third portion of path incorporates a tolerance for avoiding the section reduction or closing of any internal channel with metal cord.*

[0054] It has been observed that the deposition of material following a perimetric path, the second portion of the path, generates a narrowing of the ducts that are generated. According to this example embodiment, the deposition path is amended by causing it to enter towards the inner area a certain distance and as a result, the duct is widened.

[0055] *In some embodiments of the method, the metal cord is deposited in a direction transversal to the predetermined direction of the path, preferably in a direction*

perpendicular to the substrate.

[0056] According to this embodiment, the metal cord is deposited in a direction perpendicular to the substrate and therefore, at any change of direction imposed by the path, the deposition angle does not change, and the resulting weld bead is independent of the path. Moreover, under these conditions it is not necessary to modify the deposition orientation and the movements of the wire arc device only correspond to displacement movements without any change of orientation, simplifying the means of action and movement to achieve a deposition following a certain path.

[0057] *In an embodiment of the method, determining the representative value of the height from a sensor measurement is being processed by the computer system by:*

- *removing measurement spurious values; or*
- *removing measurements that are not maintained during a predetermined period of time; or*
- *removing both, measurement spurious values and measurements that are not maintained during a predetermined period of time.*

[0058] It has been previously described that the surface of a deposited layer in mold formation results irregular and with strong variations in height if measured at different points. When the height sensor carries out a plurality of readings, for example at or along a path, the signal received is a strongly varying signal. According to this example embodiment from this strongly varying signal a single scalar value representative of the height of the entire layer is determined.

[0059] In a first option, spurious values are eliminated, thus removing noise due to values that do not necessarily correspond to real height variations. Even if this is not the case, such values are not assessed as representative. The result is a signal that, being variable, has smaller fluctuations.

[0060] The further option assesses only values that are maintained for a predetermined period. This means that height values acquired along a path without any change in these values means that a surface area is close to flatness or does not correspond to strong height changes such as the interface between measuring outside the part and inside the part.

[0061] A third option combines the application of the first option and the second option. After one or two filters like the ones disclosed the resulting signal is more stable and can be used as a calculation reference for a representative height value.

[0062] *A method according to the previous claim, wherein the sensor measurement is being further processed by the computer system by selecting the higher value of the sensor measurements in an entire metal layer ensuring that the wire arc device does not touch the generated mold.*

[0063] The measurements used to establish the height reference value can be the directly obtained from the sensor output signal or the signal preprocessed according to any of the examples described above. In this second case, the values are closer to the real values of the height of the mold due to the elimination of unwanted effects such as reading noise or values that correspond to the beginning or end of the part following the measurement projection of the sensor. The use of the maximum value criterion ensures that the tool, the wire arc device, will never make contact with the mold at any time.

[0064] Although height is described as the measurement variable, at all times it should be interpreted as meaning that the measurement is the distance between the sensor and the measured object in the direction of growth, although the preferred example uses the vertical direction determined by the action of gravity as the direction of growth.

[0065] *Optionally, the method further comprises a final step of machining the external surface of the generated mold or of the part of said mold.* Different types of surface finishes can be applied to the formed mold or part of the mold for aesthetic or functional purposes. Preferably, the machining is milling, e.g. by means of numerical control machines with several degrees of freedom that allow the generation of complex shapes. As an example, the preform manufactured by the method and system has an excess thickness of about 5 mm on all outer surfaces, which is the area that is subsequently machined.

[0066] In the case of working surfaces that must fit precisely with other surfaces, such as the surfaces of a mold that come into contact with the surfaces of a countermold, the machining operation eliminates all the irregularities inherent to a surface generated by the contribution of a weld bead. Therefore, the 3D numerical model must be oversized in such a way that the volume generated must be delimited by surfaces distanced from the surface generated after the machining operation, distanced outwards from the body of the mold, and with a sufficient distance to ensure that the machining eliminates all irregularities. That is, even the deepest valleys of irregularities are spaced away from the final surface so that the final surface is only the result of the machining operation.

[0067] *Also optionally, the method further comprises a final step of polishing the external surface of the generated mold or of the part of said mold. Preferably, the polishing the external surface of the generated mold or of the part of said mold is a subsequent step to the step of machining the external surface of the generated mold or of the part of said mold.*

[0068] Surface polishing operations are in fact a fine machining operation. Therefore, the oversized 3D numerical model must take into account the additional reduction of volume caused by polishing the surface. This polishing step is carried out after the step of machining the external surface of the generated mold or of the part of said mold.

[0069] In a second inventive aspect, the invention pro-

vides *an additive manufacturing system for manufacturing molds, the system comprising:*

- *a substrate intended for supporting the generated mold or part of a mold;*
- *a wire arc device adapted for depositing metal cord according to a predetermined path over a surface in a direction perpendicular to the substrate and adapted to be movable in a plane parallel to the base forming a metal layer on top of each other;*
- *a sensor adapted to measure the distance between the wire arc device and a surface in a perpendicular direction to the substrate; and*
- *a computer system in communication with the wire arc device and the sensor;*

wherein the computer system is adapted to carry out the steps 1 to 3 of the method according to the first aspect of the invention.

[0070] The second aspect is an additive manufacturing system with the physical elements identified in the method description and where such a system incorporates a computational system that reads environmental variables, in particular the growth height of the layers being incorporated on the substrate by means of the sensor, and also has the ability to act. This performance is mainly to carry out the movements of the wire arc device according to the stages established by the method according to any of the described examples.

[0071] In particular, in the first aspect of the invention and the second aspect of the invention, the wire arc device is capable of carrying out movements according to the vertical direction to position itself at a height separated from the substrate sufficient to provide an additional layer of material. This distance to the substrate is the one that increases according to the described criteria and the thicknesses of the slices of the 3D numerical model that are taken as a reference each time a new layer is added.

[0072] As additional separation distance (the increment of distance to be moved) taken to separate the wire arc device when a new layer is to be deposited, the thickness of the 3D numerical model is taken as a first reference unless, as a specific example, the computational system receives information of a different distance more appropriate to the layer thickness that is actually generated when the layer is completed. In this case, although the distance taken to separate the wire arc device from the substrate is different from the thickness of the 3D numerical model, the criteria described for maintaining the reference slice or advancing to the next slice remain intact.

[0073] Preferably, the base of the system intended for supporting the generated mold or part of a mold is a metallic substrate, such as stainless steel.

[0074] *Preferably, the wire arc device is a DED-arc wire device.*

[0075] The wire arc device is preferably adapted for depositing a weldable metal cord in wire form, wherein the material may be, for example as: steel, stainless steel, nickel-chromium alloys, nickel-based alloys, titanium alloys and aluminum alloys.

[0076] Preferably, the wire arc device is movable in a plane parallel to the base by means of a robotic arm having a freedom of movement, which is connected to the wire arc device.

[0077] Once the wire arc device has increased the distance from the substrate, a new layer is applied. This layer, according to this example of realization is with movements in a plane parallel to the substrate according to the predetermined path maintaining the distance to the substrate while depositing the same layer.

[0078] In a particular embodiment of the system, the computer system is further adapted to carry out any specific example of method previously disclosed.

[0079] In a third inventive aspect, the invention provides a computer program product comprising instructions which, when the program is executed by a computer system, cause the computer system to carry out the steps 1 to 3 of the method according to the first aspect of the invention and optionally any of the additional disclosed steps of specific embodiments of the method of the first inventive aspect.

[0080] Such a computer program product provides the required software and is adapted to carry out the method of the first aspect of the invention when is executed by the computer system of the second aspect of the invention.

[0081] In a fourth inventive aspect, the invention provides a computer-readable data carrier having stored thereon the computer program of the third inventive aspect.

[0082] Advantageously, this provides a functional system for the reproduction of the sequential steps (path of the device) and/or milestones (any relevant aspect during the manufacturing process), thus achieving the required results without the presence of a user or operator.

[0083] All the features described in this specification (including the claims, description and drawings) and/or all the steps of the described method can be combined in any combination, with the exception of combinations of such mutually exclusive features and/or steps.

DESCRIPTION OF THE DRAWINGS

[0084] These and other characteristics and advantages of the invention will become clearly understood in view of the detailed description of the invention which becomes apparent from a preferred embodiment of the invention, given just as an example and not being limited thereto, with reference to the drawings.

Figure 1 This figure shows a first example of a numerical model, generated by a computer system, representing an object to be manufactured according to the method and system of additive manufacturing of the present invention.

Figure 2 This figure shows a cross-section of the numerical model of Figure 1 by the cutting plane "P".

Figure 3 This figure shows the same view of the numerical model as Figure 2, but also including the partitioning of the numerical model into a plurality of stacked slices.

Figure 4 This figure shows a view of a real situation of the system of the invention, wherein the material is being deposited on a real substrate. It also shows on a dotted line a cross-section of the numerical model being used for manufacturing. In particular, Figure 4 shows a situation in which six different layers have been deposited and the input of the last layer (i.e. the top layer) has not reached the height of the numerical model slide.

Figure 5 This figure shows the same view of the system as Figure 4, but in a different situation wherein five different layers are deposited and the last layer (i.e. the top layer) has exceeded the numerical model slide.

Figure 6 This figure shows a top view of a certain deposited layer.

Figure 7 This figure shows the same top view of Figure 6 of a certain deposited layer, but in another example including three separate openings.

Figure 8 This figure shows a top view of a certain deposited layer of a second example of a manufactured mold manufactured by the method of additive manufacturing of the invention. This second example comprises two lateral through openings and also four oil channels.

Figure 9 This figure shows a perspective view of a third example of a mold which is manufactured by the method and system of additive manufacturing of the invention.

Figure 10 This figure shows a perspective view of a forth example of a counter-mold which is manufactured by the method and system of additive manufacturing of the invention.

Figure 11 This figure shows a view of two graphs corresponding to height measuring process.

DETAILED DESCRIPTION OF THE INVENTION

[0085] As will be appreciated by one skilled in the art, aspects of the present invention may be embodied as a system, method or computer program product.

[0086] Figure 1 depicts an example of a 3d numerical model, generated by a computer system (CS), wherein the 3d numerical model represents a three-dimensional object, namely a mold, to be manufactured according to the additive manufacturing method proposed by the present invention. In this example, the 3d numerical model, which is implemented in the computer system (CS), also includes a flat base (B) on which the three-dimensional numerical model is supported. Alternatively, the numerical model could have only one plane as a base. The flat base (B) extends along a direction (Y-Y') transverse to a longitudinal direction (X-X') along which the mold (M) to be manufactured will be made to grow by adding layers of material.

[0087] In this first example, the 3d numerical model (NM) numerical model (NM) extends along a vertical axis corresponding to the longitudinal direction (X-X') and the gravity direction, which in this case is perpendicular to the direction (Y-Y') of the base (B) and will be horizontal. In this example, the shape of the 3d numerical model (NM) numerical model (NM) is not regular in the longitudinal direction (X-X') and it is regular in the direction (Z-Z'). That is, any cut according to the plane defined by the Y-Y' and X-X' directions are the same when cutting the object, as the one identified as plane "P".

[0088] In order to simplify the representation of the steps of the method of the invention, Figure 2 depicts a cross-section of the 3d numerical model of Figure 1 by cutting plane "P" of Figure 1, so a "simplified" two-dimensional numerical model is represented.

[0089] As shown in Figure 3, the "simplified" 2d numerical model of Figure 2 now includes the partitioning/segmenting of the numerical model into a plurality of stacked slices (sl_0, sl_1, sl_2,... sl s), in particular nine different stacked slices, of a predetermined thickness (e) along a predetermined longitudinal direction (X-X'). The first slice that is placed on the upper surface (B1) of the flat base (B) corresponds to slice 0 (sl_0), and the next slice that is placed on top of the upper surface of slice 0 (sl0) corresponds to slice 1 (sl_1), and so on until the last slice 8 (sl_8) is placed on top of the whole numerical model (NM). In this specific example, all nine stacked slices have the same thickness (e) but they have a different shape and width according to the transverse direction (Y-Y').

[0090] The manufacturing method uses the model as a reference so that starting from a first slice (sl_0) a first layer is deposited on the substrate in order to fill with material a volume as defined by this slice (sl_0).

[0091] The material deposition method is by arc so that once a trajectory is established in the plane parallel to the substrate, a cord of material is deposited. The deposition of material by means of a cord results in a very irregular deposition giving rise to a surface with strong fluctuations in height.

[0092] The method also makes use of height measurements, specific ways of taking a single measurement value over an irregular surface will be disclosed, which allow criteria to be applied to determine whether the volume corresponding to a slide (sl) being filled has been completed or even exceeded.

[0093] Figure 4 depicts a first real situation of the system of the invention (not in the computer system (CS), wherein the base of the object corresponds to the real substrate (S) on which material of the first layer (L_0) is deposited and also serves for supporting the generated mold (M). The computer system (CS) that is in communication with the wire arc device (A) and the sensor (H) is not represented in the figures.

[0094] In this first example of Figure 4, six stacked layers (L_0, L_1, L_2,..., L_5) have been deposited following a growth direction G-G' which is perpendicular to the direction Y-Y' of the substrate (S), so the manufacturing process is at an intermediate stage where more than half of the total of the nine slices are deposited. Furthermore, a cross-section of the numerical model that it is used for guiding the wire arc device (A) is also represented in the same figure 4 over imposed to the body generated by the deposited layers. Continuous and thick lines are those corresponding to the manufactured part of the mold (M) and dashed lines correspond to the over imposed model as a reference.

[0095] In this Figure 4, the tool (T) that is used to apply the layers (L) is also represented. Letter "L" is used for all layers or for any layer since index is not relevant. The same applies to other references with indexes.

[0096] In this case, the direction G-G' in which the mold (M) grows corresponds to the longitudinal direction X-X'. The tool (T) comprises a wire arc device (A) for depositing metal cord according to a predetermined path (PTH) over a surface in a direction perpendicular to the substrate (S). The wire arc device (A) is configured for being movable in a plane parallel to the substrate (S), see arrows indicating that direction, thus forming a metal layer (L) on top of each other. The means for automatically moving the wire arc device (A) are not represented in the figures.

[0097] These means are adapted to move according to a growing direction G-G' to a predetermined distance from the substrate (S) and a height set by the height resulting from the number of slices, and the thickness of each slice, accumulated in the manufacturing process. These means are further adapted to move in a plane parallel to the substrate (S) and according to a specific and predetermined path (PATH). Movements according to the growing direction G-G' are directed to grow one or more new layers (L) trying to fill the thickness of a specific slice (sl). If this aim is not fulfilled for a specified slice (sl) when a new layer is applied then a new layer is added. If the height resulting from a new layer exceeds the height of the accumulated slices (sl) and the next slice (sl) then such next slice (sl) is skipped taking the further next slice (sl) as a reference slice (sl).

[0098] Also the tool (T) comprises a sensor (H) that measures the vertical distance (d) between the wire arc device (A) and the current top layer of the mold (M). In particular, Figure 4 shows a situation in which the input of the current last (top) layer (i.e. the layer 5 (L_5)) has not reached the current height of the numerical model slice 4 (Sl_4), so the slide is not changed and a new layer is reapplied on top of the current top layer.

[0099] Figure 5 depicts the same view of the system as Figure 4 but in a second different method step wherein five different stacked layers (L_0, L_1, L_2,..., L_4) have been deposited. In this case, the current last (top) layer (i.e. the layer 4 (L_4)) has exceeded the current height of the numerical model slice 3 (Sl_3) and, therefore, one slide is skipped and the next slide 4 (Sl_4) is used as a reference. This criteria is more important than the former one since if the added layer (L) is higher than expected there is risk of contact between the wire are device (A) and the generated part of the mold (M) that would result in a welding of the tool and such generated part.

[0100] Both figures 4 and 5 show how the constant thickness (e) of the slices (sl_0 to Sl_8) of the numerical model does not maintain in reality, where the thickness of each deposited layer (L) is different from each other, e.g. the thickness of deposited layer 4 (L4) is substantially higher than the thickness of previous deposited layer 3 (L3).

[0101] The example shown in Figure 6 is a top view of the deposited layer 3 (L_3) having a solid rectangular configuration. It can be seen that the metal cord (MC) that forms the layer 3 (L_3) is deposited by the wire arc device (A) following a predetermined path (PTH) generated in the computer system (CS) and transmitted to the wire arc device (A) for each slice (sl) of the plurality of stacked slices of the model (NM). The path (PTH) of one slice (sl) may be different to the path PTH) of other slice (sl).

[0102] The example shown in Figure 7 is a top view of another deposited layer 3 (L_3), having also a solid rectangular configuration. Unlike Figure 6, the path (PATH) generated in the computer system (CS) and transmitted to the wire arc device (A) when manufacturing layer L_3 of a model (NM) have three separate inner conduits or openings (O) which are crossing the vertical direction. Said inner conduits or openings (O) are provided for reducing the quantity of metal of the mold, so the total weight of the mold. The path (PATH) comprises the following different regions or portions:

- a first portion of path (PTH_1) that corresponds to the rectangular perimeter of the layer L_3 determined by the perimeter of the reference slice (sl) of the model (NM) used at that stage of the manufacturing process, in particular the shape of the slice (sl) cut at the height with an horizontal plane located at the height of the layer (L);
- a second portion of path (PTH_2) that corresponds to the three inner perimeters of openings (O) sectioned by the same plane; and
- a third portion of path ($PATH_3$) that corresponds to the inner area of the same section.

[0103] Figure 8 depicts a top view of a second example of an intermediate layer of a mold (M) which has been manufactured by the method and system of additive manufacturing of an example of the invention. This second

example has a solid shape with two lateral through rectangular openings (O) and also four through oil channels (OC) for cooling the mold located at an intermediate position.

[0104] The black contour line outlines represent the paths (PATH) generated in the computer system (CS) for this specific layer (L_i). In this case, the path (PATH) generated in the computer system (CS) for this layer (L_i) comprises the following different regions or portions:

- a first portion of path (PTH_1) that corresponds to the perimeter of the layer (L);
- a second portion of path (PTH_2) that corresponds to one or more inner perimeters of inner openings (O) sectioned by the layer (L);
- a third portion of path ($PATH_3$) that corresponds to the inner area of the layer (L); and
- a forth portion of path ($PATH_4$) that corresponds to the inner perimeters of one or more inner oil channels (OC) sectioned by the layer (L_i).

[0105] The metal cord (MC) that forms the stacked layers of the mold is represented in this Figure 8 by an area with intersecting lines forming triangles. Once the mold (M) has been manufactured layer by layer, it can be subsequently machined at the outer surfaces to finally obtain the final mold.

[0106] The mold (M) and counter-mold (CM) of Figures 9 and 10 are configured for being used together, wherein the surfaces entering into contact are machined obtaining a high quality surface while the where the mold manufacturing process has required up to 25% - 45% less metal cost than a traditional casting process and a thermal inertia reduction of 38% for the core plate (the mold) and a 40% of thermal inertia reduction for the cavity plate (the counter mold).

[0107] Figure 9 depicts a perspective view of a third example of a mold (M) which has been manufactured by the method and system of additive manufacturing of the invention. This third example of a mold (M) comprises a protruding central portion (PP), three through openings (O) and also a plurality of oil channels (OC). The central portion (PP) has a lateral part that is curved and another lateral part that is rectilinear. Some oil channels (OC) of the plurality of oil channels (OC) are located in the interior of the central portion (PP) and (OC) cannot be drilled since they follow the curvature of the protruded central portion (PP).

[0108] Figure 10 depicts a perspective view of a forth example of a counter-mold (CM) which has been manufactured by the method and system of additive manufacturing of the invention. This forth example of a mold (M) comprises a recessed central portion (RP), four through openings (O) and also a plurality of oil channels (OC). The oil channels (OC) of the plurality of oil channels (OC) that are located in the peripheral area of the recessed central portion (RP) follow the curvature of said recessed central portion (RP).

[0109] Figure 11 depicts a view of two graphs corresponding to height measuring process performed by the method and system of the present invention. In particular, it shows at the top a graph of measurements captured by the height sensor (H) of the system along a given length of one of the wire arc device (A). The number of measurements retrieved from this sensor (H) is very high per unit length, so a narrow portion of the graph is plotted at the bottom of the figure, expanded to show more clearly the measurements and further signals generated from this first signal.

[0110] The black color in the two graphs shows a highly fluctuating signal (S_1) that corresponds to the height data directly obtained by the sensor (H).

[0111] The two graphs shown in gray is the value signal (S_2) of a filtered signal where the measurements directly obtained by the sensor (H) has had spurious values and, also values that are not maintained over time for a predetermined time interval are removed. The result is a more stable generated surface height tracking value.

[0112] Finally, a third signal (S_3) is shown in a lighter gray in the two graphs, almost white in the upper graph, which are constructed as the maximum values of the previous signal at predetermined length intervals thus identifying the height values to be taken as a reference to prevent the tool (T) from entering into contact with the mold (M), avoiding the welding of the tool (T) with the mold (M).

Claims

1. Method of additive manufacturing for manufacturing molds or part of molds, by means of:

   - a substrate (S) intended for supporting the generated mold (M, CM) or part of said mold;
   - a wire arc device (A) adapted for depositing metal cord (MC) according to a predetermined path (PTH) over a surface in a direction perpendicular to the substrate (S) and adapted to be movable in a plane parallel to the substrate (S) forming a metal layer (L) on top of each other;
   - a sensor (H) adapted to measure a distance (d) between the wire arc device (A) and a surface in a perpendicular direction to the substrate (S); and
   - a computer system (CS) in communication with the wire arc device (A) and the sensor (H);

   the method comprising the steps:

   1. generating by the computer system (CS) a 3D numerical model (NM) of a mold (M) or part of said mold (M);
   2. segmenting by the computer system (CS) the 3D numerical model (NM) into a plurality of stacked slices (sl_i, $i = 0,1, ...$) of a predetermined

thickness (e) according to a predetermined direction (X-X');
3. iteratively, departing from the first slice (sl_0) until the last slice (sl_N) of the 3D numerical model (NM), carrying out on each of the slices (sl_i) by the computer system (CS), according to a sequential order, the following sub-steps:

a) selecting the slice (sl_i) of the 3D numerical model (NM) to be used for determining the path (PTH) of the wire arc device (A) to form a determined metal layer (L_j);
b) determining by the computer system (CS), for the determined slice (sl_i), a path (PTH) intended to represent a trajectory of a metal cord (MC) to be deposited in respect to the slice (sl_i); and
c) commanding the wire arc device (A) by the computer system (CS) to form a determined metal layer (L_j) by depositing a metal cord (MC) on top of the previously formed metal layer (L_{j-1}), or on the substrate (S) if it is the first metal layer (L_0), following a trajectory according to the path (PTH) generated by the computer system (CS) for the slice (sl_i) to be used;

- wherein in step 3 the computer system (CS) further carries out a further action of checking for the selected slice (sl_i) the formed metal layers (L) in comparison to the slices (sl) of the 3D numerical model (NM), comprising the following sub-steps:

before step c is executed, receiving from the sensor (H) at least one measurement value of the distance (d) and determining a representative value of the height of the formed metal layers (L);
if the representative value is higher than the summation of the thicknesses € of the previous slices (sl_l, l = 0,1, ..., i - 1) of the 3D numerical model plus the thickness € of the selected slice (sl_i) to be used then at least c) of the currently checked slice is not executed and the computer system (CS) selects the next slice (sl_{i+1}).

2. A method according to claim 1, wherein after receiving from the sensor (H) the measurement of the distance (d) and determining a representative value of the height of the formed metal layers (L), the method further comprises the step:

- before step a), receiving from the sensor (H) a measurement of the distance (d) and determining a representative value of the height of the formed metal layers (L) and, if the representative value of the height is lower than the summation of the thicknesses € of the previously used slices (sl_l, l = 0,1, ..., i - 1) then steps b) and c) are executed.

3. A method according to any of the preceding claims, wherein the path (PATH), determined by the computer system (CS), generated for at least one slice (sl) of the plurality of stacked slices comprises:

- a first portion of path (PTH_1) that corresponds to the perimeter of the slice (sl);
- a second portion of path (PTH_2) that corresponds to inner perimeter/s of one or more inner conduits, openings or cavities (O) sectioned by the slice (sl); and
- a third portion of path ($PATH_3$) that corresponds to the inner area of the slice (sl).

4. A method according to the preceding claims wherein the path (PATH), determined by the computer system (CS), generated for at least one slice (sl) of the plurality of stacked slices further comprises:

- a forth portion of path ($PATH_4$) that corresponds to inner perimeter/s of one or more inner cooling ducts or channels (OC) sectioned by the slice (sl).

5. A method according to the preceding claim, wherein two sensor measurements are taken:

- a first measurement at a location corresponding to the inner area of the slice determining a representative value of the height at said location and,
- a second measurement at a location corresponding to a perimeter of the second portion or the third portion or both portions determining a representative value of the height at said location;

wherein the step c) is executed over the second portion, the third portion or both portions if the absolute value of the difference between the representative value of the height of the first measurement and the representative value of the height of the second measurement is higher than a predetermined threshold.

6. A method according to the preceding claim, wherein the generated third portion of path ($PATH_3$) incorporates a tolerance for avoiding the section reduction or closing of any inner conduits or openings (O) with metal cord (MC).

7. A method according to any of the preceding claims, wherein the metal cord (MC) is deposited in a direc-

tion of growth (G-G') transversal to the predetermined direction of the path (PATH), preferably in a direction perpendicular to the substrate (S).

8. A method according to any of the preceding claims, wherein determining the representative value of the height from a sensor measurement is being processed by the computer system (CS) by:

- removing measurement spurious values; or
- removing measurements that are not maintained during a predetermined period of time; or
- removing both, measurement spurious values and measurements that are not maintained during a predetermined period of time.

9. A method according to the previous claim, wherein the sensor measurement is being further processed by the computer system (CS) by selecting the higher value of the sensor measurements in an entire metal layer ensuring that the wire arc device (A) does not touch the generated mold (M) or part of said mold (M).

10. A method according to any of the preceding claims, further comprising the step of machining the external surface of the generated mold (M) or part of said mold (M), wherein the machining is preferably milling.

11. A method according to any of the preceding claims, further comprising the step of polishing the external surface of the generated mold (M) or part of said mold (M).

12. An additive manufacturing system for manufacturing molds (M), the system comprising:

- a substrate (S) intended for supporting the generated mold (M) or part of said mold (M);
- a wire arc device (A) adapted for depositing metal cord (MC) according to a predetermined path (PATH) over a surface in a direction perpendicular to the substrate (S) and adapted to be movable in a plane parallel to the substrate (S) forming a metal layer (L) on top of each other;
- a sensor (H) adapted to measure the distance (d) between the wire arc device (A) and a surface in a perpendicular direction to the substrate (S); and
- a computer system (CS) in communication with the wire arc device (A) and the sensor (H);

wherein the computer system (CS) is adapted to carry out the steps 1 to 3 of the method of claim 1.

13. A system according to claim 12, wherein the wire arc device (A) is a DED-arc wire device.

14. A system according to claim 12 or 13, wherein the computer system (CS) is further adapted to carry out the method according to any of claims 2 to 9.

15. A computer program product comprising instructions which, when the program is executed by a computer system (CS), cause the computer system (CS) to carry out the steps 1 to 3 of the method of claim 1 and/or any of the steps of claims 2 to 9.

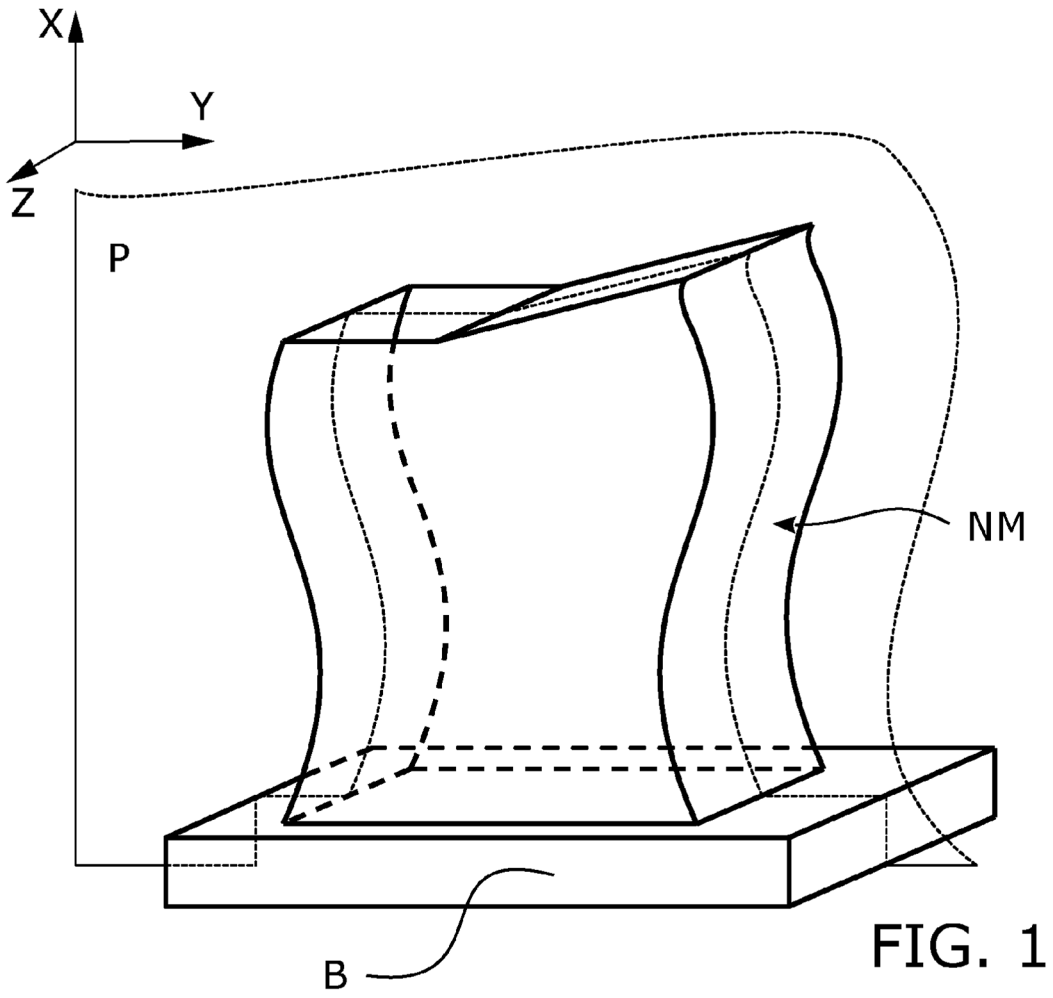

FIG. 1

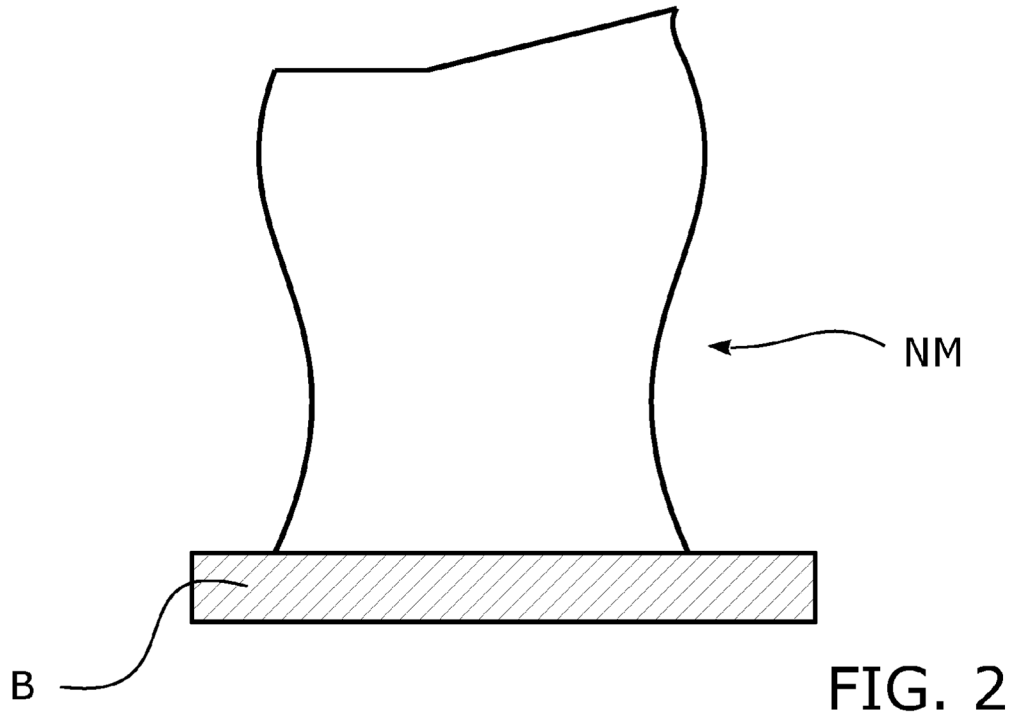

FIG. 2

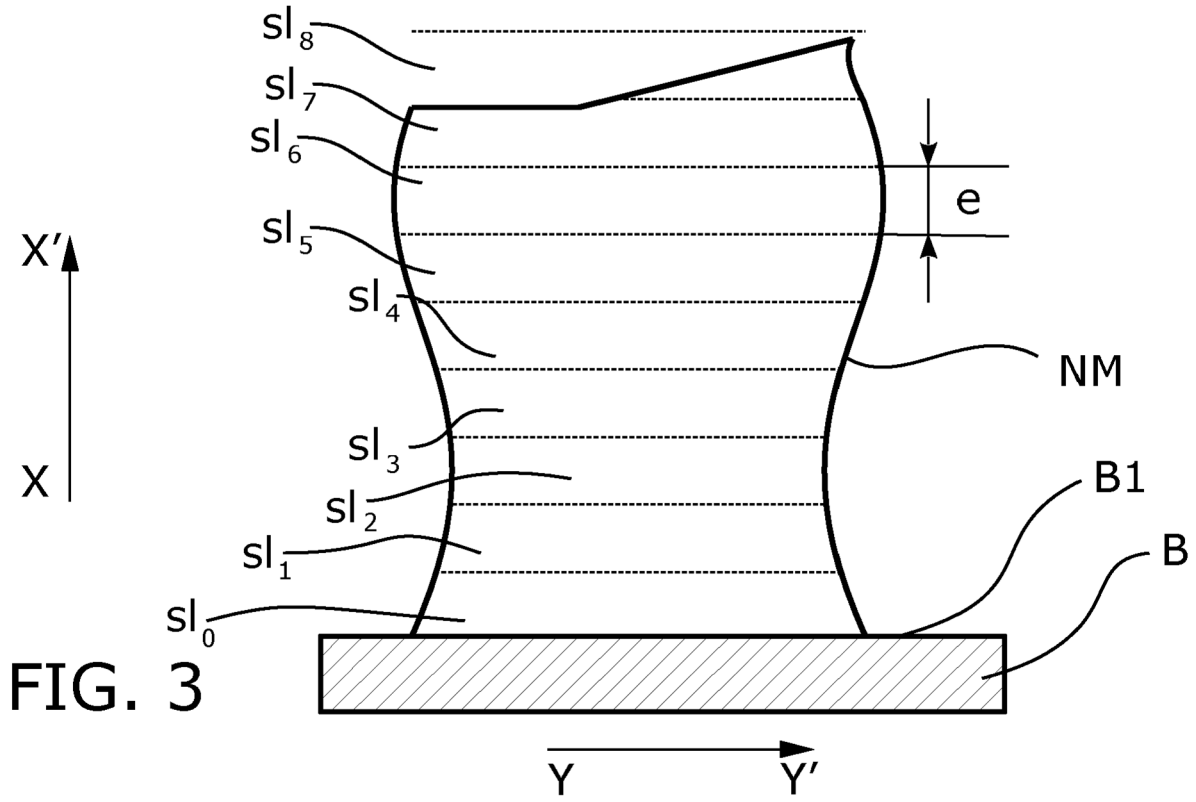
sl8
sl7
sl6
sl5
sl4
sl3
sl2
sl1
sl0
e
X'
X
NM
B1
B
Y
Y'

FIG. 3

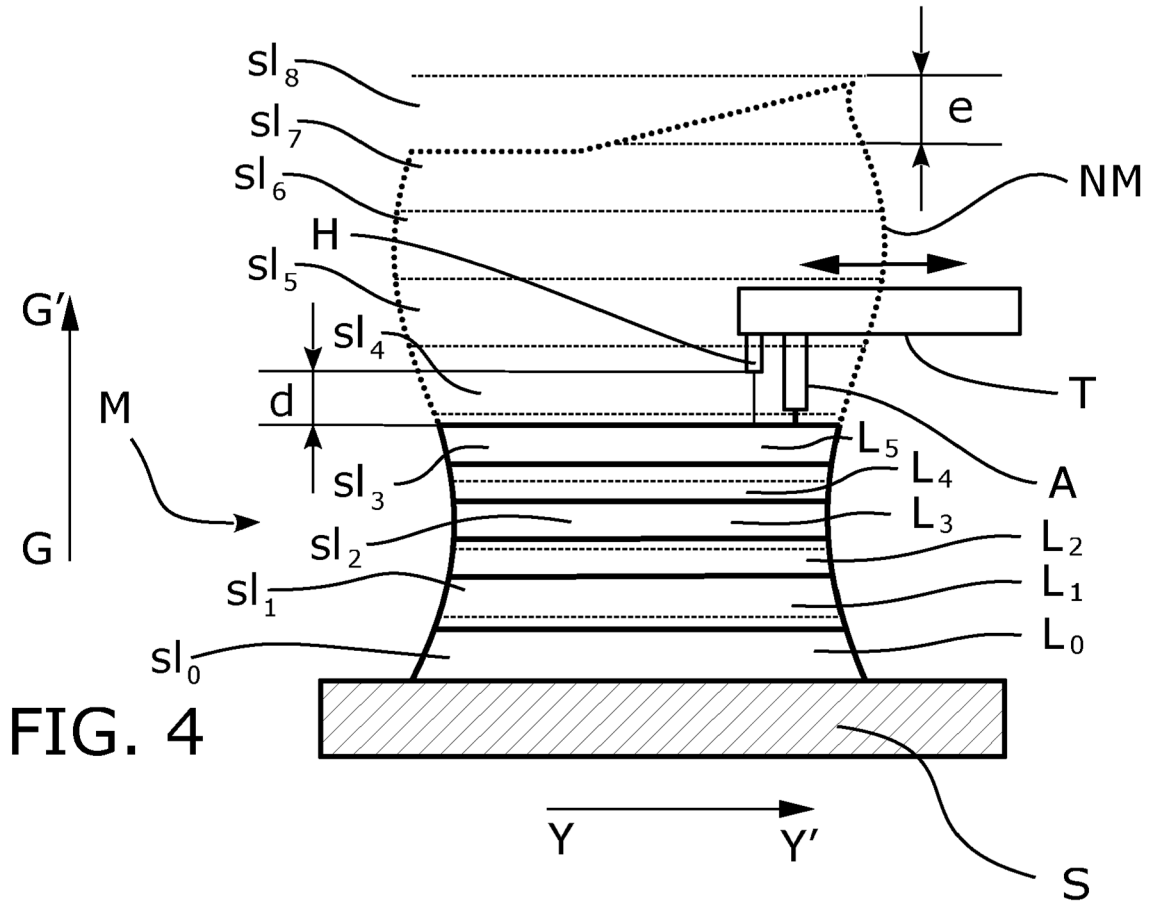
sl8
sl7
sl6
H
sl5
sl4
d
sl3
sl2
sl1
sl0
e
NM
G'
G
M
T
A
L5
L4
L3
L2
L1
L0
Y
Y'
S

FIG. 4

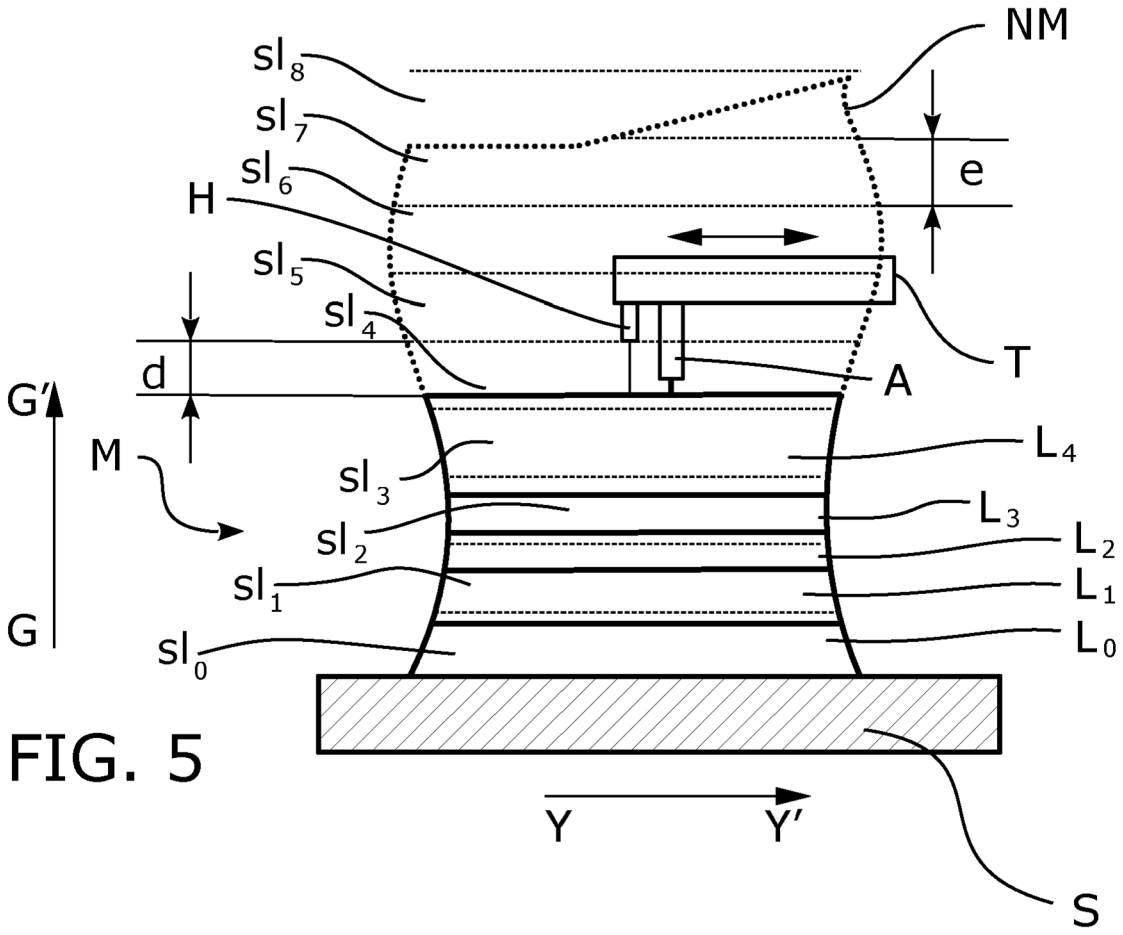
NM
sl8
sl7
sl6
H
sl5
sl4
e
T
d
A
G'
M
L4
sl3
L3
sl2
L2
sl1
L1
G
sl0
L0
Y
Y'
S

FIG. 5

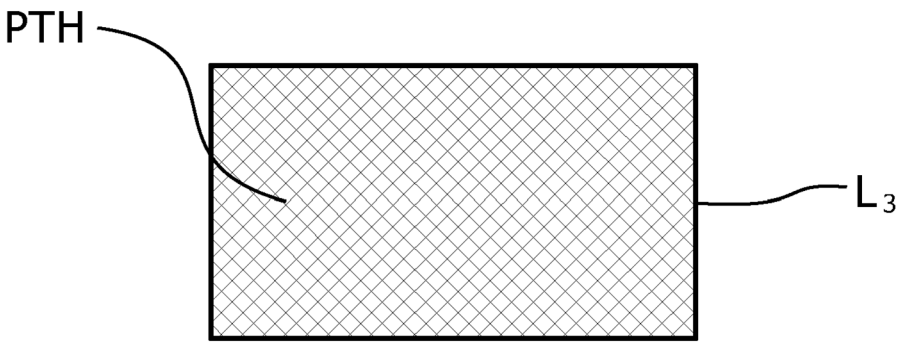
PTH
L3

FIG. 6

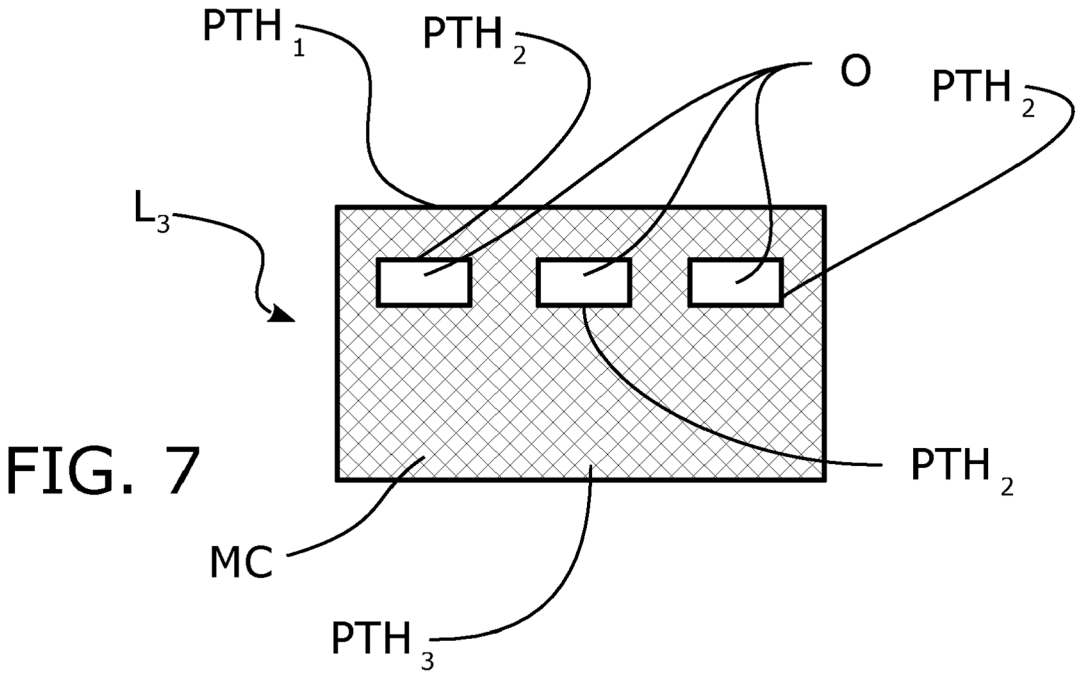

FIG. 7

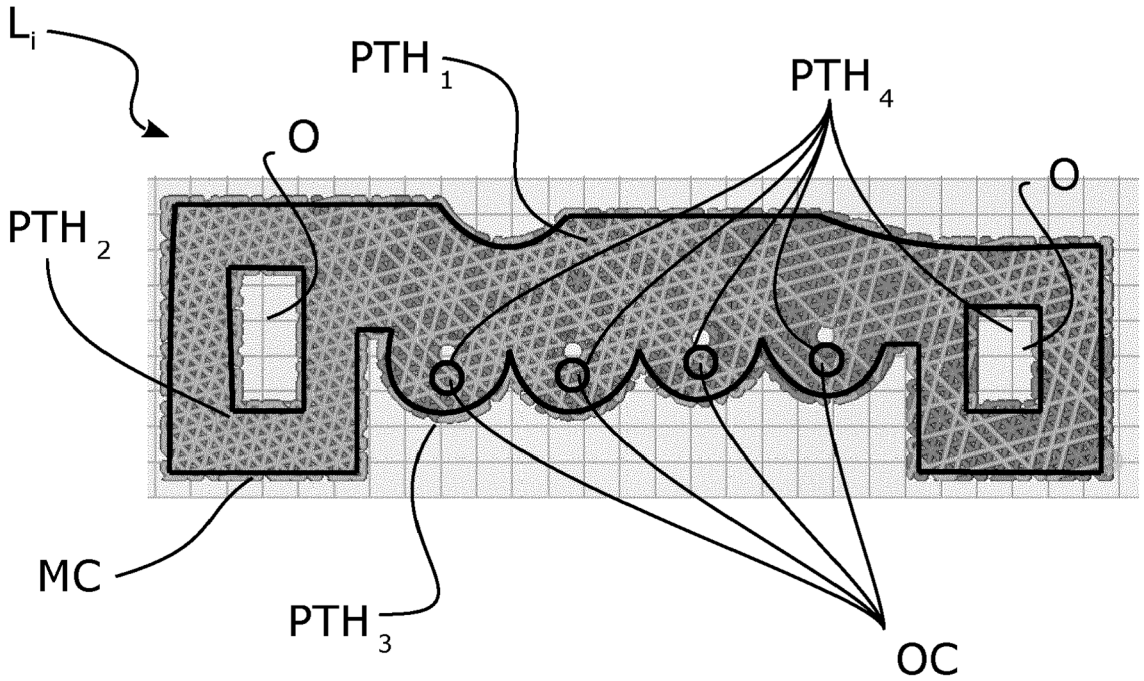

FIG. 8

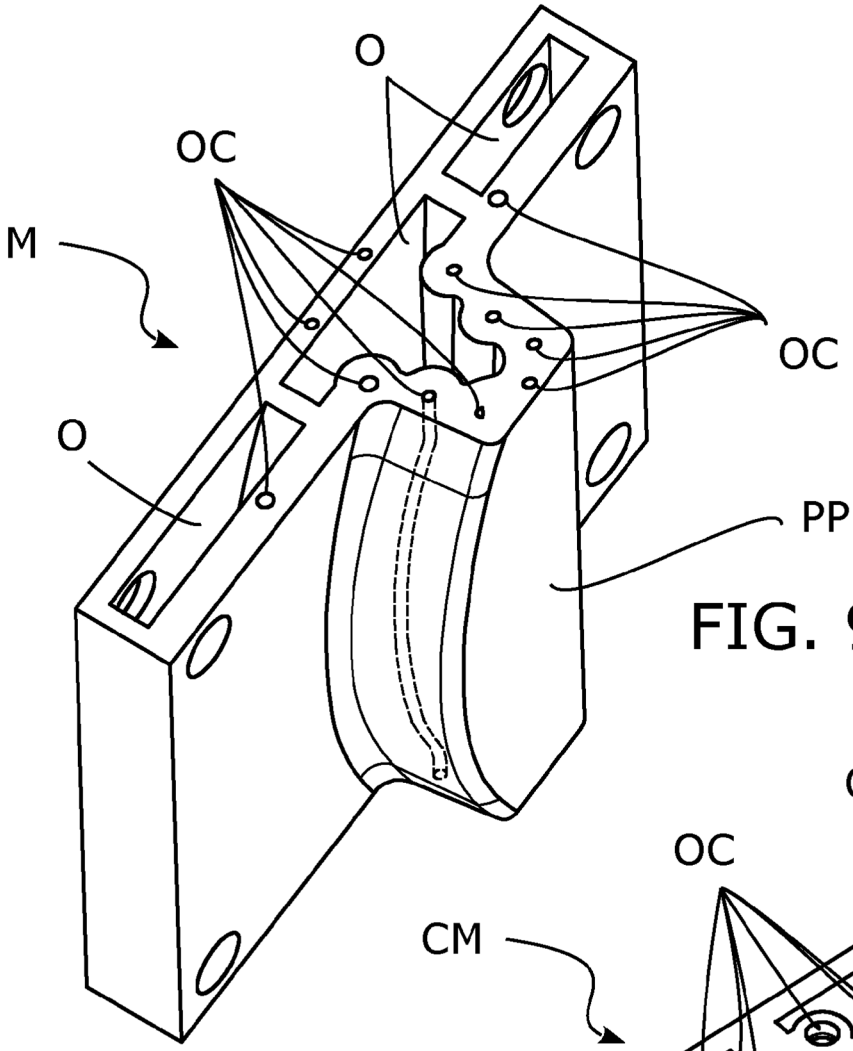

FIG. 9

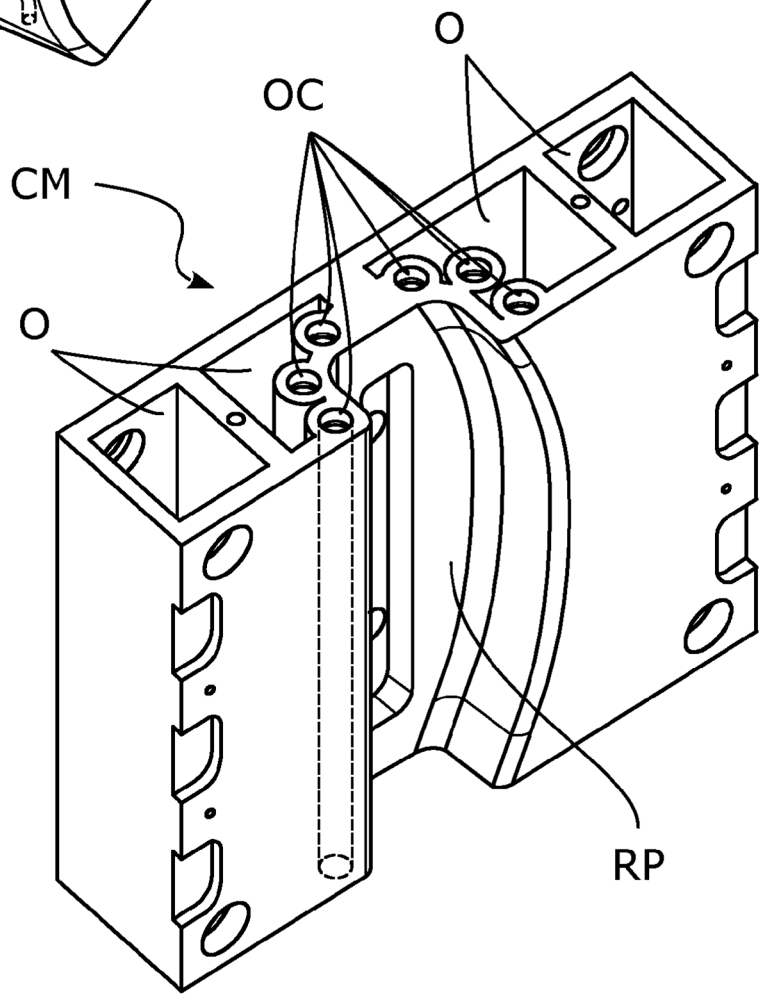

FIG. 10

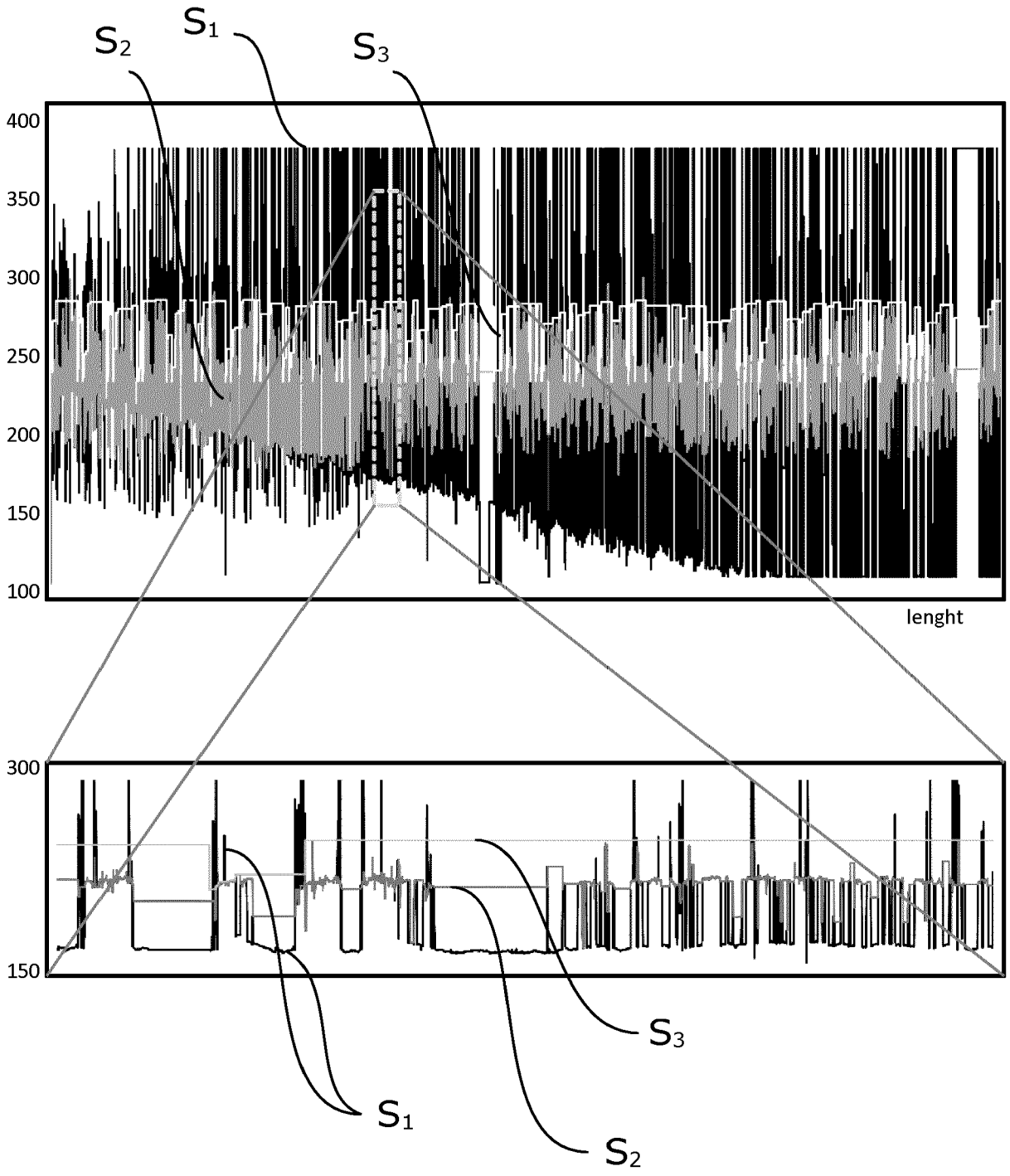

FIG. 11

Europäisches Patentamt
European Patent Office
Office européen des brevets

EUROPEAN SEARCH REPORT

Application Number
EP 23 38 2012

DOCUMENTS CONSIDERED TO BE RELEVANT

Category	Citation of document with indication, where appropriate, of relevant passages	Relevant to claim	CLASSIFICATION OF THE APPLICATION (IPC)
A	WO 2021/054894 A1 (UNIV SINGAPORE TECHNOLOGY & DESIGN [SG]) 25 March 2021 (2021-03-25) * paragraphs [0013], [0063], [0108] * * figure 3 * -----	1-15	INV. B23K9/04 B23K9/095 B33Y10/00 B33Y50/02 B33Y80/00
A	SCETINEC ALJAZ ET AL: "In-process path replanning and online layer height control through deposition arc current for gas metal arc based additive manufacturing", JOURNAL OF MANUFACTURING PROCESSES, SOCIETY OF MANUFACTURING ENGINEERS, DEARBORN, MI, US, vol. 64, 5 March 2021 (2021-03-05), pages 1169-1179, XP086543739, ISSN: 1526-6125, DOI: 10.1016/J.JMAPRO.2021.02.038 [retrieved on 2021-03-05] * sections 1, 3 and 4.4 * -----	1-15	
A	EP 3 597 342 A1 (KOBE STEEL LTD [JP]) 22 January 2020 (2020-01-22) * figures 2,3 * -----	1-15	TECHNICAL FIELDS SEARCHED (IPC) B23K B22F B33Y

The present search report has been drawn up for all claims

Place of search	Date of completion of the search	Examiner
The Hague	14 June 2023	Järvi, Tommi

CATEGORY OF CITED DOCUMENTS

X : particularly relevant if taken alone
Y : particularly relevant if combined with another document of the same category
A : technological background
O : non-written disclosure
P : intermediate document

T : theory or principle underlying the invention
E : earlier patent document, but published on, or after the filing date
D : document cited in the application
L : document cited for other reasons

& : member of the same patent family, corresponding document

EPO FORM 1503 03.82 (P04C01)

ANNEX TO THE EUROPEAN SEARCH REPORT ON EUROPEAN PATENT APPLICATION NO. EP 23 38 2012

This annex lists the patent family members relating to the patent documents cited in the above-mentioned European search report. The members are as contained in the European Patent Office EDP file on
The European Patent Office is in no way liable for these particulars which are merely given for the purpose of information.

14-06-2023

Patent document cited in search report	Publication date	Patent family member(s)	Publication date
WO 2021054894 A1	25-03-2021	NONE	
EP 3597342 A1	22-01-2020	CN 110430959 A	08-11-2019
		EP 3597342 A1	22-01-2020
		JP 6751040 B2	02-09-2020
		JP 2018149570 A	27-09-2018
		US 2019381595 A1	19-12-2019
		WO 2018168881 A1	20-09-2018

EPO FORM P0459

For more details about this annex : see Official Journal of the European Patent Office, No. 12/82

Anexo C: Patente EP4400292A1

Título

Un sistema y un método de fabricación de piezas moldeadas

Aplicantes

FUNDACIÓN AITIIP

Inventores

MARQUÉS PAOLA, Alejandro; LAGUÍA PÉREZ, Alberto; MONZÓN CATALÁN, Iván; GONZALVO BAS, Berta; DIESTE MARCIAL, José Antonio; GRACIA ARANEGA, Pascual

Prioridades y aplicación

EP23382013A·2023-01-11

Publicación y fecha

EP4400292A1·2024-07-17

(19) Europäisches Patentamt
European Patent Office
Office européen des brevets

(11) EP 4 400 292 A1

(12) EUROPEAN PATENT APPLICATION

(43) Date of publication:
17.07.2024 Bulletin 2024/29

(21) Application number: **23382013.3**

(22) Date of filing: **11.01.2023**

(51) International Patent Classification (IPC):
B29C 70/46 *(2006.01)* ***B29C 70/56*** *(2006.01)*
B29B 13/02 *(2006.01)* ***B29C 51/08*** *(2006.01)*
B29C 51/26 *(2006.01)* ***B29C 51/42*** *(2006.01)*

(52) Cooperative Patent Classification (CPC):
B29C 70/46; B29B 13/023; B29C 51/082; B29C 51/261; B29C 51/262; B29C 51/421; B29C 51/425; B29C 70/56; B29C 51/428; B29K 2105/06; B29K 2105/0863

(84) Designated Contracting States:
AL AT BE BG CH CY CZ DE DK EE ES FI FR GB GR HR HU IE IS IT LI LT LU LV MC ME MK MT NL NO PL PT RO RS SE SI SK SM TR
Designated Extension States:
BA
Designated Validation States:
KH MA MD TN

(71) Applicant: **Fundación AITIIP**
50720 Zaragoza (ES)

(72) Inventors:
- **MARQUÉS PAOLA, Alejandro**
  50720 Zaragoza (ES)
- **LAGUÍA PÉREZ, Alberto**
  50720 Zaragoza (ES)
- **MONZÓN CATALÁN, Iván**
  50720 Zaragoza (ES)
- **GONZALVO BAS, Berta**
  50720 Zaragoza (ES)
- **DIESTE MARCIAL, José Antonio**
  50720 Zaragoza (ES)
- **GRACIA ARANEGA, Pascual**
  50720 Zaragoza (ES)

(74) Representative: **ABG Intellectual Property Law, S.L.**
Avenida de Burgos, 16D
Edificio Euromor
28036 Madrid (ES)

(54) A SYSTEM AND A METHOD FOR MANUFACTURING MOLDED PIECES

(57) The present invention is related to a system and method for manufacturing molded pieces in a molding machine, preferably departing from composite plates formed from layers, e.g. carbon fiber layers, through pressing, with a pre-heating step heating the composite plate. According to a preferred embodiment, in order to reduce thermal inertia and optimize the circuits, the molds are heated using thermal fluid flowing through internal ducts with an optimized path, through molds printed using additive manufacturing techniques. In a preferred embodiment, the plate is preheated by means of a heating system with mobile lamps.

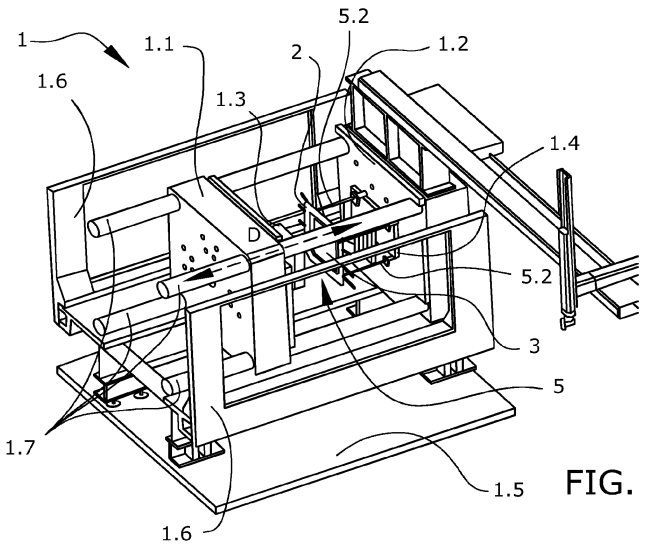

FIG. 1

EP 4 400 292 A1

Description

FIELD OF THE INVENTION

[0001] The present invention is related to a system and method for manufacturing molded pieces in a molding machine, preferably departing from composite plates formed from layers, e.g. carbon fiber layers, through pressing, with a pre-heating step heating the composite plate.

[0002] According to a preferred embodiment, in order to reduce thermal inertia and optimize the circuits, the molds are heated using thermal fluid flowing through internal ducts with an optimized path, through molds printed using additive manufacturing techniques.

[0003] In a preferred embodiment, the plate is preheated by means of a heating system with mobile lamps.

PRIOR ART

[0004] Pressing processes are performed by a mold and a counter mold installed in a molding machine.

[0005] Composite plates are known as SMCs (Sheet Molding Compounds), wherein such composite plates are produced ensuring complete integration of fibers and resin.

[0006] According to the prior art, the molding process includes a model of manufacturing which also encompasses different methodologies that seek greater efficiency in the forming of parts.

[0007] In the manufacturing process, from a general point of view, some amount of energy is applied to raw material in order to make it melt, or at least be able to flow by adapting the material to the shapes imposed by a mold.

[0008] Known processes involves the use of injection devices allowing to introduce in a forced way the material with flowing capacity inside a cavity formed inside the mold, so that the material adapts to the shape of the cavity resulting in the preset shape of the part to be manufactured. The raw material is configured according to the desired final shape, and possibly, some fraction of waste has to be removed at a later stage to provide the final product. Some of the main objectives are to optimize the variables of quality, cost and productivity.

[0009] Within the existing categorization of processes, molding is part of the mechanical processes very well known for instance in metal working, being one of the most basic operations of manufacturing by forming. In most cases the molding processes with casting involves: pouring on the mold, solidification and cooling. This method is a very versatile but complex method, since it requires taking into account numerous parameters that affect the effectiveness and quality of the process, such as the melting temperature, the pouring techniques, which at high temperatures involve the generation of trapped gases, the generation of defects, pores or cracks in the solidification process, or the difficulty in the final separation of the part from the mold. Within the casting molding processes, there are currently sand molding, shell molding, lost wax molding or gravity molding.

[0010] However, the process disclosed according to embodiments of the present invention relies on plastic deformation processes, so that it does not require the casting process of the part to be molded.

[0011] On the contrary, in metal working, deformation is possible because external forces are applied to raw material, thus causing a tensional state in the crystalline inner structure of the metal material, which, if certain values are exceeded, causes the desired permanent deformations.

[0012] Intuitively, one may come to think that casting the material is the most efficient method, achieving complicated shapes of very precise forms without the need for any machining process; or at least minimizes the subsequent machining process.

[0013] Casting has, therefore, always been a preferred option, since it allows the molding of parts very efficiently while requiring much less energy than cold, the ductility and hardening of the parts do not limit the amount of deformation of the material on the part, and its properties are mainly isotropic.

[0014] When manufacturing plastic pieces, molding processes are based on injection molds wherein the melted material shows complex fluid properties since melted plastic is a non-Newtonian fluid (without a defined and constant viscosity value) and the techniques that are valid for metals cannot be extrapolated to the model of plastic parts.

[0015] Some other known forming methods are based on cold forming, such as metal stamping techniques. Such methods involve strengthening of the area upon impact, a great deal of savings in furnace and fuel costs, and the most significant advantage is that it involves such a low amount of heating and cooling time, that for the specific case of working with large workpieces means a significantly increase in productivity.

[0016] There are also known techniques for the manufacture of parts formed by stacking layers of resin-bonded fibers. The set of layers, for example of carbon fiber, Kevlar, glass, are positioned in a mold and forced in cold to adopt the final shape.

[0017] On each of the layers, the resin is added cold, which helps the layer to adopt the shape of the mold until the total number of layers is completed. At this point, the counter-mold is superimposed, which presses the whole assembly. In many cases the set of layers with the resin that leaves the fibers embedded is inside a bag that is subjected to vacuum.

[0018] Subsequently, the set is taken to an autoclave that causes the curing and hardening process of the piece. The final part also requires additional operations such as the removal of the back mold and the bag and, finally, the extraction of the part from the mold.

[0019] This process has many drawbacks, the main one being the difficulty of automation. In most cases the

layers of fiber are applied by hand so that the worker ensures that the layer is properly adapted to the shape imposed by the mold and only when he observes that he has achieved this adaptation is when he adds resin and incorporates the next layer.

[0020] The other problem with this method is the lack of dimensional control, especially with respect to the thickness of the part.

[0021] The automation of this process and ensuring that the final dimensions are adequate is easier when the part manufactured by this procedure is a flat plate of constant thickness.

[0022] If we refer directly to the cold compression molding methodology, since it does not require such high temperatures as casting molding, it is one of the oldest plastic deformation processes in existence, being described for the first time at the beginning of the 19th century. In this process, after a previous heating at moderate temperatures, the part in its original shape is placed on the open mold. After locating the part in the mold, the mold is closed by applying force until all areas of the part come into contact with the mold. The molds used for this process are generally simpler than those used for casting and injection molding, since they do not require mold chutes or feeding systems, but they do require accessories to heat the mold.

[0023] In terms of materials, molding is also very often used for thermosets. Unsaturated polyester resins, obtained from PET, are usually used. This resin is cross-linked to form a thermosetting material, together with some kind of stress. Curing process may involve the use of heat after the material is inside of the mold. However, the method is applicable to a wide variety of thermoformable materials, such as rigid polymers or semi-finished thermoplastics. Probably the material belonging to the state of the art that is closest to the materials to be working with is the SMC (Sheet Molding Compound), which consists of laminar elements structured in deformable layers and with heat application within a specific temperature range, which, after molding, still maintains their laminar structure. They are produced by deposition of fibers projected by a cutter on a strip, which then serves as a support and on which a constant thickness of resin is already present. A recently developed variant that would also be of interest consists in the LSMC (Low Pressure Molding Compound) materials, which maintain a molding temperature with a much reduced viscosity compared to classic SMCs, allowing eight times lower molding stresses and stress addition.

[0024] Within this context, presses are normally employed to exert sufficient force on both molds, mold and counter mold. Commonly, the process is carried out with a vertical molding path, as this allows the use of gravity to mold the part by exerting both, the necessary pressure on the plate. Therefore, there is no guidance at any time in the trajectory of the plate, nor the possibility of heating both sides of it, since it is always supported by the counter-mold. And although there may be certain clamps that hold the edges of the plate, they do not follow the motion, nor do they have any type of elastic characteristic that adapts to the movement. Clamps are intended for ensuring rigidity of the edges and gravity ensures that the plate remains supported on the bottom mold.

[0025] Finally, this process is composed of two different stages: the upward stroke by the lower mold, although in some systems it remains fixed, and the downward stroke by the upper counter mold. Generally, the system is made up of a hydraulic cylinder that exerts the necessary force to carry out the molding, and commonly consists of a male and a female plunger mold, with grooved pins that ensure the perfect fitting of both parts.

[0026] There is also a need in the art for a system and method for manufacturing molded pieces in a molding machine with the aforementioned needs.

DESCRIPTION OF THE INVENTION

[0027] The present invention provides a solution for the above mentioned issues by a system for manufacturing molded pieces according to independent claim 1 and a method for manufacturing molded pieces by means of the system according to claim 20. In dependent claims, preferred embodiments of the invention are defined.

[0028] *In a first inventive aspect, the present invention provides a system for manufacturing molded pieces, comprising at least the following elements:*

- *a molding machine, comprising two supports for supporting two mold pieces, a first support adapted to receive a mold and a second support adapted to receive a counter mold, the molding machine adapted to adopt at least a first open position wherein the mold and the counter mold are spaced apart and a closed position wherein one mold piece from the mold or the counter mold exerts force against the other mold piece and, wherein the movement of one mold piece from the mold or the counter mold in respect to the other mold piece is according to a displacement direction,*
- *a frame configured for supporting a thermo-formable plate,*
- *guiding means adapted to guide the frame according to the displacement direction,*
- *heating means configured for heating the thermo-formable plate,*
- *actuating means adapted to move the heating means of least between two positions, a first position close to the thermo-formable plate for heating the same and, a second position distant from the frame and the mold pieces for allowing the mold movement.*

[0029] The present system solves all the drawbacks identified above by departing from a first piece in the form of a thermo-formable plate, for example a composite plate formed by layers of fibers embedded in a thermo-formable material.

[0030] The present invention further comprises guiding means that allow the thermo-formable plate to be positioned in any of the intermediate positions between the mold and the counter mold since guiding means are adapted to guide the frame according to the displacement direction, even when the movement of the latter is horizontal.

[0031] The present invention also comprises heating means for heating the thermo-formable plate and permit its molding even in conditions where the material, on its own, would no longer be able to maintain its stable shape before being shaped.

[0032] The term "molding machine", as used in this context, shall be interpreted as a machine comprising actuation means for applying a force by means of elements intended to move the two supports at least in an open position and in a closed position. The force is applied to the part to be molded. In this particular case, the molding machine comprises two supports for supporting at least two molding parts, a first support adapted to receive a mold and, a second support adapted to receive a counter-mold.

[0033] When the molding machine moves a support, the mold part attached to said support also moves. According to the prior art, the support usually shows a fixing area allowing at least to fix the mold piece but, the area can be larger allowing to fix additional elements.

[0034] Also according to the prior art, the actuating means of the molding machine acts on one support while the other support is immovable.

[0035] The movement of one support with its mold part relative to the other support, with the other mold part, establishes the displacement direction. The most common displacement direction is longitudinal, either vertical or horizontal.

[0036] The molding machines that make use of a vertical displacement show a fixed support, preferably the lower one, and a movable support, preferably the upper one, because the action of gravity acting on the movable elements favors the downward force against the lower fixed support, and therefore against the mold piece also arranged lower.

[0037] According to the prior art, molding machines with a vertical displacement direction are preferred for the molding of plates formed by layers. The same is true for plates that include perimeter reinforcement to increase stiffness. With this machine configuration the plate rests supported on the bottom mold piece by the action of gravity and does not need to be fixed.

[0038] In these circumstances, when the upper mold is lowered, as soon as it contacts the plate, the latter is trapped between the mold and the counter-mold, so that the friction forces determine its subsequent position as well as the way its deformation progresses.

[0039] That is, control over the position and deformation of the plate is lost and finally by trial and error the best molding conditions are determined.

[0040] Advantageously, the presence of the frame in the first aspect of the invention configured to support the thermo-formable plate to be molded and the guiding means adapted to guide the frame according to the displacement direction allows the guiding of the position of the thermo-formable plate when fixed to the frame, without the need for the operator to come into direct contact with the plate, or, according to an embodiment, even facilitating it's tensioning thus avoiding its wrinkling as a result of the molding forces acting on the plate.

[0041] The element or elements responsible for the trajectory executed by the thermo-formable plate frame are the guiding means, those being responsible for the trajectory and also centering of the frame that holds the thermo-formable plate, so that it can perform its function without getting in the way in the second position of the molding machine. According to a possible embodiment, said frame has a shape and a size such that, when the molding machine in in the second position, the frame extends perimetrically outside the mold parts.

[0042] Since the guiding means are adapted to guide the thermo-formable plate frame according to the displacement direction, any force exerted by any of the pieces of the mold, the counter-mold or both on the plate will impose a displacement of the plate which will always be limited to the direction of displacement. This ensures its correct position but does not prevent the plate from adapting its position as the deformation imposed by the mold and the counter-mold progresses as the closing position is reached.

[0043] The guiding means also makes possible to carry out an optimal heating of the thermo-formable plate just before the molding process is executed. Since the guiding means allows the frame, and therefore the plate fixed to the frame, to be located at any position between the mold and the counter mold, this condition allows to keep a space between the plate and the mold pieces at both sides of the plate. This makes it possible to heat the surface of the thermo-formable plate when it is already held by the frame and in the required position for the process.

[0044] The actuating means are the means responsible of the movement of the heating means. Among their possible positions, there are at least, a first position close to the thermo-formable plate that allows raising its temperature, thus facilitating its subsequent deformation, and a second position further away from the thermo-formable plate, which prevents either the actuating means or the heating means to hinder the molding path, or alter the thermo-formable plate from correctly acquiring the shape imposed by the mold and the counter-mold.

[0045] The specific arrangement according to the invention further allows to carry out an optimal molding process since the thermo-formable plate loses the least possible amount of heat before the molding process since the heating process is carried out close to the molding position of the plate avoiding any mounting process of a preheated piece, out of the molding machine, like in the prior art.

[0046] According to a particular embodiment of the

present invention, the *heating means are movable according to a direction perpendicular to the displacement direction.*

[0047] A preferred example where the heating means have more than one possible position with respect to the rest of the components belonging to the invention, is one in which these are disposed perpendicularly to the displacement direction, said displacement direction given by the path defined between the first and the second position of the mold, or the counter mold, or the path of the frame movement which support the thermo-formable plate.

[0048] This disposition allows equidistance between any of the points of the surface of the thermos-deformable plate and any point of the heating means, ensuring uniform heating of the surface of the thermo-formable plate. This arrangement also allows the heating medium to move independently with respect to the two mold parts; it is only necessary that the mold and counter mold be in an open position providing the space between each of these mold parts and the plate to locate the heating means.

[0049] According to another embodiment of the present invention, *the heating means comprise at least one infrared ceramic lamp,* which have the advantage, among others, of high durability and can be used 24 hours a day because their light scattering is UVA filtering.

[0050] According to a further embodiment of the present invention, *the system comprises at least one elastic deformable element that establishes the connection between the plate of one end and the frame of the opposite end.*

[0051] The at least one elastic deformable element act as connecting element between the frame and the thermo-formable plate, thus allowing its tensioning and correct positioning even during when the deformation of the plate progresses, without hindering the correct molding of the plate and avoiding the appearance of errors or wrinkles in the deformation of the thermo-formable plate due to its incorrect tensioning or positioning.

[0052] According to a further embodiment of the present invention, *the system comprises a plurality of elastic deformable joint elements distributed around the plate in order to connect a respective point of the thermo-formable plate with a respective point of the frame and also to provide stretch tension in the plate.*

[0053] According to this embodiment of the present invention, the deformable elastic joining elements are distributed along the contour of the frame, giving rise to the tensioning of the perimeter of the plate in the outward direction of the plate, and therefore favoring the correct molding of the thermo-formable plate without the appearance of wrinkles or possible errors.

[0054] That is, during the process of plate deformation, the plate is no longer contained in one plane and concave regions appear, which can cause wrinkles in the perimeter zone. The plurality of elastically deformable elements distributed perimetrically maintain a tensional state of the perimeter zone that tends to keep this region in a plane facilitating the closing of the mold and that the deformation of the plate inside is in accordance with the shape imposed by the mold and the counter-mold without the wrinkles giving rise to internal folds.

[0055] Moreover, their presence allows the spatial orientation of the assembly to be independent of the molding process and does not have to be considered for its correct functioning.

[0056] According to a possible embodiment, *the frame comprises one or more grooves and the at least one joint element is connected to the thermo-formable plate through the groove wherein the groove extends transversely to the displacement direction connecting the first and second ends of said joint element.*

[0057] The connecting elements are connected to the frame when supporting the thermo-formable plate. These grooves are arranged transversely to the direction stablished by the two ends of the connecting element, one end connected to the plate and the opposite end connected to the frame by means of the groove. This second connection allows to adjust the direction of tension applied on the plate according to a plane perpendicular to the direction of displacement. Since the tensioning direction of the joint element is perpendicular to the groove, even if the end of the joint element connected to the frame moves, its position is stable and does not tend to move to other locations along the groove.

[0058] According to another embodiment of the present invention, *the system does not have any elastic deformable element for establishing the connection between the plate and the frame; and instead the thermo-formable plate comprises respective connection portions distributed in respective positions along its perimeter. The connection between the thermo-formable plate and the inner part of the frame is performed by means of a respective fixing pin that is positioned between a respective connection portion of the thermo-formable plate and a respective point of the inner part of the frame. Preferably, said connection portions of the plate extends outwards.*

[0059] Another possible alternative to be considered by any of the embodiments, the *displacement direction is horizontal.*

[0060] According to this example of realization, the frame rests on the shanks without any tendency to move towards the mold or the counter-mold, so that the distance between the frame and the mold or the distance between the frame and the counter-mold remains stable before closing the mold parts, thus facilitating the entry of the heating means. Another advantage of this arrangement is that when the frame makes use of slots or openings of converging configuration supporting a shank, the action of gravity tends to pull the shank to the extreme position of the slot.

[0061] According to a preferred embodiment, *the frame is extended along a main plain, the plain of the thermo-formable plate when fixed to the frame.*

[0062] According to another embodiment, *the frame is adapted to be positioned perpendicular to the displacement direction.*

[0063] According to another embodiment, *the guiding means comprise a shank oriented in the displacement direction and fixed to one support of one end of the molding machine in a cantilever manner, the shank being further adapted for sliding the frame through an aperture of the frame.*

[0064] The guiding means are preferably a rod or a shank which is preferably arranged in a cantilevered arrangement. This shank is fixed at one end to the molding machine support through one of the ends. It has already been described above that the molding machine support usually has a larger area than the mold or counter mold so that fixing at some point in this extra area is possible.

[0065] According to another embodiment, *the guiding means comprise a spring and the shank comprises a stopper, being the stopper located at one end of the shank, wherein the frame when installed in the guiding means is positioned between the stopper and the spring according to the displacement direction.*

[0066] The guiding means may also comprise at least one spring. The at least one spring is oriented in the displacement direction (D) and, according to an embodiment, it butts against the support at one end of the molding machine and, the opposite end is proximal to the frame.

[0067] According to an embodiment, the frame comprises a slot or aperture intended to house the guiding means, particularly a rod or a shank. In a preferred embodiment, when the guiding means are a rod or a shank, the rod or shank is limited by an abutting element or stopper preferably located at the end in cantilever condition.

[0068] The stopper prevents the frame from slipping out of the guiding means and the spring causes a tendency on the frame so that it adopts a position close to the stopper. Therefore, the frame may move freely between the stopper and the spring.

[0069] In addition, it should be mentioned that the frame in a preferred example would be located perpendicular to the displacement direction, so that the plate is positioned parallel to the mold and the counter-mold. That way is more accurate to carry out its deformation, and no wrinkles are formed when closing the two parts of the mold.

[0070] Moreover, according to an embodiment the guiding means are made up of a spring and one or more shanks or rods. When the spring is compressed, the frame is forced to show a single position when forced by the mold parts during the closing process since the spring exerts a force against the frame that tends to pull it to one side only.

[0071] That is, the frame can move between the spring end and a stopper along its path parallel to the displacement direction except during the mold closing process where the spring exerts a force that prevents the frame from moving freely over the range of distances between which it would move freely without the spring.

[0072] According to an embodiment, *the frame comprising at least an aperture with a region of support for shank that is convex, and the convex region being oriented downwardly according to the vertical direction established by the direction of gravity.*

[0073] In a preferred example, the frame comprises one or more convex apertures or openings that allow the rod (or shank) or rods to pass through. The convex region of the opening is oriented downwardly, taking as a reference a vertical axis to the direction set by gravity. This configuration facilitates the perfect positioning of the frame by its own weight and also the limitation of its degrees of freedom. This ensures the correct trajectory of the frame and alignment with the molding machine throughout the opening and closing process.

[0074] The wider part of the opening allows a quick installation of the frame with the plate since it is sufficient to fit inside the shank, for example through the stopper. The special configuration of the opening is what establishes its correct positioning without requiring any action by an operator.

[0075] In the specific embodiment of another preferred example, the frame comprises one or more openings. A shank, among a plurality of shanks, passes through each of these openings.

[0076] According to an embodiment, *the aperture is teardrop-shaped, with the narrowest part of the teardrop-shape located in the upper part of the aperture.*

[0077] Furthermore, in a preferred example each of the openings has a tear-shaped contour oriented downwards, taking as a reference the vertical axis established by the direction of gravity. This is another specific case that allows limiting the degrees of freedom of the frame in respect to the rod or shank passing through the respective opening since the frame tends to move in the direction of gravity due to weight.

[0078] The molding of each one of the plates requires a previous heating of them, so that the material opposes less resistance at the time of carrying out the molding and thus to facilitate the process as well as to obtain more accurate results. This is possible thanks to the presence of heating means, a system that allows the preheating of the plate without hindering the manufacturing process. For this purpose, they comprise two elements spaced apart, thus making it possible to heat the plate from both sides, facing the heat-emitting surfaces on both sides of the plate to be molded.

[0079] According to an embodiment, *the heating means comprise at least two elements distanced from each other adapted to be facing both sides of the plate.*

[0080] In this embodiment, the distance from one heating element and the other heating element allows to house at least the plate wherein both sides of the plate are accessible to the heating means. This configuration facilitates the heating of the plate in an effective manner in both sides simultaneously and the plate being at a location appropriate for closing the two mold parts with

no need of expending extra time installing the heated plate in the mold machine.

[0081] By avoiding this extra time it is also possible to avoid having to raise the temperature of the plate excessively to temperatures that could degrade the properties of the plate material.

[0082] According to an embodiment, *the distance between the two elements of the heating means is adjustable.*

[0083] This feature allows a simple regulation of the heat reaching the plate without having to vary the temperature of the heat source. In addition to its simple displacement before closing between the mold and the counter-mold, so as not to hinder its contact with the plate to be molded. The minimum distance between the two elements must be such that such movement of the heating means allowing the subsequent closing of the two mold parts is not prevented.

[0084] According to an embodiment, *the heating means comprise at least two heating sources, wherein at least one heating source is activable in an independent manner.*

[0085] When the different heat sources belonging to the heating means are activated independently then these heating means also allow for the regulation of the amount of heat transmitted to the plate.

[0086] In another preferred example, either *the mold or the counter mold or both are manufactured by additive manufacturing, preferably by waam (wire arc additive manufacutring), so that there is the presence of interior ducts within the molding part or parts. As there is some thermal fluid inside, it favors both the heating and cooling process.*

[0087] The cooling process occurs through the contact of the mold with the plate to be molded, once the closing between mold and counter-mold occurs, enclosing the plate between them.

[0088] That is, during the closing phase of the two parts of the mold the plate is hot allowing its deformation. It is in this phase of closing of the two parts of the mold when there is an interaction with the plate and where all the deformation takes place. During this phase the two mold parts must also be at a high temperature in order not to cool the hot plate, since cooling during the deformation phase would harden the plate locally and cause breakage or at least defects.

[0089] In order for the mold and the counter-mold to be at a high temperature, a previous heating stage is necessary, for which a hot fluid is introduced through the internal channels.

[0090] Once the plate has acquired its final shape after the deformation process by the closing of the mold and the counter-mold, it is necessary to cool both parts of the mold to achieve again the rigidity of the molded part.

[0091] In view of these stages, the manufacturing time of a piece depends on the time required to heat the mold parts and also on the time required to cool the mold parts again after closing the mold. The overall efficiency of the process will depend on the ability to reduce these two times, which are proportional to the thermal inertia of both.

[0092] According to a preferred embodiment of the invention, in order to reduce thermal inertia and optimize the circuits, the molds (i.e. mold and a counter mold) are heated using thermal fluid flowing through internal ducts with an optimized path, through molds printed using additive manufacturing techniques. The additive manufacturing of the mold and the counter-mold allows to eliminate in the design phase material that would be present when manufacturing them from a metal block that is subsequently machined according to the state of the art but, which is not structurally necessary. This is a first factor that reduces thermal inertia.

[0093] Likewise, through additive manufacturing it is possible to configure internal ducts that adapt to complex shapes giving rise to channels and cavities that also reduce the volume of metal in the mold and, therefore, being a second factor that reduces thermal inertia. The separation walls of the mold and the counter-mold between the internal ducts and the heat exchange surface by contact with the plate can be smaller and moreover constant even if the shapes to be adopted by the plate are complicated.

[0094] In a preferred example, the thermal fluid used through the ducts flowing inside the counter-mold or both, is oil, as it prevents the phenomenon of thermal shock, and possible state changes, from occurring.

[0095] In another preferred example, the inner ducts comprise a portion of their interior adapted to the outer shape of the mold surface, so that heat transfer is optimized.

[0096] In a second aspect, the present invention provides *a method for manufacturing molded pieces by means of the system defined previously, wherein the method comprises the steps:*

a) installing a thermo-formable plate in the frame;
b) installing the frame in the guiding means while the molding machine is in open position;
c) positioning the heating means in the first position, the heating means being activated for heating the thermo-formable plate;
d) positioning the heating means in the second position;
e) positioning the molding machine in the closed position, the two mold pieces exerting force on the thermo-formable plate,
f) positioning the molding machine in the open position and removing the frame;
g) removing the molded thermo-formable plate from the frame.

[0097] According to an embodiment of the method, firstly the thermo-formable plate is placed on the frame by means of its connecting elements. Then the frame is installed into the guiding means while the molding ma-

chine is in its open position, so that it is in a fixed orientation with the displacement direction as the only degree of freedom. Then the heating means are placed close to the plate to raise its temperature, and once this process is finished, they are placed in a second position that does not obstruct the closing between the mold and the counter mold.

[0098] According to an embodiment, the mold and the counter-mold are also heated for avoiding to cool the thermo-formable plate two fast when both are closed causing the deformation of the plate.

[0099] At this point the molding machine is already in optimal conditions to close and deform the thermo-formable plate to the desired shape. Once the plate has been deformed, the mold and the counter-mold are cooled down in order to increase the rigidity of the deformed thermo-formable plate. Then the molding machine separates the two mold parts and the frame is removed from the molding machine assembly. Secondly the plate already molded with the desired shape is separated from the frame.

[0100] Additional steps may be needed depending on the specific manufactured piece, for instance cutting a perimetral part of the molded piece since such perimetral part has been only useful for supporting the thermo-formable plate with the frame.

DESCRIPTION OF THE DRAWINGS

[0101] These and other features and advantages of the invention will be seen more clearly from the following detailed description of a preferred embodiment provided only by way of illustrative and non-limiting example in reference to the attached drawings.

Figure 1 This figure shows a perspective view of an embodiment of a system for manufacturing a molded thermo-formable plate.

Figure 2 This figure shows a perspective view of an embodiment of the inner part of the system shown in figure 1, at least comprising the first support, the second support, the mold and the counter mold with the thermo-formable plate located therebetween.

Figure 3, 4 These figures show a perspective view of an embodiment of heating means configured to be installed in the system for manufacturing a molded thermo-formable plate. Figure 4 shows heating means in a first position located out of the frame supporting the thermo-formable plate and, figure 5 shows the same in a second position configured to heat the thermo-formable plate.

Figure 5 This figure shows a perspective view of an embodiment of the first support and the second support of the mold parts without the mold parts and, both being in a closed position. The first support comprises four shanks for supporting the frame.

Figure 6 This figure shows a perspective view of an embodiment of the first support and the mold showing the four shanks.

Figure 7 This figure shows a perspective view of an embodiment of a frame and a thermo-formable plate joined with a pin.

Figure 8 This figure shows a perspective view of an embodiment of a frame and a thermo-formable plate joined with a plurality of elastic deformable joint elements distributed around the thermo-formable plate.

DETAILED DESCRIPTION OF THE INVENTION

[0102] As will be appreciated by one skilled in the art, aspects of the present invention may be embodied as a system or a method.

[0103] Figure 1 depicts system for manufacturing molded pieces departing form a thermo-formable plate (3) according to a first embodiment of the invention. In this first example, system for manufacturing molded pieces is configured by the following elements:

- a molding machine (1);
- a frame (2) configured for supporting a thermo-formable plate (3);
- guiding means (5) adapted to guide the frame (2) according to a displacement direction (D);
- heating means (6) (not shown in figure 1 but shown in figures 3 and 4) configured for heating the thermo-formable plate (3); and
- actuating means (6.2) adapted to move the heating means (6) at least between two positions, a first position close to the thermo-formable plate (3) for heating the same and, a second position distant from the frame (2) and the mold pieces (1.3, 1.4) for allowing the mold movement (D).

[0104] In the example of Figure 1, the molding machine (1) comprises a base (1.5) for supporting an upper main structure that supports two supports (1.1, 1.2) identified as a first support (1.1) and a second support (1.2) for supporting two mold pieces (1.3, 1.4) also identified as a mold (1.3) and a counter mold (1.4) respectively. Furthermore, according to this embodiment two lateral parts (1.6) having a respective central apertures are also part of the main structure of this example allowing an easy access to the mold parts (1.3 ,1.4) and other inner components while protecting the operator.

[0105] Figure 1 does not show heating means (6) in

order to have a clean view of the inner components located between the mold parts (1.3, 1.4). Figure 1 shows four big bars (1.7) allowing a guided movement of the first support (1.1) for moving the mold (1.3) in respect to the second support (1.2) according to the displacement direction (D). In this specific example displacement direction is horizontal being vertical direction perpendicular to the horizontal direction and, vertical direction defined by the direction of any force caused by gravity.

[0106] The displacement of the first support (1.1) towards the second support (1.2) causes the displacement of the mold (1.3) towards the counter mold (1.4) closing the mold parts (1.3, 1.4).

[0107] During the movement of the first support (1.1), part of the big bars (1.7) on either side of the first support (1.1) are accessible. In particular a portion next to the second support (1.2).

[0108] The heating means 6 can be better appreciated in figures 3 and 4 wherein four supporting means (6.3) are configured to be fixed to the four big bars (1.7).

[0109] According to the embodiment shown in figure 3 and 4, heating means (6) comprises two elements with the purpose of placing each of the elements on either side of the thermal-deformable plate (3) allowing to heat both faces of said thermal-deformable plate (3).

[0110] In this embodiment, each element comprises a plurality of lamps (6.1) generating heat. The two elements of the heating means (6) shows a distance that is adjustable allowing to adjust the heat received by the thermo-formable plate (3).

[0111] In this embodiment, a further manner to adjust the heat received by the thermo-formable plate (3) is by activating a selection of lamps (3), preferably the activated lamps (3) being uniformly distributed preventing the overheating of a local area of the thermal-deformable plate (3).

[0112] In this example the lamps (6.1) are infrared ceramic lamps very effective heating black pieces as those made of carbon fiber.

[0113] Figure 3 shows a vertical structure keeping the plurality of lamps (6.1) located in a first position wherein the upper part comprising the plurality of lamps (6.1) is away from the supporting means (6.3), and therefore, in operative manner away from the frame (2) supporting the thermo-formable plate (3).

[0114] Figure 4 shows a second position of the heating means (6) wherein the plurality of lamps (6.1) is a lower position located in the inner region delimited by the supporting means (6.3) and, therefore located where the region destined to house the part to be molded is located.

[0115] The heating means (6) comprise actuating means (6.2) responsible for acting on the structure supporting the plurality of lamps (6.1) by moving it between the two end positions shown in figure 3 and 4 respectively.

[0116] When the lamp assembly (6.1) is in the position shown in Figure 3, that is, in an elevated position, the mold (1.3) and the counter mold (1.4) can move by opening and closing without interference between the mold parts (1.3, 1.4) and the lamps (6).

[0117] In the first position of the heating means (6), with the lamps (6.1) in the raised position, it is possible to locate the frame (2) with the thermo-formable plate (3) fixed to it (2). Once the frame (2) with the thermo-formable plate (3) is in place, the heating means (6) are lowered until the lamps (6.1) are positioned on either side of the thermo-formable plate (3). In this position and the lamps (6.1) activated the temperature of the thermo-formable plate (3) is raised, making it capable of large deformations under force.

[0118] With this configuration, rapid withdrawal of the lamps (6.1) is possible because the actuating means (6.2) raise the lamps (6.1) to a height that does not interfere with the closing of the mold (1.3) towards the counter mold (1.4) with no further operations allowing to close the mold (1.3) and the counter mold (1.4) before the heated thermo-formable plate (3) is cooled again.

[0119] Figure 2 shows a detail of the elements identified in Figure 1 but with an enlarged view in the area where the mold (1.3) and the counter mold (1.4) are located.

[0120] This view of figure 2 shows the first support (1.1) with the mold (1.3) and the second support (1.2) with the counter mold (1.4) spaced apart.

[0121] Four shanks (5.1) emerge horizontally from the second support (1.2) in a cantilevered position. Each of the shanks (5.1) has a spring (5.2) around the shank (5.1) so that the spring (5.2) is guided in its compression deformation when it occurs avoiding it from bending.

[0122] Each of the shanks (5.1) shows at the free end an stopper (5.3), in this example in the form of a disk of larger diameter than the diameter of the shank (5.1). The spring (5.3) has a shorter length than the stopper (5.3) leaving a section of the shank (5.1) free.

[0123] The frame (2), as shown in figures 7 and 8, have openings (2.1) intended to allow the passage of the shank (5.1) and also the passage of the stopper (5.3) in order to install the frame (2) in the plurality of shanks (5.1).

[0124] The frame (2) is located between one end of the spring (5.2) and the stopper (5.3). If the spring (5.2) has sufficient length then the spring (5.2), according to an embodiment, can maintain a forcing action against the stopper (5.3).

[0125] According to a preferred example, the openings (2.1) have a teardrop shape with the most restriction region located in the part which, in operative form, is located in the upper part according to the action of gravity. With this configuration, the action of the weight on the frame (2) and the thermo-formable plate (3) tends the frame (2) to descend and the shank (5.1) to be located in the narrow, convergent region of the teardrop. This tendency to position itself in the convergent region means that the natural tendency of the frame (2) is to position itself in a single position making the adjustment of its position automatic.

[0126] Another function of the spring (5.2) is to place

the position of the frame (2) in an orientation as close to perpendicular to the displacement direction (D) as possible.

[0127] Another function of the spring (5.2) is to position, according to the displacement direction (D), the frame (2) in a predetermined position that leaves space on either side of the frame (2) so that the two spaced elements of the heating means (6) can be lowered leaving the frame (2) between them safely and without mechanical interference.

[0128] Figure 2 shows the position of the frame (2) in a position close to the free end of the shanks (5.1) due to the action of the springs (5.3).

[0129] Figure 5 shows the first support (1.1) and the second support (1.2) in a close-up position where the mold (1.3) and the counter-mold (1.4) have been withdrawn to show the remaining elements in detail.

[0130] In particular, mold guiding nipples are shown to ensure in the approach that the fit between mold (1.3) and counter mold (1.4) is precise.

[0131] Also shown are the four cantilevered shanks (5.1) extending from their fixed end to the cantilevered end, the one with the stopper (5.3). The length of the shank (5.1) is sufficient so that the frame (2) can adopt any intermediate position in the movement of the mold (1.3) forcing also the movement of the thermo-formable plate (3) attached to the frame (2).

[0132] That is, at the moment of closing the mold (1.3) towards the counter mold (1.4) the frame (2) keeps the thermo-formable plate interposed between the two pieces of the mold (1.3, 1.4) ensuring the correct positioning.

[0133] Even when the thermo-formable plate (3) comes into contact with the mold (1.3) and the counter-mold (1.4) the thermo-formable plate (3) is still retained by the frame (2) allowing the thermo-formable plate (3) to deform but always maintaining the position for which it has been designed without any modification of this position from one molded piece to another.

[0134] Figure 6 shows the second support (1.2) with the counter mold (1.4) attached to it to show the shanks (5.1) of the guiding means (5) more clearly. In this specific case the counter mold (1.4) has a vertical projection shape with a central flaring. This shape is complementary to the shape of the mold (1.3) not shown in this figure. The shanks (5.1) in this embodiment are not fixed to the counter-mold (1.4) but are fixed to the second support (1.2) although the movement of all the parts shown in this figure is the same.

[0135] Figure 7 shows a first example of attachment between the frame (2) and the thermo-formable plate (3). The fastening incorporates connection portions (2.3) located in the inner area of the frame (2). In this way the connection portions (2.3) extend into the inner area of the frame (2).

[0136] Likewise, in this embodiment, the thermo-formable plate (3) has projections towards its perimeter zone with points of joint with points of the connection portions (2.3) of the frame (2). These joints are carried out by means of fixing pins (7).

[0137] When the mold (1.3) moves towards the counter-mold (1.4) with the thermo-formable plate (3) between them, there is a first approach phase in which it may not even contact the thermo-formable plate (3). Once the mold (1.3) contacts the thermo-formable plate (3) between the thermo-formable plate (3) and the counter mold (1.4) there may be a free space. By advancing the displacement of the mold even further a configuration is reached in which a part of the thermo-formable plate (3) is in contact with the mold (1.3) and, another part of the thermo-formable plate (3) are in contact with the counter mold (1.4). From this point, the advance of the mold (1.3) generates stresses in the thermo-formable plate (3) that cause its deformation and a tendency to move both in the direction of displacement (D) and in its orientation.

[0138] Since the frame (2) is guided by the guiding means (5) in the direction of displacement (D), the frame (2) moves towards the counter mold (1.4) but always being located at a point where the forces of the mold (1.3) and the counter mold (1.4) reach an equilibrium in the direction of displacement (D) while the frame (2) and the guiding means (5) always ensure its orientation perpendicular or almost perpendicular to the direction of displacement (D).

[0139] The tensile stresses between the thermo-formable plate (3) and the frame (2) can be very high depending on the shape of the part to be molded.

[0140] Figure 8 shows another embodiment where the connection between the thermo-formable plate (3) and the frame (2) has elastically deformable means (4) that allow very high deformations of the thermo-formable plate (3) without such deformations being transmitted directly to the frame (2) and, while maintaining a tensile stress between the thermo-formable plate (3) and the frame (2).

[0141] In this embodiment, Figure 8 shows the elastically deformable means (4) fixed to the frame (2) in the form of plates (4.3) fixed to the frame (2) which let pass through a perforation a traction bar (4.1) intended to connect with another joint piece (4.4) with the thermo-formable plate (3). The traction bar (4.1) is tractioned by a spring (4.2) which tends to maintain a traction force on the thermo-formable plate (3). In Figure 8, the bars (4.1) have been disconnected from the joint parts (4.4) fixed to the thermo-formable plate (3) to show the extended spring (4.2) and the details of each part.

[0142] The joint pieces (4.4) attached to the thermo-formable plate (3), in this example embodiment, have the ability to rotate relative to the thermo-formable plate (3) to reduce stresses.

[0143] According to another embodiment, the joint between the plate (4.3) through which the bar (4.1) for fixing the connecting piece (4.4) passes is in a groove (2.2) of the frame (2) in the form of a slot. The groove (2.2) allows the point of joint between the plate (4.3) and the frame (2) not to be predetermined and to be located where the least stress occurs during the progress of deformation of

the thermo-formable plate (3).

[0144] According to another embodiment, the groove (2.2) of the frame (2) extends in a direction contained in the main plane of the frame (2) but transverse to the direction taken by the bar (4.1) pulling the thermo-formable plate (3) to ensure the stability of the joint.

Claims

1. A system for manufacturing molded pieces by means of:

   - a molding machine (1) comprising two supports (1.1, 1.2) for supporting two mold pieces (1.3, 1.4), a first support (1.1) adapted to receive a mold (1.3) and a second support (1.2) adapted to receive a counter mold (1.4), the molding machine (1) adapted to adopt at least a first open position wherein the mold (1.3) and the counter-mold (1.4) are spaced apart and a closed position wherein one mold piece (1.3, 1.4) exerts force against the other mold piece (1.4, 1.3) and, wherein the movement of one mold piece (1.3, 1.4) in respect to the other mold piece (1.4, 1.3) is according to a displacement direction (D);
   - a frame (2) configured for supporting a thermo-formable plate (3);
   - guiding means (5) adapted to guide the frame (2) according to the displacement direction (D);
   - heating means (6) configured for heating the thermo-formable plate (3);
   - actuating means (6.2) adapted to move the heating means (6) at least between two positions, a first position close to the thermo-formable plate (3) for heating the same and, a second position distant from the frame (2) and the mold pieces (1.3, 1.4) for allowing the mold movement (D).

2. A system according to claim 1, wherein the heating means (6) are movable according to a direction perpendicular to the displacement direction (D).

3. A system according to any of previous claims, wherein the heating means (6) comprise at least one infrared ceramic lamp (6.1).

4. A system according to any of previous claims, which comprises at least one elastic deformable joint element (4) that establishes the connection between the thermo-formable plate (3) at one end and the frame (2) at the opposite end.

5. A system according to claim 4, wherein it further comprises a plurality of elastic deformable joint elements (4) distributed around the thermo-formable plate (3) in order to connect a respective point of the thermo-formable plate (3) with a respective point of the frame (2) and also to provide stretch tension in the plate (3).

6. A system according to claims 4 or 5, wherein the frame (2) comprises one or more grooves (2.2) and the at least one joint element (4) is connected to the thermo-formable plate (3) through the groove (2.2) wherein the groove (2.2) extends transversely to the displacement direction (D) connecting the first and second ends of said joint element (4).

7. A system according to any of claims 1 to 3, wherein the thermo-formable plate (2) comprises respective connection portions (2.3) distributed in respective positions along its perimeter and, wherein the connection between the thermo-formable plate (2) and the inner part of the frame (3) is performed by means of a respective fixing pin (7) that is positioned between a respective connection portion (2.3) of the thermo-formable plate (2) and a respective point (3.1) of the inner part of the frame (3).

8. A system according to any of previous claims, wherein the displacement direction (D) is horizontal.

9. A system according to any of previous claims, wherein the frame (2) is extended along a main plain, the plain of the thermo-formable plate (3) when fixed to the frame (2).

10. A system according to any of previous claims, wherein the frame (2) is adapted to be positioned perpendicular to the displacement direction (D).

11. A system according to any of previous claims, wherein the guiding means (5) comprise a shank (5.1) oriented in the displacement direction (D) and fixed to one support at one end of the molding machine (1) in a cantilever manner, the shank (5.1) being further adapted for sliding the frame (2) through an aperture of the frame (2.1).

12. A system according to the previous claim, where the guiding means (5) comprise a spring (5.2) and the shank (5.1) comprises a stopper (5.3), being the stopper (5.3) located at one end of the shank (5.1), wherein the frame (2) when installed in the guiding means (5) is positioned between the stopper (5.3) and the spring (5.2) according to the displacement direction (D).

13. A system according to claim 11 or 12, wherein the frame (2) comprising at least an aperture with a region of support for shank (5.1) that is convex, and the convex region being oriented downwardly according to the vertical direction established by the direction of gravity.

14. A system according to the previous claim, where the aperture is teardrop-shaped, with the narrowest part of the teardrop-shape located in the upper part of the aperture.

15. A system according to any of previous claims, wherein the heating means (6) comprise at least two elements distanced from each other adapted to be facing both sides of the thermo-formable plate (3).

16. A system according to the previous claim, wherein the distance between the two elements of the heating means (6) is adjustable.

17. A system according to any of previous claims, wherein the heating means (6) comprise at least two heating sources, wherein at least one heating source is activable in an independent manner.

18. A system according to any of previous claims, wherein the mold (1.3) , the counter mold (1.4) or both mold pieces (1.3, 1.4) is manufactured by additive manufacturing, preferably by waam; and, the mold piece/pieces (1.3, 1.4) comprises internal ducts for conducting a thermal fluid, wherein the internal ducts are for the heating and/or cooling process.

19. A system according to claims 1 and 16, wherein the internal ducts comprises an internal portion that mimics the shape of at least a portion of the surface adapted to be in contact with the thermo-formable plate (3).

20. A method for manufacturing molded pieces by means of a system according to any of previous claims, wherein the method comprises the steps:

a) installing a thermo-formable plate (3) in the frame (2);
b) installing the frame (2) in the guiding means (5) while the molding machine (1) is in open position;
c) positioning the heating means (6) in the first position, the heating means (6) being activated for heating the thermo-formable plate (3);
d) positioning the heating means (6) in the second position;
e) positioning the molding machine (1) in the closed position, the two mold pieces (1.3, 1.4) exerting force on the thermo-formable plate (3);
f) positioning the molding machine (1) in the open position and removing the frame (2);
g) removing the molded thermo-formable plate (3) from the frame (2).

21. A method according to previous claim, wherein before positioning the molding machine in the open position and removing the frame (2), the mold (1.3) and the counter mold (1.4) are cooled down in order to increase the rigidity of the deformed thermo-formable plate (3).

22. A method according to any of claims 20 to 21, wherein before positioning the molding machine in the closed position, the mold (1.3) and the counter mold (1.4) are heated.

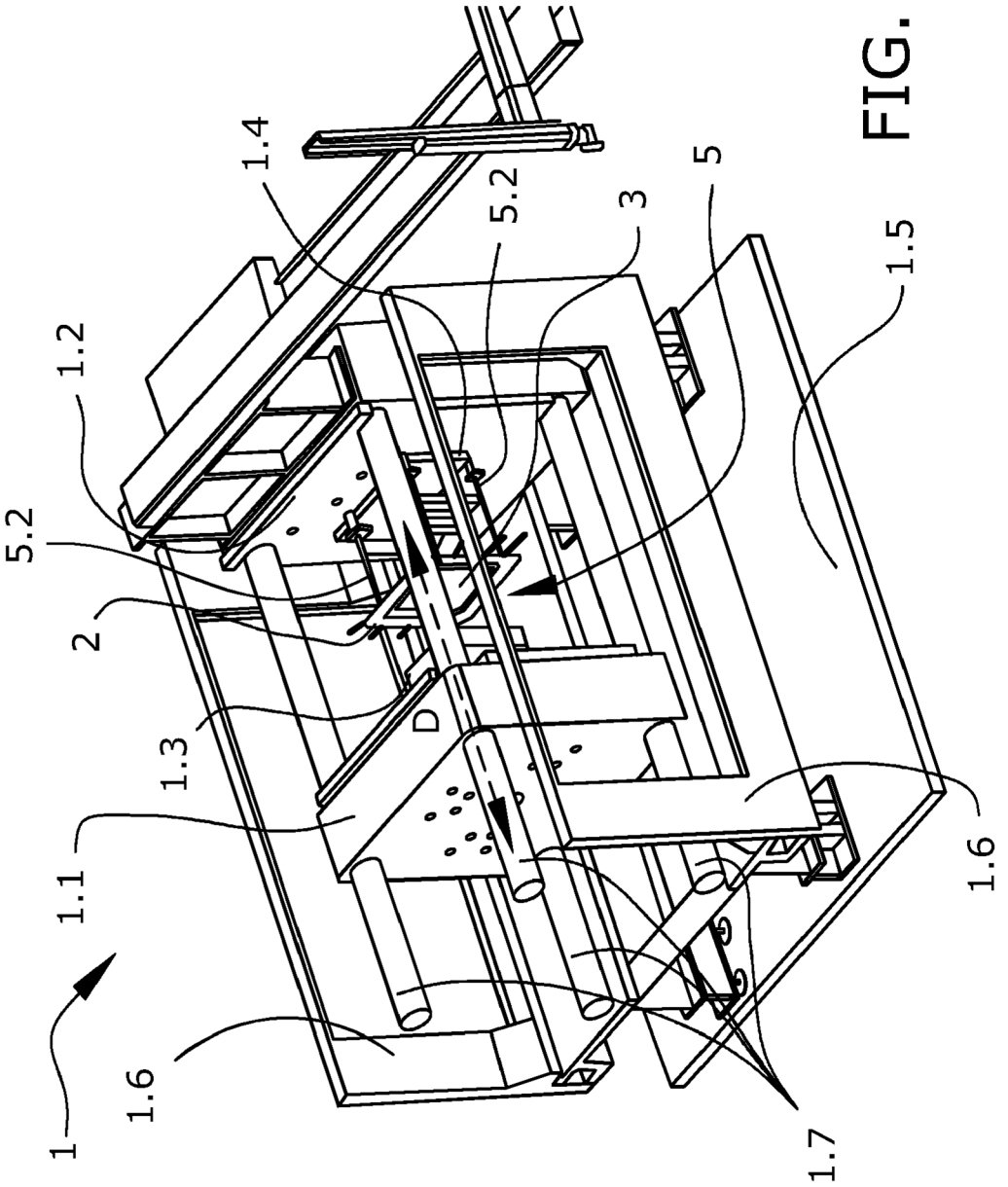

FIG. 1

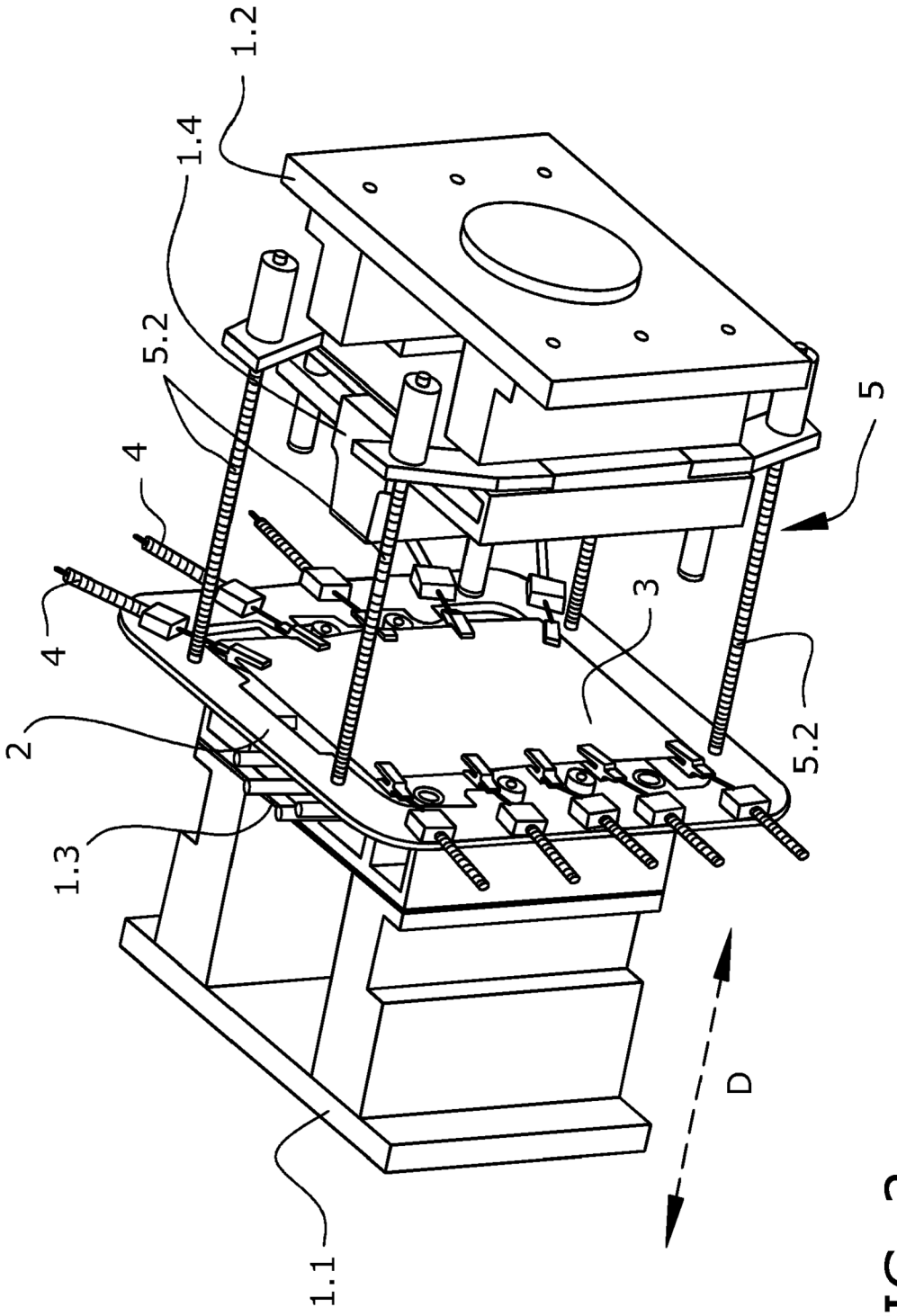

FIG. 2

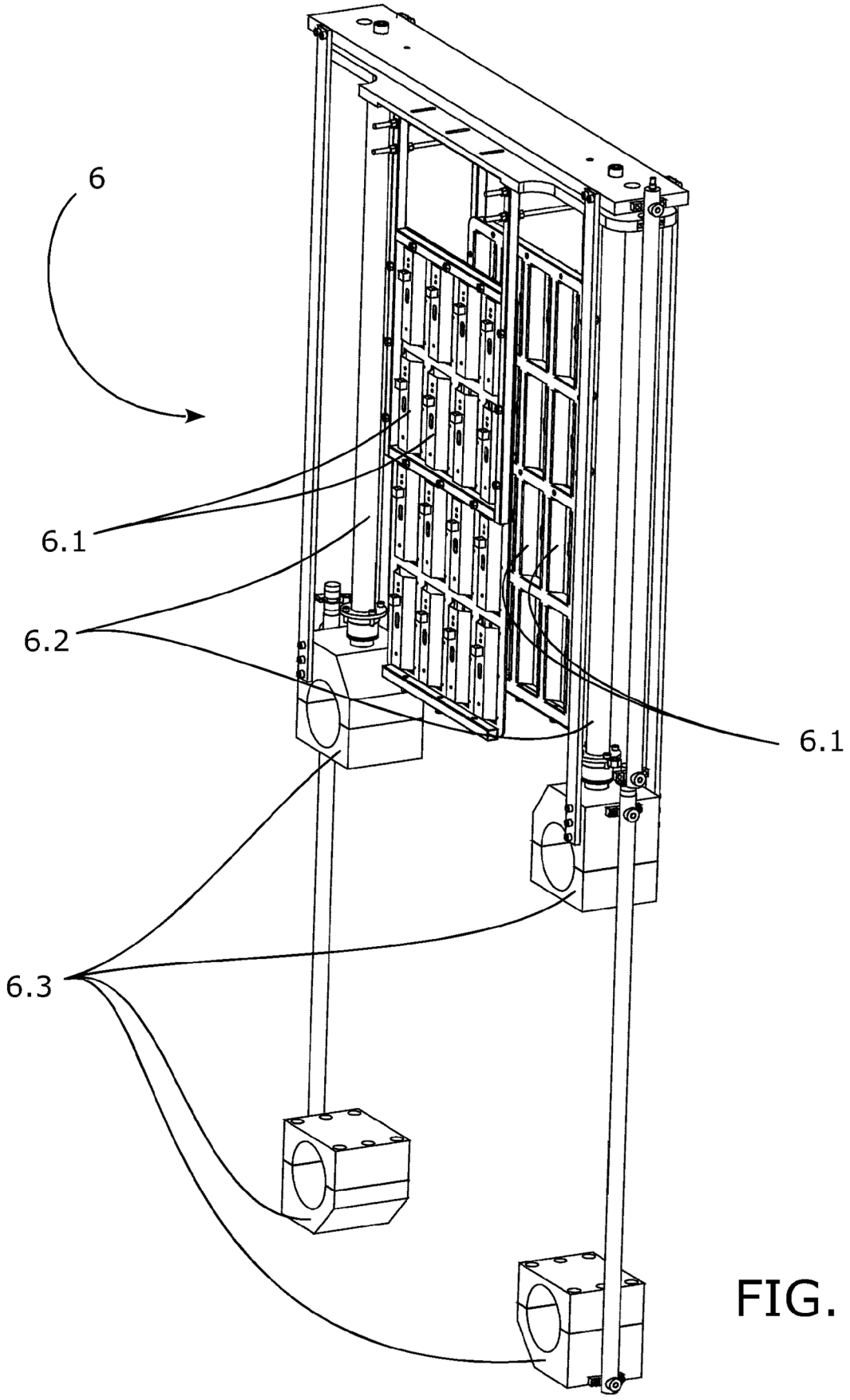

FIG. 3

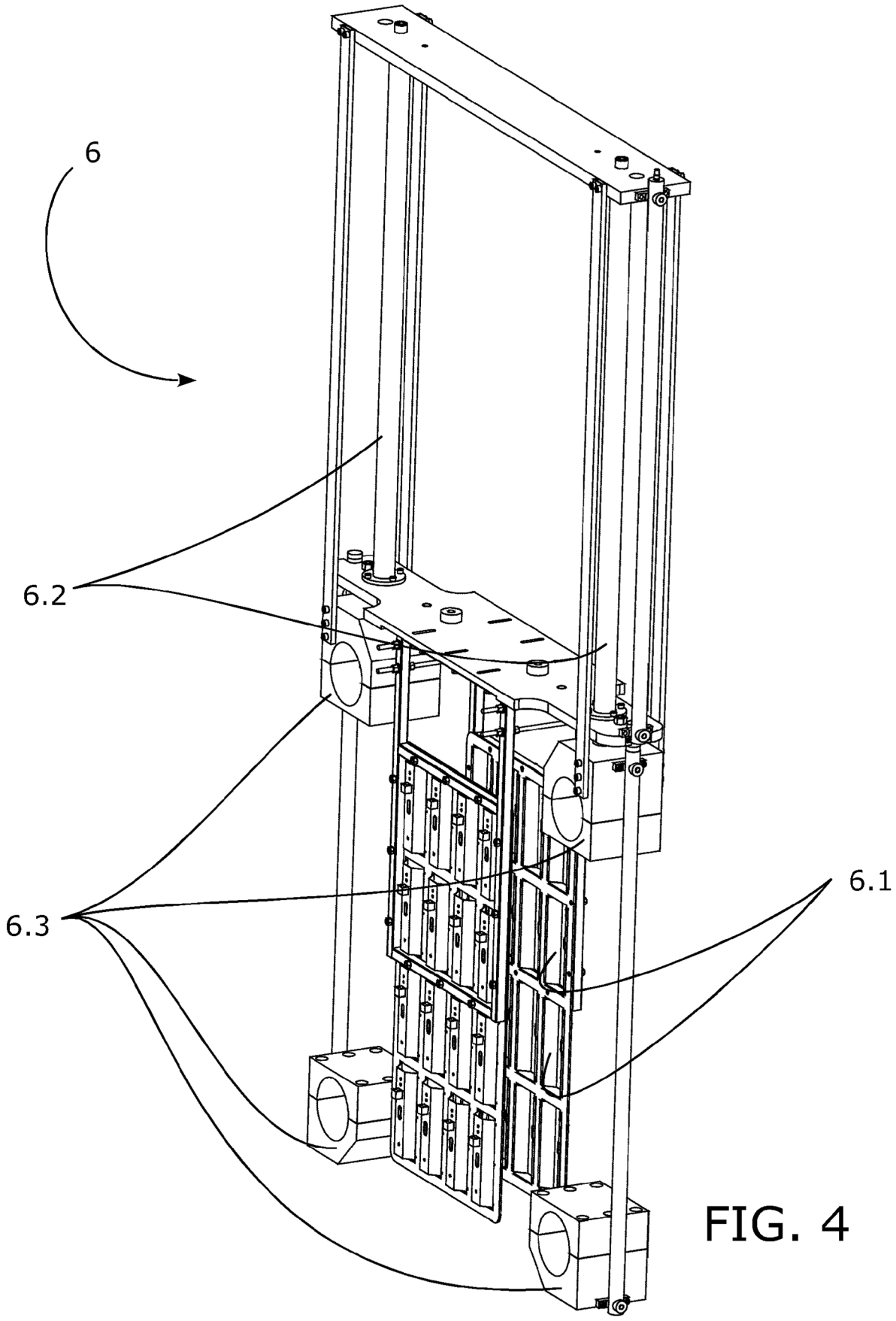

FIG. 4

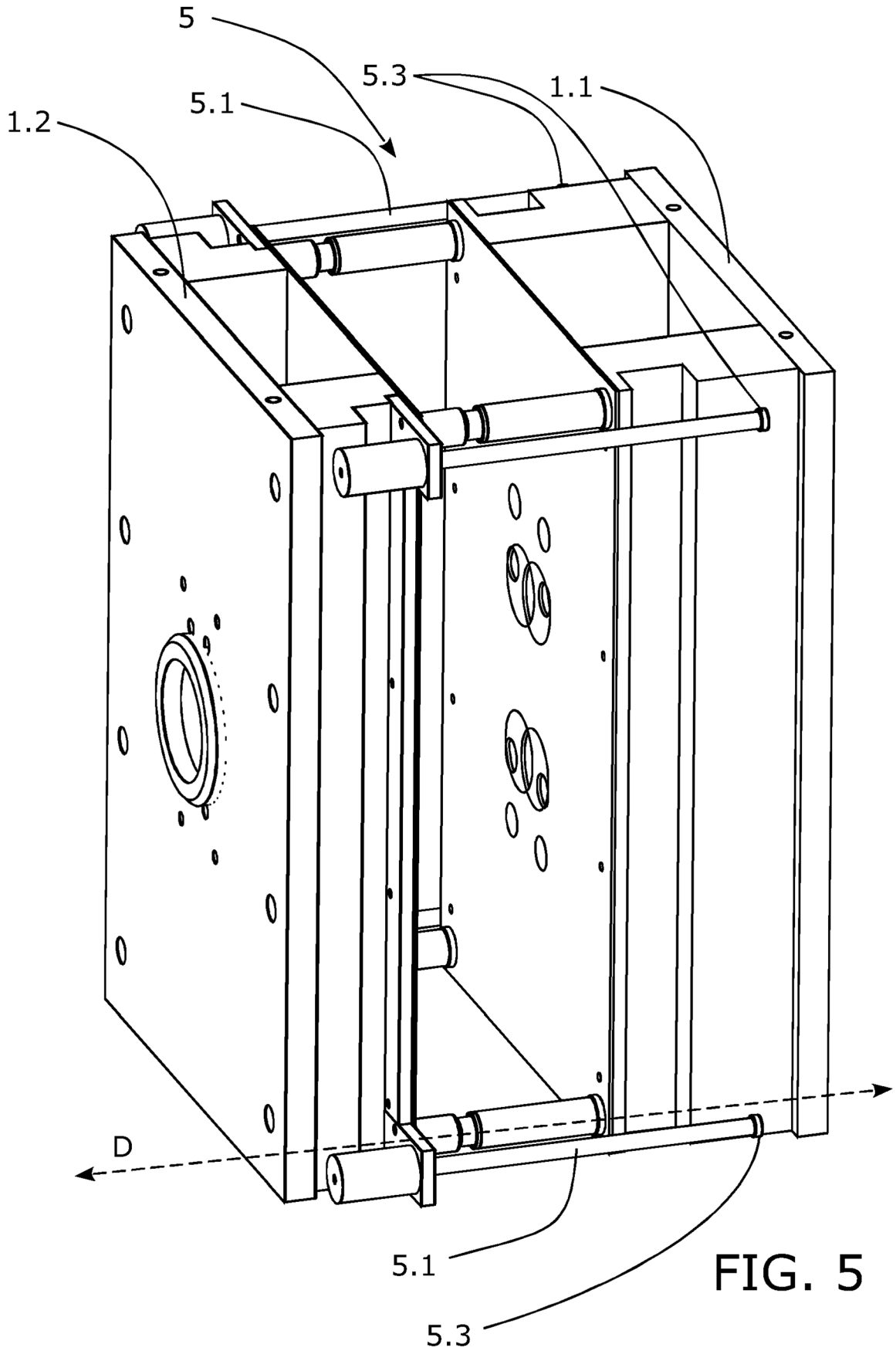

FIG. 5

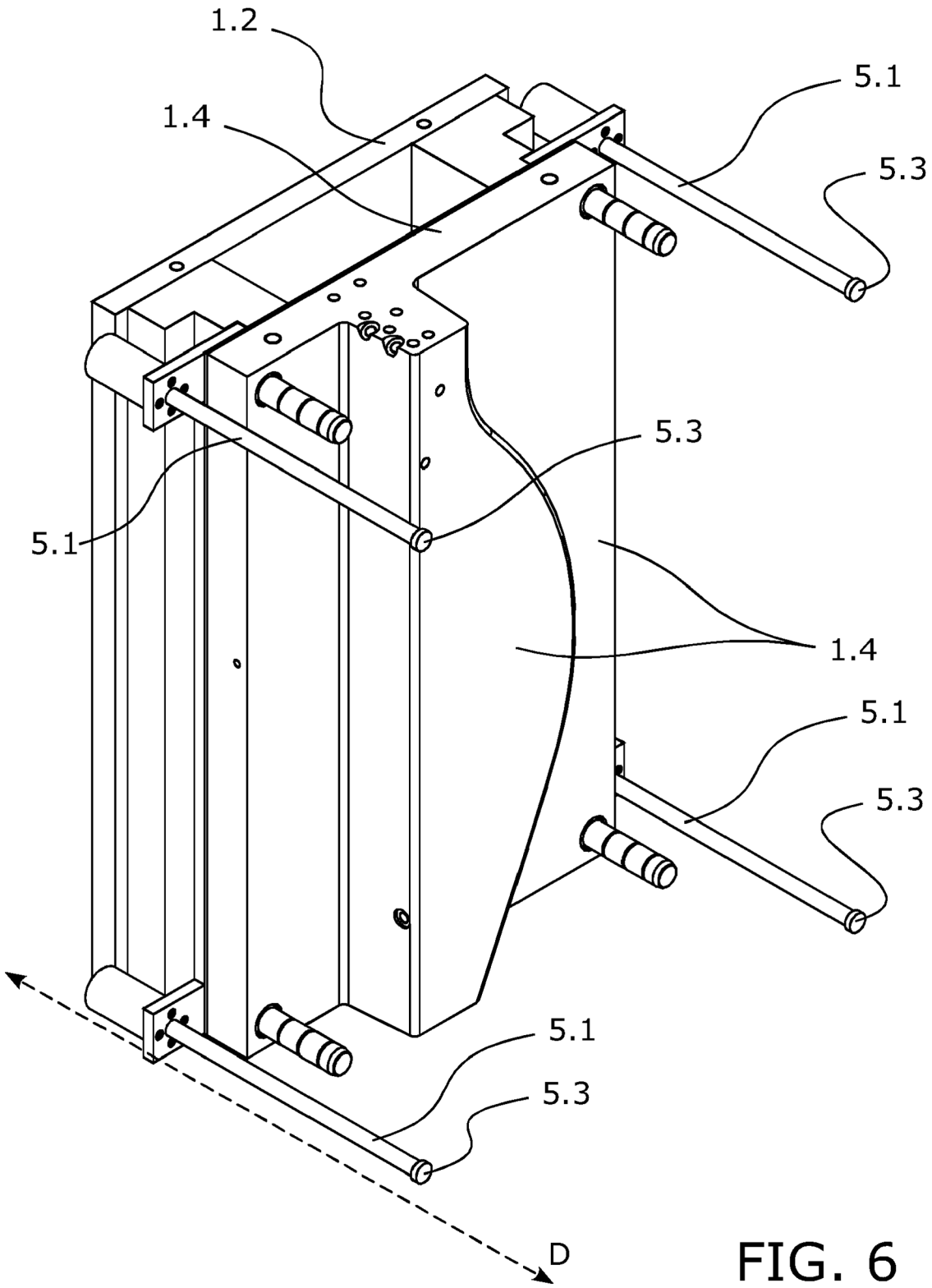

FIG. 6

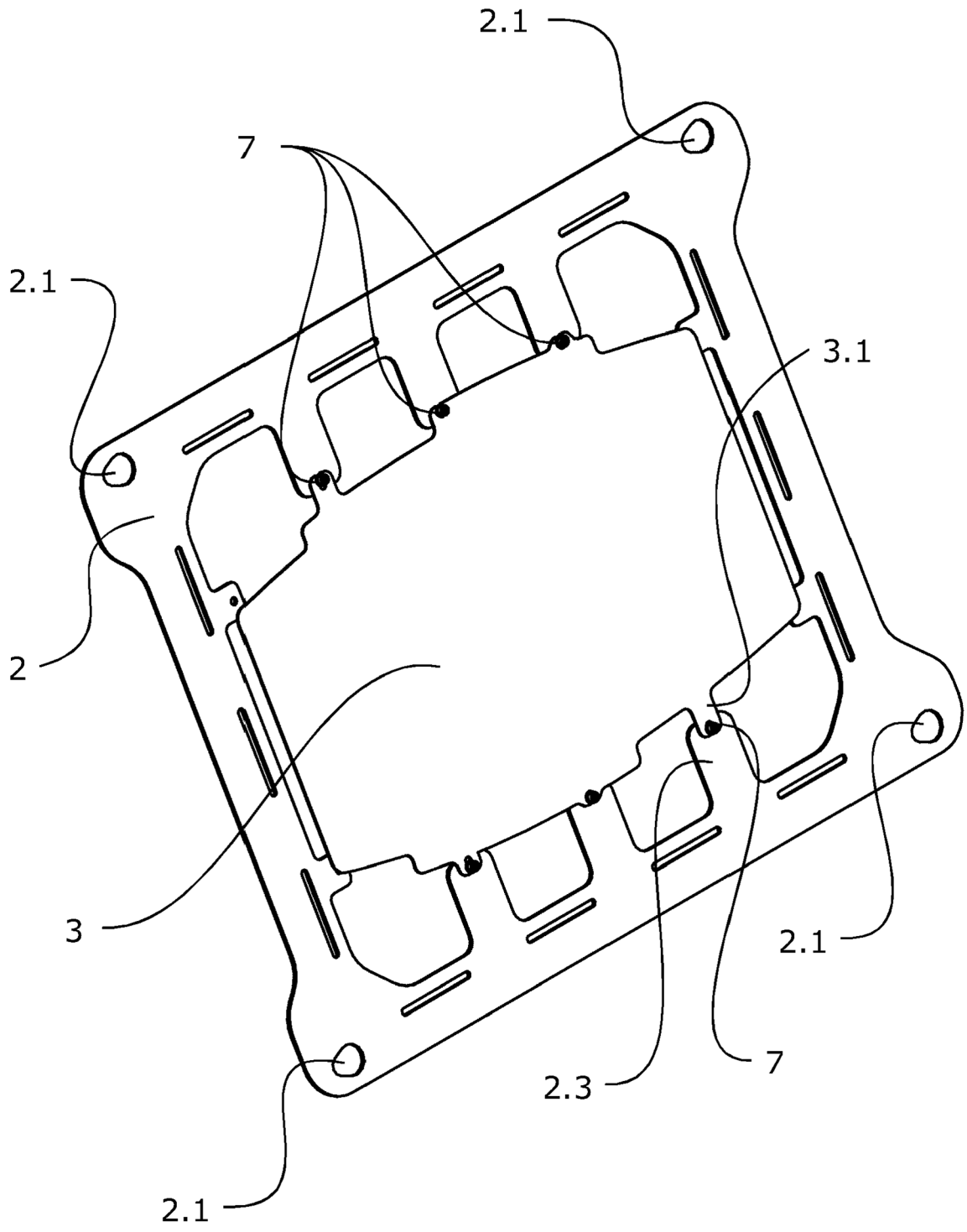

FIG. 7

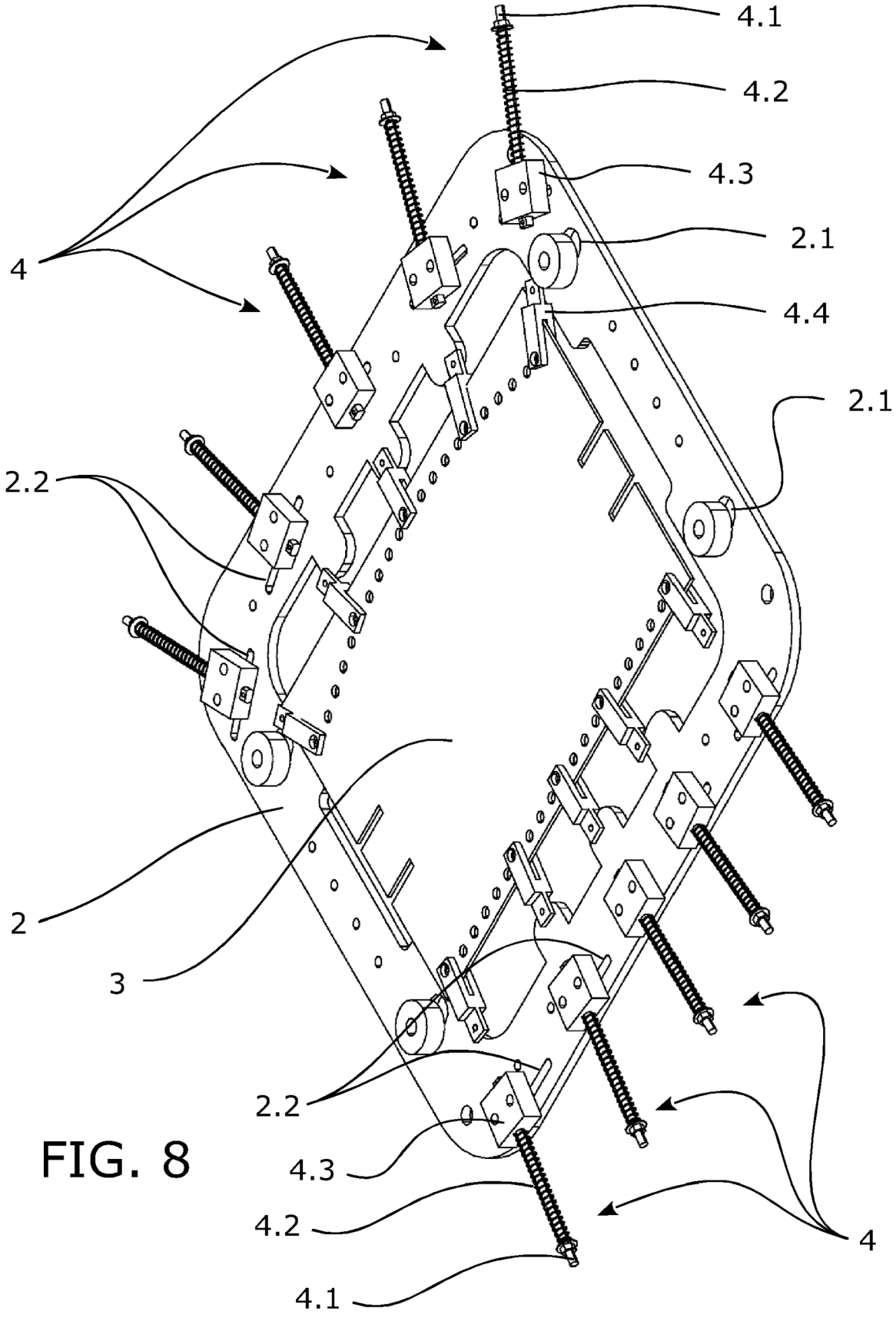

FIG. 8

Europäisches Patentamt
European Patent Office
Office européen des brevets

EUROPEAN SEARCH REPORT

Application Number
EP 23 38 2013

DOCUMENTS CONSIDERED TO BE RELEVANT

Category	Citation of document with indication, where appropriate, of relevant passages	Relevant to claim	CLASSIFICATION OF THE APPLICATION (IPC)
X	US 2020/269487 A1 (DANDO KERRICK ROBERT [US]) 27 August 2020 (2020-08-27)	1-3, 7-10, 15-17,20	INV. B29C70/46 B29C70/56
Y	* page 1 - page 4; claims 1-20; figures 1-7 *	4,5,18, 19	B29B13/02 B29C51/08
A	* paragraphs [0008], [0028]; claims 4, 11 * * paragraphs [0034], [0038] *	6,13,14	B29C51/26 B29C51/42
X	CN 114 474 685 A (SUZHOU TIANXI COMPOSITE CO LTD) 13 May 2022 (2022-05-13)	1-3, 7-12, 15-17,20	
Y	* page 1 - page 4; claims 1-7; figure 1 * * paragraph [0038] *	4,5,18, 19	
A		6,13,14	
Y	EP 2 881 234 A1 (PREMIUM AEROTEC GMBH [DE]) 10 June 2015 (2015-06-10)	4,5	
A	* page 1 - page 6; claims 1-10; figures 1-6 * * paragraphs [0040], [0065]; figures 1, 2, 6 *	7	
Y	US 5 026 514 A (HAUWILLER PAUL B [US] ET AL) 25 June 1991 (1991-06-25)	4,5	
A	* figures 1-3 * * columns 4-8; claims 1-10 *	7	
Y	CN 108 480 821 B (UNIV FUZHOU) 15 October 2019 (2019-10-15) * pages 1-5; claims 1-9; figures 1-3 *	18,19	

-/--

TECHNICAL FIELDS SEARCHED (IPC)

B29B
B29C
B29K

The present search report has been drawn up for all claims

Place of search	Date of completion of the search	Examiner
Munich	14 July 2023	Brunswick, André

CATEGORY OF CITED DOCUMENTS

X : particularly relevant if taken alone
Y : particularly relevant if combined with another document of the same category
A : technological background
O : non-written disclosure
P : intermediate document

T : theory or principle underlying the invention
E : earlier patent document, but published on, or after the filing date
D : document cited in the application
L : document cited for other reasons

& : member of the same patent family, corresponding document

EPO FORM 1503 03.82 (P04C01)

Europäisches Patentamt
European Patent Office
Office européen des brevets

EUROPEAN SEARCH REPORT

Application Number
EP 23 38 2013

DOCUMENTS CONSIDERED TO BE RELEVANT

Category	Citation of document with indication, where appropriate, of relevant passages	Relevant to claim	CLASSIFICATION OF THE APPLICATION (IPC)
A	US 2003/146543 A1 (LEBRUN GILBERT [US] ET AL) 7 August 2003 (2003-08-07) * paragraph [0035] - paragraph [0054]; figures 2-5 * * paragraphs [0088] - [0093] * * paragraphs [0098] - [0102] * * claims 16-19 *	1-22	
A	US 2015/217488 A1 (ALLMAN DANIEL [US] ET AL) 6 August 2015 (2015-08-06) * pages 1-3; claims 1-21; figures 5, 6, 1a-4 *	1-22	
A	US 11 524 425 B2 (ALEDA SA [CH]) 13 December 2022 (2022-12-13) * the whole document * * figures 8-11, 35, 38 *	1-22	
			TECHNICAL FIELDS SEARCHED (IPC)

The present search report has been drawn up for all claims

Place of search	Date of completion of the search	Examiner
Munich	14 July 2023	Brunswick, André

CATEGORY OF CITED DOCUMENTS

X : particularly relevant if taken alone
Y : particularly relevant if combined with another document of the same category
A : technological background
O : non-written disclosure
P : intermediate document

T : theory or principle underlying the invention
E : earlier patent document, but published on, or after the filing date
D : document cited in the application
L : document cited for other reasons

& : member of the same patent family, corresponding document

EPO FORM 1503 03.82 (P04C01)

ANNEX TO THE EUROPEAN SEARCH REPORT ON EUROPEAN PATENT APPLICATION NO. EP 23 38 2013

This annex lists the patent family members relating to the patent documents cited in the above-mentioned European search report. The members are as contained in the European Patent Office EDP file on
The European Patent Office is in no way liable for these particulars which are merely given for the purpose of information.

14-07-2023

Patent document cited in search report	Publication date	Patent family member(s)	Publication date
US 2020269487 A1	27-08-2020	NONE	
CN 114474685 A	13-05-2022	NONE	
EP 2881234 A1	10-06-2015	DE 102013018148 A1	11-06-2015
		EP 2881234 A1	10-06-2015
		ES 2597278 T3	17-01-2017
		US 2015151507 A1	04-06-2015
US 5026514 A	25-06-1991	NONE	
CN 108480821 B	15-10-2019	NONE	
US 2003146543 A1	07-08-2003	AU 2003201562 A1	02-09-2003
		CA 2473692 A1	31-07-2003
		US 2003146543 A1	07-08-2003
		WO 03061930 A2	31-07-2003
US 2015217488 A1	06-08-2015	CN 104602896 A	06-05-2015
		EP 2892709 A1	15-07-2015
		US 2015217488 A1	06-08-2015
		WO 2014039965 A1	13-03-2014
US 11524425 B2	13-12-2022	CN 111448042 A	24-07-2020
		EP 3473397 A1	24-04-2019
		EP 3700727 A1	02-09-2020
		US 2020346419 A1	05-11-2020
		WO 2019082055 A1	02-05-2019

EPO FORM P0459

For more details about this annex : see Official Journal of the European Patent Office, No. 12/82